EUROCONTROL
Experimental Centre

Sandrine CARLIER
James SMITH
Frank JELINEK

GAES – Future Engine Technology Environmental Impact

EEC/SEE/2005/002

EUROCONTROL

Title : GAES – Future Engine Technology Environmental Impact

Authors: Sandrine Carlier, James Smith

Review:
Frank Jelinek – frank.jelinek@eurocontrol.int

EUROCONTROL EXPERIMENTAL CENTRE, Bretigny sur Orge, France

EEC Note: EEC/SEE/2005/002

EXECUTIVE SUMMARY

A growing shortage of fuel supply and an ever-increasing interest in environmental concerns are encouraging the aeronautical community to develop new types of aircraft propulsion. Among the different possibilities studied, hydrogen seems to be the most promising mode of propulsion for the next decades.

Apart from helping to overcome the fuel supply problem, hydrogen engines offer the great advantage of exhausting only water vapour and NO_x.

Conversion of conventional engines to hydrogen is more straightforward than it appears at first sight since the engine's basic principle is the same. However higher volumes of fuel to be transported would require modification in aircraft airframes.

The first hydrogen-powered aircraft could operate around 2015. A conversion of the whole fleet to hydrogen could not be carried out before 2050.

The current study aims at comparing the situation in term of environmental concerns if:

- No aircraft is converted to hydrogen, i.e. a reduction of emission is obtained through technological improvement on today's kerosene engines only,
- The entire fleet is converted to hydrogen.

The current study does not reflect the future situation but focuses on the environmental impact or benefit of one factor: evolution of technologies. Therefore traffic growth is not considered in the current study. Results are not marred by traffic growth.

The environmental analysis leads to a contrasted assessment depending on the pollutant:

- If focussing on environmental impact of **CO, HC, CO_2 and SO_x only**, the hydrogen engine is unquestionably an **ideal solution** since these emissions would totally disappear from aviation's pollutant list.
- The assessment of **NO_x** is more ambivalent since, in the long term (2050), emission of NO_x will stay **significant whichever technology** is used, even if kerosene engines would produce at least twice as much NO_x as hydrogen engines, or even more if pre-mixing technology is used. No decision can be made if focussing on NO_x only.
- Concerning **H_2O**, hydrogen engines have a **significant disadvantage**: the amount of water vapour emitted is 2.6 times higher than water emitted from today's conventional engines. This translates into a higher probability of contrail formation.

With regard to contrail production for the baseline scenario, the aircraft fleet of 2004, on average for the 20 days studied, produced contrails on **15.93%** of the flight legs >= FL240. Flight legs refer to short flight segments in the CPR data, each of approximately 2 minutes duration. The percentage of contrail-producing flight legs increased to **17.54%** for the fleet of 2028, to **19.05%** for the fleet of 2050 (with increased fuel efficiency) and to **27.13%** for the all hydrogen fleet of 2050.

This indicates that, in comparison with 2004, an estimated increase in contrail sky coverage of approximately **1.61%** can be expected in 2028, **3.12%** in 2050 with increased fuel efficiency, and **11.20%** in 2050 with hydrogen aircraft. For all three future scenarios, this increase appears to be consistent over both days of low and high contrail coverage.

This also indicates an increase of **8.08%** in contrail sky coverage using hydrogen aircraft compared to using kerosene aircraft in 2050.

In order to identify which future engine technology would be the best from an environmental point of view, emissions were normalized using environmental shadow costs (see section 7.4). Figure 1 represents the sum of emission costs in 2050 for kerosene and hydrogen technology.

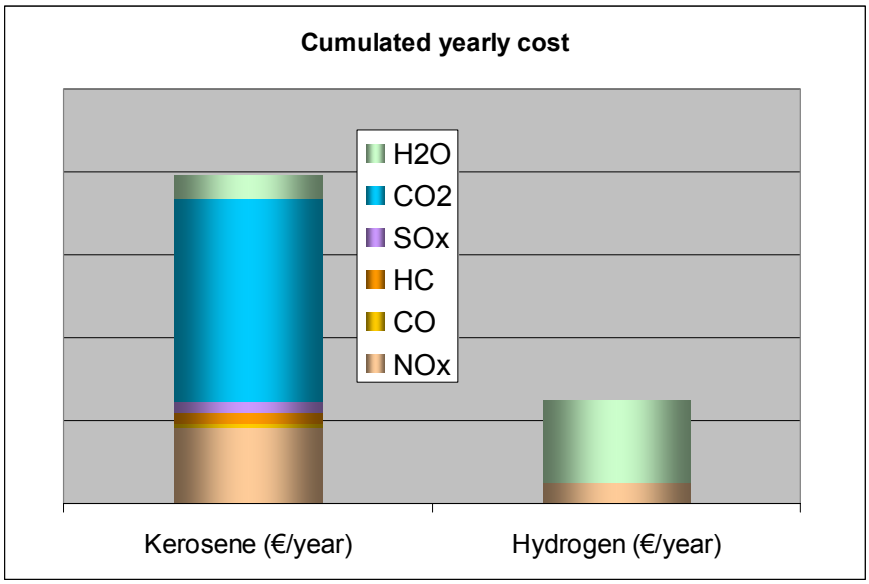

Figure 1: Cumulative yearly emissions costs[1]

It appears that the sum of emissions exhausted by kerosene engines have on average a shadow cost almost 3 times higher than the sum of emissions from hydrogen engines. On an environmental point of view, the assessment is in hydrogen's favour; hydrogen is a "clean" technology in comparison with kerosene.

Nevertheless this result has to be used with caution since the study does not consider all the parameters necessary to draw conclusions. In particular the production of liquid hydrogen may induce emissions at ground level, which would decrease the interest of hydrogen technology from a global environmental point of view.

Moreover the evaluation of the cost of H_2O emission is subject to modifications following recent findings from NASA and DLR ([Ref 18] & [Ref 19]).

[1] Based on an averaged estimation of future emissions.

REPORT DOCUMENTATION PAGE

Reference: EEC/SEE/2005/002	**Security Classification:** Unclassified
Originator: Society, Environment, Economy Research Area	**Originator (Corporate Author) Name/Location:** EUROCONTROL Experimental Centre Centre de Bois des Bordes B.P.15 91222 BRETIGNY SUR ORGE CEDEX France Telephone: +33 1 69 88 75 00
Sponsor: EUROCONTROL EATM	**Sponsor (Contract Authority) Name/Location:** EUROCONTROL Agency Rue de la Fusée, 96 B –1130 BRUXELLES Telephone: +32 2 729 90 11

TITLE:
GAES - Future Engine Technology Environmental Impact

Authors :	**Date**	**Pages**	**Figures**	**Tables**	**Appendix**	**References**
Frank Jelinek, Sandrine Carlier, James Smith	09/05	xiii+158	72	28	7	34

EATMP Task Specification	Project	Task No. Sponsor	Period
-	Future Engine Technology	-	2005

Distribution Statement:
(a) Controlled by: EUROCONTROL Project Manager
(b) Special Limitations: None
(c) Copy to NTIS: ~~YES~~ / NO

Descriptors (keywords):
Global Emissions – AEM – TEA – Condensation Trail – Contrail – NO_x – CO – HC – CO_2 – H_2O – SO_x – Future Aircraft Engine Technology – Hydrogen – EEC – SEE – etc.

Abstract:
The future engine technology environmental impact study investigates the potential environmental benefit of hydrogen engines compared to the evolution of technology for conventional kerosene engines. Contrail maps are presented to compare both situations.

TABLE OF CONTENTS

LIST OF TABLES

LIST OF FIGURES

ABBREVIATIONS

ACARE ..... Advisory Council for Aviation Research in Europe
AEM ..... Advanced Emission Model
AEM3 ..... Advanced Emission Model, 3rd version
ANCAT ..... Abatement of Nuisances Caused by Air Transport
APU ..... Auxiliary Power Unit
ASPO ..... Association for the Study of Peak Oil
CAEP/2 ..... Committee on Aviation Environmental Protection – 2nd formal meeting
CFMU ..... Central Flow Management Unit
CO ..... Carbon Monoxide
CO_2 ..... Carbon Dioxide
Contrail ..... Condensation trail
CPR ..... Correlated Position Reports
DLR ..... German Aerospace Centre
EEC ..... EUROCONTROL Experimental Center
EEC-BM2 ..... The EUROCONTROL modified Boeing Method 2
EI ..... Emission Index
EPA ..... Environmental Protection Agency
ESA ..... European Space Agency
FESG ..... Forecast and Economic Support Group
FL ..... Flight Level
FNL ..... Global Final Analyses
GDAS ..... Global Data Assimilation System
GIFAS ..... Groupement des Industries Françaises Aéronautiques et Spatiales
GIS ..... Geographical Information System
GTS ..... Global Telecommunications System
GWP ..... Global Warming Potential
H_2O ..... Water
HC ..... Hydrocarbon
ICAO ..... International Civil Aviation Organisation
IPCC ..... Intergovernmental Panel on Climate Change
KNMI ..... Royal Netherlands Meteorological Institute
Lat ..... Latitude
Long ..... Longitude
LTO ..... Landing- and Take-Off cycle
Max ..... Maximum

Min ..... Minimum
MM5 ..... Numerical weather model
MS ..... Microsoft
MTOW ..... Maximum Take-Off Weight
MTU ..... Motoren und Turbinen Aero Engines
NASA ..... National Aeronautics and Space Administration
NCAR ..... National Centre for Atmospheric Research
NESDIS ..... National Environmental Satellite, Data, and Information Service
NM ..... Nautical Mile
NO_x ..... Oxides of Nitrogen
OWE ..... Operating Weight Empty
ppb ..... parts per billion (10^9)
SEE ..... Society, Environment, Economy
SO_x ..... Oxides of Sulphur
TEA ..... Toolset for Emission Analysis
TOG ..... Total Organic Gases
VOC ..... Volatile Organic Compounds
yr ..... Year

Intentionally left blank

1 INTRODUCTION

1.1 Context

This study is motivated by the findings of DLR and NASA studies that focussed on the impact of contrails on the environment. As detailed in section 3.3, research conducted mainly by NASA and DLR in 2003 ([Ref 18] and [Ref 19]) give every indication that the impact of H_2O on environment, and especially the resulting apparition of contrails, is much higher than estimated by the IPCC. The contribution of H_2O emission to radiative forcing might be one of the most penalizing to the environment. Indeed air emissions of H_2O, on top of being a greenhouse gas, contributes to the apparition of contrails which are likely to eventually affect the weather (see section 7.3.1 for more details).

As upcoming technologies may lead to aircraft exhausting significantly more H_2O than today's aircraft do, this issue could become critical during the next decades. It must therefore be investigated.

Moreover, a deep-seated motive for this study was the interest to better understand possible means for the aircraft industry to contribute to the goals defined for all industry sectors by the Kyoto conference. The Kyoto protocol requires the global emission output to be reduced 5.2%l by 2008/2012, and an even higher target of 8 % reduction has been fixed for EUROPE [Ref 5].

Within the transport sector aviation is not currently the highest polluter, however, the growth rate in the aviation sector remains significantly higher than for other forms of transport. In light of this, aviation and all its stakeholders have the responsibility to redouble efforts in order to try to reach the goals set in Kyoto. Major efforts in the airframe and aircraft engine manufacturing industry have led to significant reductions in fuel burn and emissions per passenger-kilometre over the last 40 years. Although this process of technical improvements is still ongoing, the progress that has been made through technological advances has been rapidly absorbed by the continuous traffic increase. For this reason, other stakeholders in the aviation transport sector must increase their efforts to improve the situation.

The threat of fuel supply's exhaustion in the next decades motivated the aeronautical community to study new modes of propulsion. The gap between world oil consumption and discoveries is now negative and increasing (Figure 2) presaging oil shortages in the long term.

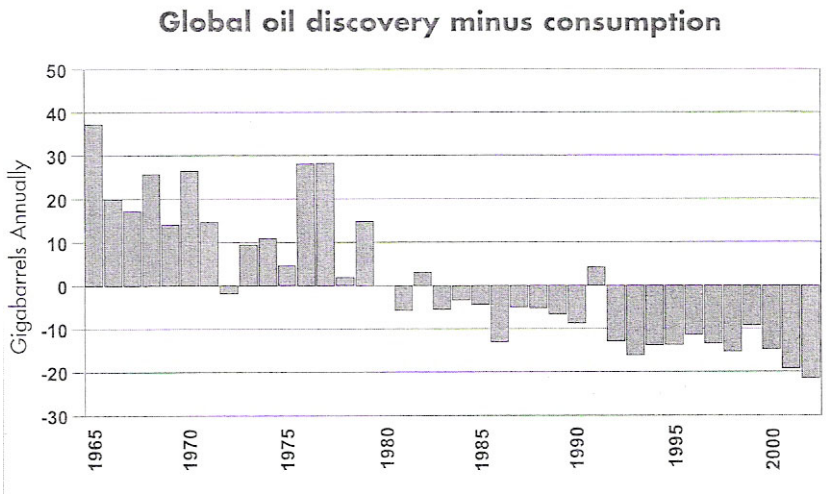

Figure 2: Gap between world oil consumption and discoveries (source: ASPO)

Studies like this one help to estimate the potential environmental benefits of the different program's elements and bring an extra environmental component into context.

1.2 Study process plan

The methodology shown below was applied to this study. This report is presented following the same steps.

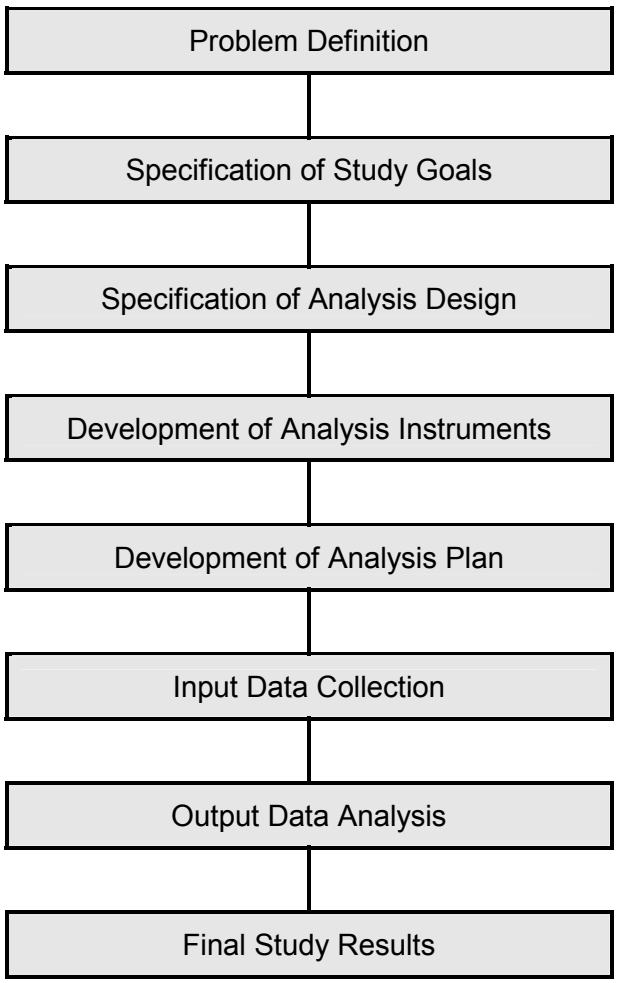

Figure 3: Process phases for the future engine technology study

Intentionally left blank

2 PROBLEM DEFINITION – NEW ENGINE TECHNOLOGY[2]

The global supply of fossil fuels is expected to be exhausted sometime in this century, even if opinions about the exact date may differ. This is the date by when we will need alternative forms of energy at our disposal. They will have to be developed well enough not to just work in the laboratory but also to be used safely and reliably in operational service.

A second motivation for the aeronautical community to develop a new mode of propulsion is the strengthening of environmental concerns, and especially the level of CO_2 emissions. Both engines and aircraft have to be improved to reduce or even eliminate aircraft emissions.

The IPCC ([Ref 3]) reports that subsonic aircraft being produced today are about 70% more fuel efficient per passenger-km than 40 years ago. In the same period the amount of pollutant emitted by aircraft engines decreased significantly. The majority of this gain was achieved through engine improvements and the remainder from airframe design improvement. However, further technological enhancements on kerosene engines are limited.

Although synthetic kerosene might replace current kerosene, the main alternatives to kerosene that have been proposed and investigated as potential fuels for aircraft gas turbines are discussed in section 7.8.4 of the IPCC report [Ref 3]. All but one of them can be dismissed from further consideration here, on the grounds that the economic or environmental benefits they offer are thought unlikely ever to justify a change from kerosene. The one exception is cryogenic hydrogen.

2.1 Hydrogen as an alternative to kerosene

Hydrogen can be used just like conventional fuels – burnt in engines or boilers to provide heat and power – or it can be chemically reacted with oxygen in a fuel cell to produce electricity directly. If the conventional combustion route is taken, then some small amounts of polluting emissions will result, such as NO_x due to high-temperature reactions involving the nitrogen in the air, though far less than with traditional fossil fuels. In the case of a fuel cell, the only emission will be water vapour. The benefits of using hydrogen are thus simple and clear – used in power generation or as a vehicle fuel, it contains nothing that pollutes and so all emissions are dependent on the way in which it is combusted.

2.2 Hydrogen as an energy carrier

Hydrogen, however, is not a true fuel; rather it is an energy carrier[3], like electricity. It cannot be mined, drilled-for or cut down but must be manufactured from other compounds that are widely available on earth. The two most abundant hydrogen-containing compounds are water (H_2O) and hydrocarbon fuels (H_xC_y). 99% of this hydrogen is currently produced from fossil

[2] This paragraph sums up the main of information from the literature (especially [Ref 9] and [Ref 26] to [Ref 32]). It aims at helping the reader to familiarize himself with hydrogen aircraft technology.

[3] An energy carrier can be thought of as a means of delivering energy to end-use, as distinct from a primary source of energy. It may be used to provide energy services in a handier or cleaner form. Many things can serve this role, for example gasoline, electricity or hydrogen.

fuels, primarily natural gas, with chemical production and renewable energy sources accounting for the rest.

However, producing hydrogen from hydrocarbons yields the greenhouse gas carbon dioxide (CO_2) as a by-product. At present, all of the CO_2 generated is released to atmosphere. As climate change and reductions in greenhouse gas emissions are a concern by the Kyoto protocol, ways of producing hydrogen without emitting CO_2 will be needed. The great variety of designs to produce hydrogen does not allow the calculation of one "true" value to estimate the amount of CO_2 emissions avoidable in the future. The economic challenge of producing hydrogen cost efficiently also has to be met.

This study focuses exclusively on assessing emissions from the final use of hydrogen. Even if not considered in this document, the overall energy used to produce hydrogen has to be investigated. The complete chain of processes for hydrogen production and use has to be examined, to find out whether overall greenhouse gas emissions would rise or fall by the substitution of hydrogen for other energy carriers.

2.3 Hydrogen aircraft

Hydrogen aircraft have been the subject of much research in Europe, the USA, Russia and elsewhere since the 1950s. In the long term, H_2 could be used in place of kerosene to fuel jet aircraft, although major changes in aircraft design would be required.

A very important consideration in using hydrogen as aircraft fuel is the possibility of a significant reduction in harmful emissions. During the combustion of kerosene in today's engines, carbon dioxide (CO_2) and water (H_2O) are produced. Additionally lesser amounts of sulphur dioxide (SO_2), carbon monoxide (CO), nitrogen oxides (NO_X) and unused hydrocarbons (HC) are also emitted. The last three substances are considered to be greenhouse gases.

However, if hydrogen is used, water is the principal product of combustion. The emission of water, which acts as a greenhouse gas at altitudes of eleven to twelve km, is significantly higher than with a kerosene-fuelled engine. In addition, the forming of nitrogen oxide (NO_x) cannot be avoided.

However, according to Dasa's Dr. Hans-Wilhelm Pohl and Dr. Hans-Günter Klug, project managers of Cryoplane ([Ref 9]), NO_x emissions are significantly lower than with a comparative kerosene engine. Since the greenhouse effect of water depends very much on altitude, the harmful effects of water emissions can be reduced significantly by lowering the flight altitude. The downside of this is slightly higher drag and an increase in fuel consumption.

Hydrogen has one further advantage: In principle there is an unlimited supply of it, although it is fixed in the form of water. Energy has to be used to extract hydrogen from water to make it useable. If this problem is solved elegantly - for example with regenerative energies - a closed loop is created with its combustion: water→hydrogen→water (see [Ref 26]).

2.3.1 Technical aspect of hydrogen aircraft

- **Hydrogen is lighter than kerosene**

Hydrogen's energy per kg (120,000kJ/kg) is 2.8 times higher than kerosene's energy (42,800kJ/kg). This means that only one third of the kerosene amount is necessary for a hydrogen aircraft to cover the same range. This allows the aircraft's maximum load to be boosted. Dasa reports an increase of about five per cent with regional and short haul aircraft and around 20 per cent with long distance jets.

- **Hydrogen requires a larger volume than kerosene**

The significantly lower density of hydrogen prevents the storage of hydrogen in its gaseous form. In order to reduce the space needed for the storage of hydrogen, hydrogen is stored in liquid form in designated tanks at 20 degrees Kelvin (minus 253 Degrees Celsius), or even in a "slush" state (minus 260 Degrees Celsius, 50% liquid, 50% solid hydrogen). A trade-off has to be done since the "slush" state is much more expensive and requires a smaller volume but a heavier tanks' structure than liquid state (notably due to higher pressure inside the tanks and to greater insulation needs), thus impacting directly on fuel consumption. But even then the specific volume of hydrogen is roughly twelve times larger than kerosene's one.

Taking into account that only one third of the weight of kerosene has to be transported, a hydrogen fuel tank is 4.3 times bigger than a kerosene tank to cover the same range.

Airframes would have to be fundamentally redesigned to accommodate the larger volumes of fuel. Designs include planes similar to current large passenger aircraft but with additional fuel tanks running above the length of the passenger compartment, or the more radical “blended wing body” or “flying wing”. However the form of the fuel tank is imposed by the storage pressure of liquid hydrogen. Only spherical and cylindrical tanks would support pressure of liquid hydrogen, which largely influences the overall aircraft design. The extra structural weight due to tanks and modifications in the design of aircraft has to be calculated.

Consequences of the large volume of tanks might affect the number of passengers to be transported in an equivalent aircraft because seats would be replaced by fuel tanks. At the same time aerodynamic properties of the aircraft would be affected, causing excess drag.

Engines would have to be modified, in particular to keep NO_x emissions within acceptable levels. The combustion chamber needs to be redesigned to overcome the problems of nitrogen oxides in the emissions of hydrogen engines. The formation of nitrogen oxide is dependent on the peak temperatures reached in the combustion chamber and on the residence time that the gas mixture spends inside of the combustor. A short residence time at high temperature would reduce the formation of NO_x. Fortunately the combustion chamber can be shortened, because hydrogen gas burns spontaneously, and the fuel-air-mixture does not need to stay for long in the combustion chamber.

Without modification, a hydrogen engine may generate more nitrogen oxide than a kerosene engine. Nevertheless conversion of conventional turbo engines can be done. Modifications to the engine are only minor, because the general working of the engine basically does not change. The biggest change is that kerosene is being replaced with hydrogen.

Although cryogenic engines are widely used in space technology, components from space launchers cannot be copied directly because aviation requires a much longer component

lifetime. Moreover the level of safety to be met in aviation is incomparably higher than for space missions, since aircraft carry many civilian passengers.

According to the Cryoplane project ([Ref 9]), hydrogen engines run 30 to 50K cooler than kerosene engines for the same thrust level. This lower temperature would increase engine life.

Moreover, as hydrogen's heat-absorption capacity is much higher than kerosene's, hydrogen could also be used in engine and aircraft cooling systems. Increasing turbine cooling efficiency would allow an increase of the temperature in front of the turbine, hence enhancing compressor pressure ratio. Even if small, the benefits are not negligible.

In order to be able to use hydrogen for civil aviation in a few decades, not only technical problems have to be solved. A whole new infrastructure has to be put in place: airports have to be converted and production and availability of H_2 have to be guaranteed on a bigger scale than today.

2.3.2 Safety aspects

Public perception of H_2 safety is nowadays negative following the spectacular accident of the airship Hindenburg in 1937. H_2 flames are invisible, making optical sensing difficult in case of fire. Additional proof will thus be essential to help public opinion get over this psychological problem. Hydrogen aircraft will clearly be required to meet the same stringent safety standards as conventional ones.

Nevertheless the first safety assessments are optimistic ([Ref 9]). Indeed:

- In free atmosphere, hydrogen rises quickly. Hence the danger zone is small if hydrogen leaks or is spilled.
- Hydrogen will burn at concentrations significantly below the limit for detonation.
- There is no detonation in free atmosphere.
- Hydrogen will not form a fire carpet.
- Hydrogen burning is fast, producing very low heat radiation.
- Combustion products are not toxic.
- Practical experience has proved a clear safety advantage of hydrogen versus gasoline.

First safety assessments thus seem to indicate that hydrogen engines would be at least as safe as kerosene engines.

2.3.3 Hydrogen vs. kerosene aircraft

Table 1 gives a quick overview of hydrogen aircraft compared to kerosene aircraft.

	Kerosene	Hydrogen
Energy by kg (kJ/kg)	42,800kJ/kg	120,000kJ/kg
Weight	100%	36% (÷ 2.8)
Volume of fuel	100%	1200% (× 12)
Volume of fuel tank	100%	430% (× 4.3)
MTOW of long range aircraft	100%	85% to 105%[4]
OWE	100%	120-125%
Drag	100%	110%
CO_2, SO_x, CO, HC	100%	0%
H_2O	100%	260% (× 2.6)
NO_x	100%	5 to 25%[5]

Table 1: Hydrogen versus kerosene aircraft ([Ref 9] and [Ref 26] to [Ref 32])

2.3.4 Summary

Hydrogen jet aircraft use liquid hydrogen to combust in a modified turbine jet engine. The hydrogen is stored in liquid or in a "slush" state of part liquid, part solid hydrogen. Storage tanks must be very large.

Main advantages:

- zero-emissions except for small-to-medium amounts of nitrogen-oxides (controllable to a great extent with fuel injection),
- powerful enough to drive large jet aircraft,
- light fuel load allows use of smaller engines to do the same job, or longer flights between refuelling,
- unlimited supply.

Main disadvantages:

- voluminous hydrogen requires large fuel tanks which may cause excess drag,
- loud (although not as loud as normal jet engines),
- requires a new infrastructure to be put in place at airports,
- presently, much more expensive than kerosene.

[4] depending on the aircraft configuration and mission.

[5] Depending on combustion chambers technology

On balance it appears that current types of aviation fuel will continue to be the preferred option for gas turbine powered aircraft. This situation could change if liquid hydrogen could be produced by an environmentally acceptable and economically competitive method or if the need to reduce CO_2 emissions from aviation becomes overwhelming.

2.4 Fuel cell aircraft

Along with the discussion about future energies for aircraft propulsion appears fuel cell technology. Although probably applicable for APU only, the fuel cell's principle is presented here for completeness reasons.

Fuel cell aircraft are electric aircraft that generate electricity from hydrogen fuel cells to drive an electric motor/propeller. These planes would be refuelled rather than recharged.

2.4.1 What is a fuel cell?

In principle, a fuel cell operates like a battery. Unlike a battery, a fuel cell does not run down or require recharging. It will produce energy in the form of electricity and heat as long as fuel is supplied.

A fuel cell consists of two electrodes sandwiched around an electrolyte. Oxygen passes over one electrode and hydrogen over the other, generating electricity, water and heat.

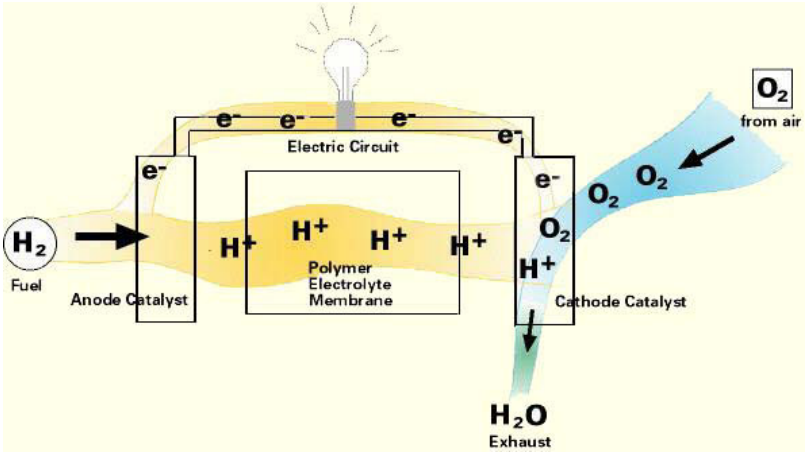

Figure 4: Fuel cell principle[6]

Hydrogen fuel is fed into the "anode" of the fuel cell. Oxygen (or air) enters the fuel cell through the cathode. Encouraged by a catalyst, the hydrogen atom splits into a proton and an electron, which take different paths to the cathode. The proton passes through the electrolyte. The electrons create a separate current that can be used before they return to the cathode, to be reunited with the hydrogen and oxygen in a molecule of water.

6 Source: http://www.fuelcells.org

2.4.2 Fuel cells and aviation

A fuel cell system which includes a "fuel reformer" can utilize the hydrogen from any hydrocarbon fuel – from natural gas to methanol, and even gasoline. Since the fuel cell relies on chemistry and not combustion, emissions from this type of a system would still be much smaller than emissions from the cleanest fuel combustion processes.

Fuel cell vehicles operating on hydrogen stored on-board the vehicles produce zero pollution in the conventional sense. Neither conventional pollutants nor greenhouse gases are emitted. The only by-products are water and heat.

Systems that rely on a reformer on board to convert a liquid fuel to hydrogen produce small amounts of emissions, but would still reduce smog-forming pollution by up to 90 percent compared to traditional combustion engines, depending on the choice of fuel.

In addition to being inherently cleaner and quieter than current technology gas turbines, fuel cells can generate approximately twice as much electricity from the same amount of fuel. Unlike a battery, which needs to be recharged, fuel cells keep working as long as the fuel lasts.

Nevertheless it is quite unrealistic that fuel cells alone would be used to move aircraft. A fuel cell aircraft's flight range for a small aircraft is around 500 to 800 miles between hydrogen refuelling. Fuel cells would be adapted to power small passenger carrying aircraft only, especially propeller-driven aircraft (which are small contributor to global emissions), if future fuel cell engines could ever overcome working temperature limitation problem. For this reason, the current study only focuses on hydrogen engines and does not address a highly hypothetical "all fuel cell fleet" scenario.

Fuel cells could potentially replace the current gas turbine auxiliary power units (APUs), which provide electricity and air for airplane systems, for large commercial aircraft powered by hydrogen engines.

Fuel cells would thus be part of the new infrastructure to be developed at airports, in the framework of large liquid hydrogen-powered aircraft development. The impact of fuel cell APUs on the environment would need to be assessed if such a technology is proved as being concretely viable.

2.5 Timescale

Although technology for hydrogen aircraft is available today in theory, it is not realistic to consider that commercial hydrogen powered aircraft will be mass-produced within the next few years. Indeed production of such aircraft has not been launched. Neither are airports equipped to welcome hydrogen aircraft.

According to the Cryoplane project ([Ref 9]) work package 8, both small and medium-sized aircraft (i.e. up to 220 seats) would be hydrogen-converted first. Liquid hydrogen on the large aircraft would be introduced ten years later. Operation of a hydrogen-fuelled aircraft will not be attractive to the market at this time due to high costs for hydrogen. Therefore setting-up of a 100% liquid hydrogen fleet would highly depend on a firm line of policy regulation taken by ICAO to lead to a worldwide introduction of liquid hydrogen aircraft. With the support of such a regulatory framework, optimistic estimates expect a 100% hydrogen fleet for about 2050. This estimation does not consider potential delays due to industrial production.

3 SPECIFICATION OF STUDY GOALS

The main goal of this study is to compare the evolution of fuel burn and emissions depending on the technological direction the aeronautic community will move toward in the next decades. Growing shortage of fuel in the next decades as well as increasingly important environmental concerns will condition these choices to a great extent.

Two directions are addressed in this study:

- Evolution of current kerosene engines, including fuel and propulsion efficiency improvement and reduction of the amount of emissions.
- Radical transformation of engines toward cryogenic technology, which would be an alternative to exhaustion of fuel supply and would lead to the disappearance of all aircraft emissions except H_2O and a small amount of NO_x.

The consequences of the direction chosen will be critical from an environmental point of view. This study will specifically investigate the potential environmental impact of the two directions mentioned above, in particular in terms of CO_2, NO_x and H_2O, since those three emissions are seen to be the main factors in the chemical processes leading to radiative forcing (greenhouse effect) and a reduced ozone layer. The investigation of CO and HC emissions (and therefore VOC and TOG, which are linked to HC emissions) is also addressed, even if these are mostly emitted at a low level.

Unfortunately today's state of the art does not allow precise predictions of the evolution of technology in the long term. In particular, emission reduction in future engines is highly dependent on trade-offs between the pollutants to reduce and thus almost not quantifiable today. The emission analysis of this study hence does not claim to present a precise analysis of the situation in the next decades but tends to indicate trends.

The focus is on contrail production, since hydrogen engines would produce much more water vapour than kerosene engine, thus probably affecting the contrail and cirrus clouds coverage.

The paragraphs below present an overview of the main emissions covered by the study.

3.1 Aviation Environmental Impacts from Carbon Dioxide (CO_2)

CO_2 is a stable component in atmospheric chemistry. CO_2 is naturally occurring and is mixed homogeneously throughout the atmosphere. CO_2 affects the atmosphere directly and depending on the concentrations of molecules it affects the ability of the earth to absorb outgoing radiation emitted by the earth's surface and lower atmosphere. In terms of global warming this is of great concern as CO_2 can reside in the atmosphere for hundreds of years.

The CO_2 emitted by aircraft is mixed with CO_2 from other sources. As jet aircraft have only been in service over the last 50 years, CO_2 concentrations from aircraft alone are difficult to assess. Nevertheless, the aviation sector is estimated to produce 2 – 3 % of overall man-made CO_2 emissions [Ref 3]. For an analysis of its impact on the atmosphere, precise knowledge of the geographical position and altitude of the emission source is of low importance, and atmospheric CO_2 cannot be associated with local emitters. CO_2 emissions have to be reviewed in a global context.

3.2 Aviation Environmental Impacts from Nitrogen Oxides (NO_X)

NO_x is a common term used to refer mostly to two species of oxides of nitrogen collectively reported as NO_2 –equivalent: nitrous dioxide (NO_2) and nitrous oxide (NO), a greenhouse gas which accumulates in the atmosphere with other greenhouse gases leading to a rise in the earth's temperature over time. NO_2 is a strong oxidizing agent that reacts in the air to form corrosive nitric acid, as well as toxic organic nitrates. It also plays a major role in the atmospheric reactions that produce ground-level ozone or photochemical smog.

NO_x has two contradictory effects on ozone. In high altitudes of the stratosphere NO_x emissions contribute to the reduction of ozone, while in typical Cruise altitudes (8-13 km) NO_x emissions cause an ozone increase.

NO_x can react with other substances in the air to form acids which are deposited as rain, fog, snow (wet deposition) or dry particles (dry deposition). It can be carried by wind for hundreds of kilometres causing trans-boundary air pollution impacts such as acid rain damage to material, buildings and historical monuments, and the acidification and eutrophication of lakes and streams.

Apart from lightning, aircraft are responsible for all NO_x emissions at 8-15 km altitudes. The contribution of aviation to global NO_x emissions is currently estimated to be only 1.8 % [Ref 12]. However, several studies predict, for the North Atlantic track system, an increase of NO_x from aircraft emissions of 10 – 100 % [Ref 13], [Ref 14], [Ref 15].

3.3 Aviation Environmental Impacts from water vapour (H_2O)

Water vapour is a greenhouse gas and is formed as a by-product of the combustion of kerosene. At high altitude water vapour condenses to form thin cloud trails (contrails) in the sky.

Depending on meteorological conditions (such as air temperature and prevailing wind) these contrails can persist visibly for many hours often spreading out to join with other mature contrails, which may then influence the formation of cirrus clouds. Moreover, water vapour can reside in the troposphere for up to nine days before being eliminated in the form of precipitation. In the stratosphere it can last weeks or months, adding to the potential radiative forcing effect and man-made climate change over this period.

Following the 9/11 terrorist attacks in the US, almost all aircraft were grounded for 24-48 hours. Over the following days diurnal temperatures were between 1 and 2 degrees C higher than normal ([Ref 16]). This may be explained because contrails were not produced in that period and so did not contribute to cirrus cloud formation. This allowed sunlight to enter the earth's atmosphere unimpeded, raising daytime temperature, and, as the returning radiation was not trapped by the cloud, lowering night-time temperature.

Approximately 10-20 % of all jet aircraft flights occur in air masses that are humid enough to cause contrails. With air traffic growing and contrails becoming more prevalent, the natural variation will further decline and some scientists speculate that this could disrupt regional ecosystems.

Figure 5 illustrates this with a ‘snap-shot’ of the situation over Northern Europe.

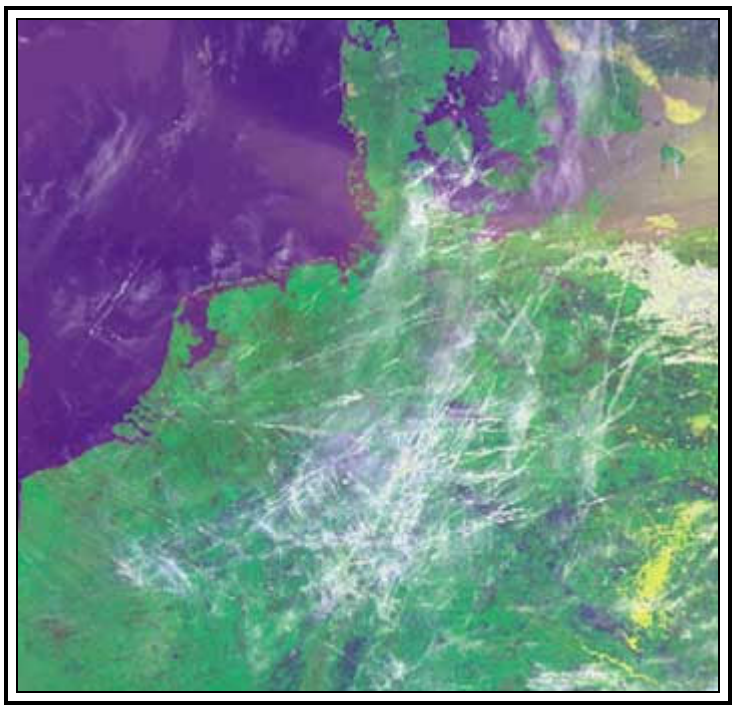

Figure 5: NOAA-12AVHRR Satellite photograph; Central Europe; May 4, 1995, proc. by DLR

Currently the contrail cover remains weak. The annual average contrail coverage is about 0.1 % of the earth's surface while the natural cirrus clouds global mean coverage reaches about 20 %. However over regions with intense air traffic, the local contrail cover can reach up to 5 % of the sky [Ref 11]. According to the IPCC (Intergovernmental Panel on Climate Change) reference scenario documented in 1999, the global contrail cover is projected to grow to 0.5 % by 2050 ([Ref 3]).

The most recent research of mainly NASA ([Ref 18]) and DLR ([Ref 19]) during 2003 indicates that the environmental impact in terms of radiative forcing resulting from contrails and contrail-caused cirrus clouds might be significantly higher than initially estimated by IPCC and might even be more important than the overall impact of the sum of all other greenhouse gases emphasised in the past.

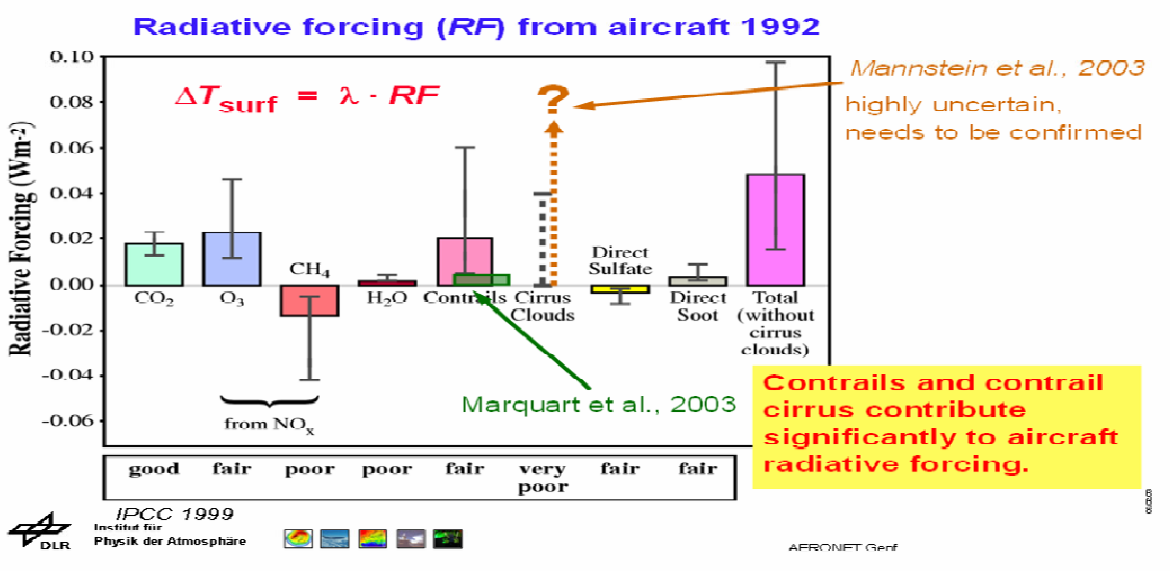

Figure 6: Increased RF by aviation-caused Contrails and Cirrus Clouds ([Ref 19])

Since the scientific case is not yet sufficiently proven with the required statistical reliability, aviation can not yet adopt measures that might later prove to be ineffective or, worse, counter-productive.

To test the scientific case the EUROCONTROL Experimental Centre (EEC) is working with and supports the European Space Agency's two-year project CONTRAILS ([Ref 20] & [Ref 10]). Part of the project is also to validate the EEC's contrail prediction model. Such a model would be required if contrail-related research results in the societal need to re-organise traffic flows to avoid the cold, damp air masses in which contrails form. Final results of ESA's CONTRAILS project are expected for End 2005.

For additional information, the influence of different emissions on health is detailed in Appendix A of [Ref 17].

4 DEVELOPMENT OF ANALYSIS INSTRUMENTS

4.1 The Advanced Emission Model (AEM)

The current study used the AEM3 Advanced Emission Model 3 to estimate today's (i.e. 2004) aviation fuel burn and atmospheric emissions. The AEM3 model and the underlying calculation methodology are described in this section.

The Advanced Emission Model version 3 (AEM3) is used to estimate aviation emissions and fuel burn for a given set of traffic movements in an analysis region.

AEM3 is a stand-alone system able to analyse flight profile data, on a flight-by-flight base, for air traffic scenarios of almost any scope. It uses 4D-flight profile information to calculate fuel burn and, in addition, emissions produced (CO_2, H_2O, SO_x, NO_x, HC, CO, VOC, TOG).

The model is based on the use of several underlying databases, including a set of default databases that hold information related to aircraft, aircraft engines, fuel burn rates and emission indices. These default databases rely on external data providers, assuring the quality of the information provided. The user of the system is responsible to assure that the relation between those default databases is representative for the specific study purpose. This default system information is combined with dynamic input data, represented by the air traffic flight profiles.

Flight tracks were superposed over geographical data using the ArcView GIS package. Further analysis has been performed using standard spreadsheet and database software such as MS Excel and MS Access.

4.1.1 AEM3 Fuel burn calculation

4.1.1.1 Calculations for operation below 3000ft

Below 3000 ft, the fuel burn calculation is based on the Landing and Take-Off Cycle (LTO) defined by the ICAO Engine Certification specifications. ICAO LTO covers four engine operation modes, which are used to model the following six phases of aircraft operations in AEM3:

- Taxi-Out,
- Take-Off,
- Climb-Out,
- Approach,
- Landing,
- Taxi-In.

Landing is considered as an Approach phase (and thus uses Approach fuel flow and emission indices) which lasts for the same duration as the Take-Off phase.

The *ICAO Engine Exhaust Emissions Data Bank* [Ref 21] includes emission indices and fuel flow for a very large number of aircraft engines. AEM3 links each aircraft appearing in the input traffic sample to one of the engines in the *ICAO Engine Exhaust Emissions Data Bank*.

The standard LTO cycle can be added to all input flight profiles, even when real data for those operations is available. The application of the ICAO LTO cycle is common practice in aviation emission estimation and assures complete information for all profiles during those phases of flight.

4.1.1.2 Calculations for operation above 3000ft

Above 3000 ft, fuel burn calculation is based on the "Base of Aircraft Data" (BADA). This database provides altitude and attitude dependent performance and fuel burn data for more than 150 aircraft types. The version 3.5, used with AEM3 for this study, covers nearly 90 % of the aircraft types that make up the European air traffic. BADA is developed and maintained by the EUROCONTROL Experimental Centre.

AEM3 links each aircraft performing one of the input flight profiles to the BADA fuel burn data. Where no data for a specific aircraft type is available, representative aircraft types are used to create the most realistic indirect link; e.g. the A319 is the reference aircraft for the A319 and A318, etc.

4.1.2 AEM3 Emissions calculation

4.1.2.1 Calculations for operation below 3000ft

Below 3000 ft, the emission calculation is based on the *ICAO Engine Exhaust Emissions Data Bank* [Ref 21].

4.1.2.2 Calculations for operation above 3000ft

Above 3000 ft, the emission calculation is also based on the *ICAO Engine Exhaust Emissions Data Bank*, but emission factors and fuel flow are adapted to the atmospheric conditions at altitude using a method initially developed by The Boeing Company (The Boeing Method 2 – BM2) and subsequently modified by the EUROCONTROL Experimental Centre Business Unit for Environmental Studies (EEC-BM2) (see Annex 1 "Boeing method 2 – EUROCONTROL Modified"). In this way, emissions for the pollutants NO_x, HC and CO can be estimated for the entire flight operation.

The emissions for the pollutants H_2O and CO_2 are direct results of the oxidation process of carbon and the hydrogen contained in the fuel with the oxygen contained in the atmosphere. SO_x emissions depend directly on the sulphur content of the fuel used. All three are directly proportionally to the fuel burn, and can thus be calculated directly from fuel burn estimates.

An understanding of fuel composition is vital for determining the proportional coefficients between fuel burn and emissions. The constants used in AEM3 during this study are presented below.

Pollutant	Coefficient
CO_2	3.149 kg / kg Fuel
H_2O	1.230 kg / kg Fuel
SO_2	0.00084 kg / kg Fuel

Table 2: Coefficients for emissions calculation – CO_2, H_2O, SO_2

These are average values obtained from an intensive literature review [Ref 22] at the EUROCONTROL Experimental Centre Business Unit Environmental Studies.

Volatile Organic Compounds (VOC) and Total Organic Gases (TOG) emissions are estimated using a method developed by the U.S. Environmental Protection Agency (U.S. EPA). These are estimated in proportion to the HC emissions. Many individual organic gas emissions (e.g. benzene) are directly estimated from VOC and TOG value. The constants used in AEM3 during this study are presented below.

Pollutant	Coefficient
VOC = HC × 1.0947 VOC/HC correction factor	
acetaldehyde	VOC × 0.0519 acetaldehyde / VOC correction factor
Acrolein	VOC × 0.0253 acrolein / VOC correction factor
POM as16-PAH	VOC × 1.166E-4 16-PAH / VOC correction factor
POM as 7-PAH	VOC × 1.049E-6 7-PAH / VOC correction factor
Styrene	VOC × 0.0044 styrene / VOC correction factor
TOG = VOC × 1.1167 TOG/VOC conversion factor	
1,3-butadiene	TOG × 0.0180 1,3-butadiene fraction
benzene	TOG × 0.0194 benzene fraction
ethylbenzene	TOG × 0.0017 ethylbenzene fraction
formaldehyde	TOG × 0.1501 formaldehyde fraction
propionaldehyde	TOG × 0.0095 propionaldehyde fraction
toluene	TOG × 0.0052 toluene fraction
xylene	TOG × 0.0048 xylene fraction

Table 3: Coefficients for emissions calculation – VOC, TOG

Note that emission calculations presented above are applicable for kerosene combustion only. Emission calculations for cryogenic engines are based on parametric values from literature.

4.1.3 AEM3 fuel burn and emissions calculations : Summary

The following graphic indicates in a simplified way the different approaches applied in AEM3 to obtain the most realistic fuel burn and emission estimations for all phases of each flight profile.

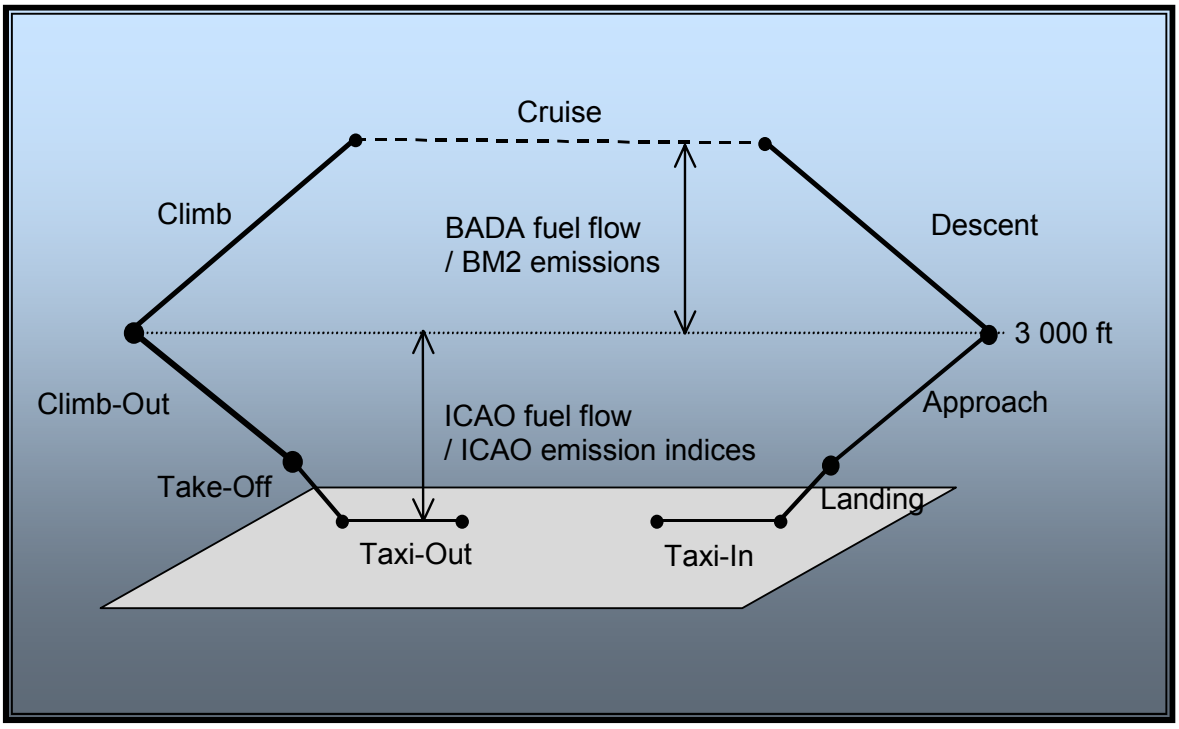

Figure 7: The AEM3 calculation cycle

4.1.4 The AEM3 4D – Analysis Window

The most widely separated geographical coordinates (min and max altitude, longitude, latitude), and the time limits given by the traffic and flight files, automatically define the 4D analysis window inside which fuel burn and emissions from aircraft operation are calculated. Nevertheless, AEM3 also provides the possibility to overwrite those values and to manually define the 3D airspace block and the start / end times a user wishes the system to use. Moreover, to overcome the potential limitations of such a rectangular analysis window, AEM3 allows the user to "cut" its output data into a geographical area defined by an irregular polygon.

Intentionally left blank

5 DEVELOPMENT OF ANALYSIS PLAN

This study investigates and compares the potential environmental impact of future engine technologies:

- Current combustion technology,
- Hydrogen technology.

5.1 Data sources

60 traffic days of 2004 CPR data from an earlier emission project (contrail project, see section 7.3.3 and [Ref 10]) were available for this study. The study was based on days showing atmospheric conditions with high and low contrails formation identified by Earth Observation Satellites. From these 60 days, two days per month from January to October 2004 (i.e. 20 days) were selected as presented in Table 4 below.

Month	High Contrails Day	Low Contrails Day
Jan	20 Jan	10 Jan
Feb	11 Feb	26 Feb
Mar	18 Mar	08 Mar
Apr	29 Apr	22 Apr
May	28 May	17 May
Jun	01 Jun	22 Jun
Jul	24 Jul	01 Jul
Aug	31 Aug	01 Aug
Sep	17 Sep	11 Sep
Oct	03 Oct	18 Oct

Table 4: Days of traffic selected for the study

5.2 Geographical footprint

During the contrail project, the initial CPR data set was reduced as follows:

- Longitude: 10W-20E
- Latitude: 40N-60N
- FL: >FL240 (altitude corresponding to contrail formation)

The current study does not address contrail formation only. Emissions produced at flight levels below FL240 have to be assessed. Therefore, it is necessary to use the complete set of CPR data and not only a reduced subset above FL240.

For consistency reasons the same geographical region of interest as for the Contrails project is chosen for the current study : 40N – 60N and 10W – 20E.

Contrail maps for new technology engines will thus be easily and directly comparable with maps produced during the contrail project.

5.3 Scenarios

The base idea of the study is to compare the current (i.e. 2004) situation, in terms of emissions and impact on contrails formation, with the same traffic performed with new technologically improved engines.

As the focus is on technological improvement, traffic growth is not considered in the current study. Neither is the airport capacity increase considered.

5.3.1 Scenario 'Baseline': The CONTRAIL movements

For the selected days the contrail maps were already produced.

Nevertheless the calculation of fuel burn and emissions below FL240 had to be done. AEM3 thus had to be executed for all days under study.

It was assumed that flight completion in AEM3 was not necessary. Indeed:

- The study consists of a comparison between scenarios; no absolute figure is required.
- Added portions of flights would be identical in all the scenarios.
- One emphasis of the study is the formation of contrails, which occurs at high altitudes. The situation at low altitude is out of the scope of the study.

5.3.2 Scenario 'Kerosene' (2028K & 2050K): Current combustion technology but improved

Airbus Global Market Forecast (Airbus GMF) 1999 ([Ref 2]), reports an average replacement of aircraft after 24 years of operation[7]. As a result, this means that the 2004 fleet will be totally replaced by the year 2028. The current study thus estimates the situation in 2028 (scenario 2028K). A scenario for 2050 (scenario 2050K) is also considered to fit with a probable timescale for hydrogen aircraft fleet development (see section 2.5).

IPCC ([Ref 3]) reports a yearly average of 1-2% improvement in aircraft fuel efficiency of new production aircraft since the dawn of the jet age. Examined over several decades, these improvements represent a relatively steady and continuous rate of improvement. IPCC assumes a similar trend when fuel efficiency improvements are projected forward to 2050. If the conservative value of 1% per year is considered, this means that 2028's aircraft should burn about 21.4% less fuel for the same mission as today's (2004) aircraft, while 37.0% less fuel would be burnt in 2050.

In parallel a method was developed at EEC in 2000 based on a formula allowing a parametric estimation of fuel efficiency. Even if confirmed by GIFAS ([Ref 5]) findings, results from this methodology are pessimistic when compared to the IPCC estimation.

As a consequence, both methods were used during the study (scenarios 2028K and 2050K).

[7] This estimation dates from 1999. As the duration of aircraft life tends to get longer (especially for freight aircraft), the average life may be slightly higher in 2004. Even if confirmed, the actual averaged aircraft replacement age would not change results of the study fundamentally.

Percentages of emission evolution were available in the literature. The estimation of fuel burn and emissions were hence deduced from baseline results.

It has to be underlined that, in spite of technological improvements, future flight profiles are considered as identical to actual 2004 CPR profiles.

The increase of propulsion efficiency due to future technological improvements may lead to the formation of more contrails since temperatures of gases exhausted out of engines will evolve. Contrail maps were thus produced for each day of 2028 (i.e. when all 2004's fleet will be replaced) and for each day of 2050 and compared with 2004 maps.

5.3.3 Scenario 'Hydrogen' (2050H): Use of Hydrogen technology

The study considers an extreme case scenario: the entire fleet powered by hydrogen engines. As detailed in section 2.5, it is not realistic to expect such a fleet before 2050.

Formulae relating energy output to fuel burn/hydrogen burn and emissions are available in the literature (see details in section 5.6). These formulae were used to estimate fuel burn/hydrogen burn and emissions exhausted by hydrogen engines, based on 2004 fuel burn.

The adaptation of the contrail algorithm (especially engine propulsion efficiency) for such hydrogen engines was developed in this study (see section 7.3.6). The output is a set of contrail maps to be compared with the 2004 situation. A comparison between scenario 2050K and 2050H is of interest since both indicate the situation at the same date (2050), with two different options depending on the effort put into engine technology improvement.

5.4 Estimation of fuel burn

Improvements to the fleet's fuel efficiency for existing aircraft (through modifications or in-life upgrades) are difficult to predict. Indeed fuel efficiency enhancement is not only the result of engines technology improvement. Aircraft aerodynamic properties, structure lightening, or system evolutions are also involved.

A technology improvement curve was developed at EUROCONTROL based on engine manufacturer's fuel efficiency data between 1958 and 1997 (Figure 8). Note that the calculation is based on current kerosene. Fuel consumption and emissions if synthetic kerosene is used are not assessed in this study[8].

[8] Emissions are highly dependent on fuel composition and especially hydrogen and sulphur content. Oil source and refining process for synthetic kerosene may lead to a slightly different composition, thus influencing actual emissions.

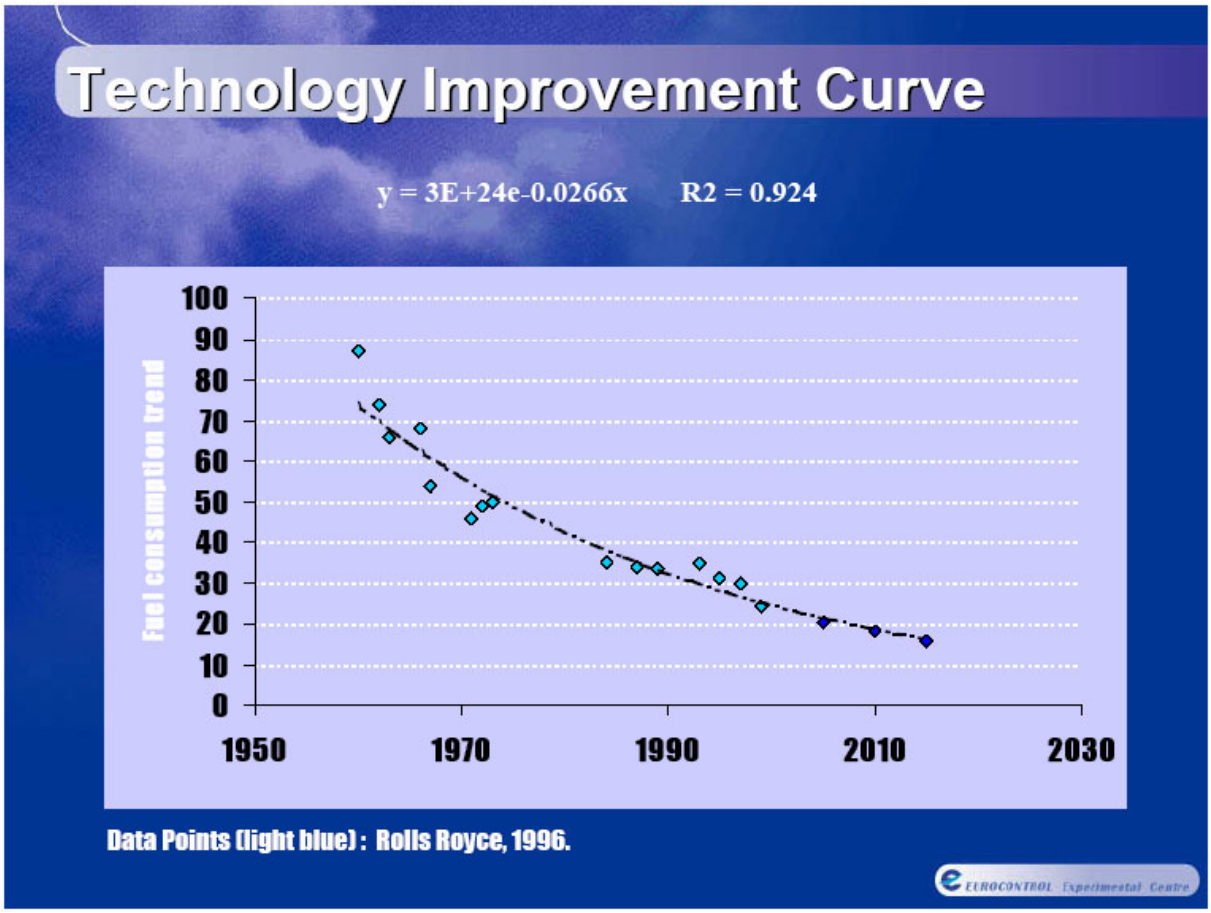

Figure 8: Technology Improvement Curve

The best equation to represent historical values of yearly technological improvement was established to be the following:

$$Fuel\ Efficiency\ (\%) = (3E + 24) \times e^{-0.0266 \times Year}$$

An extrapolation of the technology improvement curve using the previous equation gives the following results:

Year	Fuel efficiency improvement for replaced traffic
2028	+10.01%
2050	+14.97%

Table 5: Fuel efficiency improvement in 2028 and 2050 as compared to 2004

As stated earlier, the entire fleet of the 2004 traffic sample is considered as completely renewed by 2028. The same is true between 2028 and 2050. Fleet change thus does not have to be broken down year by year to obtain state of the art in 2028.

As a result, based on the values found from the trend line, fuel burn in 2028 is thus expected to be 10.0% lower than 2004 fuel burn while the reduction by 2050 should be 15.0% lower.

The evolution of the EUROCONTROL's technology improvement curve is in accord with the following statement from GIFAS ENVIRONMENT GROUP ([Ref 5]): "*Present and future actions will go on bringing significant gains [in term of environmental benefits] but future improvements will be reduced regarding achievements obtained during the last 40 years."* Nevertheless fuel efficiencies estimated with the EUROCONTROL methodology are pessimistic regarding most of the forecasts available in the literature. For instance, Aero2K project ([Ref 4]) forecasts 19% reduction in fuel burn by 2025 while ACARE targets indicate a reduction of fuel burn by 50% between 2000 and 2020.

Indeed historically, improvements for new production aircraft have globally averaged 1-2% per year in fuel efficiency. The conservative value of 1% a year is used as basis for most fuel burn forecasts. Therefore, a constant global improvement value of around 1% per year based on averaged improvements is considered feasible in the framework of this study.

Hence, two scenarios are considered in this study:

- Scenario α (alpha): Use of EUROCONTROL's technology improvement curve.
- Scenario β (beta): 1% improvement a year in fuel efficiency.

NO_x, CO and HC estimates in this study do not depend directly on the scenario (α or β):

As NO_x, CO and HC emissions are not directly proportional to fuel burn, the variation of NO_x, CO and HC estimations for scenarios α & β is not considered in this study. However, a better fuel efficiency would actually lead to a reduced emissions level.

As detailed in section 5.5, NO_x, CO and HC estimations rely on the Aero2k project, which considers 19% fuel burn reduction between 2002 and 2025. This value enters the current study range (scenario α – 10% reduction in 24 years and scenario β – 21.4% in the same timeframe). Estimations of NO_x, CO and HC are thus assumed as valid for both scenarios α and β.

5.5 Estimation of emissions for kerosene engines

During the combustion of kerosene in conventional engines, carbon dioxide (CO_2) and water (H_2O) are produced. Additionally lesser amounts of sulphur oxides (SO_x), carbon monoxide (CO), nitrogen oxide (NO_x) and unused hydrocarbons (HC) are also emitted, as detailed in section 3 ("Specification of study goals"). The last three substances are considered to be greenhouse gases.

CO_2, H_2O and SO_x emissions are proportional to fuel burn. NO_x, CO and HC emissions are difficult to quantify precisely in the medium/long term since they are based on hypothetical future technological improvements.

5.5.1 Trade-off to reduce emissions

At least conceptually the reduction of CO, HC and smoke is straightforward: the combustion should be prolonged for as long as possible at high temperature in the presence of ample excess oxygen. This also has the effect of increasing the combustion efficiency.

The problem of reducing NO_x is more subtle. NO_x is formed in chemical reactions, which are much slower than those leading to the formation of CO_2 and H_2O, but the rate of formation of NO_x increases rapidly with temperature. Because of the comparatively slow rate of formation of NO_x, the amount created depends on both the temperature and the residence time at that temperature. Unfortunately the long residence time that would reduce CO, HC and smoke would therefore favour the formation of NO_x. Any subsequent breakdown of NO_x is much slower.

The standard approach to reducing NO_x is to reduce the residence time as much as possible, keeping in mind both the other pollutants and the need to keep an acceptable level of combustion efficiency at high altitude and low fuel flow rate. The very hot gases are then rapidly quenched to drop the temperature below that at which the NO_x formation is significant. This has led to a reduction in the size of the combustor in relation to the flow rates of air and fuel.

The strong dependence of NO_x formation on temperature means that there is a tendency for the level to increase as the temperature entering the combustor increases. In other words, as the design pressure ratio for the engines increases it gets more difficult to maintain low levels of NO_x. It is not surprising that raising the turbine inlet temperature also makes it harder to maintain low levels of NO_x.

The requirement to keep NO_x low at high thrust (a short residence time at high temperature) and to keep CO and HC low at low thrust (a long residence time) are fundamentally contradictory.

5.5.2 Emission reduction trends in the last decades

Greater progress has already been made with some individual pollutants than with others, as stated by the FAA in the document "aviation & emissions – A primer" ([Ref 1]).

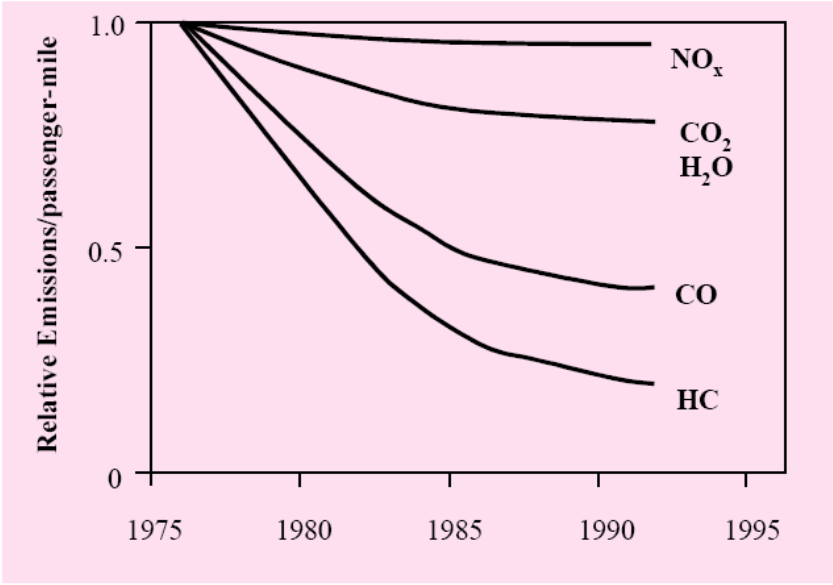

Aircraft emissions of all species have declined over time, however, considerably more progress has been made with HC and CO than with NO_x.

Figure 9: Historical evolution in aircraft pollutant emissions – Source FAA [Ref 1]

NO_x has proven to be the most difficult pollutant to control and may thus lead to great improvement in the future. In contrast, a great deal of progress was obtained since the 70's in reducing emissions of CO and HC (by 50% to 80%), leading to a mature technology. This results in the forecast that percentages of CO and HC reduction in the next decades will probably be lower than past reductions. Nevertheless, CO and HC emissions are expected to be indirectly reduced through the increase in fuel efficiency.

5.5.3 NO_x

IPCC ([Ref 3]) forecasts that average NO_x emissions of production aircraft will be 30-50% below the current CAEP/2 NO_x limit by 2020 and 50-70% below the current CAEP/2 limit by 2050 if emphasis is put on greater NO_x reduction. Lesser NO_x reduction can be expected if future aircraft and engine designs consider both improved fuel efficiency and NO_x reduction.

ACARE (Advisory Council for Aviation Research in Europe) environmental targets expect a reduction of 80% of NO_x emissions by 2020 for standard aircraft compared to operating conditions in 2000.

Other figures were found in the literature. However it appeared that the objectives are most of the time directly issued from the targets defined by the European Commission under the ACARE project. It was not possible to estimate if those objectives were likely to be met due to the duration of the time course (24 years).

Such general trends are not precise enough to directly quantify future emissions.

Based on an in-depth study of worldwide traffic in year 2002, and on future emission prediction methodologies, the Aero2K project[9] ([Ref 4]) estimates that the amount of NO_x burnt by 2025 will be 38% lower than 2002 NO_x emissions without considering traffic growth. NO_x emissions saved as a consequence of fuel efficiency increases are included in this figure.

Regarding imprecision in NO_x emissions estimation within the medium term, this value is assumed as valid to estimate NO_x in 2028 in the framework of this project in spite of a slight discrepancy in the dates (2002-2025 instead of 2004-2028). Aero2k results are valid for an average to high growth scenario with particularly successful embodiment of NO_x reduction technology in new aircraft over the period.

Concerning 2050, very little information is available since long term technical evolution is particularly difficult to predict. As stated above, CAEP/2 evaluates a gain of 20% NO_x between 2020 and 2050. If considering a constant evolution, NO_x reduction between 2028 and 2050 will then be around 14.7%.

A study conducted by GIFAS environmental group ([Ref 5]) predicts 10 to 15% NO_x reduction between 2020 and 2050, which corresponds to 7.3 to 11% between 2028 and 2050.

The two extreme values (7.3% and 14.7% NO_x reduction between 2028 and 2050) are considered in the study.

[9] Global aviation emissions inventory for 2002 and forecast of emissions for the year 2025

5.5.4 CO and HC

Based on the historical evolution reported by Airbus, CO and HC evolution trends were obtained as plotted in Figure 10.

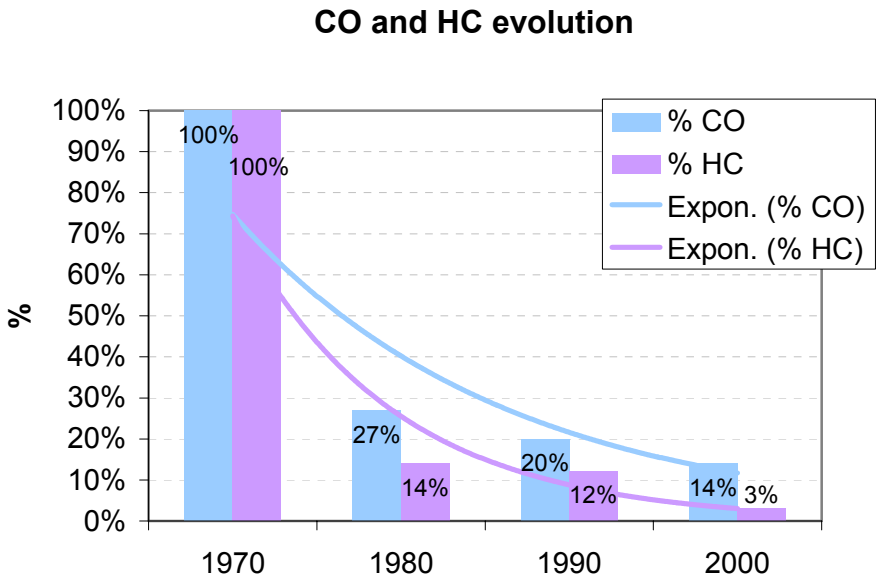

Figure 10: CO and HC evolution based on standard ICAO LTO cycle – source Airbus [Ref 6]

As large improvements in CO and HC emissions were made in the last decade, an extrapolation to medium term scenarios leads to 0 CO and HC emitted. This indicates that such an extrapolation is not accurate for these pollutants and confirms that future technical progress may not be as important as past improvement in this field.

Once again, the Aero2K project's estimations had to be used in this project, even if based on a comparison of 2002 and 2025. An average of 12% CO and HC reduction is thus used for 2028.

No sufficiently accurate information was found to forecast CO and HC emissions in 2050. The 2050 scenario thus concentrates on NO_x, fuel burn and related pollutants only.

5.5.5 Fuel burn and emissions of kerosene engines – summary

Table 6 summarises fuel burn and emission applicable to kerosene engines.

To enrich the current study, an estimation of fuel burn and NO_x in 2015 was assessed, since 2015 was studied during the ANCAT/EC2 emissions inventory and forecast ([Ref 8]). The methodologies used to determine percentages of fuel burn and NO_x reduction are detailed in Annex 2.

	Fuel burn and related pollutants		NO_x	CO	HC
	Scenario α	Scenario β			
2004	100%	100%	100%	100%	100%
2015	98.4%	89.5%	84%	n/a	n/a
2028	90.0%	78.6%	62%	88%	88%
2050	85.0%	63.0%	52.9 to 57.5%[10]	n/a	n/a

Table 6: Fuel burn and emissions of kerosene engines

5.6 Estimation of fuel burn and emissions for hydrogen engines

As 0.36kg of hydrogen offers the identical energy content as 1kg of kerosene (see section 2.3.1), the mass of hydrogen burnt represents 0.36 times the quantity of kerosene burnt for the same route in 2004.

The only two emissions produced by hydrogen engines are water vapour and NO_x.

5.6.1 Water vapour

Emission of water vapour due to hydrogen engines is estimated in literature as 2.6 times higher than emissions due to kerosene engines. Indeed, 0.36kg of hydrogen contains as much energy as one kg of kerosene but generates 3.21kg of water vapour instead of 1.23kg for a kerosene engine. The value of '2.6 times kerosene's emission' appears in many documents from different sources (among which [Ref 27], [Ref 28] and [Ref 31]) and is thus assumed to represent an average value.

Although not a problem at ground level, water vapour at high altitude (above 10km) is a greenhouse gas. The harmful effects of water vapour emissions can thus be reduced significantly by lowering the flight altitude. If the effects on climate change are estimated to be too important, hydrogen aircraft may be re-routed to altitudes lower than 10km. The downside of this is slightly higher drag and an increase in fuel consumption.

[10] 7.3 to 14.7% reduction between 2028 and 2050

Water vapour is also responsible for the formation of contrails, which may then influence the development of cirrus clouds. In the case of hydrogen propulsion, no particles are emitted. Contrails are only constituted by ice crystals formed in the atmosphere. This phenomenon is detailed in this study.

5.6.2 NO_x

The estimation of NO_x from hydrogen engines is not as well defined as for H_2O emissions. It is strongly dependant on technological trade-offs to be decided.

Indeed the high temperature inherent in jet-type combustion causes the production of copious amounts of nitrogen-oxides. Various techniques are employed to avoid the high temperatures but unfortunately NO_x production is not completely avoidable. The amount of NO_x is controllable to a great extent with fuel injection.

Combustion chambers with pre-mixing seem to be the best solution: the homogenous fuel-air-mixture guarantees an even combustion. During trials at MTU in Munich, the use of a so called "Premixing Perforated Plate" reduced nitrogen emissions by 95% when compared with a modern kerosene turbofan. However, putting this idea into practice has its pitfalls. Extreme lean or rich mixtures can cause self-ignition during premixing or a backlash from the combustion chamber into the pipes, in which the premixing is taking place.

Along with the conventional option of using a combustion chamber without premixing there is still the so-called Micromix procedure, which was initially developed at the Technical University in Aachen. Premixing is not required with this procedure. The big combustion chamber is replaced with many small ones, thus controlling inhomogeneous mixtures.

As detailed in Cryoplane project ([Ref 9]), three "generations" of Micromix hydrogen combustors were developed and tested. For the most advanced Micromix combustor of the third generation, a 77.6% NO_x reduction was measured during tests at full shaft power of the load compressor and zero generator power, compared with kerosene operation. Using this result, Cryoplane's team made a theoretical assessment of NO_x emission reductions by application of the Micromix hydrogen combustion principle to eight different typical aircraft main engines. For the selected set of gas turbines, an average NO_x emission reduction of about 75% was calculated as compared to an engine running on kerosene, for aircraft categories in commercial operation (from business jets to very large long range aircraft such as A380).

This value is used in the current study to estimate NO_x emissions in 2050. NO_x reduction expected if pre-mixing combustion chambers are used is also indicated even if this technology is not completely mastered today.

As a result, percentages used for the study for 2050 as compared to the 2004 situation are the following:

- Hydrogen fuel burn (by mass): 36%
- H_2O emissions: 260%
- NO_x emissions: 5 to 25%
- Other emissions: 0%

Noise measurements showed that the noise level of the hydrogen combustor is approximately at the same level as the kerosene engine, so no striking improvement in terms of noise is foreseen with the use of hydrogen engines.

Intentionally left blank

6 INPUT DATA COLLECTION

6.1 Data preparation

The data was consistent and without error and thus required very little preparation and formatting before AEM3 execution.

6.2 Number of flights

A total of 387,457 flights over 20 traffic days were available for the study. A number of flights were deleted during data preparation:

- One flight was deleted because its departure airport was not identifiable.
- 231 other flights operated by unidentified aircraft types were ignored. This deletion concerns 0.06% of the traffic.
- 286 flights constituted by one single flight point were not exploitable.
- As a result of the geographical limitation of the traffic for this study, 10,691 flights (2.76% of the traffic) not entering the study geographical area were ignored.
- Flights lasting less than 10 minutes in the study geographical area were also ignored in order to keep a representative data set.

As a result, 372,198 realistic flight profiles were used for the study, as detailed in Table 7 below, corresponding to more than 96% of the initial traffic. An average of 18,600 flights per traffic day can be considered as a statistically reliable data set.

Date	In the initial data set	Unknown aircraft	Unknown airport	Single point flights	Outside of study geographical area	Lasting less than 10 minutes in the study geographical area	Remaining number of flights for the study
20040110	13646	-5		-7	-375	-110	13149
20040120	17622	-11		-10	-449	-229	16923
20040211	17366	-12		-13	-496	-198	16647
20040226	18077	-14		-14	-494	-177	17378
20040308	17911	-5		-10	-506	-237	17153
20040318	18696	-8		-14	-543	-202	17929
20040422	19724	-17		-10	-525	-229	18943
20040429	19341	-23		-20	-605	-208	18485
20040517	20011	-15		-23	-455	-184	19334
20040528	22156	-27		-18	-601	-245	21265
20040601	20421	-5		-21	-575	-192	19628
20040622	20984	-10		-12	-579	-203	20180
20040701	21628	-14		-12	-627	-227	20748
20040724	19005	-8		-21	-467	-180	18329
20040801	19313	-10		-11	-571	-168	18553
20040831	21872	-10	-1	-21	-600	-261	20979
20040911	18424	-4		-9	-460	-159	17792
20040917	22590	-11		-19	-700	-195	21665
20041003	18298	-10		-6	-555	-172	17555
20041018	20372	-12		-15	-508	-274	19563
Total	**387457**	**-231**	**-1**	**-286**	**-10691**	**-4050**	**372198**
Percentage of initial traffic	**100%**	**-0.06%**	**0.00%**	**-0.07%**	**-2.76%**	**-1.05%**	**96.06%**

Table 7: Number of flights available and deleted for the study

7 OUTPUT DATA ANALYSIS AND RESULTS

A direct comparison of the absolute amount of emissions in 2004, 2028 and 2050 would not make any sense in this study since future figures are directly deduced from the 2004 traffic scenario. This section will thus concentrate on the relative evolution of the different pollutants over the time period.

Nevertheless, Table 8 presents the amount of pollutant for the whole traffic sample, and averaged per flight.

Total traffic sample		Fuel		NO_x		CO	HC	H_2O	
		fuel scenario α	fuel scenario β	Low	High			fuel scenario α	fuel scenario β
Kerosene	2004	1,024,265,810		11,582,240		7,528,541	743,054	1,259,846,946	
	2015	1,009,926,088	917,064,362	9,729,081				1,242,209,089	1,127,989,165
	2028	921,839,229	804,743,257	7,180,989		6,625,116	653,887	1,133,862,251	989,834,206
	2050	870,625,938	645,106,812	6,127,005	6,659,788			1,070,869,904	793,481,378
Hydrogen	2050	368,735,692		579,112	2,895,560	0	0	3,275,602,060	

Average per flight		Fuel		NO_x		CO	HC	H_2O	
		fuel scenario α	fuel scenario β	Low	High			fuel scenario α	Fuel scenario β
Kerosene	2004	2752		31.1		20.2	2.0	3385	
	2015	2713	2464	26.1				3337	3031
	2028	2477	2162	19.3		17.8	1.8	3046	2659
	2050	2339	1733	16.5	17.9			2877	2132
Hydrogen	2050	991		1.6	7.8	0	0	8801	

Table 8: Summary of fuel burn and emissions obtained in the study (in kg)

For more readability, CO_2 and SO_x emissions are not presented above. They are proportional to fuel burn for kerosene engines and equal to zero for hydrogen engines. The same is true for VOC and TOG, which are proportional to HC for kerosene engines.

7.1 Evolution of fuel burn and emissions from 2004 to 2050

The evolution of fuel burn, H_2O and NO_x estimated for the next decades is presented in Figure 11 to Figure 13. Values appearing on the plot correspond to average value per flight. On each figure, the amount of fuel/emissions for a hydrogen engine is plotted to provide a visual comparison.

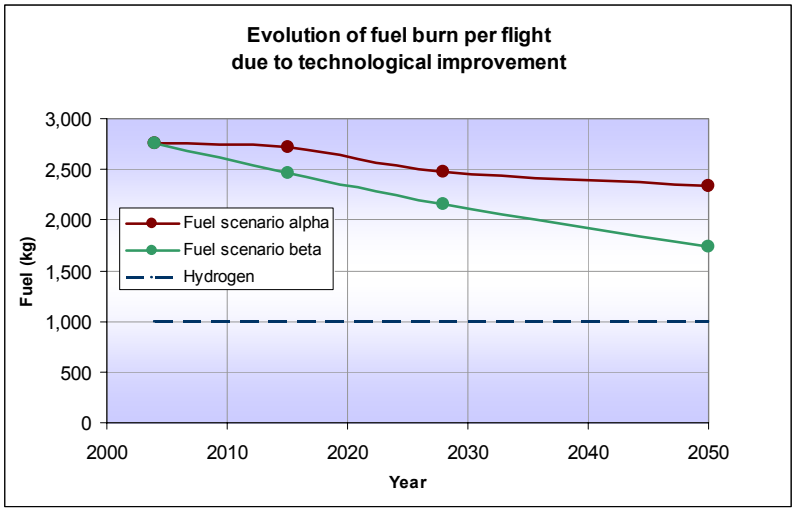

Figure 11: Evolution of fuel burn due to technological improvement

Depending on the methodology used to estimate future fuel burn, there is a wide range of values in the long term. The actual fuel burn in the future will probably lie between the green and red curve plotted above.

It must be kept in mind that the value corresponding to the hydrogen engine on Figure 11 does not reflect a technological improvement in fuel efficiency but an intrinsic physical property of hydrogen (i.e. weight). This plot can thus not be compared with any fuel cost decrease.

Similarly the airframe improvements and drag are not taken into account in this section.

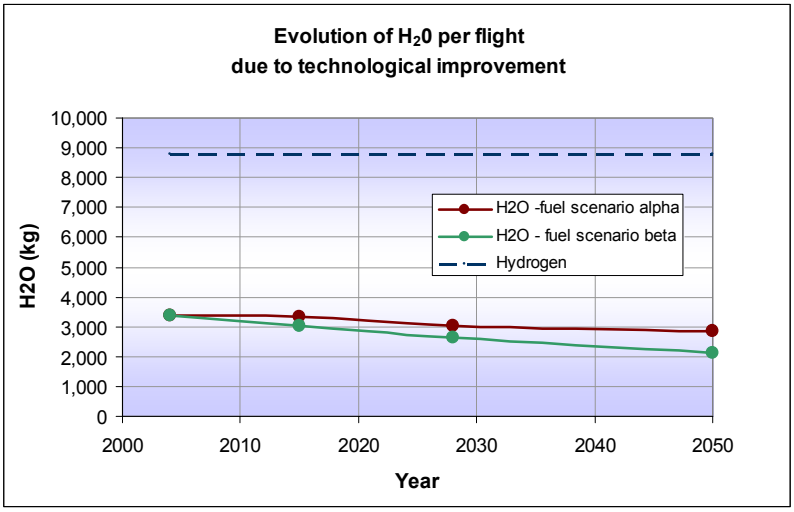

Figure 12: Evolution of H_2O due to technological improvement

As anticipated, the amount of H_20 emitted by kerosene engines is much lower than the emissions hydrogen engines would produce. The impact of this concern is assessed in section 7.3 dedicated to contrails formation.

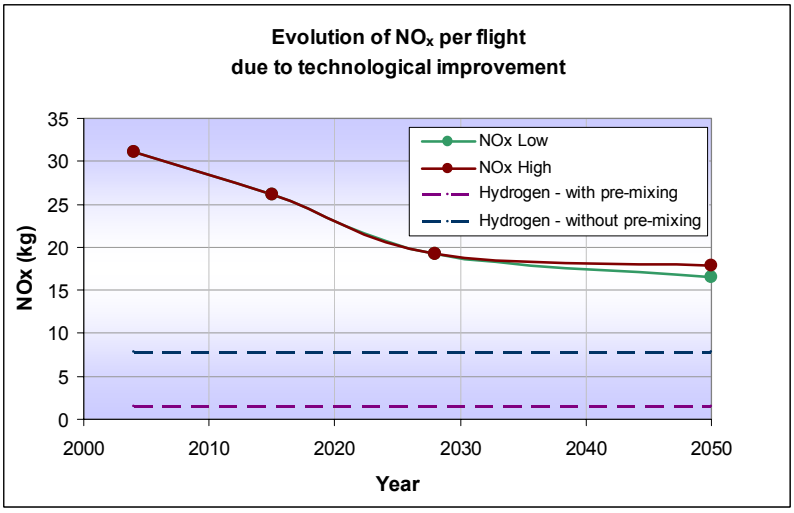

Figure 13: Evolution of NO_x due to technological improvement

If technological improvements follow the forecasts, kerosene engine technology would not become comparable to hydrogen technology in terms of the amount of NO_x emitted between 2040 and 2045. Nevertheless, if concentrating on NO_x only, improvements also have to be made on hydrogen engines (especially on control of pre-mixing engines) to obtain significantly low emissions and justify the migration toward hydrogen technology.

7.2 Extrapolation of emissions from 2004 to 2050

The aim of this section is to give a rough estimation of emissions due to aviation until the total conversion of fleet to hydrogen. It has to be kept in mind that fossil fuel stocks may become scarce or exhausted before 2050.

The following statements are considered:

- Introduction of the first hydrogen aircraft in 2015,
- Replacement of the last kerosene aircraft in 2050 (see section 2.5 "Timescale"),
- Aircraft are replaced at the same rate during all the period and without regard to their category and size,
- CO and HC values for kerosene aircraft after 2028 are extrapolated from the evolution between 2004 and 2028,
- Technological improvement for kerosene engines is considered.

Results are presented for one day of traffic in the geographical zone used for this study, i.e. 18610 flights or portion of flight on average.

"Do nothing scenario" graphics are included to indicate the situation if no hydrogen aircraft are introduced before 2050.

7.2.1 Visualisation of improvement due to technology

Figure 14 to Figure 17 give an indication of future emissions if hydrogen technology is adopted from 2015 (left-hand plots) and if only kerosene aircraft are used in the future (right-hand plots). The plots have to be read as "cumulative" curves. For example, on Figure 14, blue + firebrick areas correspond to the total NO_x emitted. This quantity is divided into kerosene contribution (blue areas) and hydrogen contribution (firebrick areas). Figure 14 to Figure 17 reflect technological enhancements only.

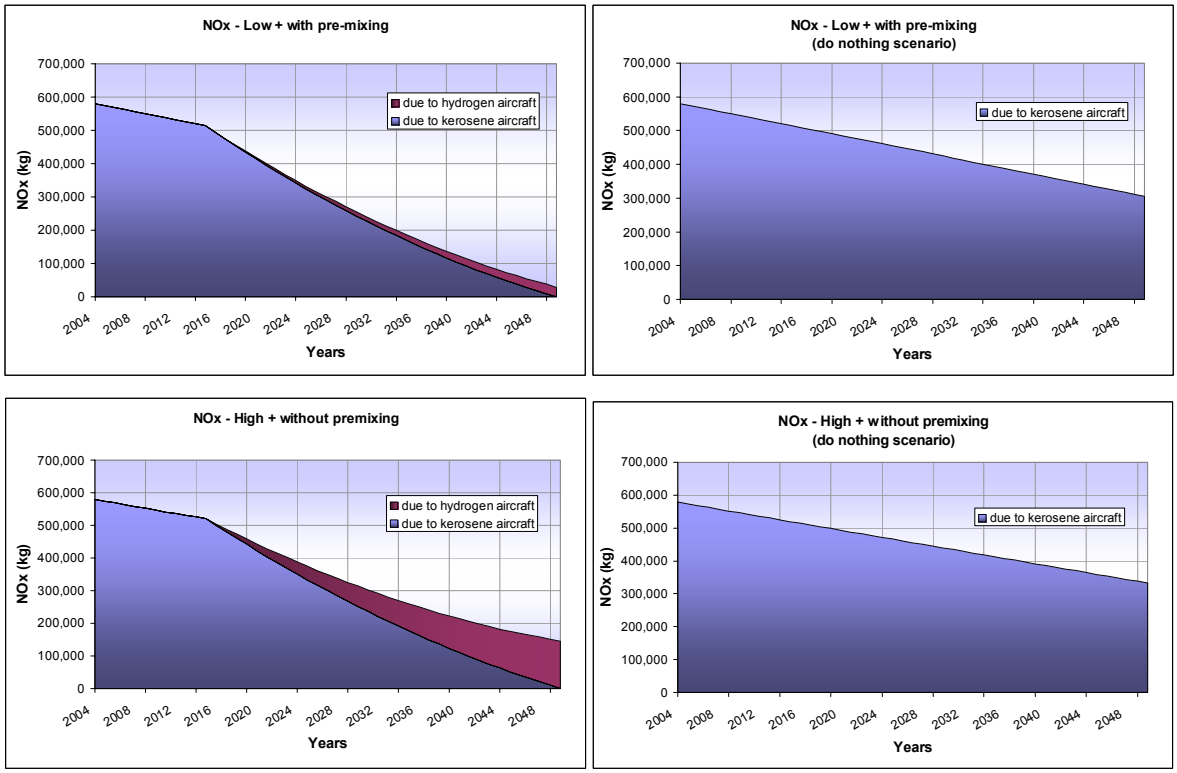

Figure 14: Total amount of NO_x emitted per day

Two scenarios are plotted on Figure 14, corresponding to two extreme configurations:

- Low estimation of NO_x for kerosene engines and pre-mixing technology used for hydrogen engines,
- High estimation of NO_x for kerosene engines and no pre-mixing technology used for hydrogen engines.

Whichever estimation is the closest to reality, a great reduction of NO_x emissions per engine is expected. Nevertheless upcoming kerosene engines are expected to be twice less efficient in term of NO_x emission than hydrogen engines by the year 2050.

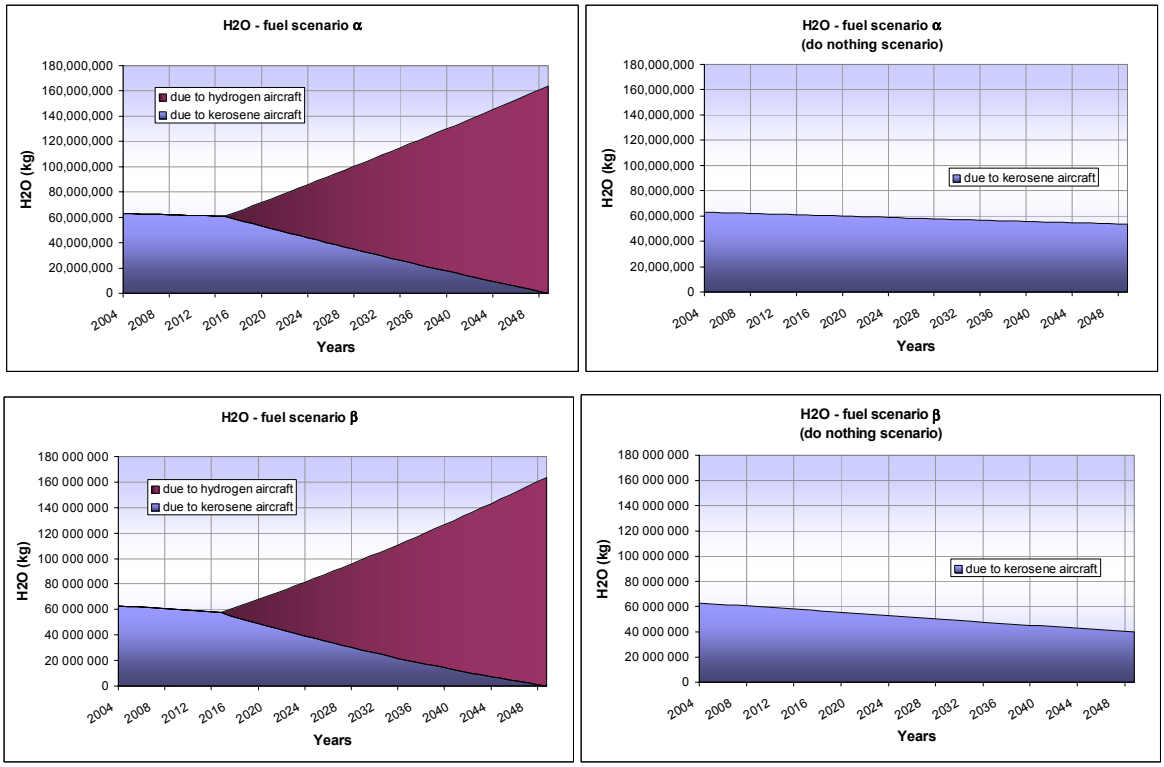

Figure 15: Total amount of H_2O emitted per day

Figure 15 gives an estimation of the level of H_2O emitted, depending on the scenario used for the estimation of fuel burn. The introduction of hydrogen aircraft would clearly lead to a rapid growth of H_2O emissions once hydrogen aircraft enter service.

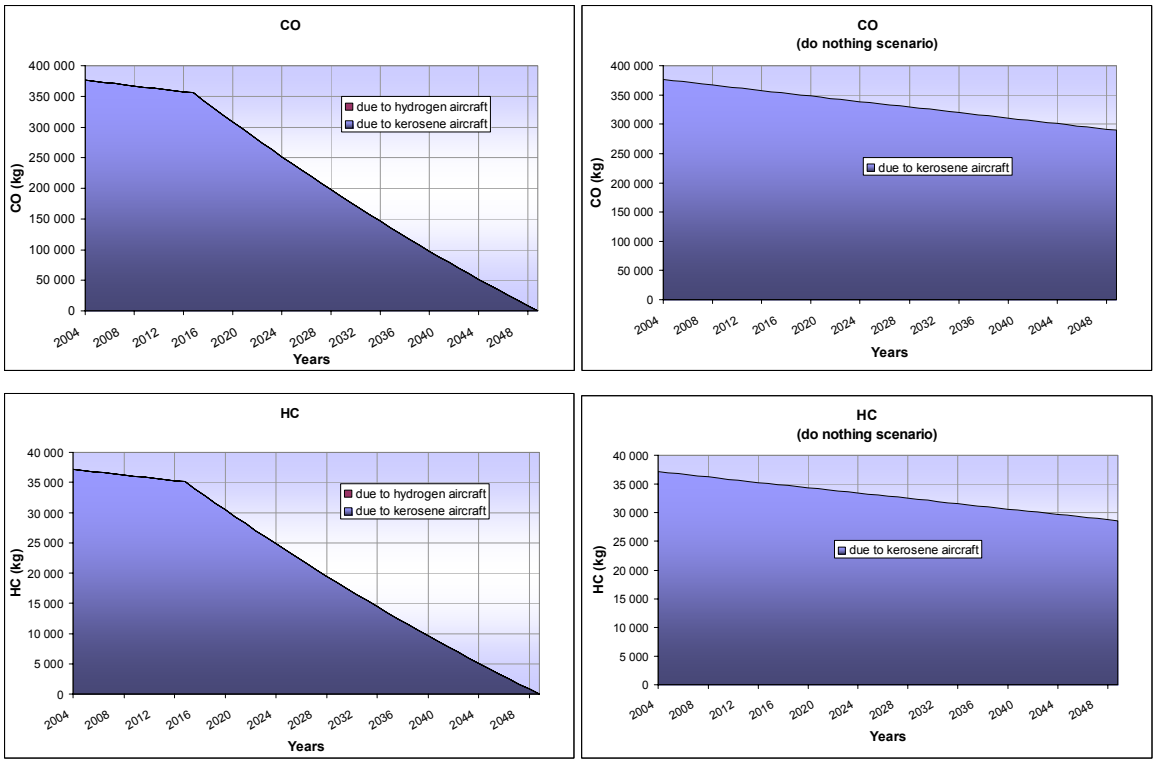

Figure 16: Total amount of CO and HC emitted per day

As no CO or HC are emitted by hydrogen engines (no firebrick colour on the left-hand plots), the replacement of kerosene aircraft by cryogenic aircraft would lead to a progressive reduction of CO and HC amount reaching zero if all the fleet is converted to hydrogen.

Without introduction of hydrogen aircraft, the level of CO and HC is expected to remain relatively high.

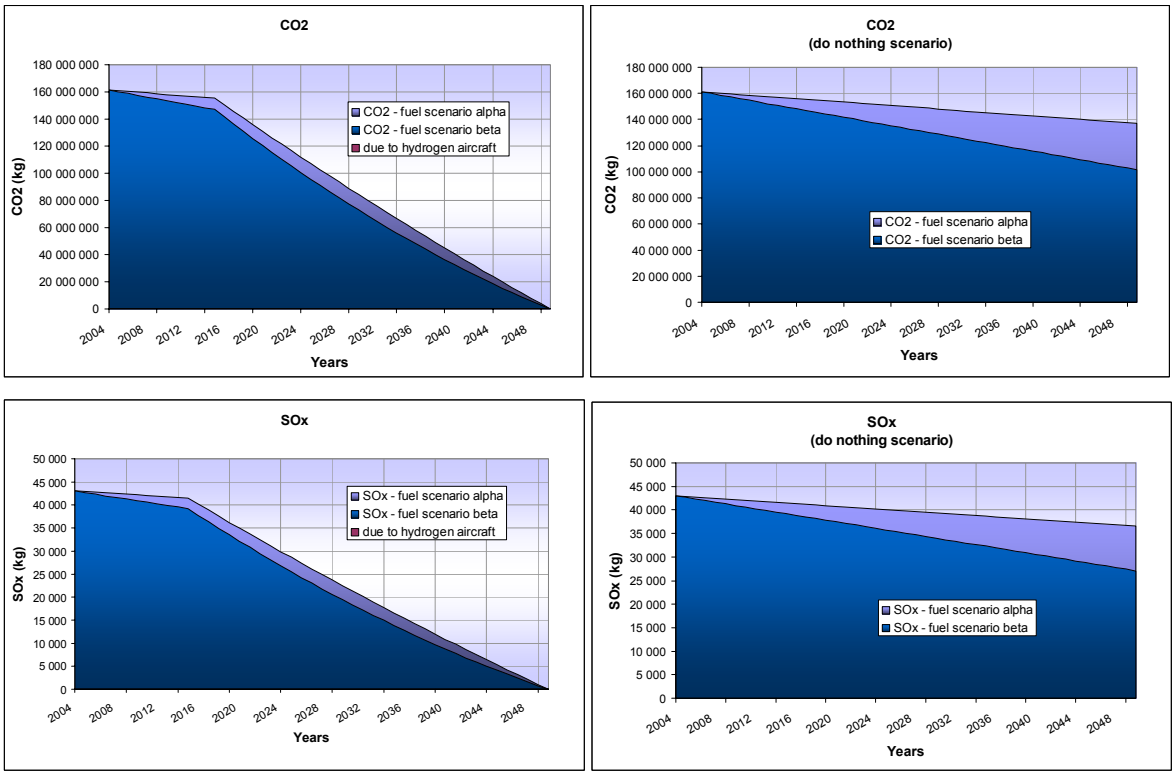

Figure 17: Total amount of CO_2 and SO_x emitted per day

As highlighted by Figure 17, the same is true for CO_2 and SO_x. Once again the estimation of CO_2 and SO_x depends on the scenario used for fuel burn estimation.

The fading of CO_2 emissions is a key factor for the adoption of hydrogen technology. Indeed, if CO_2 emission due to aviation represents "only" 2 to 3% of today's overall man-made CO_2 emissions [Ref 3], this percentage will grow in the next decade, following the reduction of CO_2 emitted by others contributors.

7.2.2 Conclusion

Regardless of any fuel shortage, which tends to give the advantage to hydrogen engines, Figure 14 to Figure 17 show the following:

- The level of NO_x emissions would decrease faster if hydrogen aircraft are introduced, especially if premixing technology becomes standard. However the level of NO_x emissions expected by the year 2050 is not negligible whichever technology is used. No decision can be made if focussing on NO_x only.
- Even with the best improvement possible on kerosene engines, this kind of technology will always produce CO, HC, CO_2 and SO_x. As hydrogen engines are free from these emissions, the advantage will always be given to hydrogen engines from an environmental point of view.
- The quantity of H_2O produced by hydrogen engines is 2.6 higher than water emitted from today's conventional engines. The impact of H_2O on the environment is significant and seems to be underestimated ([Ref 18] and [Ref 19]). It is worth going into depth on the H_2O discussion, especially regarding the subsequent formation of contrails, since this pollutant is the key feature for any decision.

7.3 Impact of H_2O emission on contrail formation

7.3.1 Contrail formation

Contrails are ice-crystal clouds that originate from aircraft exhaust emissions of particles and water. Contrails are commonly observed to have different life-times varying from the very short (typically a fast disappearing cloud the length of the aircraft) to the very long (when they may be persistent and eventually spread out to form a cirrus-like coverage) that is in its final form eventually indistinguishable from natural cirrus cloud.

Three main factors control contrail formation: water released from the combustion of fuel, ambient temperature, and relative humidity. The water released is a simple function of the amount of fuel burned at cruise altitudes. In addition to these factors, the specific design of a given engine may result in varying temperatures of the exhaust gases between engines and this will dictate whether a contrail is triggered or not for the same ambient temperature and humidity.

The formation of contrails arises from the increase in relative humidity that occurs during the mixing of the warm and moist exhaust gases from the aircraft engines with the colder and less humid ambient air. A contrail will form when saturation with respect to ice is reached or surpassed in the exhaust plume. The thermodynamic relation for contrail formation (Figure 18) requires knowledge of the air pressure, temperature, and relative humidity at a given flight level, as well as the fuel properties such as the emission index of H_2O, the combustion heat, and the overall aircraft propulsion efficiency. See Annex 4 of this report for the equations used by the Contrail Model.

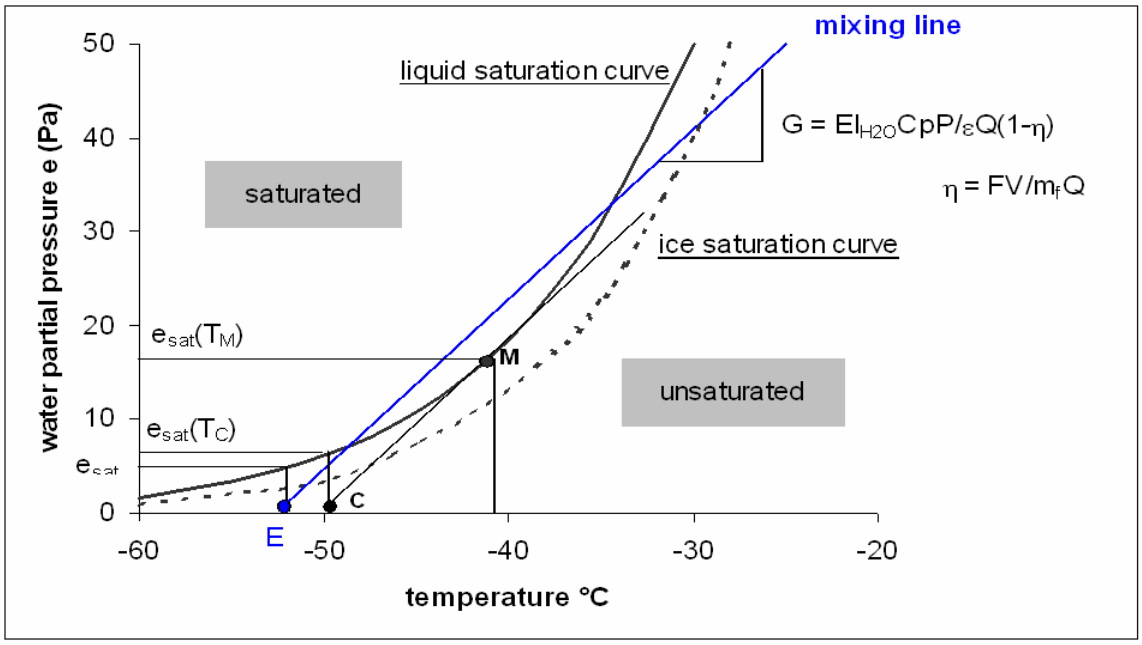

Figure 18: Thermodynamics Of Contrail Formation

7.3.2 The CONTRAIL Model

The CONTRAIL Model is part of EUROCONTROL's Toolset for Emission Analysis (TEA). TEA is a set of three inter-connected models, namely: AEM3, a EUROCONTROL system for estimating aviation emissions and fuel burn; MM5, a numerical weather model that provides forecast and analysis data for other EUROCONTROL models; and CONTRAIL, a EUROCONTROL tool for determining the probability and amount of contrail formation from aircraft (Figure 19).

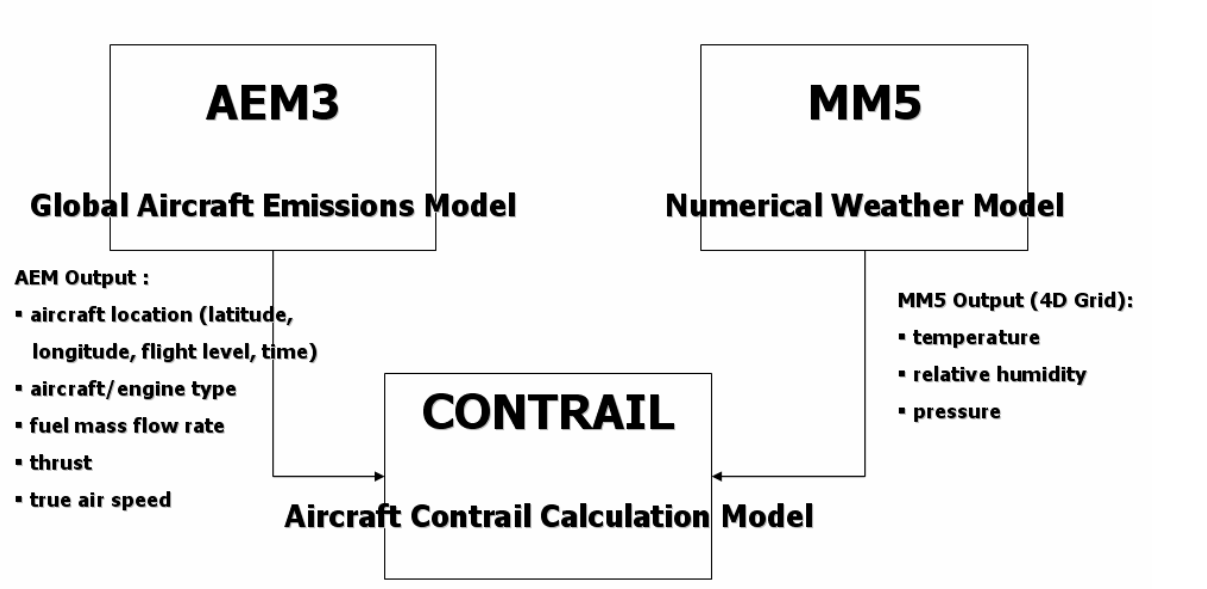

Figure 19: Overview Of Eurocontrol's Toolset For Emission Analysis (TEA)

AEM has been described above in section 4.1. The meteorological model MM5 is a 'state-of-the-art' system developed by the National Centre for Atmospheric Research (NCAR) and Pennsylvania State University. MM5 provides the surface and upper air meteorological data needed for local and global emission studies and contrail estimations, namely: pressure; geopotential height; temperature; horizontal and vertical wind speeds; and humidity. MM5 has been used for a broad spectrum of theoretical and real-time studies, including applications of both predictive simulation and four-dimensional data assimilation to monsoons, hurricanes, and cyclones. MM5 has been used by a wide range of agencies for studies involving convective systems, fronts, land-sea breezes, mountain-valley circulations, and urban heat islands.

MM5 is the latest in a series of weather models that developed from a mesoscale model used at Pennsylvania State University in the early 1970's. Since that time, it has undergone many changes designed to broaden its usage. These include: (i) a multiple-nest capability, (ii) non-hydrostatic dynamics, which allows the model to be used at a few-kilometer scale, (iii) multitasking capability on shared-and distributed-memory machines, (iv) a four-dimensional data-assimilation capability, and (v) more physics options. The model is supported by several auxiliary programs, which are referred to collectively as the MM5 modeling system.

The CONTRAIL model developed by the EEC is used to calculate contrails from actual aircraft flight tracks. This program uses the output from AEM3 and meteorological data from MM5. The CONTRAIL model first outputs the flight tracks that produce contrails and that would be visible to a satellite passing overhead at specific times during the day.

The CONTRAIL model then uses the output from AEM3 combined with meteorological data from MM5 to evaluate contrail formation. The required data provided by AEM3 for the CONTRAIL model are the 4D aircraft location (latitude, longitude, flight level, and time), the aircraft/engine type, fuel mass flow rate, thrust, and true air speed). For CONTRAIL, MM5 provides air temperature, relative humidity and air pressure at the AEM3 4D aircraft locations. The stages that make up the calculation of contrails consist of the following steps:

7.3.2.1 MM5 Stage

- Collect gridded meteorological analyses and observations for each time period.
- Run the MM5 model using these data.
- Reformat the MM5 output to allow direct input to the CONTRAIL model.

7.3.2.2 AEM3 Stage

- Collect the relevant Flight and Traffic data.
- Verify and validate these data.
- Run AEM3 using these data.
- Reformat and grid the AEM3 output be compatible with the MM5 data and to allow input to the CONTRAIL model.

7.3.2.3 CONTRAIL Stage

- Run the CONTRAIL model using the data from the MM5 and AEM3 stages.
- Create output files identifying the flight legs that would be visible to a satellite which would pass overhead at set, predetermined times.
- Grid these contrail output files to allow direct comparison with the actual satellite images.

7.3.3 Scenario 'Baseline': the CONTRAILS Project

The baseline scenario uses the output data from the CONTRAIL model which was used as part of a project, entitled “CONTRAILS: Aircraft Condensation Trails Monitoring Service”, between the European Space Agency (ESA), The EUROCONTROL Experimental Centre (EEC), the German Aerospace Centre (DLR), the Royal Netherlands Meteorological Institute (KNMI), and the Dundee Satellite Receiving Station (United Kingdom). The CONTRAILS project ([Ref 10] & [Ref 20]) seeks to support the continuous assessment of the environmental effects of increasing volumes of air traffic by monitoring the daily contrail and cirrus cloud coverage, for one year, over Europe and the North Atlantic. As part of this project, which focuses primarily on mapping observed contrails by satellite as well as on changes in cirrus cloud coverage, and on properties that can be related to changes in air traffic density, a complete and independent assessment of the EUROCONTROL CONTRAIL formation model shall be made by comparing model-based contrail maps with the satellite derived contrail maps. The results described in this paper are based on the first stages of this assessment.

For this project, the EUROCONTROL Experimental Centre produced 60 days of contrail maps consisting of 6 days for each of January though October 2004 for each overpass of a weather satellite (NOAA 16 or NOAA 17, etc.) which can record the observation of contrails. The dates chosen for each month are the fixed dates: the 5th, the 14th, and the 23rd, plus 3 days chosen by DLR (one a “high” contrail day, i.e. a lot of observed contrails; a “low” contrail day, i.e. with very few observed contrails and a “medium” contrail day). The output is in NetCDF format with a grid size of 0.25° x 0.25° lat/long grid. The geographical limits were 40°N-60°N latitude and 10°W-20°E longitude, which allowed complete coverage by EUROCONTROL’s Correlated Position Reports (CPR) data.

7.3.3.1 Flight Data Used For AEM3

The flight data used as input for AEM3 in the CONTRAILS project were the EUROCONTROL Correlated Position Reports (CPR) provided by the Central Flow Management Unit (CFMU). These data contain the actual geographical position and altitude of each aircraft based upon radar tracks correlated with flight plan data and normally sent every minute. Figure 20 shows the typical daily geographical extent of EUROCONTROL's CPR data for 2004.

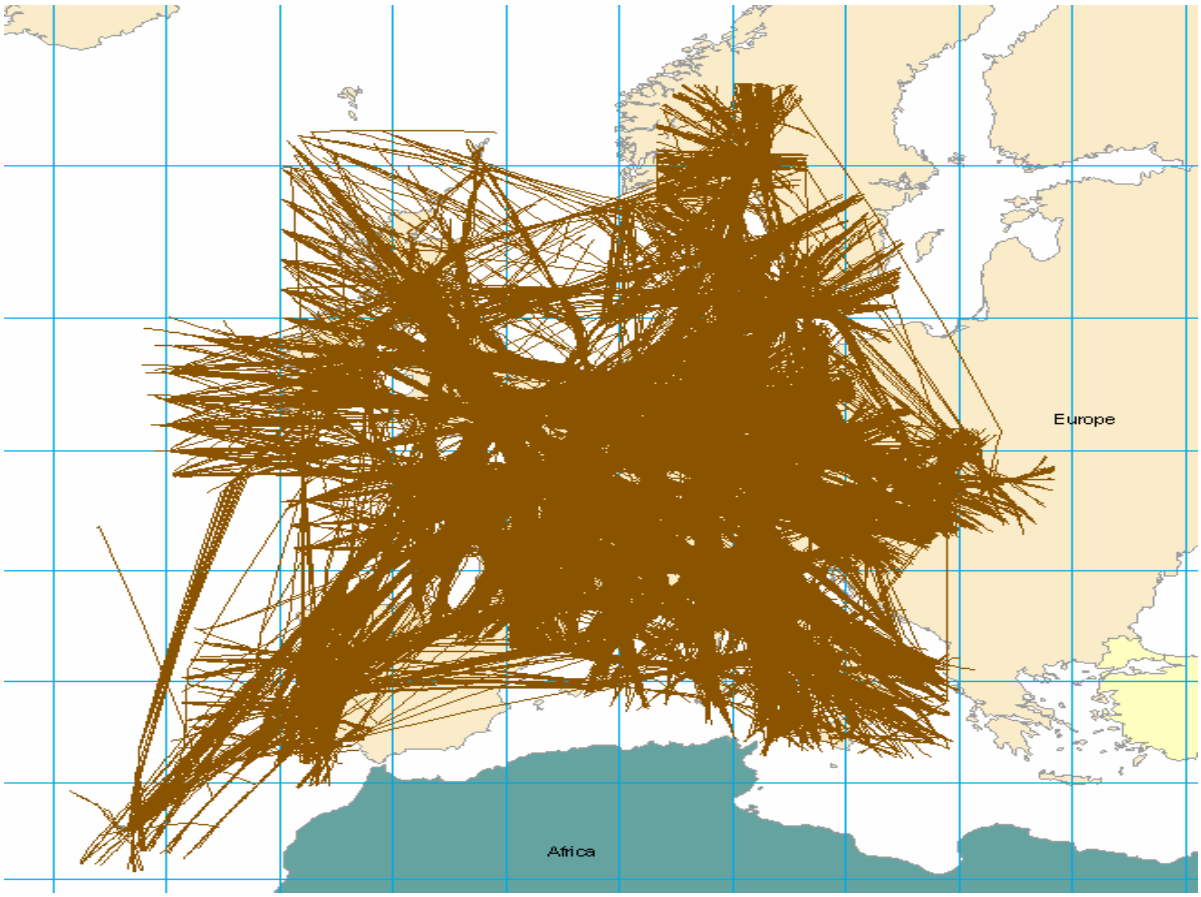

Figure 20: Typical Daily Extent Of EUROCONTROL's Correlated Position Reports (CPR) Radar Data.

7.3.3.2 Input Meteorological Data For MM5

The input meteorological data for MM5 for the CONTRAILS Project were the NCEP/DOE AMIP-II Reanalysis 2 gridded analysis data as well as the NCEP ADP Upper Air and Surface Observational Data.

7.3.3.2.1 NCEP/DOE AMIP-II Reanalysis 2

The NCEP/NCAR Reanalysis project uses a state-of-the-art analysis/forecast system to perform data assimilation using past data from 1948 to the present. There are over 80 different variables, (including geopotential height, temperature, relative humidity, U and V wind components, etc.) on 17 pressure levels (heights) on 2.5x2.5 degree grids, four times daily. The goal of Reanalysis-2 is to improve upon the NCEP/NCAR Reanalysis by fixing the errors and by updating the parameterizations of the physical processes.

7.3.3.2.2 NCEP ADP Upper Air Observational Data

NCEP ADP Global Upper Air Observation Subsets are a global synoptic set of 6 hourly upper air data reports. These were operationally collected by NCEP. They include radiosondes, pibals and aircraft reports received via the Global Telecommunications System (GTS) and satellite data from the National Environmental Satellite, Data, and Information Service (NESDIS). This data is the primary input to the Global Data Assimilation System (GDAS), which is used to make forecasts and the Global Final Analyses (FNL). It was also a major input for the NCEP/NCAR and ECMWF Reanalysis Projects. This data set includes upper air station data from land and ship-launched radiosondes. This involves, at 00Z and 12Z, about 650 - 1000 stations. It also includes satellite winds derived from cloud drift analysis and data from aircraft takeoff and landings with between 5000 and 10000 reports every 6 hours.

7.3.3.2.3 NCEP ADP Surface Observational Data

NCEP ADP Global Surface Observations are global synoptic set of 3 hourly surface data reports. These were operationally collected by NCEP. They include land and marine reports received via the Global Telecommunications System (GTS). This dataset is DSS' primary surface observation set. This data set includes the following land surface station report types: SYNOP, METAR, AWOS and ASOS. It also incorporates data from moving ships, fixed ships, MARS (moving and fixed) and buoy (moored and drifting).

7.3.4 Baseline Scenario CONTRAIL Model Output

Although the CONTRAILS project is still ongoing, preliminary results are presented here in the form of two examples: one of a day with a lot of visible contrails over Central Europe and the other with very few contrails over the same area. This first example is of a day where many contrails were produced over central Europe.

7.3.4.1 Heavy Contrails Example: 18-03-2004

Contrails are produced in areas of high humidity and very low temperatures. The following Figure 21 shows the humidity and temperature plots (from Reanalysis 2) for 12Z 18-03-2004 at flight level 300.

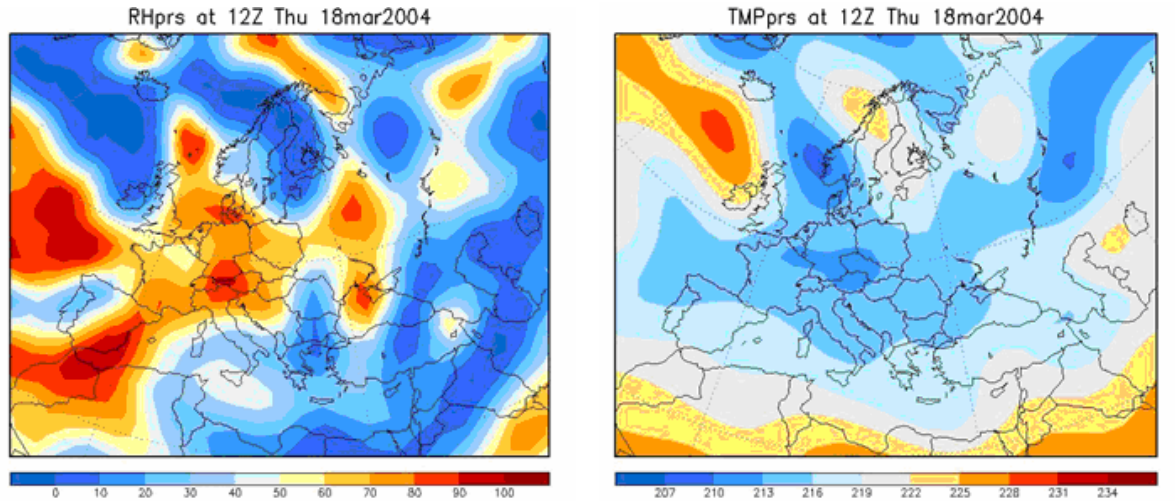

Figure 21: Relative Humidity (left) and Temperature (right) at FL 300: 12:00 March 18, 2004

The relative humidity plot (on the left) indicates areas of high humidity in red and the temperature plot (on the right) indicates areas of very cold air in blue. It can then be seen that the area above Central Europe is both very humid and very cold and this would then indicate that this area would be expected to produce contrails.

The following plots show the comparison of the CONTRAIL Model plot with the corresponding observed contrails from the satellite image over the same geographical area. The plot on the left shows where, on a map of Europe, contrails were modelled to be (using the Contrail Model). The plot on the right shows where, on a similar map and at the same scale, contrails were observed by satellite at the same time. Indeed, a very close correlation can be observed. The coloured boxes on the Contrail Model plots (left) are areas of "contrail density" (number of contrails per area) within a 0.25 degree latitude by 0.25 degree longitude grid cell.

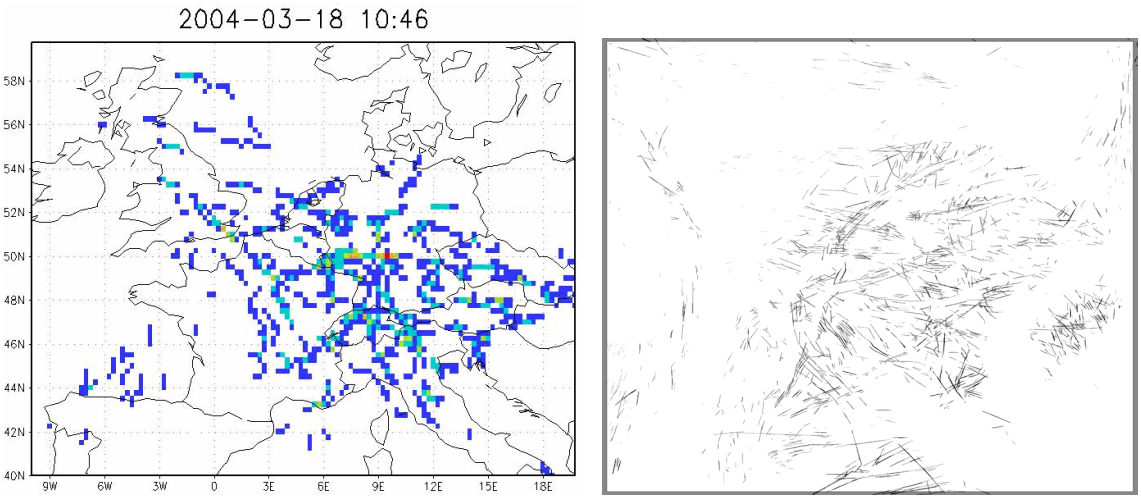

Figure 22: Modelled contrails (left) and observed contrails (right) at 10:46 March 18, 2004

7.3.4.2 Light Contrails Example: 09-03-2004

The second example is an example of a day where very few contrails were produced over central Europe. The humidity and temperature plots (from Reanalysis 2) for 12Z 09-03-2004 at flight level 00 are shown in Figure 23. It can be seen that the area over Central Europe is not very humid and not very cold which is the area where contrails are not expected. Rather, contrails would be expected over the ocean off the western coast of France.

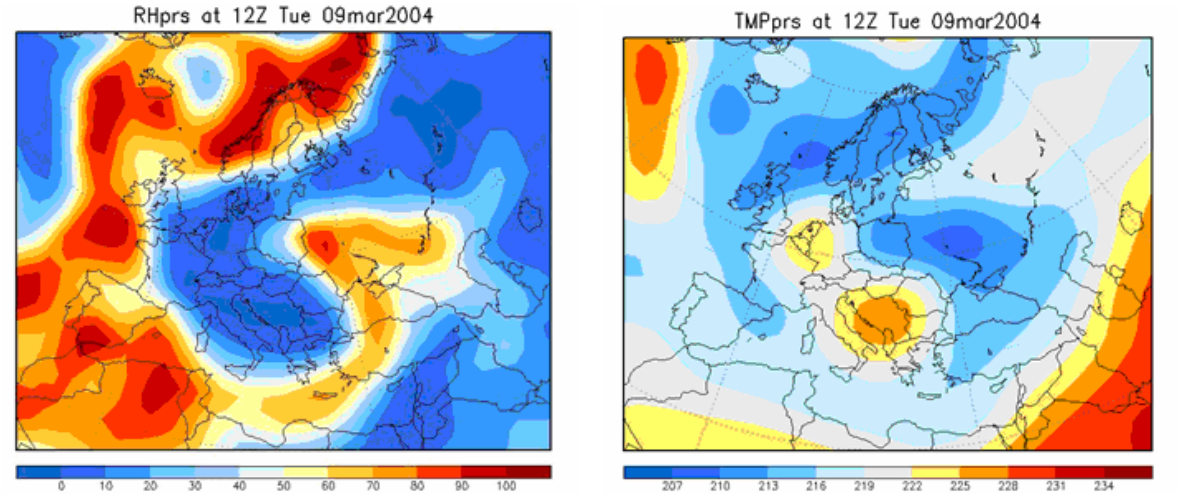

Figure 23: Relative Humidity (left) and Temperature (right) at FL 300: 12:00 March 09, 2004

As in the heavy contrails example, the following figures show the comparison of the Contrail Model plot with the corresponding observed contrails from the satellite image over the same geographical area. Again, a very close correlation can be observed.

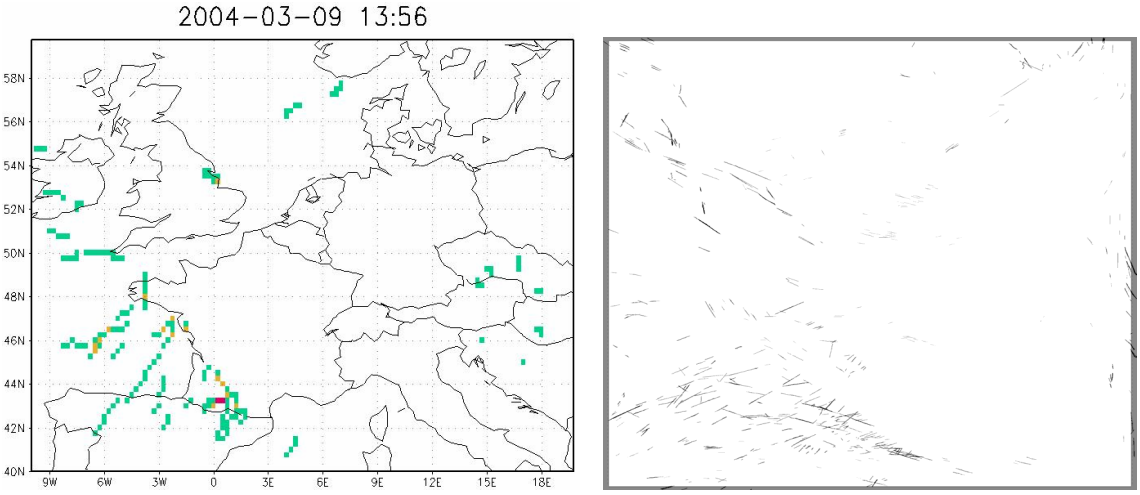

Figure 24: Modelled contrails (left) and observed contrails (right) at 13:56 March 09, 2004

7.3.5 Scenario 'Kerosene': Current combustion technology but improved

Two different situations have been analyzed for this scenario. Firstly Scenario 2028K examines the effect of improved combustion technology on contrail coverage for the year 2028 and secondly Scenario 2050K examines the effect for the year 2050.

As described in section 5.3.2, the entire 2004 fleet will be totally replaced by the year 2028. Growth in fuel efficiency is estimated at around 1% per year[11]. This means that 2028's fleet should burn about 24% less fuel for the same missions as the 2004 fleet (Scenario 2028K). Similarly, following this same trend, the fleet of 2050 would burn 46% less fuel (Scenario 2050K).

In order to estimate the contrail coverage, for each leg of a flight the contrail model calculates the Engine Propulsion Efficiency (η) using the following equation. The complete equations used by the Contrail Model are given as Annex 4 of this report.

Engine Propulsion Efficiency:

$\eta = FV/M_f Q$

where:

F = engine thrust (N)

V= air speed (m/s)

M_f = mass fuel flow (Kg/s)

Q = combustion heat of fuel (taken as constant 43 MJ/kg)

For Scenario 2028K, the mass fuel flow (M_f) is **decreased** by 24%. Similarly for Scenario 2050K, the mass fuel flow is decreased by 46%.The other factors, namely; engine thrust, air speed and combustion heat of fuel are taken to be the same as the baseline scenario. The Engine Propulsion Efficiency would, by this equation, therefore be **increased** by 24% for Scenario 2028K and 46% for Scenario 2050K. Propulsion efficiency is calculated by the Contrail Model for each aircraft on each flight leg with typical average 2004 values on the order of 0.3. This would increase, for Scenario 2028K, to values around 0.37 and around 0.44 for Scenario 2050K. An increase in the Engine Propulsion Efficiency would lead to an **increase** of the slope of the exhaust/ambient air mixing line (See Figure 18 and Annex 4). This increases the maximum temperature at which contrails would be formed, and thereby the growth of propulsion efficiency will lead to more contrails formation.

[11] For simplification reasons, in the section 7.3 only one scenario was assessed to estimate future fuel burn. It was considered that '1% per year' is equivalent to '1% of 2004's technology per year'. This assumption is valid since technological improvement yearly average reported by IPCC ([Ref 3]) is 1 to 2%. The value considered in section 7.3 is within IPCC's limits.

7.3.5.1 Scenario 2028K: Contrail Model Output

The Contrail Model was run for the 20 days of Scenario 2028K. Also produced were contrail maps for the same satellite overpass times (a total of 179) as the Baseline Scenario. A comparison of Scenario 2028K with the Baseline Scenario is shown below:

Date	Flight Legs >= FL 240 in the initial data set	Number of Contrails			% Contrails			
		Baseline Scenario	Future Scenario #2028K	Difference Baseline to #2028K	Baseline Scenario	Future Scenario #2028K	Difference in Contrail Number Baseline to #2028K	Increase of Contrail Coverage Baseline to #2028K
20040110	570525	167853	173089	5236	29.42%	30.34%	3.12%	0.92%
20040120	566918	173507	178549	5042	30.61%	31.49%	2.91%	0.89%
20040211	570747	180025	186457	6432	31.54%	32.67%	3.57%	1.13%
20040226	611619	20440	21365	925	3.34%	3.49%	4.53%	0.15%
20040308	597653	28763	29720	957	4.81%	4.97%	3.33%	0.16%
20040318	602841	203739	211868	8129	33.80%	35.14%	3.99%	1.35%
20040422	653073	136030	144773	8743	20.83%	22.17%	6.43%	1.34%
20040429	650359	122017	127677	5660	18.76%	19.63%	4.64%	0.87%
20040517	695851	89972	94380	4408	12.93%	13.56%	4.90%	0.63%
20040528	763449	133459	142187	8728	17.48%	18.62%	6.54%	1.14%
20040601	717164	38466	46434	7968	5.36%	6.47%	20.71%	1.11%
20040622	729812	69766	102939	33173	9.56%	14.10%	47.55%	4.55%
20040701	759129	21319	25337	4018	2.81%	3.34%	18.85%	0.53%
20040724	776039	46327	65518	19191	5.97%	8.44%	41.43%	2.47%
20040801	770995	81288	103768	22480	10.54%	13.46%	27.65%	2.92%
20040831	770571	69059	77334	8275	8.96%	10.04%	11.98%	1.07%
20040911	771282	172982	197876	24894	22.43%	25.66%	14.39%	3.23%
20040917	774843	204091	222048	17957	26.34%	28.66%	8.80%	2.32%
20041003	731943	178382	202449	24067	24.37%	27.66%	13.49%	3.29%
20041018	712615	60409	65838	5429	8.48%	9.24%	8.99%	0.76%
Total	**13797428**	**2197894**	**2419606**	**221712**	**15.93%**	**17.54%**	**10.09%**	**1.61%**

Table 9: Output statistics from the Contrail Model: Comparison of Baseline and Scenario 2028K (2028)

The data indicate that, on average and for the 20 days studied, **15.93%** of the flight legs >= FL240 in 2004 produced contrails in 2004. Flight legs refer to short flight segments in the CPR data, each of approximately 2 minutes duration. The percentage of contrail-producing flight legs increased to **17.54%** with the estimated fleet fuel efficiency increase of 2028 (Scenario 2028K). This indicates an estimated increase in contrail number of approximately **10.09%** in 2028 compared with 2004 (2419606 contrails from flight legs in 2028 compared to 2197894 contrails from flight legs in 2004). In order to gauge the percentage change in contrail sky coverage, this difference in contrail number can be compared to the total number of flight legs giving an estimation of an increase of **1.61%** (221712 contrail difference / 13797428 flight legs).

When the data is split into two parts, high contrail days and low contrail days, as defined in Table 4 of section 5.1, we get the following results. First, the following table shows the data for high contrail days.

Date (HIGH Contrails)	Flight Legs >= FL 240 in the initial data set	Number of Contrails			% Contrails			
		Baseline Scenario	Future Scenario #2028K	Difference Baseline to #2028K	Baseline Scenario	Future Scenario #2028K	Difference in Contrail Number Baseline to #2028K	Increase of Contrail Coverage Baseline to #2028K
20040120	566918	173507	178549	5042	30.61%	31.49%	2.91%	0.89%
20040211	570747	180025	186457	6432	31.54%	32.67%	3.57%	1.13%
20040318	602841	203739	211868	8129	33.80%	35.14%	3.99%	1.35%
20040429	650359	122017	127677	5660	18.76%	19.63%	4.64%	0.87%
20040528	763449	133459	142187	8728	17.48%	18.62%	6.54%	1.14%
20040601	717164	38466	46434	7968	5.36%	6.47%	20.71%	1.11%
20040724	776039	46327	65518	19191	5.97%	8.44%	41.43%	2.47%
20040831	770571	69059	77334	8275	8.96%	10.04%	11.98%	1.07%
20040917	774843	204091	222048	17957	26.34%	28.66%	8.80%	2.32%
20041003	731943	178382	202449	24067	24.37%	27.66%	13.49%	3.29%
Total	**6924874**	**1349072**	**1460521**	**111449**	**19.48%**	**21.09%**	**8.26%**	**1.61%**

Table 10: Output statistics from the Contrail Model: Comparison of Baseline and Scenario 2028K (High contrail days only)

The data indicate that, on average and for the 10 high contrail days studied, **19.48%** of the flight legs >= FL240 in 2004 produced contrails in 2004. The percentage of contrail-producing flight legs increased to **21.09%** with the estimated fleet fuel efficiency increase of 2028 (Scenario 2028K). This indicates an estimated increase in contrail number of **8.26%** (which is less than the 10.09% for both high and low contrail days) in 2028 compared with 2004 (1460521 contrails from flight legs in 2028 compared to 1349072 contrails from flight legs in 2004). The percentage change in contrail sky coverage is estimated as an increase of **1.61%** (111449 contrail difference / 6924874 flight legs). Interestingly the contrail sky coverage for the high contrails days is the same as for both high and low contrail days combined (see Table 9).

It should be noted that this increase refers to an increase in terms of contrail "density" but not in terms of contrail "lifetime". With these "increased contrail coverage" scenarios the amount of contrails are increased because of the different technology of the engines but the lifetime of the contrails (how long the contrail exists before it dissipates) remains the same because this is a function of the atmospheric conditions and not the engine characteristics. In other words, the contrails will not last "longer" in the air for the different scenarios proposed (since each scenario uses the same atmospheric conditions).

Next, the following table shows the data for low contrail days. The data indicate that, on average and for the 10 low contrail days studied, **12.35%** of the flight legs >= FL240 in 2004 produced contrails in 2004. The percentage of contrail-producing flight legs increased to **13.96%** with the estimated fleet fuel efficiency increase of 2028 (Scenario 2028K). This

indicates an estimated increase in contrail number of **12.99%** in 2028 compared with 2004 (959085 contrails from flight legs in 2028 compared to 848822 contrails from flight legs in 2004). It should be noted that this figure is greater than both the 10.09% for both high and low contrail days and the 8.25% for high contrails only. However, the percentage change in contrail sky coverage for the low contrail days is estimated as an increase of **1.60%** (110263 contrail difference / 6872554 flight legs). Which is practically the same value of the contrail sky coverage for the high contrails days and for both high and low contrail days combined (see Table 9).

Even though there is a higher percent change in the number of contrails on low contrail days as compared with high contrail days, the effect on the contrail sky coverage is the same. In sum, the effect, then, on the contrails of the improved engine technology scenario 2028K as compared to the present day is estimated to be an approximate **1.61%** increase in total contrail sky coverage consistent throughout the year.

Date (LOW Contrails)	Flight Legs >= FL 240 in the initial data set	Number of Contrails			% Contrails			
		Baseline Scenario	Future Scenario #2028K	Difference Baseline to #2028K	Baseline Scenario	Future Scenario #2028K	Difference in Contrail Number Baseline to #2028K	Increase of Contrail Coverage Baseline to #2028K
20040110	570525	167853	173089	5236	29.42%	30.34%	3.12%	0.92%
20040226	611619	20440	21365	925	3.34%	3.49%	4.53%	0.15%
20040308	597653	28763	29720	957	4.81%	4.97%	3.33%	0.16%
20040422	653073	136030	144773	8743	20.83%	22.17%	6.43%	1.34%
20040517	695851	89972	94380	4408	12.93%	13.56%	4.90%	0.63%
20040622	729812	69766	102939	33173	9.56%	14.10%	47.55%	4.55%
20040701	759129	21319	25337	4018	2.81%	3.34%	18.85%	0.53%
20040801	770995	81288	103768	22480	10.54%	13.46%	27.65%	2.92%
20040911	771282	172982	197876	24894	22.43%	25.66%	14.39%	3.23%
20041018	712615	60409	65838	5429	8.48%	9.24%	8.99%	0.76%
Total	**6872554**	**848822**	**959085**	**110263**	**12.35%**	**13.96%**	**12.99%**	**1.60%**

Table 11: Output statistics from the Contrail Model: Comparison of Baseline and Scenario 2028K (Low contrail days only)

7.3.5.2 Scenario 2050K: Contrail Model Output

The Contrail Model was also run for the 20 days of Scenario 2050K. Contrail maps for the same satellite overpass times (a total of 179) as the Baseline Scenario were produced. A comparison of Scenario 2050K with the Baseline Scenario is shown below:

Date	Flight Legs >= FL 240 in the initial data set	Number of Contrails			% Contrails			
		Baseline Scenario	Future Scenario #2050K	Difference Baseline to #2050K	Baseline Scenario	Future Scenario #2050K	Difference in Contrail Number Baseline to #2050K	Increase of Contrail Coverage Baseline to #2050K
20040110	570525	167853	178018	10165	29.42%	31.20%	6.06%	1.78%
20040120	566918	173507	183574	10067	30.61%	32.38%	5.80%	1.78%
20040211	570747	180025	190164	10139	31.54%	33.32%	5.63%	1.78%
20040226	611619	20440	22029	1589	3.34%	3.60%	7.77%	0.26%
20040308	597653	28763	30554	1791	4.81%	5.11%	6.23%	0.30%
20040318	602841	203739	218166	14427	33.80%	36.19%	7.08%	2.39%
20040422	653073	136030	150309	14279	20.83%	23.02%	10.50%	2.19%
20040429	650359	122017	134034	12017	18.76%	20.61%	9.85%	1.85%
20040517	695851	89972	96944	6972	12.93%	13.93%	7.75%	1.00%
20040528	763449	133459	149789	16330	17.48%	19.62%	12.24%	2.14%
20040601	717164	38466	51534	13068	5.36%	7.19%	33.97%	1.82%
20040622	729812	69766	127255	57489	9.56%	17.44%	82.40%	7.88%
20040701	759129	21319	31119	9800	2.81%	4.10%	45.97%	1.29%
20040724	776039	46327	82324	35997	5.97%	10.61%	77.70%	4.64%
20040801	770995	81288	134351	53063	10.54%	17.43%	65.28%	6.88%
20040831	770571	69059	87057	17998	8.96%	11.30%	26.06%	2.34%
20040911	771282	172982	224507	51525	22.43%	29.11%	29.79%	6.68%
20040917	774843	204091	245883	41792	26.34%	31.73%	20.48%	5.39%
20041003	731943	178382	218062	39680	24.37%	29.79%	22.24%	5.42%
20041018	712615	60409	72709	12300	8.48%	10.20%	20.36%	1.73%
Total	**13797428**	**2197894**	**2628382**	**430488**	**15.93%**	**19.05%**	**19.59%**	**3.12%**

Table 12: Output statistics from the Contrail Model: Comparison of Baseline and Scenario 2050K (2050)

The data indicate that, on average and for the 20 days studied, **15.93%** of the flight legs >= FL240 in 2004 produced contrails in 2004. The percentage of contrail-producing flight legs increased to **19.05%** with the estimated fleet fuel efficiency increase of 2050 (Scenario 2050K). This indicates an estimated increase in contrail number of approximately **19.59%** in 2050 compared with 2004 (2628382 contrails from flight legs in 2050 compared to 2197894 contrails from flight legs in 2004). The percentage change in contrail sky coverage is estimated as an increase of **3.12%** (430448 contrail difference / 13797428 flight legs).

When the data is split into two parts, high contrail days and low contrail days, as defined in Table 4 of section 5.1, we get the following results. First, the following table shows the data for high contrail days.

Date (HIGH Contrails)	Flight Legs >= FL 240 in the initial data set	Number of Contrails			% Contrails			
		Baseline Scenario	Future Scenario #2050K	Difference Baseline to #2050K	Baseline Scenario	Future Scenario #2050K	Difference in Contrail Number Baseline to #2050K	Increase of Contrail Coverage Baseline to #2050K
20040120	566918	173507	183574	10067	30.61%	32.38%	5.80%	1.78%
20040211	570747	180025	190164	10139	31.54%	33.32%	5.63%	1.78%
20040318	602841	203739	218166	14427	33.80%	36.19%	7.08%	2.39%
20040429	650359	122017	134034	12017	18.76%	20.61%	9.85%	1.85%
20040528	763449	133459	149789	16330	17.48%	19.62%	12.24%	2.14%
20040601	717164	38466	51534	13068	5.36%	7.19%	33.97%	1.82%
20040724	776039	46327	82324	35997	5.97%	10.61%	77.70%	4.64%
20040831	770571	69059	87057	17998	8.96%	11.30%	26.06%	2.34%
20040917	774843	204091	245883	41792	26.34%	31.73%	20.48%	5.39%
20041003	731943	178382	218062	39680	24.37%	29.79%	22.24%	5.42%
Total	**6924874**	**1349072**	**1560587**	**211515**	**19.48%**	**22.54%**	**15.68%**	**3.05%**

Table 13: Output statistics from the Contrail Model: Comparison of Baseline and Scenario 2050K (High contrail days only)

The data indicate that, on average and for the 10 high contrail days studied, **19.48%** of the flight legs >= FL240 in 2004 produced contrails in 2004. The percentage of contrail-producing flight legs increased to **22.54%** with the estimated fleet fuel efficiency increase of 2050 (Scenario 2050K). This indicates an estimated increase in contrail number of **15.68%** (which is less than the 19.59% for both high and low contrail days) in 2050 compared with 2004 (1560587 contrails from flight legs in 2050 compared to 1349072 contrails from flight legs in 2004). The percentage change in contrail sky coverage is estimated as an increase of **3.05%** (211515 contrail difference / 6924874 flight legs). The contrail sky coverage for the high contrails days is lower but very close to the value for both high and low contrail days combined (see Table 12).

It should be noted that this increase refers to an increase in terms of contrail "density" but not in terms of contrail "lifetime". With these "increased contrail coverage" scenarios the amount of contrails are increased because of the different technology of the engines but the lifetime of the contrails (how long the contrail exists before it dissipates) remains the same because this is a function of the atmospheric conditions and not the engine characteristics. In other words, the contrails will not last "longer" in the air for the different scenarios proposed (since each scenario uses the same atmospheric conditions).

Next, the following table shows the data for low contrail days. The data indicate that, on average and for the 10 low contrail days studied, **12.35%** of the flight legs >= FL240 in 2004 produced contrails in 2004. The percentage of contrail-producing flight legs increased to

15.54% with the estimated fleet fuel efficiency increase of 2050 (Scenario 2050K). This indicates an estimated increase in contrail number of **25.80%** in 2050 compared with 2004 (1067795 contrails from flight legs in 2050 compared to 848822 contrails from flight legs in 2004). It should be noted that this figure is greater than both the 19.59% for both high and low contrail days and the 15.68% for high contrails only. The percentage change in contrail sky coverage is estimated as an increase of **3.19%** (218973 contrail difference / 6872554 flight legs). The contrail sky coverage for the low contrails days is higher but very close to the value for both high and low contrail days combined (see Table 12).

Even though there is a higher percent change in the number of contrails on low contrail days as compared with high contrail days, the effect on the contrail sky coverage is the same. In sum, the effect on the contrails of the improved engine technology scenario 2050K as compared to the present day is estimated to be an approximate **3.12%** increase in total contrail sky coverage consistent throughout the year.

Date (LOW Contrails)	Flight Legs >= FL 240 in the initial data set	Number of Contrails			% Contrails			
		Baseline Scenario	Future Scenario #2050K	Difference Baseline to #2050K	Baseline Scenario	Future Scenario #2050K	Difference in Contrail Number Baseline to #2050K	Increase of Contrail Coverage Baseline to #2050K
20040110	570525	167853	178018	10165	29.42%	31.20%	6.06%	1.78%
20040226	611619	20440	22029	1589	3.34%	3.60%	7.77%	0.26%
20040308	597653	28763	30554	1791	4.81%	5.11%	6.23%	0.30%
20040422	653073	136030	150309	14279	20.83%	23.02%	10.50%	2.19%
20040517	695851	89972	96944	6972	12.93%	13.93%	7.75%	1.00%
20040622	729812	69766	127255	57489	9.56%	17.44%	82.40%	7.88%
20040701	759129	21319	31119	9800	2.81%	4.10%	45.97%	1.29%
20040801	770995	81288	134351	53063	10.54%	17.43%	65.28%	6.88%
20040911	771282	172982	224507	51525	22.43%	29.11%	29.79%	6.68%
20041018	712615	60409	72709	12300	8.48%	10.20%	20.36%	1.73%
Total	**6872554**	**848822**	**1067795**	**218973**	**12.35%**	**15.54%**	**25.80%**	**3.19%**

Table 14: Output statistics from the Contrail Model: Comparison of Baseline and Scenario 2050K (Low contrail days only)

7.3.6 Scenario 'Hydrogen' (2050H): Use of Hydrogen Technology

It is estimated that by the year 2050 the entire fleet of commercial aircraft could possibly be replaced entirely by hydrogen-burning aircraft. Since a major by-product of hydrogen engines is water vapour (more so than for kerosene aircraft), it is important to investigate the level of contrail product from these hydrogen-burning aircraft.

In order to estimate the contrail coverage, for each leg of a flight the contrail model calculates the Engine Propulsion Efficiency (η) using the following modifications for hydrogen aircraft:

From section 7.3.5: $\eta = FV/M_f Q$

Now, the same energy content (producing the same thrust and same airspeed) of 1 kg of kerosene, a hydrogen aircraft burns 0.36 kg of hydrogen. Therefore in the formula for Engine Propulsion Efficiency the Mass Fuel Flow (M_f) of hydrogen aircraft will be **decreased** by 36% (compared to the mass fuel flow of kerosene). However, the combustion heat of hydrogen is 120 MJ/kg and not the 43 MJ/kg of kerosene, which is a 36% **increase**. This results in a net zero change in fuel efficiency. The change in the amount of contrails produced by hydrogen aircraft in comparison with 2004 aircraft is not in the Engine Propulsion Efficiency but in the increased amount of water vapour emitted. This is taken into account, in the Contrail Model, in the calculation of the slope of the exhaust/ambient air mixing line:

Slope Of The Exhaust/Ambient Air Mixing Line:

$G = EL_{H2O} C_P P/\varepsilon Q(1-\eta)$

where:

EL_{H2O} = Water emission index;

C_P = specific heat capacity of air at constant pressure = 1004 J/KgK

P = pressure (hPa)

ε = ratio of the gas constants of air and water vapour = 0.622

η = engine propulsion efficiency

Q = combustion heat of fuel (taken as constant 120 MJ/kg) (hydrogen)

For hydrogen:

EL_{H2O} = 3.21 kg/kg hydrogen burned (2.6 times larger than the value for kerosene, which is 1.230 kg/kg kerosene burned)

7.3.6.1 Scenario 2050H: Contrail Model Output

The Contrail Model was also run for the 20 days of Scenario 2050H. Also produced were contrail maps for the same satellite overpass times (a total of 179) as the Baseline Scenario. A comparison of Scenario 2050H with the Baseline Scenario is shown below:

Date	Flight Legs >= FL 240 in the initial data set	Number of Contrails			% Contrails			
		Baseline Scenario	Future Scenario #2050H	Difference Baseline to #2050H	Baseline Scenario	Future Scenario #2050H	Difference in Contrail Number Baseline to #2050H	Increase of Contrail Coverage Baseline to #2050H
20040110	570525	167853	210880	43027	29.42%	36.96%	25.63%	7.54%
20040120	566918	173507	221140	47633	30.61%	39.01%	27.45%	8.40%
20040211	570747	180025	218926	38901	31.54%	38.36%	21.61%	6.82%
20040226	611619	20440	25548	5108	3.34%	4.18%	24.99%	0.84%
20040308	597653	28763	32569	3806	4.81%	5.45%	13.23%	0.64%
20040318	602841	203739	271793	68054	33.80%	45.09%	33.40%	11.29%
20040422	653073	136030	210176	74146	20.83%	32.18%	54.51%	11.35%
20040429	650359	122017	193389	71372	18.76%	29.74%	58.49%	10.97%
20040517	695851	89972	105417	15445	12.93%	15.15%	17.17%	2.22%
20040528	763449	133459	200269	66810	17.48%	26.23%	50.06%	8.75%
20040601	717164	38466	90224	51758	5.36%	12.58%	134.56%	7.22%
20040622	729812	69766	217947	148181	9.56%	29.86%	212.40%	20.30%
20040701	759129	21319	60801	39482	2.81%	8.01%	185.20%	5.20%
20040724	776039	46327	161213	114886	5.97%	20.77%	247.99%	14.80%
20040801	770995	81288	233232	151944	10.54%	30.25%	186.92%	19.71%
20040831	770571	69059	123068	54009	8.96%	15.97%	78.21%	7.01%
20040911	771282	172982	353500	180518	22.43%	45.83%	104.36%	23.40%
20040917	774843	204091	372038	167947	26.34%	48.01%	82.29%	21.67%
20041003	731943	178382	330201	151819	24.37%	45.11%	85.11%	20.74%
20041018	712615	60409	110934	50525	8.48%	15.57%	83.64%	7.09%
Total	**13797428**	**2197894**	**3743265**	**1545371**	**15.93%**	**27.13%**	**70.31%**	**11.20%**

Table 15: Output statistics from the Contrail Model: Comparison of Baseline and Scenario 2050H

For Hydrogen aircraft in 2050 (Scenario 2050H), the data indicate that, on average and for the 20 days studied, **27.13%** of the flight legs >= FL240 produced contrails. This is an increase over the value of 15.93% in 2004 (from the previous section). This indicates an estimated increase in contrail coverage of approximately **70.09%** in 2050 compared with 2004 (3743265 contrails from flight legs in 2050 compared to 2197894 contrails from flight legs in 2004). This suggests a very large increase in contrail number using hydrogen aircraft. This large increase in contrail number translates into an estimate of the percentage change in contrail sky coverage as an increase of **11.20%** (1545371 contrail difference / 13797428 flight legs).

The following table shows the data for high contrail days:

Date (HIGH Contrails)	Flight Legs >= FL 240 in the initial data set	Number of Contrails			% Contrails			
		Baseline Scenario	Future Scenario #2050H	Difference Baseline to #2050H	Baseline Scenario	Future Scenario #2050H	Difference in Contrail Number Baseline to #2050H	Increase of Contrail Coverage Baseline to #2050H
20040120	566918	173507	221140	47633	30.61%	39.01%	27.45%	8.40%
20040211	570747	180025	218926	38901	31.54%	38.36%	21.61%	6.82%
20040318	602841	203739	271793	68054	33.80%	45.09%	33.40%	11.29%
20040429	650359	122017	193389	71372	18.76%	29.74%	58.49%	10.97%
20040528	763449	133459	200269	66810	17.48%	26.23%	50.06%	8.75%
20040601	717164	38466	90224	51758	5.36%	12.58%	134.56%	7.22%
20040724	776039	46327	161213	114886	5.97%	20.77%	247.99%	14.80%
20040831	770571	69059	123068	54009	8.96%	15.97%	78.21%	7.01%
20040917	774843	204091	372038	167947	26.34%	48.01%	82.29%	21.67%
20041003	731943	178382	330201	151819	24.37%	45.11%	85.11%	20.74%
Total	**6924874**	**1349072**	**2182261**	**833189**	**19.48%**	**31.51%**	**61.76%**	**12.03%**

Table 16: Output statistics from the Contrail Model: Comparison of Baseline and Scenario 2050H (High contrail days only)

The data indicate that, on average and for the 10 high contrail days studied, **31.51%** of the flight legs >= FL240 in 2004 produced contrails in 2050. This indicates an estimated increase in contrail number of **61.76%** (which is less than the 70.31% for both high and low contrail days) in 2050 compared with 2004 (2182261 contrails from flight legs in 2050 compared to 1349072 contrails from flight legs in 2004). The percentage change in contrail sky coverage is estimated as an increase of **12.03%** (833189 contrail difference / 6924874 flight legs). The contrail sky coverage for the high contrails days is higher but within 1% of the value for both high and low contrail days combined (see Table 15).

Next, the following table shows the data for low contrail days:

Date (LOW Contrails)	Flight Legs >= FL 240 in the initial data set	Number of Contrails			% Contrails			
		Baseline Scenario	Future Scenario #2050H	Difference Baseline to #2050H	Baseline Scenario	Future Scenario #2050H	Difference in Contrail Number Baseline to #2050H	Increase of Contrail Coverage Baseline to #2050H
20040110	570525	167853	210880	43027	29.42%	36.96%	25.63%	7.54%
20040226	611619	20440	25548	5108	3.34%	4.18%	24.99%	0.84%
20040308	597653	28763	32569	3806	4.81%	5.45%	13.23%	0.64%
20040422	653073	136030	210176	74146	20.83%	32.18%	54.51%	11.35%
20040517	695851	89972	105417	15445	12.93%	15.15%	17.17%	2.22%
20040622	729812	69766	217947	148181	9.56%	29.86%	212.40%	20.30%
20040701	759129	21319	60801	39482	2.81%	8.01%	185.20%	5.20%
20040801	770995	81288	233232	151944	10.54%	30.25%	186.92%	19.71%
20040911	771282	172982	353500	180518	22.43%	45.83%	104.36%	23.40%
20041018	712615	60409	110934	50525	8.48%	15.57%	83.64%	7.09%
Total	**6872554**	**848822**	**1561004**	**712182**	**12.35%**	**22.71%**	**83.90%**	**10.36%**

Table 17: Output statistics from the Contrail Model: Comparison of Baseline and Scenario 2050H (Low contrail days only)

The data indicate that, on average and for the 10 low contrail days studied, **22.71%** of the flight legs >= FL240 in 2004 produced contrails in 2050. This indicates an estimated increase in contrail number of **83.90%** (1561004 contrails from flight legs in 2050 compared to 848822 contrails from flight legs in 2004). It should be noted that this figure is greater than both the 70.31% for both high and low contrail days and the 61.76% for high contrails only. The percentage change in contrail sky coverage is estimated as an increase of **10.36%** (712182 contrail difference / 6872554 flight legs). The contrail sky coverage for the low contrails days is lower but very close to the value for both high and low contrail days combined (see Table 15).

Even though there is a higher percent change in the number of contrails on high contrail days as compared with low contrail days, the effect on the contrail sky coverage is approximately the same. In sum, the effect on the contrails of the use of hydrogen technology scenario 2050H as compared to the present day is estimated to be an approximate **11.20%** increase in total contrail sky coverage consistent throughout the year.

7.3.7 Comparison of Scenario 2050K and Scenario 2050H

In comparing the two future scenarios for 2050 (Scenario 2050K, with increased fuel efficiency and Scenario 2050H with hydrogen aircraft), the data indicate, on average and for the 20 days studied, an estimated increase in contrail coverage of approximately **42.42%** with hydrogen-burning over future aircraft with more efficient kerosene-burning engines in 2050 (3743265 contrails from flight legs with hydrogen compared to 2628382 contrails from kerosene). This suggests a large increase in contrail number using hydrogen aircraft over using kerosene aircraft in 2050. This large increase in contrail number translates into an estimate of the percentage change in contrail sky coverage as an increase of **8.08%** (1114883 contrail difference / 13797428 flight legs).

Date	Flight Legs >= FL 240 in the initial data set	Number of Contrails			% Contrails			
		Future Scenario #2050K	Future Scenario #2050H	Difference #2050K to #2050H	Future Scenario #2050K	Future Scenario #2050H	Difference in Contrail Number #2050K to #2050H	Increase of Contrail Coverage #2050K to #2050H
20040110	570525	178018	210880	32862	31.20%	36.96%	18.46%	5.76%
20040120	566918	183574	221140	37566	32.38%	39.01%	20.46%	6.63%
20040211	570747	190164	218926	28762	33.32%	38.36%	15.12%	5.04%
20040226	611619	22029	25548	3519	3.60%	4.18%	15.97%	0.58%
20040308	597653	30554	32569	2015	5.11%	5.45%	6.59%	0.34%
20040318	602841	218166	271793	53627	36.19%	45.09%	24.58%	8.90%
20040422	653073	150309	210176	59867	23.02%	32.18%	39.83%	9.17%
20040429	650359	134034	193389	59355	20.61%	29.74%	44.28%	9.13%
20040517	695851	96944	105417	8473	13.93%	15.15%	8.74%	1.22%
20040528	763449	149789	200269	50480	19.62%	26.23%	33.70%	6.61%
20040601	717164	51534	90224	38690	7.19%	12.58%	75.08%	5.39%
20040622	729812	127255	217947	90692	17.44%	29.86%	71.27%	12.43%
20040701	759129	31119	60801	29682	4.10%	8.01%	95.38%	3.91%
20040724	776039	82324	161213	78889	10.61%	20.77%	95.83%	10.17%
20040801	770995	134351	233232	98881	17.43%	30.25%	73.60%	12.83%
20040831	770571	87057	123068	36011	11.30%	15.97%	41.36%	4.67%
20040911	771282	224507	353500	128993	29.11%	45.83%	57.46%	16.72%
20040917	774843	245883	372038	126155	31.73%	48.01%	51.31%	16.28%
20041003	731943	218062	330201	112139	29.79%	45.11%	51.43%	15.32%
20041018	712615	72709	110934	38225	10.20%	15.57%	52.57%	5.36%
Total	**13797428**	**2628382**	**3743265**	**1114883**	**19.05%**	**27.13%**	**42.42%**	**8.08%**

Table 18: Output statistics from the Contrail Model: Comparison of Scenario 2050K and Scenario 2050H

The following table shows the data for high contrail days. The data indicate that, on average and for the 10 high contrail days studied, an estimated increase in contrail number of **39.84%** with hydrogen over kerosene in 2050 (2182261 contrails from flight legs with hydrogen compared to 1560587 contrails from flight legs with kerosene). This is less than the 42.42% for both high and low contrail days. The percentage change in contrail sky coverage is estimated as an increase of **8.98%** (621674 contrail difference / 6924874 flight legs). The contrail sky coverage for the high contrails days is higher but within 1% of the value for both high and low contrail days combined (see Table 18).

Date (HIGH Contrails)	Flight Legs >= FL 240 in the initial data set	Number of Contrails			% Contrails			
		Future Scenario #2050K	Future Scenario #2050H	Difference #2050K to #2050H	Future Scenario #2050K	Future Scenario #2050H	Difference in Contrail Number #2050K to #2050H	Increase of Contrail Coverage #2050K to #2050H
20040120	566918	183574	221140	37566	32.38%	39.01%	20.46%	6.63%
20040211	570747	190164	218926	28762	33.32%	38.36%	15.12%	5.04%
20040318	602841	218166	271793	53627	36.19%	45.09%	24.58%	8.90%
20040429	650359	134034	193389	59355	20.61%	29.74%	44.28%	9.13%
20040528	763449	149789	200269	50480	19.62%	26.23%	33.70%	6.61%
20040601	717164	51534	90224	38690	7.19%	12.58%	75.08%	5.39%
20040724	776039	82324	161213	78889	10.61%	20.77%	95.83%	10.17%
20040831	770571	87057	123068	36011	11.30%	15.97%	41.36%	4.67%
20040917	774843	245883	372038	126155	31.73%	48.01%	51.31%	16.28%
20041003	731943	218062	330201	112139	29.79%	45.11%	51.43%	15.32%
Total	**6924874**	**1560587**	**2182261**	**621674**	**22.54%**	**31.51%**	**39.84%**	**8.98%**

Table 19: Output statistics from the Contrail Model: Comparison of Scenario 2050K and Scenario 2050H (High contrail days only)

Next, the following table shows the data for low contrail days:

Date (LOW Contrails)	Flight Legs >= FL 240 in the initial data set	Number of Contrails			% Contrails			
		Future Scenario #2050K	Future Scenario #2050H	Difference #2050K to #2050H	Future Scenario #2050K	Future Scenario #2050H	Difference in Contrail Number #2050K to #2050H	Increase of Contrail Coverage #2050K to #2050H
20040110	570525	178018	210880	32862	31.20%	36.96%	18.46%	5.76%
20040226	611619	22029	25548	3519	3.60%	4.18%	15.97%	0.58%
20040308	597653	30554	32569	2015	5.11%	5.45%	6.59%	0.34%
20040422	653073	150309	210176	59867	23.02%	32.18%	39.83%	9.17%
20040517	695851	96944	105417	8473	13.93%	15.15%	8.74%	1.22%
20040622	729812	127255	217947	90692	17.44%	29.86%	71.27%	12.43%
20040701	759129	31119	60801	29682	4.10%	8.01%	95.38%	3.91%
20040801	770995	134351	233232	98881	17.43%	30.25%	73.60%	12.83%
20040911	771282	224507	353500	128993	29.11%	45.83%	57.46%	16.72%
20041018	712615	72709	110934	38225	10.20%	15.57%	52.57%	5.36%
Total	**6872554**	**1067795**	**1561004**	**493209**	**15.54%**	**22.71%**	**46.19%**	**7.18%**

Table 20: Output statistics from the Contrail Model: Comparison of Scenario 2050K and Scenario 2050H (Low contrail days only)

The data indicate that, on average and for the 10 low contrail days studied, an estimated increase in contrail number of **46.19%** with hydrogen over kerosene (1561004 contrails from flight legs with hydrogen compared to 1067795 contrails from flight legs with kerosene). This figure is greater than both the 42.42% for both high and low contrail days and the 39.84% for high contrails only. The percentage change in contrail sky coverage is estimated as an increase of **7.18%** (493209 contrail difference / 6872554 flight legs). The contrail sky coverage for the low contrails days is lower but very close to the value for both high and low contrail days combined (see Table 18).

As for the previous case, even though there is a higher percent change in the number of contrails on high contrail days as compared with low contrail days, the effect on the contrail sky coverage is approximately the same. In sum, the effect on the contrails of the use of hydrogen technology scenario 2050H compared to improved engine technology of the same year is estimated to be an approximate **8.08%** increase in total contrail sky coverage consistent throughout the year.

7.3.8 Sample Contrail Model Maps

The difference in contrail coverage the four scenarios mentioned: Baseline Scenario (2004), Scenario 2028K (2028 – increases fuel efficiency), Scenario 2050K (2050 – increased fuel efficiency) and Scenario 2050H (2050 – hydrogen engines) is demonstrated by a presentation of several of the maps produced by the Contrail Model. The Contrail Model produced maps for each satellite overpass (179 in total). Presented here is one map per day for each Scenario (the map closest to 12:00 noon).

Each map has coloured boxes which indicate areas of "contrail density" (number of contrails per area) within a 0.25 degree latitude by 0.25 degree longitude grid cell. The colour of the box indicates the number of contrails on a "sliding scale" with dark blue or purple being the smallest density (smallest number of contrails in that particular area) at that time whereas red or dark red indicates the largest density at that time (for that map). The important thing to note is that in each of the samples, it can be seen that the contrail density (number of contrails) is increased from the baseline scenario to scenarios 2028K to 2050K and finally to Scenario 2050H.

7.3.8.1 January 10:

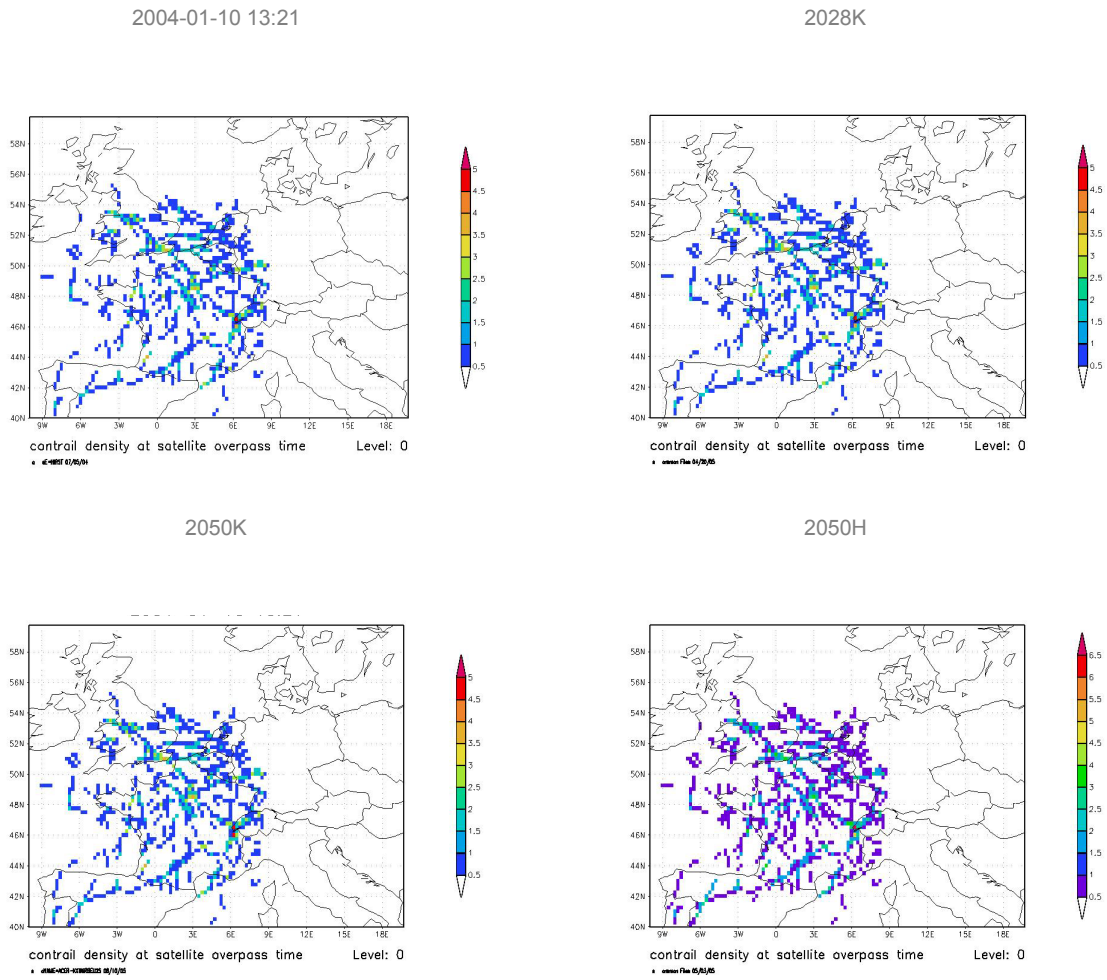

Figure 25: January 10: Baseline Scenario (Top Left), 2028K (Top Right), 2050K (Bottom Left), 2050H (Bottom Right)

7.3.8.2 January 20:

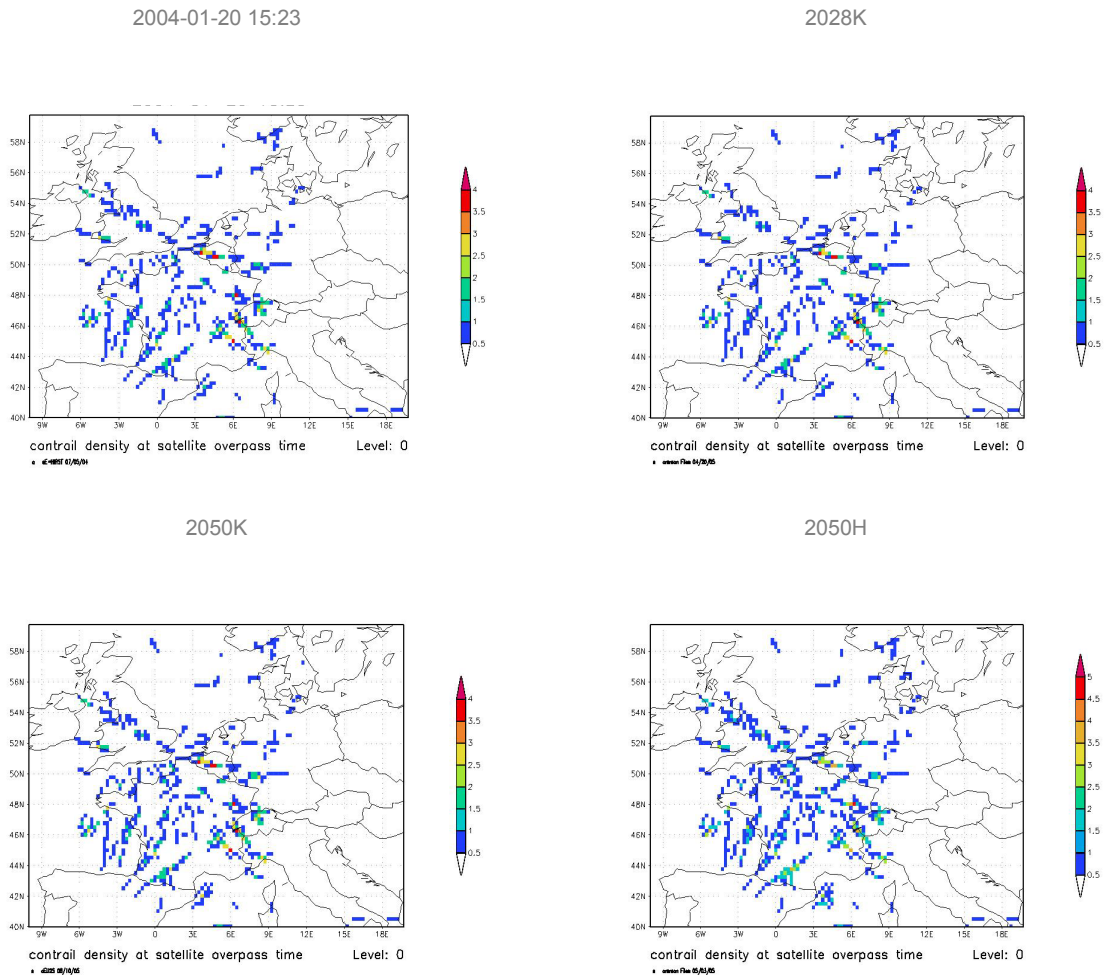

Figure 26: January 20: Baseline Scenario (Top Left), 2028K (Top Right), 2050K (Bottom Left), 2050H (Bottom Right)

7.3.8.3 February 11:

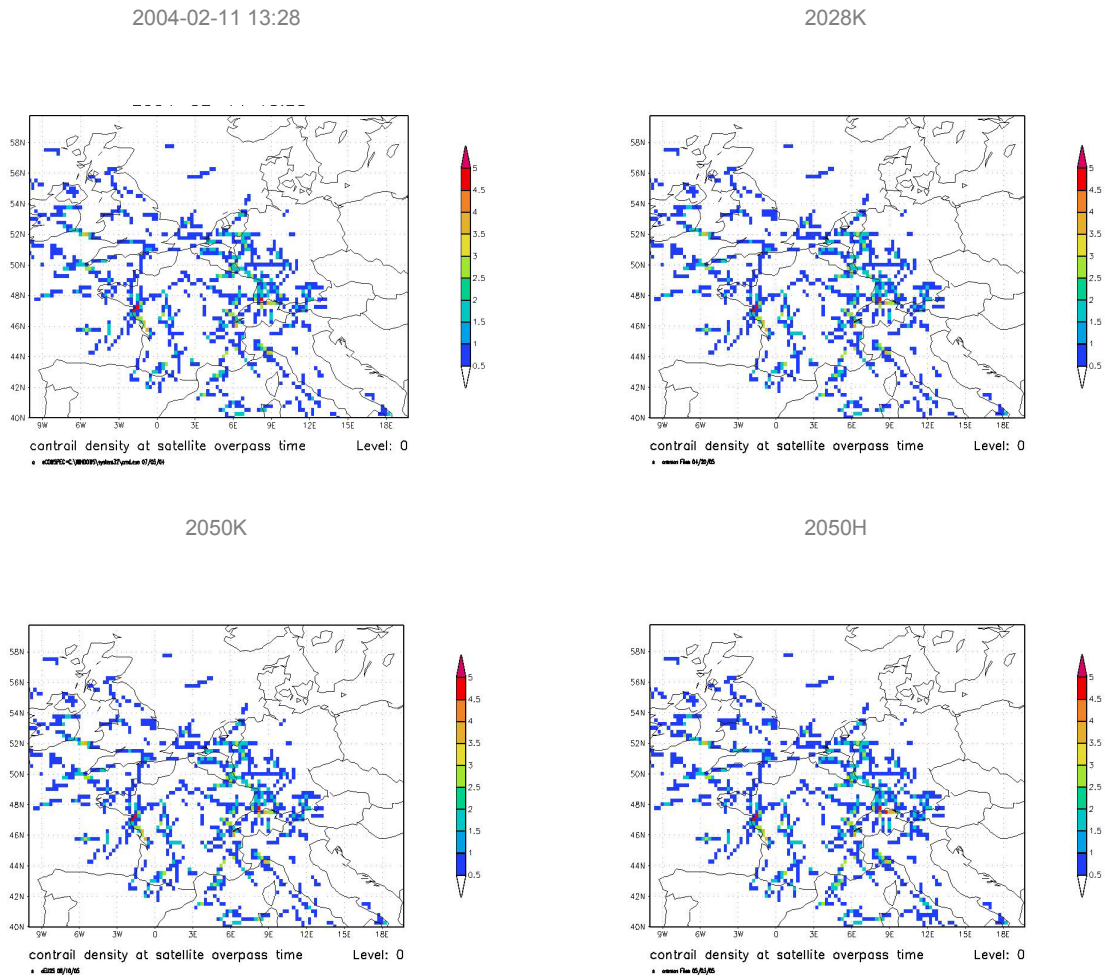

Figure 27: February 11: Baseline Scenario (Top Left), 2028K (Top Right), 2050K (Bottom Left), 2050H (Bottom Right)

7.3.8.4 February 26:

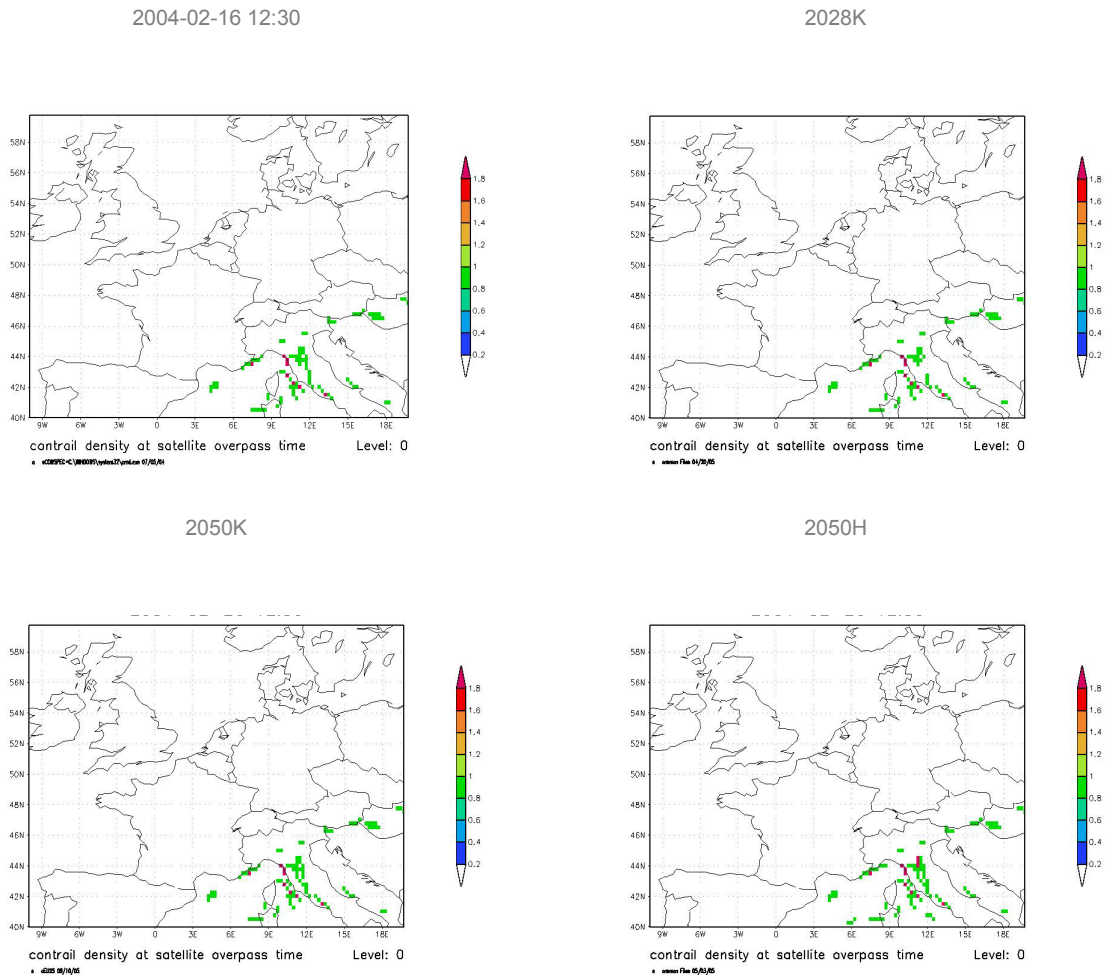

Figure 28: February 26: Baseline Scenario (Top Left), 2028K (Top Right), 2050K (Bottom Left), 2050H (Bottom Right)

7.3.8.5 March 08:

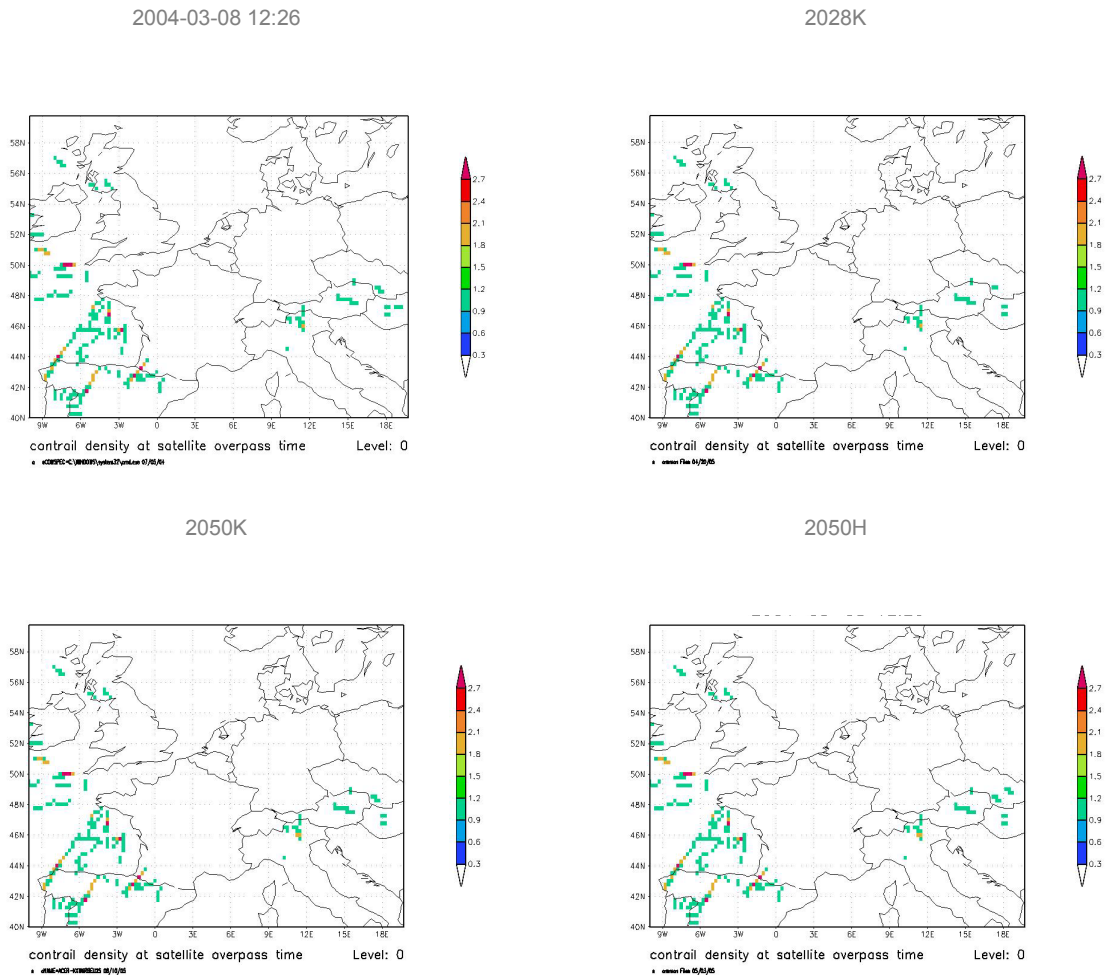

Figure 29: March 08: Baseline Scenario (Top Left), 2028K (Top Right), 2050K (Bottom Left), 2050H (Bottom Right)

7.3.8.6 March 18:

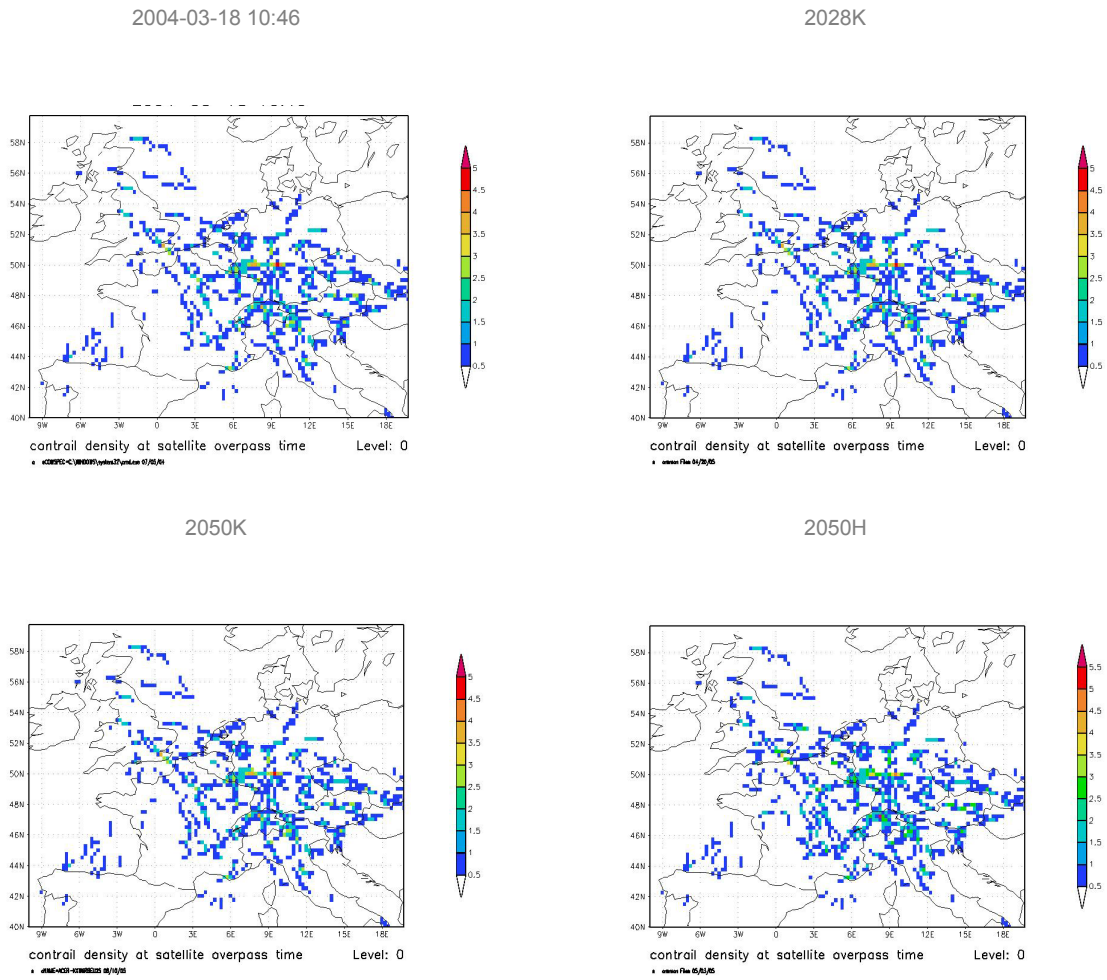

Figure 30: March 18: Baseline Scenario (Top Left), 2028K (Top Right), 2050K (Bottom Left), 2050H (Bottom Right)

7.3.8.7 April 22:

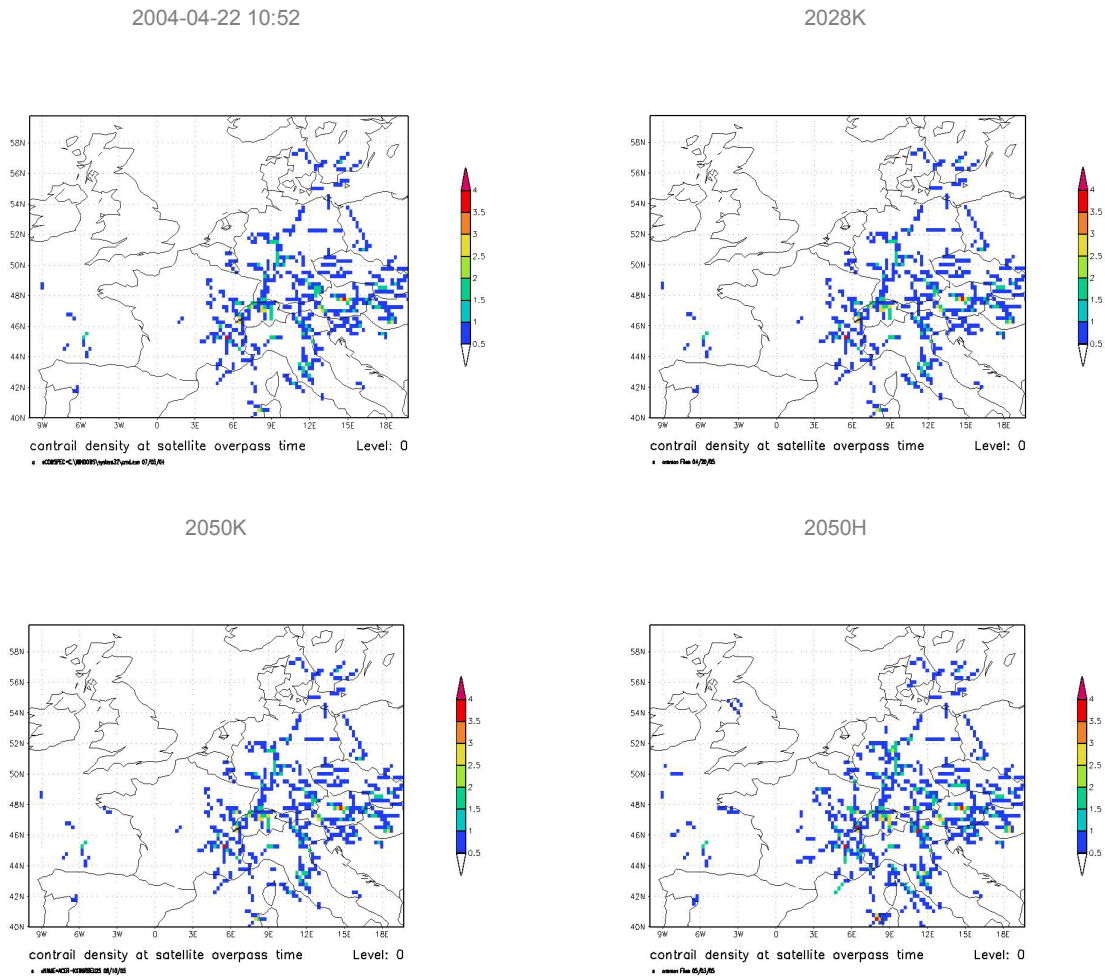

Figure 31: April 22: Baseline Scenario (Top Left), 2028K (Top Right), 2050K (Bottom Left), 2050H (Bottom Right)

7.3.8.8 April 29:

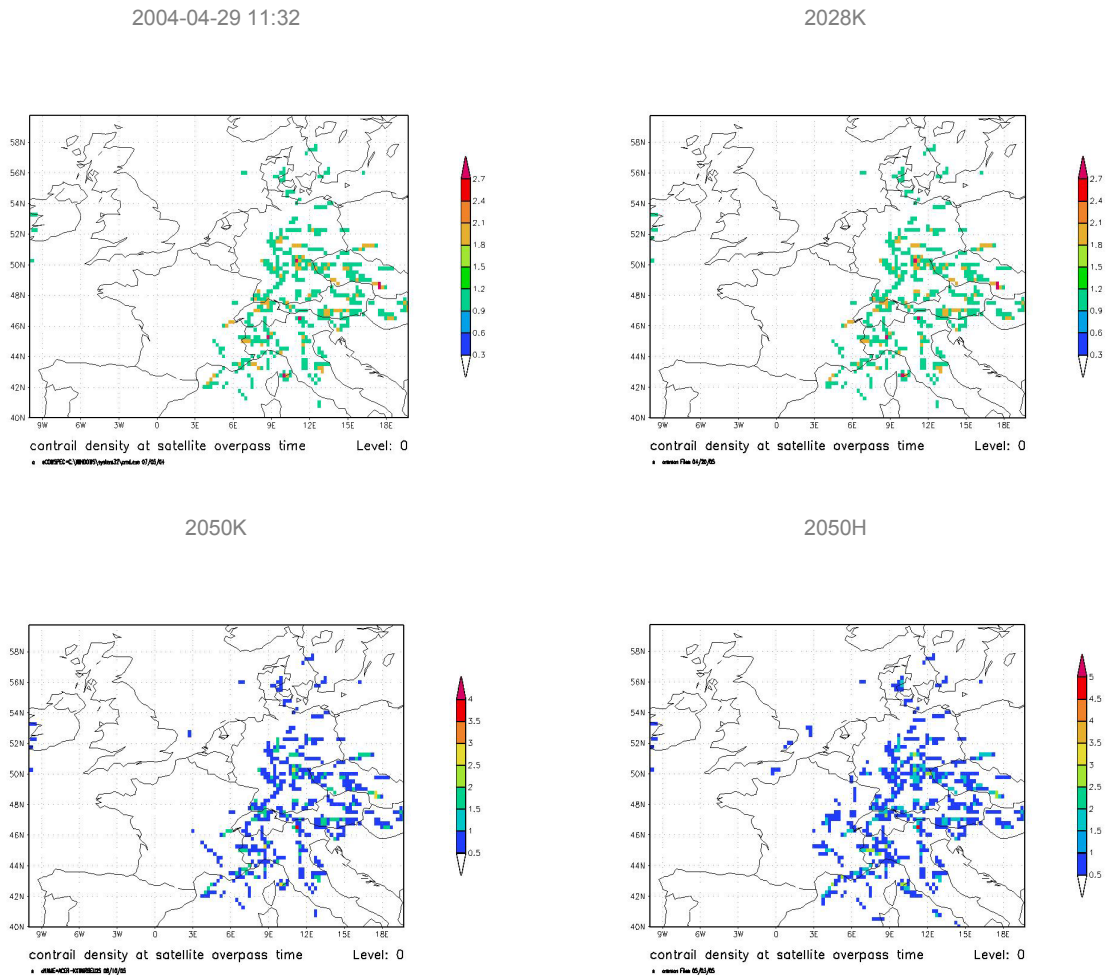

Figure 32: April 29: Baseline Scenario (Top Left), 2028K (Top Right), 2050K (Bottom Left), 2050H (Bottom Right)

7.3.8.9 May 17:

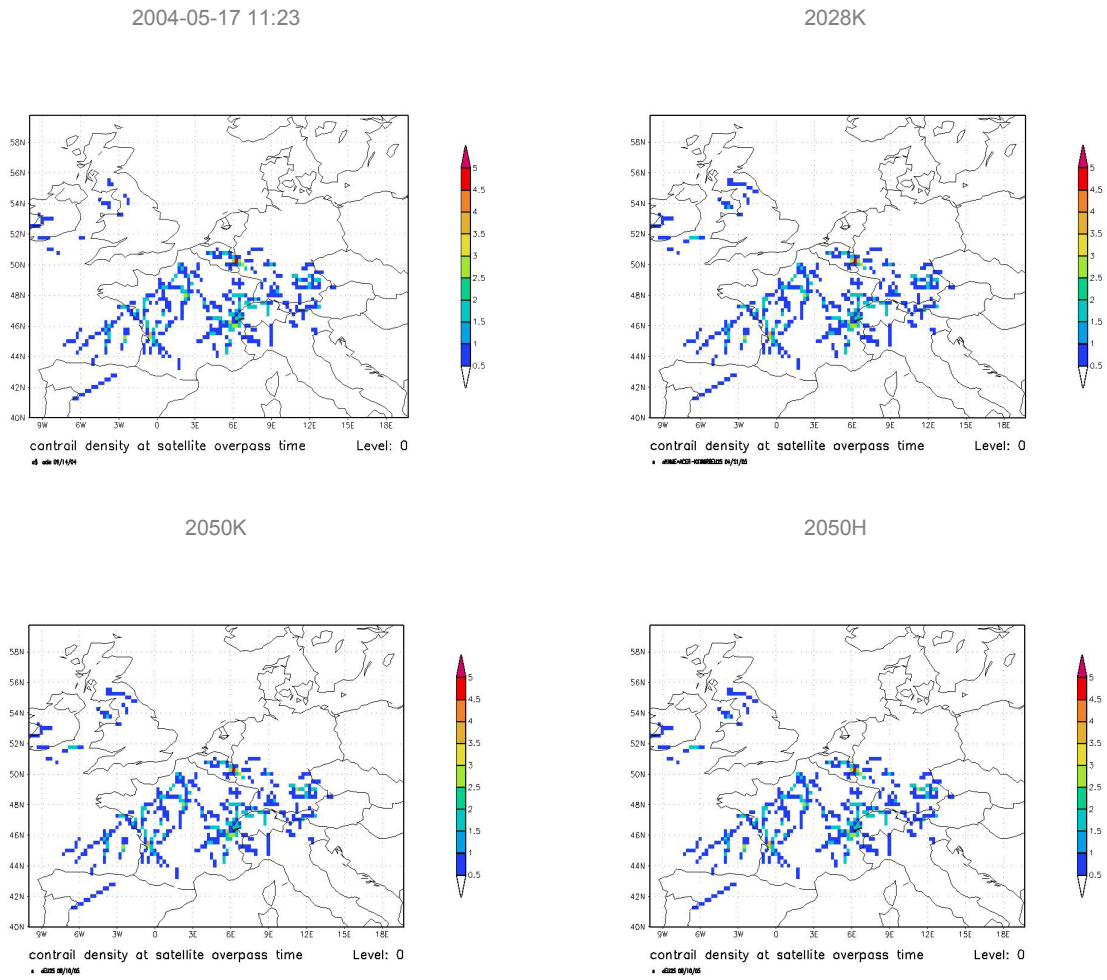

Figure 33: May 17: Baseline Scenario (Top Left), 2028K (Top Right), 2050K (Bottom Left), 2050H (Bottom Right)

7.3.8.10 May 28:

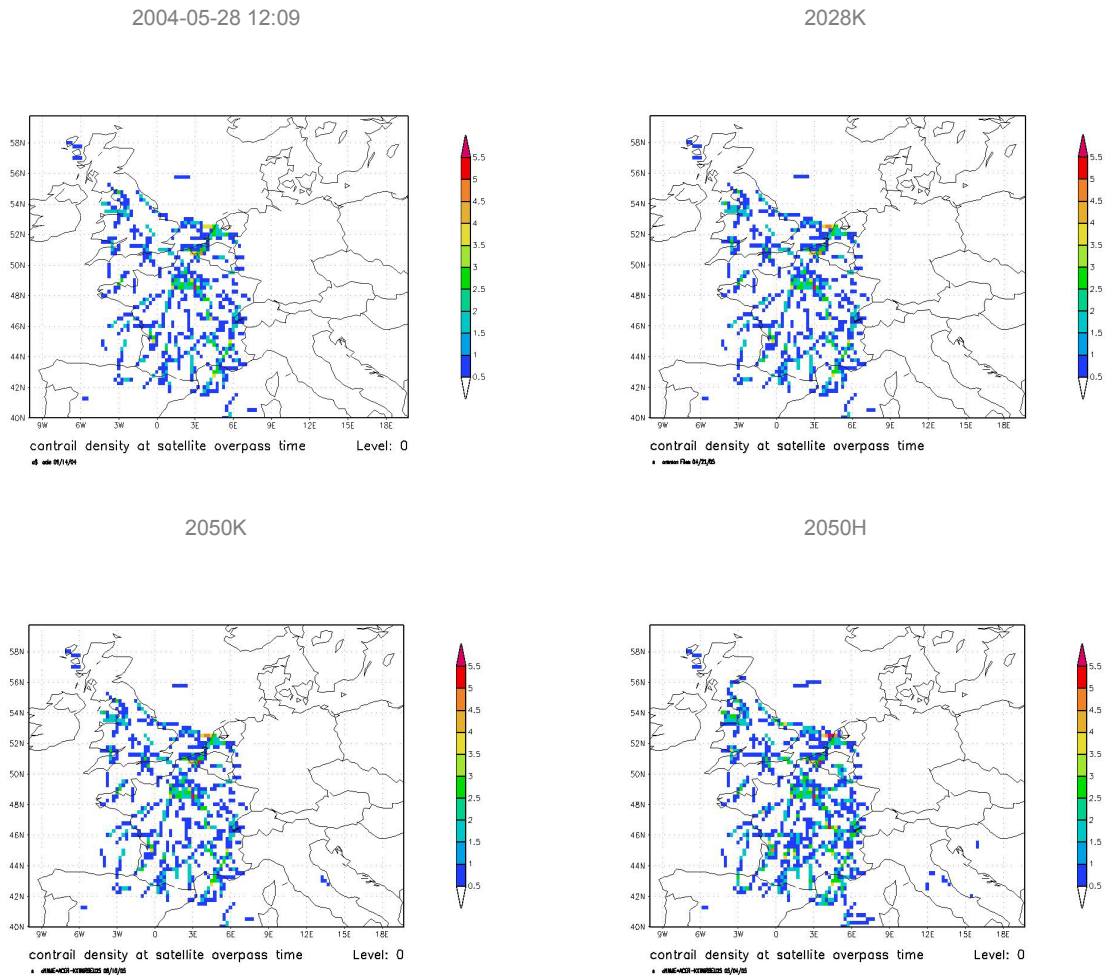

Figure 34: May 28: Baseline Scenario (Top Left), 2028K (Top Right), 2050K (Bottom Left), 2050H (Bottom Right)

7.3.8.11 June 01:

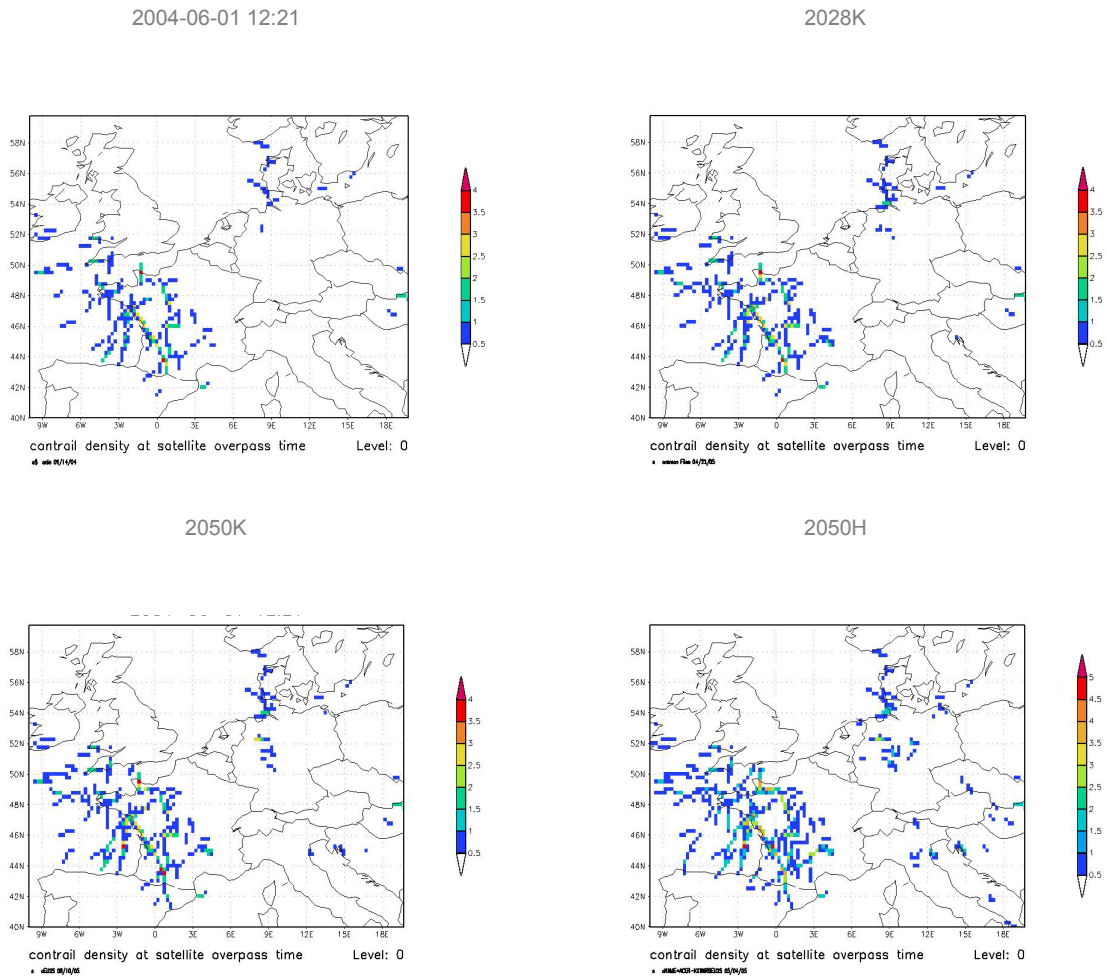

Figure 35: June 01: Baseline Scenario (Top Left), 2028K (Top Right), 2050K (Bottom Left), 2050H (Bottom Right)

7.3.8.12 June 22:

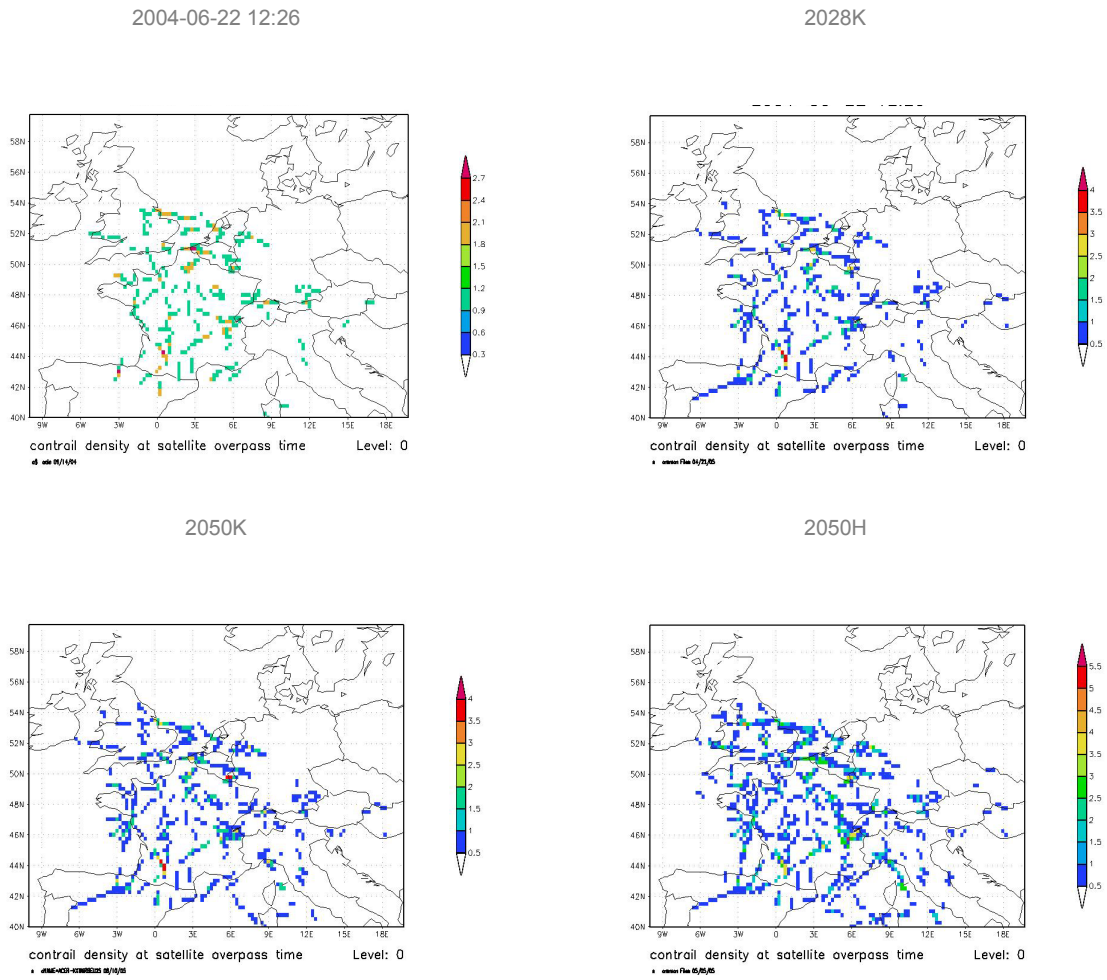

Figure 36: June 22: Baseline Scenario (Top Left), 2028K (Top Right), 2050K (Bottom Left), 2050H (Bottom Right)

7.3.8.13 July 01:

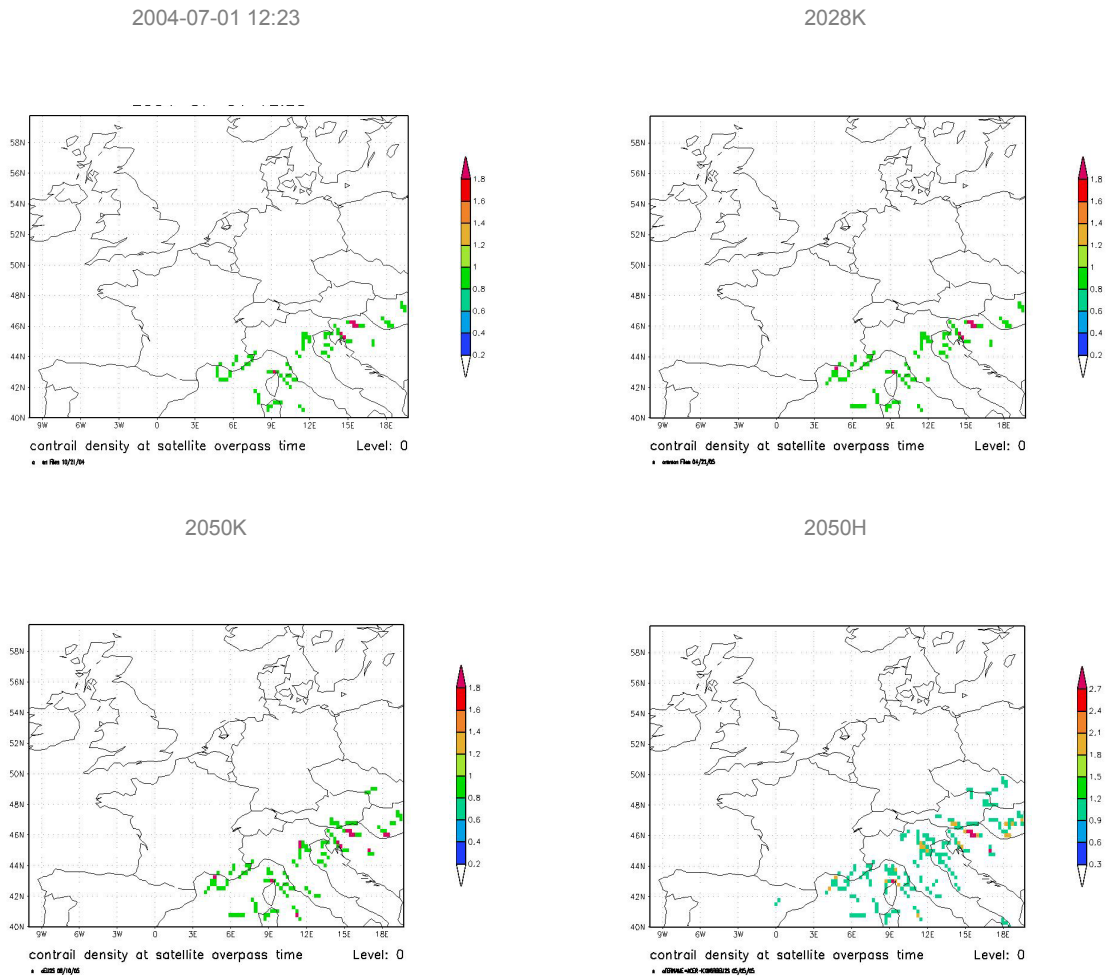

Figure 37: July 01: Baseline Scenario (Top Left), 2028K (Top Right), 2050K (Bottom Left), 2050H (Bottom Right)

7.3.8.14 July 24:

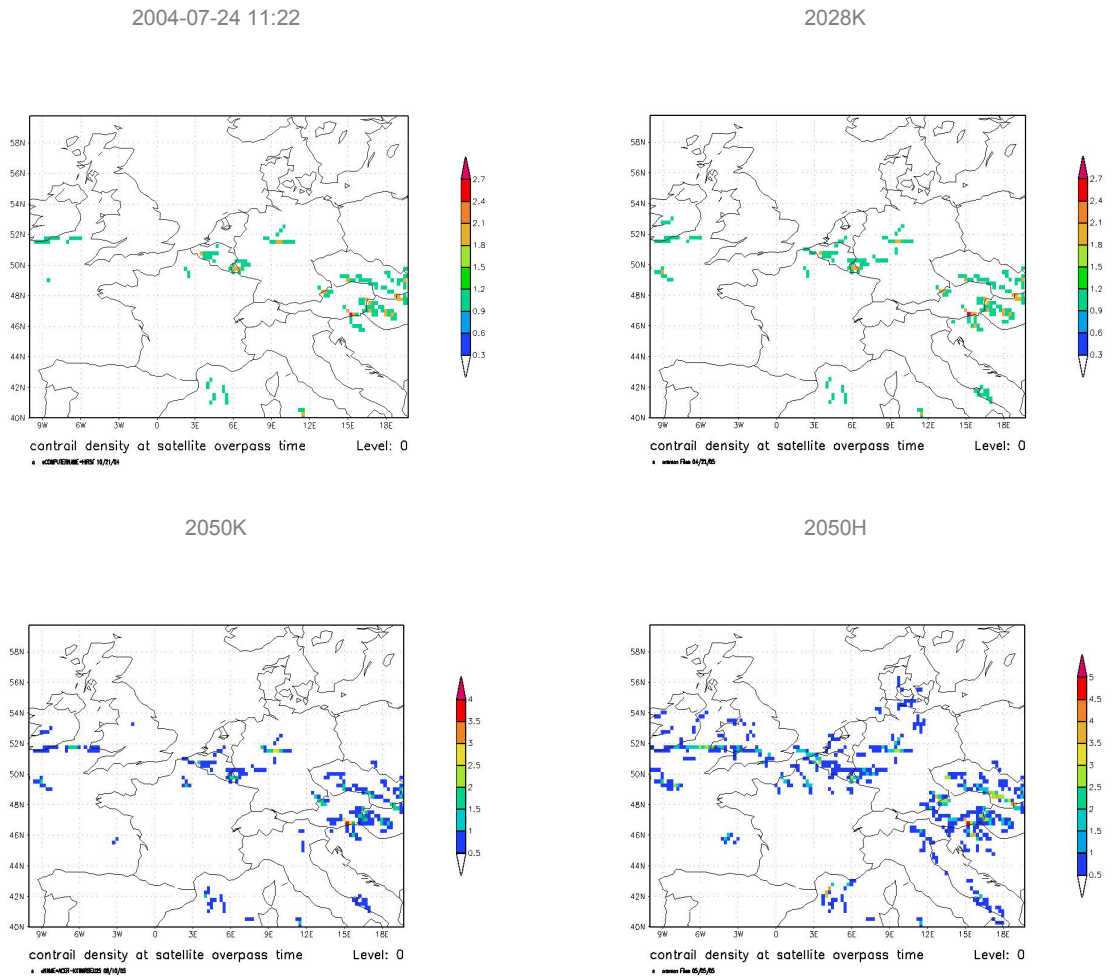

Figure 38: July 24: Baseline Scenario (Top Left), 2028K (Top Right), 2050K (Bottom Left), 2050H (Bottom Right)

7.3.8.15 August 01:

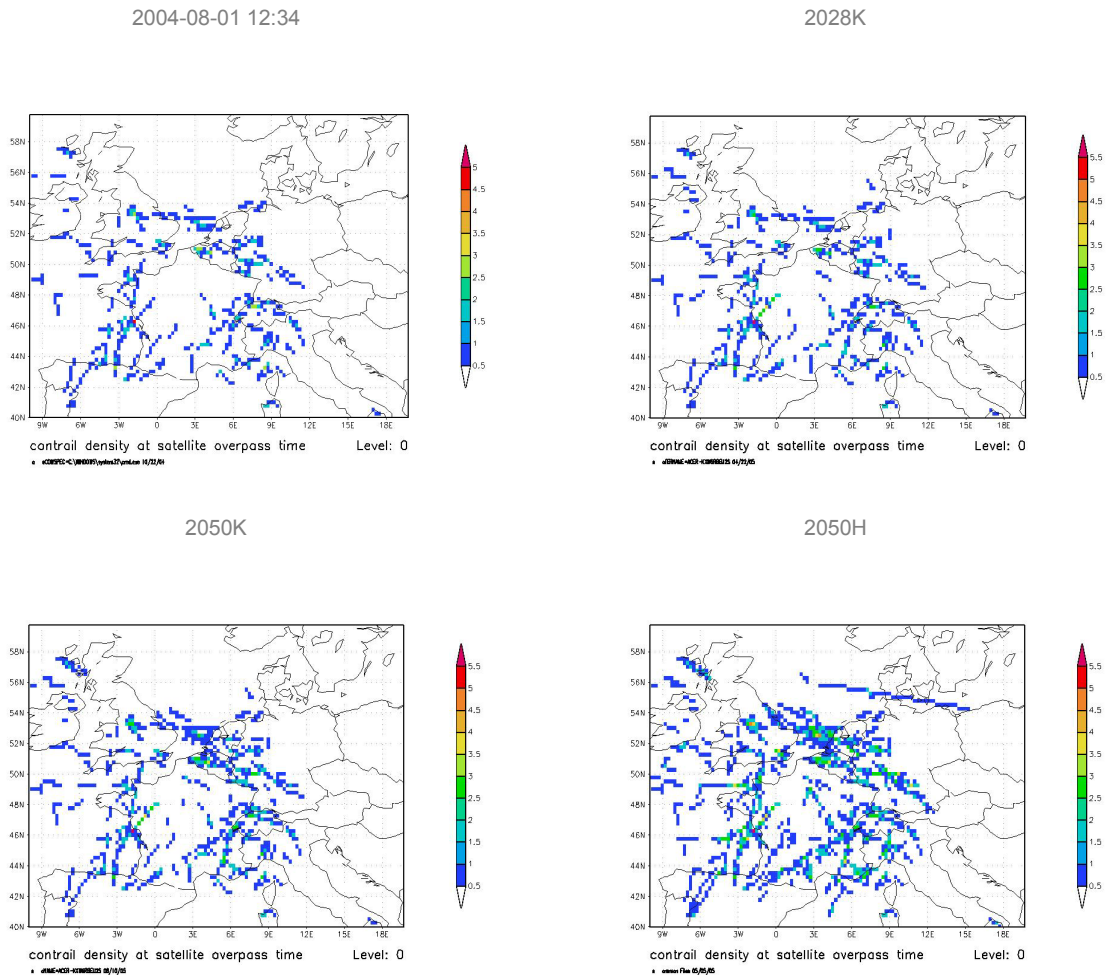

Figure 39: August 01: Baseline Scenario (Top Left), 2028K (Top Right), 2050K (Bottom Left), 2050H (Bottom Right)

7.3.8.16 August 31:

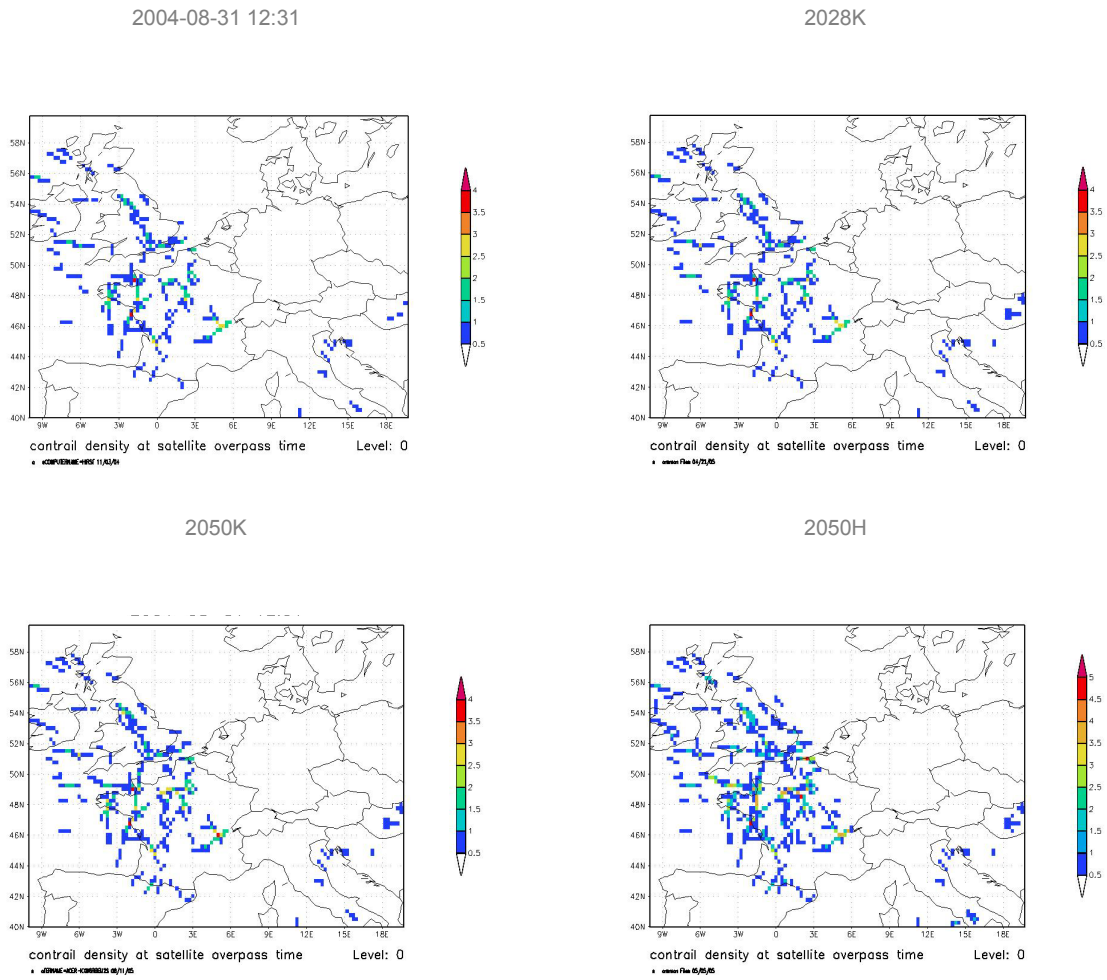

Figure 40: August 31: Baseline Scenario (Top Left), 2028K (Top Right), 2050K (Bottom Left), 2050H (Bottom Right)

7.3.8.17 September 11:

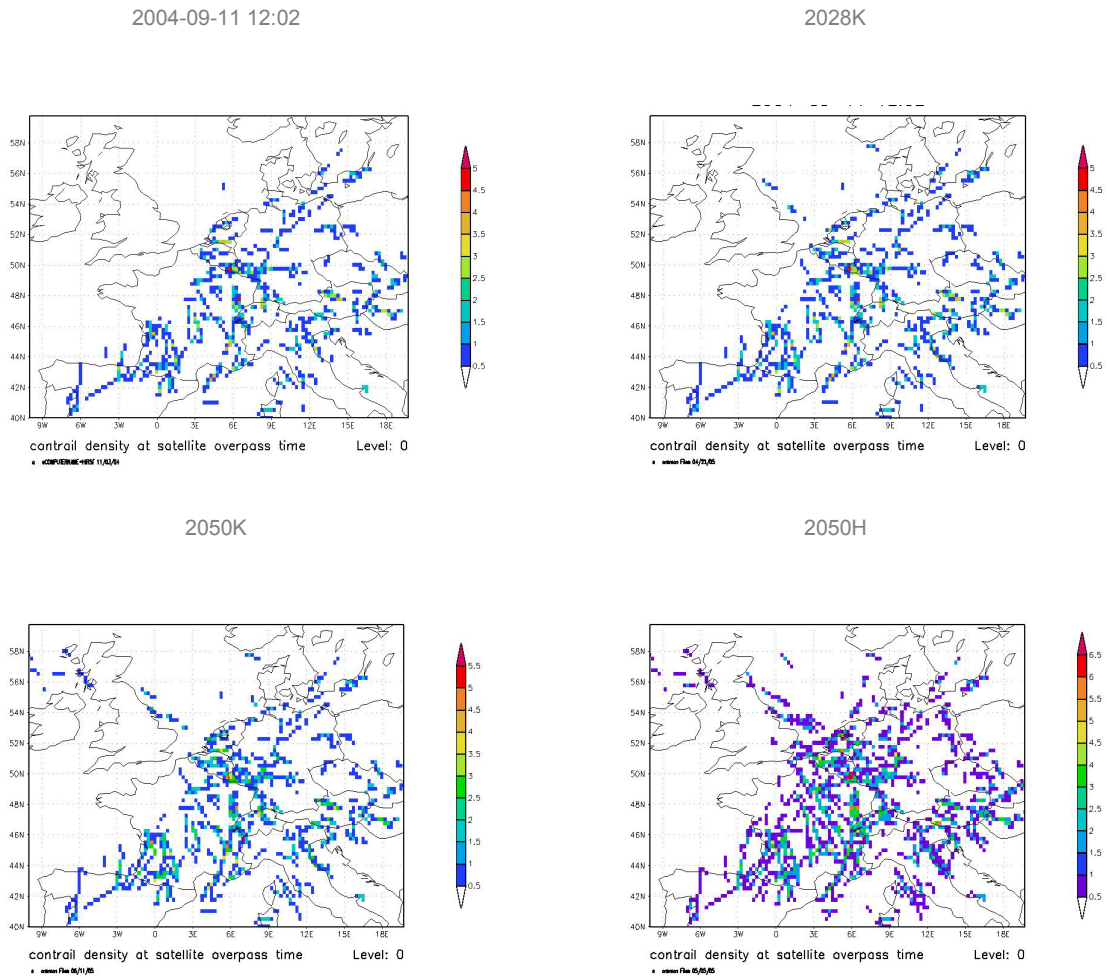

Figure 41: September 11: Baseline Scenario (Top Left), 2028K (Top Right), 2050K (Bottom Left), 2050H (Bottom Right)

7.3.8.18 September 17:

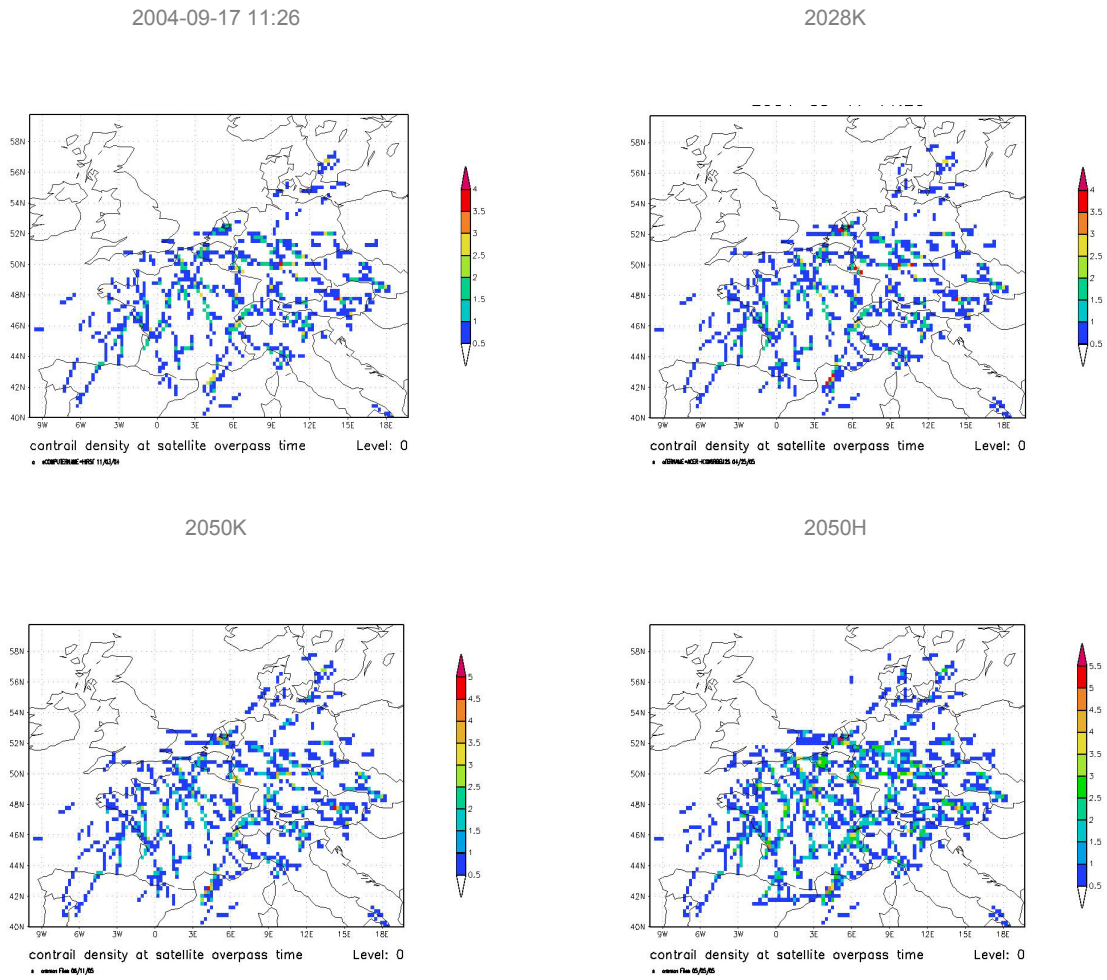

Figure 42: September 17: Baseline Scenario (Top Left), 2028K (Top Right), 2050K (Bottom Left), 2050H (Bottom Right)

7.3.8.19 October 03:

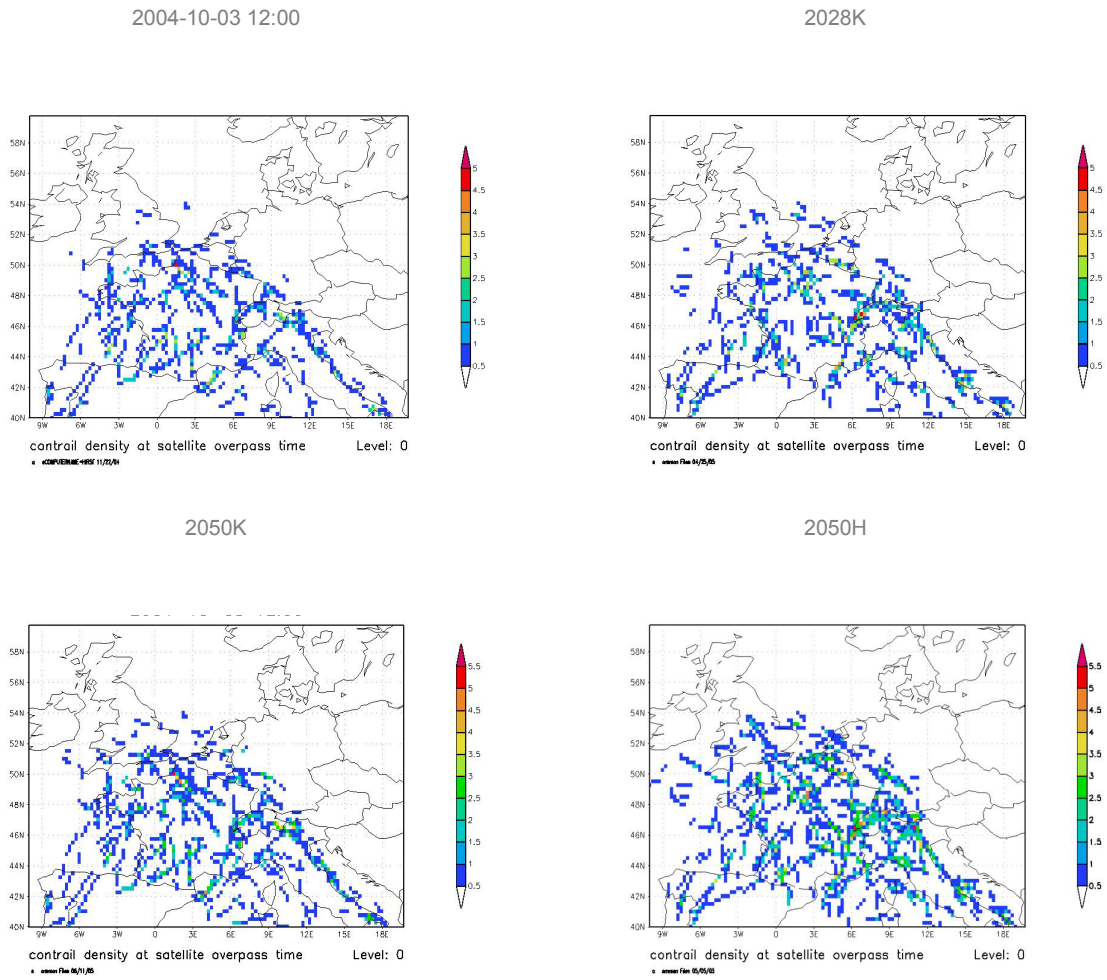

Figure 43: October 03: Baseline Scenario (Top Left), 2028K (Top Right), 2050K (Bottom Left), 2050H (Bottom Right)

7.3.8.20 October 18:

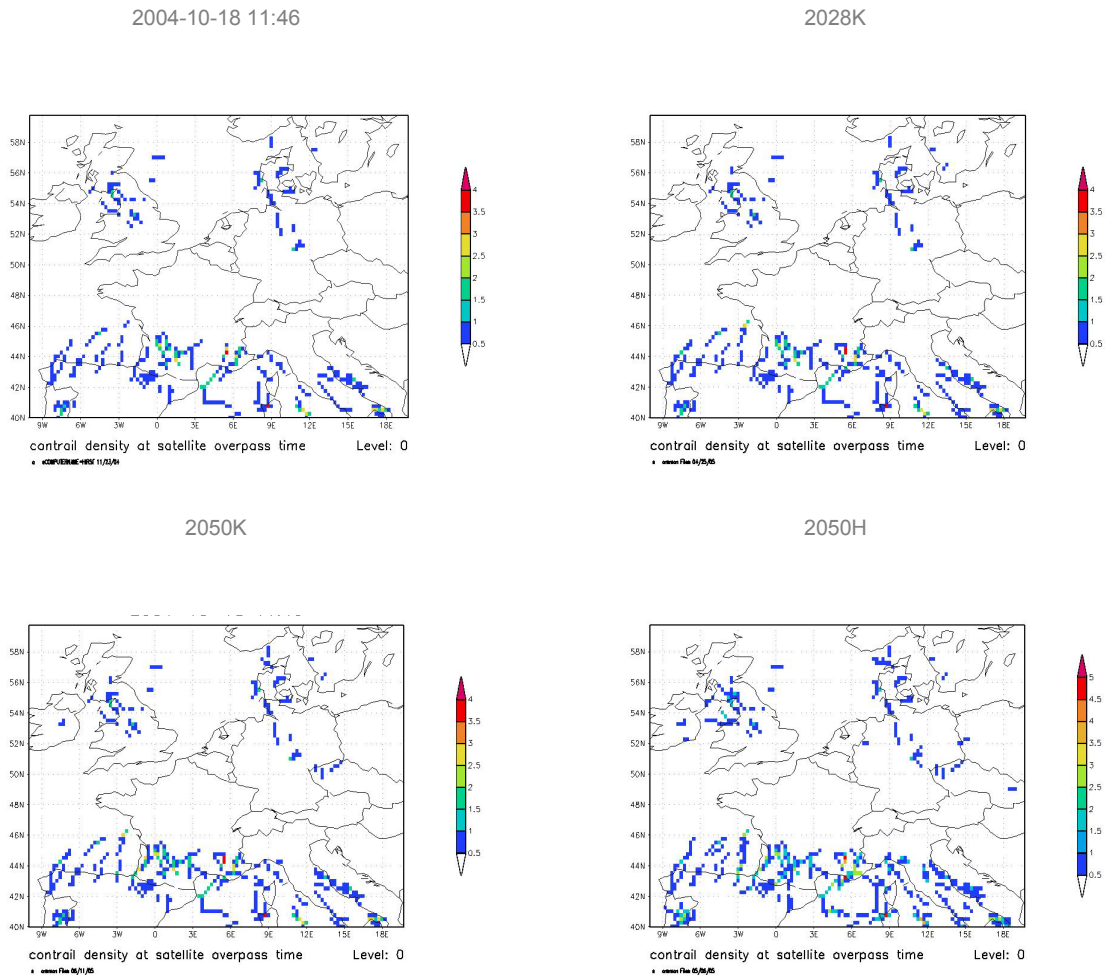

Figure 44: October 18: Baseline Scenario (Top Left), 2028K (Top Right), 2050K (Bottom Left), 2050H (Bottom Right)

7.4 Normalisation of emissions

An estimation of comparative environmental effects of future aircraft technologies requires a normalization of emissions. In other words, the impact of the different pollutants should be converted to comparable figures.

7.4.1 Global Warming Potential

The first idea was to use global warming potential (GWP) to normalize emissions. GWP is an index that relates the impact of emissions of a gas to that of emission of an equivalent mass of CO_2.

However, GWP do not appear to be a suitable index to normalize aircraft emissions in the scope in this study. As developed by IPCC ([Ref 3] chapter 6.2.2), "*GWPs were meant to compare emissions of long-lived, well-mixed gases such as CO_2, CH_4, N_2O, and hydrofluorocarbons (HFC) for the current atmosphere; they are not adequate to describe the climate impacts of aviation.*"

(…)

"*There is a basic impossibility of defining a GWP for "aircraft NO_x" because emissions during takeoff and landing would have one GWP; those at cruise, another; those in polar winter, another; and those in the upper tropical troposphere, yet another. Different chemical regimes will produce different amounts of ozone for the same injection of NO_x, and the radiative forcing of that ozone perturbation will vary by location.*"

In addition, "Climate Change 2001" ([Ref 33]) states that "*CO trend is very sensitive to the time period chosen. The value for 1996 to 1998 is +6ppb/yr. For the period 1991 to 1999, the CO trend was -0.6ppb/yr*". The value to use and the evolution within 2050 are thus difficult to predict.

Lastly, no explicit information on H_2O was found, while H_2O is a determining pollutant in this study.

In view of all these problems, derivation of GWP indices for emissions was not attempted in this study.

7.4.2 Shadow Cost

Failing GWP normalization, it was decided to use Euro (€) as a basis.

Environmental costs for carbon dioxide (CO_2), nitrous oxides (NO_x), and water vapour (H_2O) were established as follows:

- CO_2 is among the easiest to handle. Its levels are a constant rate of fuel consumption. Whatever the conditions, each kilogram of fuel burn generates 3.149 kilograms of CO_2. However, the long residence time of CO_2 in the atmosphere, around 100 years, makes it not straightforward to cost for the economists. Debates on the discount rate to use (reflecting at one extreme the preference for the present and at the other extreme the right for future generation to live in a "clean" environment) generate very wide ranges of cost estimates for CO_2.

- NO_x effects are more complex to assess. Actually, NO_x is not a greenhouse gas as such, but its presence in the atmosphere leads to:
  i) an increase in atmospheric ozone when released at altitudes around the tropopause[12],
  ii) a decrease in atmospheric ozone when released at higher altitudes, and
  iii) a decrease in methane (CH_4) concentration, which is a greenhouse gas.
  However, the opposite indirect effects of NO_x emissions on ozone and methane do not compensate, and on average, the net result probably contributes to warming the atmosphere. One should thus stay cautious in the interpretation of NO_x cost results.

- H_2O is, as CO_2, directly proportional to fuel burn. Each kilogram of kerosene fuel consumed generates 1.23 kilogram H_2O while each 0.36 kilogram of hydrogen fuel consumed (same energy content as 1kg of kerosene fuel, see section 5.6.1) generates 3.21 kilogram of H_2O. Water vapour is a greenhouse gas, but as its time residence in the atmosphere is short, and most of it is evacuated in the form of rain within one or two weeks.

  In a recent report ([Ref 34]), a wide review on the cost evaluation for CO_2 was performed (a dozen references were used). It was shown that both damage and prevention costs for CO_2 gave similar ranges, from a few Euros to around €100 per tonnes. Eliminating extreme values, the authors suggest an average of €30 per tonne, with a range of €10-50 to consider the uncertainties.[13]

  In the same report, a methodology to derive a cost for NO_x and H_2O emissions is proposed (based on IPCC simulation results on relative radiative forcing of each emission). It consists in computing the ratio of relative emissions on relative impacts. 1 kilogram of NO_x emitted in the atmosphere has the same impact as 132 kilogram of CO_2, and 1 kilogram of H_2O has the same impact as 0.28 kilogram of CO_2.

[12] The tropopause is the limit between troposphere and stratosphere, varying in function of the geographical locations, and roughly situated around 10 kilometres altitude, which corresponds to the subsonic aircraft cruise level.

[13] Value based on the comprehension of cost of H_2O as published in IPCC ([Ref 3]). This cost may increase if the hypothesis put forward by NASA ([Ref 18]) and DLR ([Ref 19]) is confirmed (see section 3.3).

As the three emissions can now be expressed relative to each other in terms of environmental impacts, one can easily translate values found for CO_2 to H_2O and NO_x.

Specie	Low	Recommended	High
CO_2 (€ per tonne)	10	30	50
H_2O (€ per tonne)	2.8	8.3	14
NO_x (€ per tonne)	1300	4000	6600

Table 21: Values of emissions resulting from their relative impacts – CO_2, H_2O, NO_x

Note that "Recommended" figures correspond to IPCC 1992 cost factors.

In addition to the detailed investigations which lead to the validated results of Table 21, a study carried out in 2004 aimed at estimating emissions cost as indicated in the literature to deduce "averaged" values.

Result ranges for pollutants not covered by Table 21 are the following:

Specie	Low	Recommended	High
CO (€ per ton)	104	142	205
HC (€ per ton)	2569	5543	8518
SO_x (€ per ton)	2110	6094	11133

Table 22: Values of emissions resulting from their relative impacts – CO, HC, SO_x

As they are not published yet, figures in Table 22 are to be used with caution. They attempt only to give a trend in the scope of this study.

Moreover, costs indicated in Table 21 and Table 22 are valid in 2004 (i.e. for baseline). They are used as comparative values between hydrogen and kerosene in 2050, but should NOT be considered as absolute figures for future scenarios.

Fuel is a key budget item for airlines. Nevertheless the cost for fuel was not estimated in this study since (not exhaustive list):

- The cost for kerosene fuel is highly dependent on the dollar exchange rate. In 2004, it was assumed to be €342 per tonne with a range of €279 to €454 per tonne. With such disparities on baseline and with a very hypothetic evolution of the dollar's exchange rate in the next 45 years, the estimation of kerosene cost in 2050 is considered as hazardous in the scope of this study.
- Fuel shortage may induce exponential prices of fuel in the future, affecting fuel cost predictions.

- As fuel becomes scarce, aircraft technology may have recourse to synthetic kerosene. The price of production/purchase of synthetic kerosene is not known at this time. Neither can estimates be made of the date of introduction of synthetic kerosene, nor of the portion of the future fleet using synthetic kerosene compared to conventional kerosene use.
- The future price of hydrogen fuel and the cost of liquid hydrogen production are not established at this time. The future production method for liquid hydrogen has not been established either. The consideration of ecology in the production of hydrogen may influence the price.

7.4.3 Hydrogen vs. kerosene in 2050

Based on the cost of emissions in 2004, Figure 45 plots the yearly cost of 2050 emissions for both kerosene and hydrogen technologies (one line per emission). "Low" and "high" values correspond to the bottom and top of each vertical line. Horizontal dashes indicate "recommended" values (as defined in Table 21 and Table 22).

Only one scenario was considered for each emission: when the study indicates two extreme masses of emissions, the averaged mass was used in the plots. In other word, the only parameter fluctuating in the section is the estimation of emissions' cost.

Note that, even if plotted for readability reasons, CO[14], HC, CO_2 and SO_x emissions out of hydrogen engines are equal to zero.

[14] Assumption: CO and HC emissions for 2050 were not estimated in this study. Nevertheless, the value for 2028 was used on Figure 45 and Figure 46. Is was assumed that, as the cost of CO and HC emissions is very low regarding decisive pollutants such as CO_2 and H_2O, the error on CO and HC evolution between 2028 and 2050 is negligible in this section. Even if slightly overestimated, CO and HC costs indicated in the following figures give correct trends.

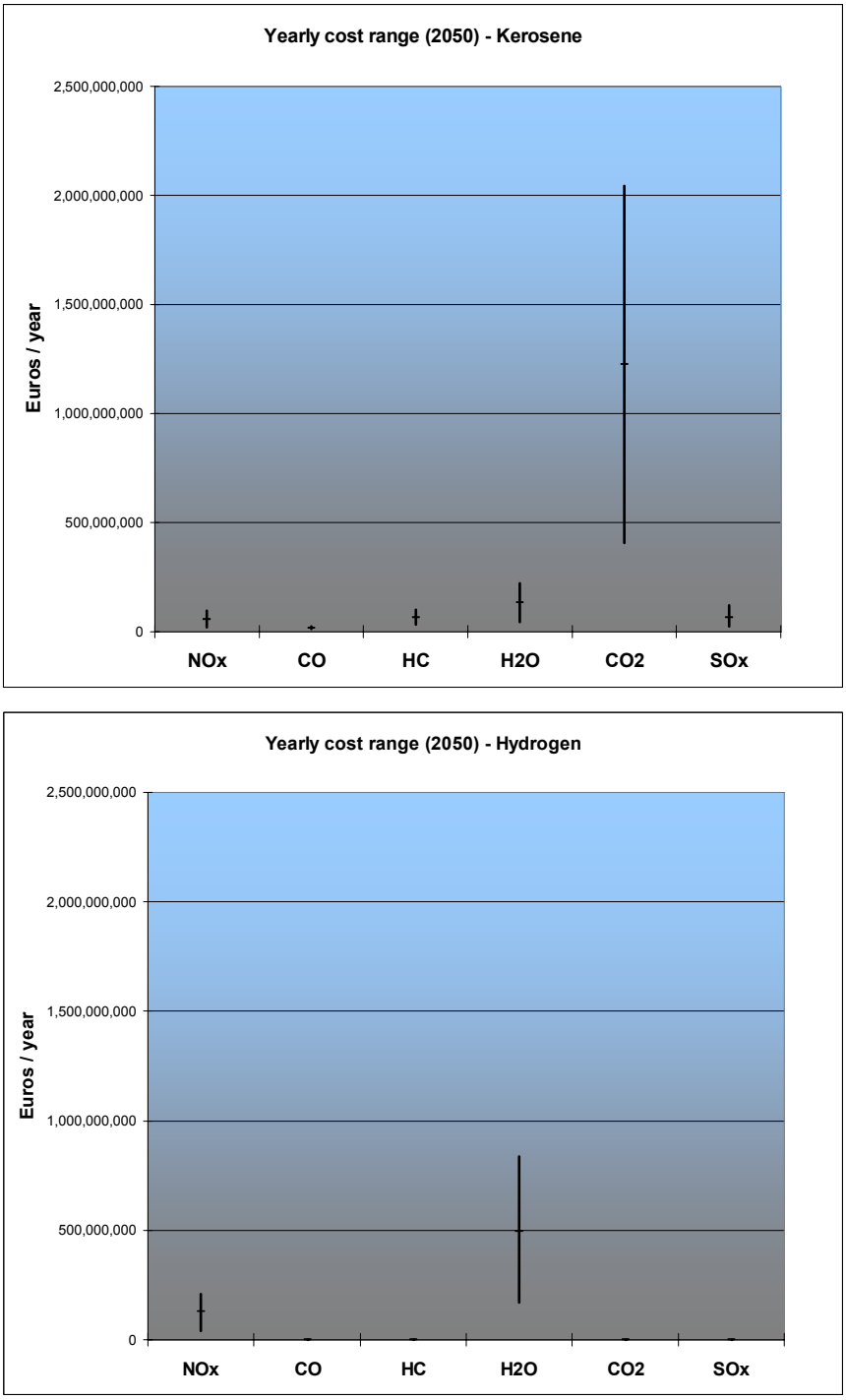

Figure 45: Yearly emissions cost range for kerosene and hydrogen technology (2050)

As expected, CO_2 is highly penalizing to kerosene engines while H_2O from hydrogen engines is the second most expensive emission.

NO_x is the second penalizing emission for both technologies but reads much higher for kerosene engines.

If emission costs are cumulated, Figure 46 is obtained. For each plot, "low", "recommended" and “high” cost estimates are given.

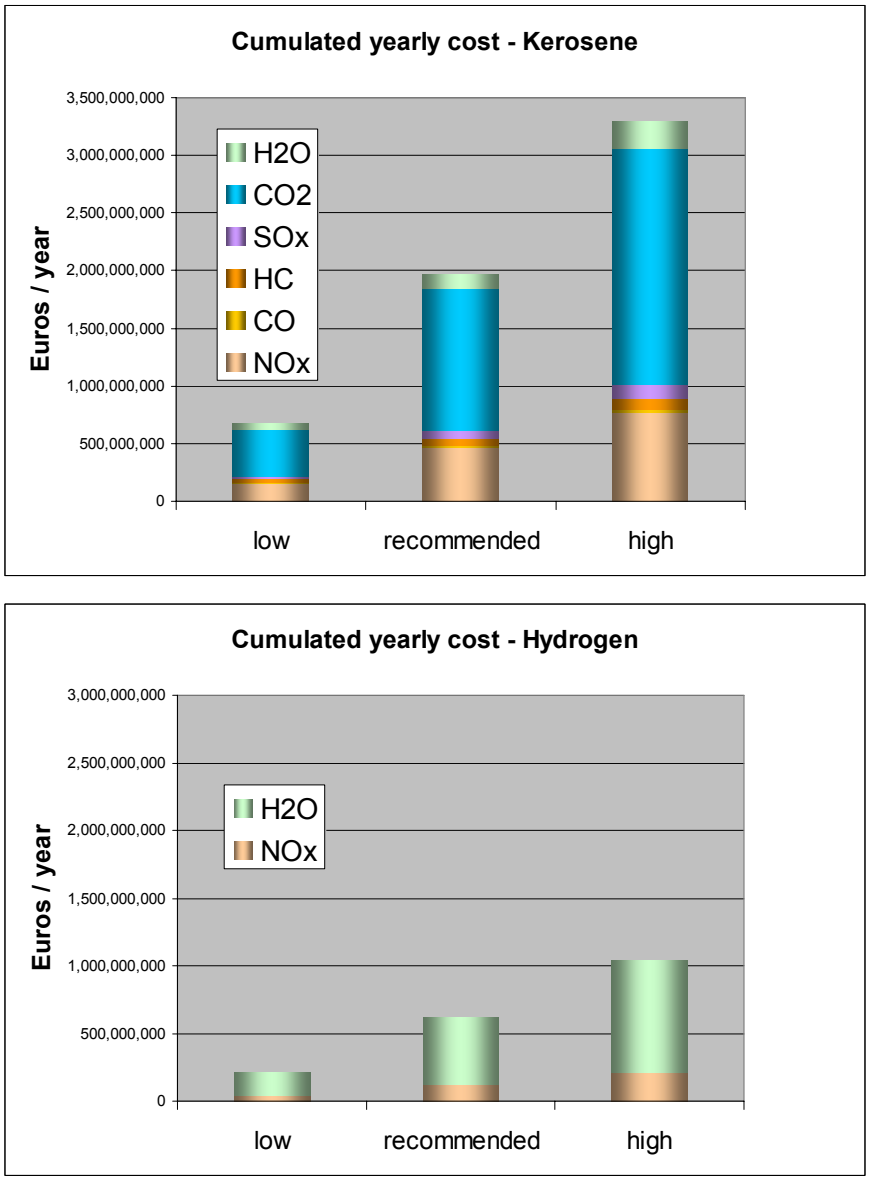

Figure 46: Cumulated yearly emissions costs for kerosene and hydrogen technology (2050)

A visual comparison of 2050 emissions costs for kerosene and hydrogen technology seem to indicate that hydrogen technology is 3 times more environmental friendly than kerosene technology. Moreover other emissions not addressed in this study (ozone, methane, etc) penalize kerosene engines.

Nevertheless these results are complete only if the following items are kept in mind:

- Emissions produced during hydrogen's production process are not known, since they will depend on the mode of production adopted/developed. Such emissions would be exhausted at ground level, as opposed to kerosene's exhaust emissions. As the same pollutant does not have the same effect depending on the altitude of production (see section 4 and references indicated in section 4), the impact on environment would be bound up with both quantities and type of emissions produced. These highly probable emissions would have an additional cost not estimated here, hanging over hydrogen's technology.
- The impact of H_2O seems to be underestimated (see section 3.3). Indeed, if the direct impact of H_2O emissions is more and more precisely estimated, the actual impact of contrails is clearly not mastered by the scientific community. The additional impact of contrails would probably disadvantage hydrogen technology. If, as suggested by [Ref 18] and [Ref 19], it turns out that the impact of H_2O emissions is more important than the overall impact of the sum of all other greenhouse gases, the trend could even be reversed into kerosene's favour.
- The probable use of synthetic kerosene (produced from natural gas, coal, residue from petroleum, biomass, etc.) in the future may improve kerosene engines from an environmental point of view, even if the production of synthetic kerosene would generate emissions at ground level. Indeed synthetic kerosene could be enhanced in order to meet higher environmental performances.

As a conclusion, Figure 46 has to be interpreted with caution since the study does not consider all the parameters necessary to draw conclusions, especially in term of hydrogen production process. Limitations mentioned above have to be considered when presenting Figure 46.

7.5 Conclusion of 'output data analysis and results'

This section addressed two possible future evolutions of fuel burn and emission based on two extreme scenarios:

- No hydrogen aircraft,
- Replacement of all the fleet by hydrogen aircraft.

Based on the results of this study, the second item seems to lead to a better situation in term of environment by the year 2050. Nevertheless limitations mentioned all along section 7 (and especially in section 7.4) have to be kept in mind.

In reality, the whole fleet will probably not be hydrogen powered. Only a portion of aircraft may be converted to hydrogen while other aircraft may be powered by other kinds of fuel, whether conventional or synthetic kerosene. Bi-fuelled aircraft could also be developed if extra weight due to dual technology is not a handicap.

Moreover the evolution from kerosene to hydrogen powered aircraft will depend on the category of aircraft (i.e. commercial, business, military, size of aircraft, etc), as discussed in Annex 3.

Anyway the situation in the future will probably correspond to a mix between the two scenario assessed in this study, unless a brand new technology is discovered.

Intentionally left blank

8 OUTPUT SENSIBILITY ANALYSIS

This chapter aims to indicate the level of confidence in the absolute figures obtained by AEM3 for the baseline results of this study. The results depend strongly on the quality of the input data, the quality of the underlying databases for engines, aircraft performance and fuel burn, and the realism of the applied methods to estimate the emission output in the AEM3 model. For a more detailed analysis of the level of confidence in AEM3, see "AEM3 Validation Report" [Ref 24].

Note that this entire section is valid for kerosene aircraft only. Results linked to hydrogen aircraft are based on the state of the art as documented in the literature.

Sensibility analysis of the cost assessment was carried out previously in section 7.4 and is not repeated here.

8.1 CO_2, H_2O, SO_x estimation with AEM3

The emissions for CO_2, H_2O and SO_x are directly proportional to the fuel burn. Any error level estimated for the fuel burn estimation will propagate, for that reason, for exactly the same level, into the results for those pollutants. The emission coefficients representing the degree of proportionality between fuel burn and the above pollutants were based on an in-depth literature review [Ref 22]. There is only a slight variation for those coefficients in the different literature sources, and the values applied for this study have been qualified reasonable by a variety of domain experts.

Pollutant	Current Study	Max	Min	Max %	Min %
	(kg/kg fuel)			(%)	
CO_2	3.149	3.22	3.1	2.25	-1.56
H_2O	1.23	1.25	1.17	1.63	-4.88
SO_x	0.00084	0.0012	0.000267	42.86	-68.21

Table 23: Variation in published coefficients for fuel proportional emissions (%)

The above table indicates the variation for the different coefficients in the different literature sources compared to the coefficients applied in this study. The variation indicates at the same time the level of error, which may apply to the results through the emission coefficients used for CO_2, H_2O, and SO_x estimations of this study.

It has to be reminded that the effect of H_2O emissions on the environment may be much higher than stated by IPCC (see [Ref 18] & [Ref 19] and Figure 6 of section 3.3). The maximum value of radiative forcing of cirrus clouds due to H_2O emissions is highly uncertain and needs more investigation from scientific community before any meaningful sensibility analysis can be carried out.

8.2 NO_x, HC, CO estimation with AEM3

The estimation of the level of realism for the NO_x, HC and CO emissions calculated by AEM3 is based on information available from several other research projects, since real data for validation purpose is not available directly.

Note that VOC and TOG are assumed to be proportional to HC[15] and therefore suffer from the same level or error and sensibility as HC.

8.2.1 NASA study

A NASA study [Ref 23] provides an internal distribution between NO_x, CO and HC for a total mission (Taxi-Out to Taxi-In) of a B757-200, for standard mission ranges of 400 and 3000 nautical miles:

- NO_x 90 to 72.5%,
- CO 25 to less than 10%,
- HC 2.5 to less than 1%.

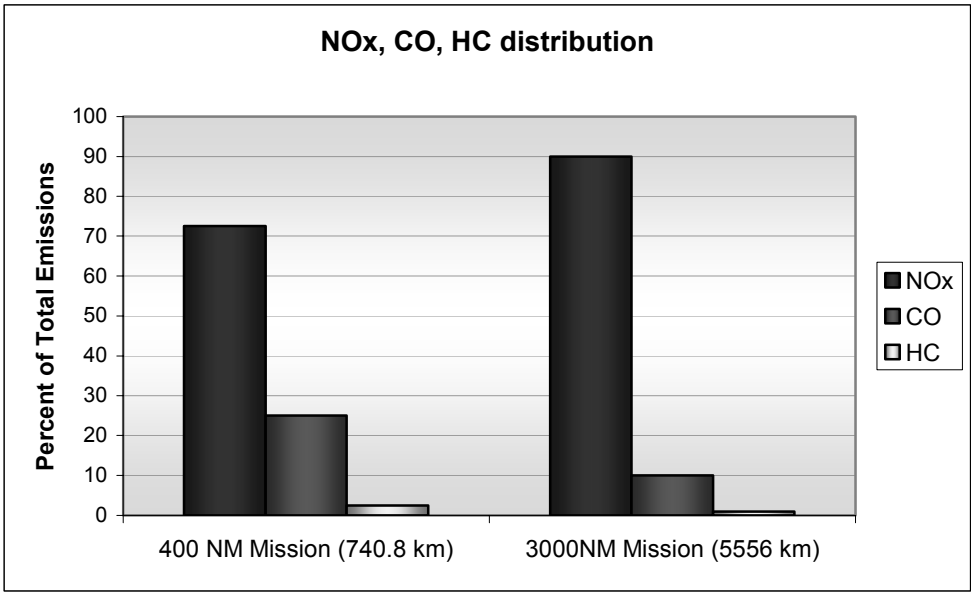

Figure 47: Emissions Comparison of 757-200 for 400 NM and 3000 NM Mission

[15] VOC and TOG are based on e.g. average US EPA chemical specification factors for jet engine emissions, but they can vary between engines and for different fuel compositions of kerosene.

By comparison, Figure 48 represents the distribution of average NO_x, CO and HC in the total emissions for the current study (2004's scenario), for an average mission range of 750km.

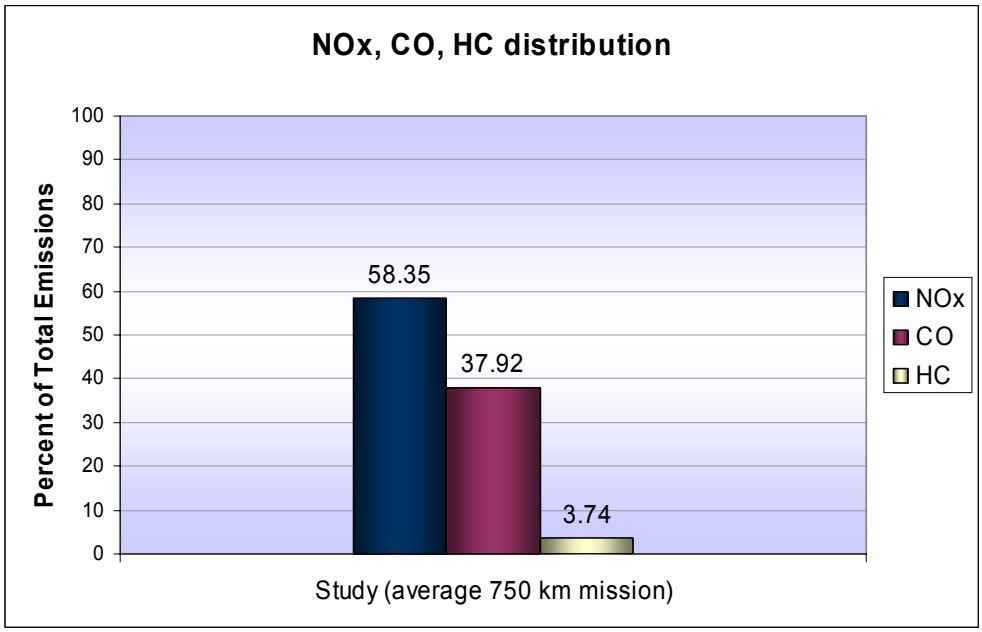

Figure 48: Emissions Comparison of overall traffic for Baseline and FL-Limited scenarios

The distributions for the current study and the reference information published by NASA have the same trend. Nevertheless, the proportion of NO_x is significantly lower in this study. This phenomenon is mainly due to the fact that unlike NASA's traffic used for estimations, flights in the study are not necessarily complete.

NO_x is mainly exhausted during climb and cruise phase (high engine trust setting) while CO and HC are characteristic from descent phase (low engine trust setting). In the data set under study, a portion of flight is missed at low level, especially take-off and climb-out phases where a lot of NO_x is emitted. In parallel, even if CO and HC exhausted during landing phase are ignored, the significant amount of CO and HC emitted at high level, when aircraft begin the descent phase, are part of the study. The proportion of CO and HC taken into account in this study is thus relatively higher compared to the NO_x proportion, as reflected by Figure 48.

The "AEM3 validation report" [Ref 24] confirmed that the distribution given by AEM3 for complete flights and nominal engine use is of high realism and very close to NASA's distribution.

8.2.2 NOx average emission indices from ANCAT and NASA inventories

NASA and ANCAT researchers analysed the NO_x emissions estimation for larger traffic samples. They put the calculated amount of NO_x emissions in relation to the estimated amount of fuel burn by those traffic scenarios, to obtain an indication for average NO_x Emission Indices. This analysis led to the following estimations for average NO_x Emissions Indices ($EINO_x$) in g per kg fuel burn:

	ANCAT 1A	ANCAT 2	NASA	NASA
	1992	1992	1990	1992
Horizontal resolution (°)	2.8 × 2.8	1 × 1	1 × 1	1 × 1
Vertical resolution (km)	1	1	1	1
$EINO_x$ (g/kg)	16.8	13.7	10.9	11.1

Table 24: Published average $EINO_x$ (g/kg fuel) of reference projects [Ref 25]

ANCAT 1A results were obtained using a thermodynamic NO_x emission model. This model was replaced during ANCAT 2 by the DLR NO_x estimation method. NASA results are based on Boeing Method 1 and Method 2.

A comparison by Rolls-Royce experts between the Boeing Method 2 and the DLR NO_x emission method indicates a difference of 3.6 %, with the DLR method giving the higher NO_x estimation.

The results published in the present report are obtained using AEM3, which applies a modified version of Boeing Method 2 (see Annex 1 "Boeing method 2 – EUROCONTROL Modified"). The modification compared to the original Boeing Method 2 covers a correction in the formula to correct for humidity at flight level.

A brief comparison during earlier studies, between DLR method, Boeing Method 2 and the EUROCONTROL modified Boeing Method 2 (EEC-BM2) indicates DLR method to deliver 4.28 % higher results than the Boeing Method 2 and 3.56 % higher results than the EEC-BM2.

The average $EINO_x$ obtained in this study lies at 11.3g/kg fuel burnt. These results are about 1.8 % higher than NASA results from 1992, and 17.5 % lower than ANCAT2 results.

Averaged $EINO_x$ obtained for this study thus enters NASA and ANCAT2 range of value. Nevertheless this value should read slightly higher if complete flight profiles were considered in the study. Moreover the average distance flown in the study is short (750km). The NASA and ANCAT values presented in Table 24 were obtained with a much more complete and varied data set.

9 CONCLUSION

A commercial aircraft fleet at any particular date is mainly composed of aircraft developed up to 30 to 35 years earlier. Thus technology introduced at a given date will produce a significant impact on the environment up to 30 to 35 years later.

From the operating cost point of view hydrogen remains unattractive under today's condition: kerosene is much cheaper than hydrogen and production/infrastructure is completely missing. Nevertheless the cost for emissions from kerosene technology is much higher than hydrogen's emissions, which may influence airlines in the future.

In the middle term (30 to 40 years), synthetic kerosene could be used to counter a shortage of fossil reserves and maybe help making today's aircraft generation profitable. In the long term (> 40 years), cryogenic fuel may find its way, but only if it presents real advantages and clear environmental compensations compared to synthetic kerosene.

With regard to contrail production: the baseline scenario, using the aircraft fleet of 2004, 2004 produced contrails on **15.93%** of the flight legs >= FL240 (average for the 20 days studied). Flight legs refer to short flight segments in the CPR data, each of approximately 2 minutes duration. The percentage of contrail-producing flight legs increased to **17.54%** for the fleet of 2028, to **19.05%** for the fleet of 2050 (with increased fuel efficiency) and to **27.13%** for the all-hydrogen fleet.

This indicates that, in comparison with 2004, an estimated increase in sky contrail coverage of approximately **1.61%** can be expected in 2028, **3.12%** in 2050 with increased fuel efficiency, and **11.20%** in 2050 with hydrogen aircraft. For all three future scenarios, this increase appears to be consistent over both days of low and high contrail coverage.

Given the increase in contrail production with hydrogen aircraft when compared with future kerosene aircraft with increased fuel efficiency, it should be stressed that this negative impact of hydrogen technology must be carefully weighed against the fact of increased NO_x and other pollutants associated with kerosene burning aircraft. In addition, use of kerosene has an associated detrimental effect on the global energy balance, and the diminishing resources of fossil fuels may well make the move to hydrogen engines necessary and inevitable.

Indeed, kerosene engines would exhaust significantly higher amounts of pollutants at altitude, which could be avoided by using hydrogen technology.

A trade-off has to be found between both technologies to maintain an acceptable environmental situation in the future in spite of traffic growth. A solution to explore could be bi-fuelled systems. Synthetic kerosene could be used during some flight phases while cryogenic engines would propel the aircraft during other phases.

Intentionally left blank

ANNEX 1. BOEING METHOD 2 – EUROCONTROL MODIFIED

This annex describes the EUROCONTROL modified Boeing Method 2 (EEC-BM2)

1 The original Boeing Method 2 (BM2)

The International Civil Aviation Organisation (ICAO) has established standards and recommended practices (Annex 16 to the ICAO Conference, "Environmental Protection") for the testing of aircraft emissions on turbojet and turbofan engines. The world's jet engine manufacturers have been required to report to ICAO the results of required testing procedures, which pertain to aircraft emissions. ICAO regulations require reporting of emissions testing data on the following gaseous emissions: NO_x, HC, CO and smoke. In addition to this, ICAO requires that information be reported on the rate of fuel flow at various phases of flight. Hence, ICAO maintains a database of this where information is available to find out this information for each of the phases of flight as ICAO defines them:

Operating Mode	Throttle Setting (percent of maximum rated output)
Take-Off	100 %
Climb-Out	85 %
Approach	30 %
Taxi/ground idle	7 %

The Boeing Aircraft Company conducted an extensive study for NASA on emission inventories for scheduled civil aircraft worldwide (see Baugham et al., 1996). The Boeing 2 Method is an empirical procedure developed for this study, which computes in-flight aircraft emissions using, as a base, the measured fuel flow and the engine ICAO data sheets. Whereas the first Boeing method took into account ambient pressure, temperature and humidity, the second method was more complicated (and accurate). This new method allowed for ambient pressure, temperature and humidity as well as Mach number.

1.1 Methodology

The Boeing Method uses English units and not S.I. therefore the first step is to convert the Fuel Flow (W_f) from the ICAO data for a specific engine from kg/s to lbs/hr (multiply by 7936). The Emission Index (EI) values from ICAO are to be read as lbs/1000 lbs (same number as g/kg).

The ICAO fuel flow values are then to be modified by a correction for aircraft installation effects (W_f):

Take-Off	1.010
Climb-Out	1.013
Approach	1.020
Taxi/ground idle	1.100

STEP 1: Curve fitting the Data

The Emission Indices (NO_x, HC, CO) are to be plotted (log-log) against the corrected fuel flow (W_f).

STEP 2: Fuel Flow Factor

a) Calculate the values ∂_{amb} (ambient pressure correction factor) and θ_{amb} (ambient temperature correction factor) where:

$\partial_{amb} = \frac{P_{amb}}{14.696}$ (P_{amb} = ambient (inlet) pressure) and

$\theta_{amb} = \frac{T_{amb} + 273.15}{288.15}$ (T_{amb} = ambient (inlet) temperature)

b) The fuel flow values are further modified by the ambient values:

$W_{ff} = \frac{W_f}{\partial_{amb}} \times \theta_{amb}^{3.8} \times e^{0.2 \times M^2}$, where M is the Mach number.

c) Calculate the humidity correction factor H:

H = -19.0 × (ω - 0.0063), ω = specific humidity,

$$\omega = \frac{0.62198 \times \Phi \times P_v}{P_{amb} - \Phi \times P_v}.$$

where Φ is relative humidity and P_v = saturation vapour pressure in psia. For a correction to this formula, please see the EUROCONTROL corrected Boeing 2 Method below.

$P_v = (0.014504) \times 10^{\beta}$

and,

$$\beta = 7.90298 \times \left(1 - \frac{373.16}{T_{amb} + 273.16}\right) + 3.00571 + 5.02808 \times \log_{10}\left(\frac{373.16}{T_{amb} + 273.16}\right)$$

$$+ 1.3816 \times 10^{-7} \times \left(1 - 10^{11.344 \times \left(1 - \frac{T_{amb} + 273.16}{373.16}\right)}\right) + 8.1328 \times 10^{-3} \times \left(10^{3.49149\left(1 - \frac{373.16}{T_{amb} + 273.16}\right)} - 1\right)$$

STEP 3: Compute EI

Calculate the emission indices of HC, CO and NO_x:

$$EIHC = REICH \times \frac{\theta_{amb}^{3.3}}{\partial_{amb}^{1.02}}$$

$$EICO = REICO \times \frac{\theta_{amb}^{3.3}}{\partial_{amb}^{1.02}}$$

$$EINOx = REINOx \times e^{H} \times \sqrt{\frac{\partial_{amb}^{1.02}}{\theta_{amb}^{3.3}}}$$

Where the REIHC, REICO, and $REINO_x$ values are read off the graph (STEP 1) by substituting W_{ff} for $W_{f.}$

STEP 4: Total Emission

$$\text{Total (HC, CO, NO}_x\text{)} = \text{Number of Engines} \times \sum_i \left[(EIHC, EICO, EINOx)_i \times W_{f_i} \times time_i \times 10^{-3} \right] \text{ in lbs}$$

1.2 Bibliography

[Ref 21] & [Ref 23]

2 EUROCONTROL modified Boeing Method 2 (EEC-BM2)

Eurocontrol has implemented an improved version of the Boeing Method2 as part of its AEM3 emission calculations used to obtain the results for the current study. The improvement covers a mistake within the published Boeing Method, specifically with regard to the humidity calculation (see above). The formula for the humidity correction factor should read:

$$\omega = \frac{0.62198 \times \Phi \times P_v}{P_{amb} - 0.37802 \times \Phi \times P_v}$$

The reason is that specific humidity, ω, is defined as the ratio of the mass of water vapour in a sample of moist air to the total mass of moist air, i.e.:

$$\omega = \frac{M_w}{M_w + M_d}$$

where M_w is the mass of water vapour and M_d is the mass of dry air.

Specific humidity can also be calculated from the actual vapour pressure (P_a) and ambient Pressure (P_{amb}) as:

$$\omega = \frac{e \times P_a}{P_{amb} - (1-e) \times P_a}$$

The factor e is the ratio of the mole weight of water vapour to that of air (18.016 / 28.966 - both in g/mol) = 0.62198 (a dimensionless quantity).

Please note also that actual vapour pressure (P_a) is related to relative humidity (Φ) and the saturation vapour pressure (P_v) by the formula:

$$\Phi = \frac{P_a}{P_v}$$

Therefore the correct formula for specific humidity is

$$\omega = \frac{0.62198 \times \Phi \times P_v}{P_{amb} - 0.37802 \times \Phi \times P_v}$$

Note that the factor 0.37802 appearing is 1 – e = 1 – 0.62198 (= 0.37802) and must be included in the formula. This correction has been implemented as the Boeing Method 2 - EUROCONTROL modified.

ANNEX 2. DETERMINATION OF FUEL BURN AND NO_X REDUCTION IN 2015

Fuel burn – Scenario α

Based on EUROCONTROL's technology improvement curve, fuel efficiency for replaced traffic within 2015 was calculated. Aircraft manufactured by the year 2015 would be on average **5.40%** more efficient than 2004's aircraft.

As opposed to other scenarios assessed in this study (i.e. 2028 and 2050), not all of the 2004's fleet will be replaced by 2015. The percentage of fleet replaced was thus estimated.

For that purpose, the aircraft registration number was not available. As a result no actual exhaustive list of aircraft's manufacturing year was obtained.

The estimation was thus based, for each aircraft type, on averaged manufacturing year out of JPFleet database. Information out of JPFleet was reduced to European aircraft since European aircraft are representative of CPR traffic data of the study. 98.75% of aircraft types in the traffic data were accessible in JPFleets; the estimation is thus statistically reliable.

As a result, **29.77%** of 2004's fleet is estimated to be replaced in 2015, which means that 70.23% of 2015's fleet will still have 2004's efficiency.

For that reason, 2015's fleet will be only **1.60%** more efficient than 2004's fleet.

NO_x

The ANCAT/EC2 emissions inventory provides forecast NO_x emissions for 2015 based on 1991/1992 data. Considering a constant yearly evolution from 1992 to 2015, an estimation of 2004's situation in terms of total NO_x emissions due to ANCAT/EC2 traffic sample was done. 2015 NO_x emissions appear to be 1.3 times higher than the total amount of NO_x emitted in 2004.

For the purpose of the ANCAT/EC2 emissions inventory and forecast it was assumed by ANCAT/EC2 team that traffic recorded in the 1992 inventory will grow at the world average rate of about 5% per annum each year until 2015. As a result, based on ANCAT/EC2 findings, the reduction of NO_x emissions is estimated to reach 16% between 2004 and 2015 for the same traffic sample.

ANNEX 3. DISCUSSION ON AIRCRAFT CATEGORIES

The data set under study is based on radar tracks. Five main aircraft families can be identified:

- Commercial aircraft (for passenger and freight)
- Military aircraft (fighters as well as troop transportation)
- Business jets
- Helicopters
- Propeller driven light aeroplanes (less than 6-8 tons)

This list does not claim to be exhaustive.

The data set is distributed as follows:

Aircraft category	% of the fleet
Commercial aircraft	86.76
Military aircraft	0.07
Business jets	8.91
Helicopters	0.18
Propeller driven light aeroplanes	4.08

Table 25: Distribution of fleet in the traffic sample under study

The differentiation between freighter and commercial aircraft was unfortunately not feasible since no registration number was available to identify each aircraft individually.

Research and development to reduce fuel burn and emissions will probably be radically different depend on the category.

1. Commercial and freight

Commercial and freight aviation will definitely be the category which will benefit primarily and even originate future technological improvements. Indeed this category represents the majority of the flights, and operating costs are an important issue.

When becoming too old for commercial exploitation, some aircraft are converted into freighters. The average age of the freight fleet is thus higher than for the commercial fleet and benefits from technological improvements will be seen several years after the commercial fleet.

2. Military aviation

If the commercial aircraft category will probably originate most of the technological developments, environmental concerns may not be the first priority for military aircraft. Troop carriers will probably benefit from the evolution of commercial aircraft technologies. The focus for fighters will probably be put on issues like weight or distance range, with an impact on fuel burn, but most probably not on emissions.

Nevertheless, even if not precisely quantified, military activities generate today a tiny fraction of fuel consumption and emissions regarding commercial activities, although each military aircraft individually (especially fighters) is particularly pollutant and fuel consuming. However, the number of military flights above Europe is small and fighter flights are often operated in specific areas.

3. Business jets

As detailed in [Ref 5], there is almost parity between commercial aircraft and business jets in term of number of aircraft in operation in the world.

However, according to IPCC ([Ref 3]), the quantity of fuel burnt by little commercial aircraft and aircraft from general aviation (business jets, helicopters, light aircraft) lies at around 5% of the total quantity of fuel burnt by the fleet from the entire world. An estimation obtained by a different approach indicates that business aviation only contributes to 2% of total fuel burnt by commercial aviation on a worldwide scale.

FESG (Forecast and Economic Support Group) from ICAO foresees a decrease of this number down to a maximum of 1% by 2050 (i.e. technological improvements will greatly offset the growth of traffic). The contribution of business aviation to global pollution will hence be almost negligible.

Moreover, today's business jets are particularly fuel-efficient since they are aimed at a demanding clientele. In addition business jets are designed to operate in every kind of airport, including small airfields which may be in environmentally critical regions or subject to specific local regulations. Hence noise and emissions requirements to satisfy customers' needs are strict.

4. Helicopters

The total number of helicopters in operation in the world (apart from the Russian Federation) is estimated to reach 18,000, burning 1.2 millions of tons of kerosene yearly, hence less than 1% of all fuel burnt by aeronautic in the same time period ([Ref 3]). Unlike commercial aviation, the future market prospects for helicopters are limited. At the very most fuel burn could double by 2050, hence representing an even smaller fraction of total fuel burnt for aeronautics purposes.

In addition, because of its low flight level, the small range flown and its usage mainly outside airport concentrations, the helicopter resembles more a land vehicle than an aircraft. It has no direct climatic impact on troposphere and no massive environmental impact at ground level in term of emissions.

The contribution of helicopters to damage on the environment is thus extremely small and localized. For this reason helicopters are not yet submitted to emission regulations as with commercial aviation. This will probably not motivate helicopter manufacturers to improve fuel efficiency and emissions in the next years. The main issue for helicopters improvements in the next decades is noise, since noise experienced by populations at ground level is one of the biggest restraints for expansion of use.

5. Propeller driven light aeroplanes

Even if regulatory constraints are applicable to light airplanes, the engines used and small ranges flown make this category a small contributor to the total fuel burnt by aviation. Moreover, the low flight levels used by this fleet reduce the impact on global warming.

Nevertheless light aeroplanes may in the future benefit from technological improvement from engine manufacturers. The potential development of fuel cell propulsion for a portion of this fleet could reduce emissions, since fuel cells only generate electricity, water and heat.

ANNEX 4. CONTRAIL CALCULATION PROCEDURE

In order to calculate contrails in each grid cell, the CONTRAIL model performs the following calculations. These equations are based on the generally accepted “Schmidt-Appleman” criterion for contrail formation:

Engine Propulsion Efficiency:

$\eta = FV/M_f Q$

where:

F = engine thrust (N)

V= air speed (m/s)

M_f = mass fuel flow (Kg/s)

Q = combustion heat of fuel (taken as constant 43 MJ/kg)

Slope Of The Exhaust/Ambient Air Mixing Line:

$G = EL_{H2O}C_P P/\varepsilon Q(1-\eta)$

where:

EL_{H2O} = Water emission index (water is a result of the oxidation process of carbon and hydrogen contained in the aviation fuel with the oxygen in the atmosphere) = 1.230 kg/kg fuel burn;

C_P = specific heat capacity of air at constant pressure = 1004 J/KgK

P = pressure (hPa)

ε = ratio of the gas constants of air and water vapour = 0.622

η = engine propulsion efficiency

Q = combustion heat of fuel (taken as constant 43 MJ/kg)

Saturation Vapour Pressure Over Water:

$E_{satW}(T) = 6.112\exp[6816(1/273.15-1/T) + 5.1309\ln(273.15/T)]$ (hPa)

with T = ambient temperature measured in K

Saturation Vapour Pressure Over Ice:

$E_{satI}(T) = 6.112\exp[4648(1/273.15-1/T) – 11.64\ln(273.15/T) + 0.02265(273.15-T)]$ (hPa)

with T = ambient temperature measured in K

Ambient Vapor Pressure:

$E = U_W E_{satW} / 100$ (hPa)

where

U_W = ambient relative humidity over water

Ambient Relative Humidity Over Ice:

$U_I = E/E_{satI} * 100$ (%)

Threshold Temperature For Saturated Air:

$T_M = -46.46 + 9.43\ln(G-0.053) + 0.720(\ln(G-0.053))^2$ (C)

using the slope of the exhaust / ambient air mixing line G

Threshold Temperature For Dry Air:

$T_C = T_M – (E_{sat}W(T_M)/G)$ (C)

this is also known as critical temperature

Exhaust/Ambient Air Mixing Line Intercept Temperature:

$T_E = T – (E/G)$ (C)

where

U = ambient relative humidity and T = ambient temperature in C

Contrails form when $T_E < T_C$. However, persistent contrails form when $T_E < T_C$ and $E > E_{satI}$ (i.e. in very moist cold air).

ANNEX 5. METEOROLOGICAL SITUATION

This brief report will outline the meteorological situation for the 20 days in 2004: January 10 and 20, February 11 and 26, March 8 and 18, April 22 and 29, May 17 and 28, June 1 and 22, July 1 and 24, August 1 and 31, September 11 and 17, October 3 and 18. Information is presented for general weather conditions and the relative humidity and temperature at flight level FL 300.

1. Surface Analysis

January 10, 2004: Meteorological Analysis

A low pressure system situated over northern Britain, with an associated occluded front down through Ireland brought heavy precipitation and strong westerly winds to Scotland. A deep low pressure system over Iceland with a warm front running through northern Norway brought with it strong southerly winds. A series of low pressure systems over the north Atlantic had associated warm front with extended eastward over south and central France. A warm front extended through the eastern Mediterranean from a low centred over southern Italy brought heavy rain but relatively weak north-westerly winds to southern Greece. Highs located over central Turkey and the central and northern parts of Russia brought mild conditions to these regions.

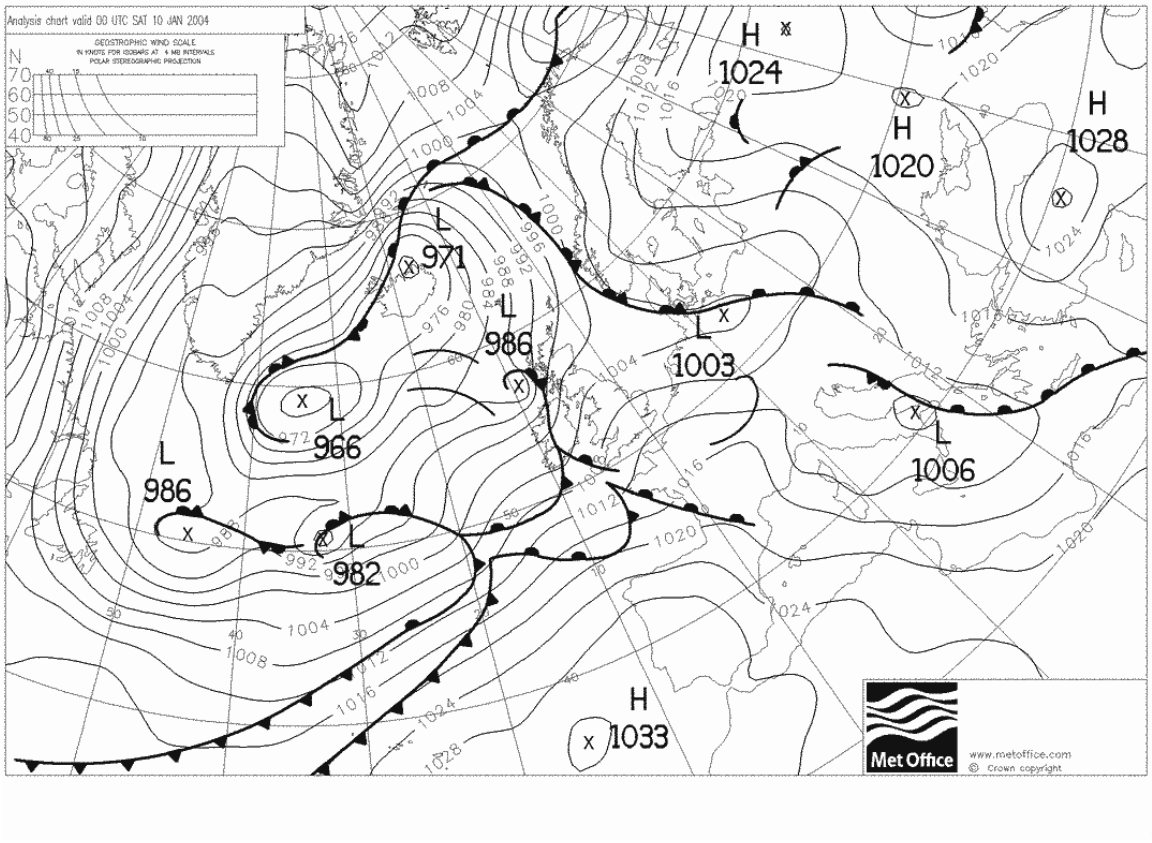

Figure 49: Meteorological Analysis: January 10, 2004

January 20, 2004: Meteorological Analysis

A low pressure system with an occluded front centred over Lithuania brought precipitation, light winds to the Baltic States. Also associated with this system were warm fronts located over central France and southern and central Germany bringing light precipitation throughout the region. In addition a cold front stretching through Britain to Iceland and extending to the north Atlantic brought heavy precipitation to northern Scotland and Iceland. A low pressure system over western Libya brought heavy rain and light winds to Tunisia. High pressure systems over Turkey brought clear skies and almost calm conditions to the eastern Mediterranean and southern Russia.

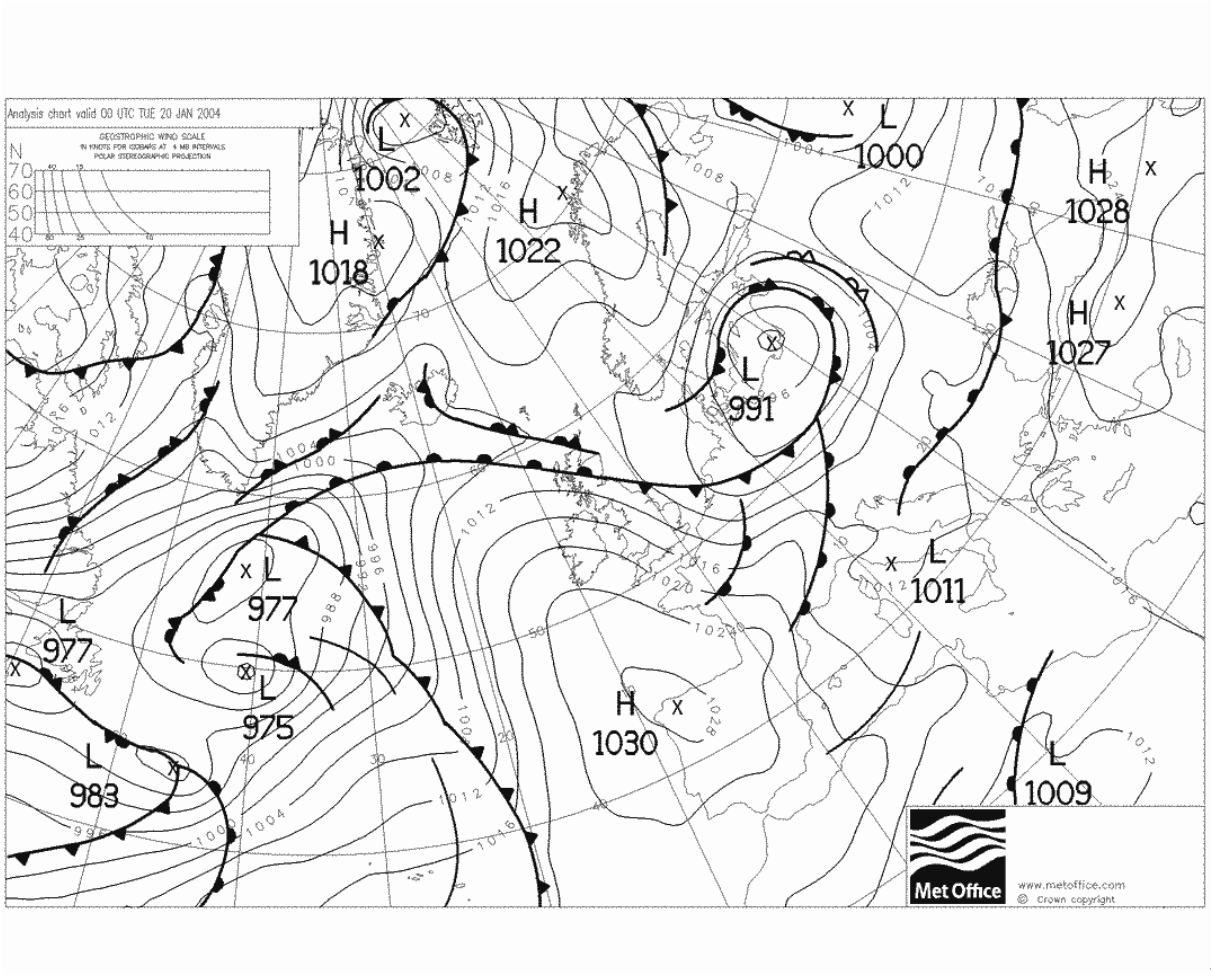

Figure 50: Meteorological Analysis: January 20, 2004

February 11, 2004: Meteorological Analysis

A low pressure system centred over Denmark with a cold front changing to a warm front extending to Iceland brought strong north-easterly winds to Britain and northern Europe. A fast-moving low-travelling eastward through south-central Russia had associated with it a cold front extending through the central Mediterranean region. This brought heavy but break rain to southern Italy and also to northern Romania. Also associated with this same fast-moving low was a cold front extending through Turkey which brought very heavy rain to Armenia and southern Russia. Highs located over western France, Norway and central Germany brought light winds and calm conditions to these regions.

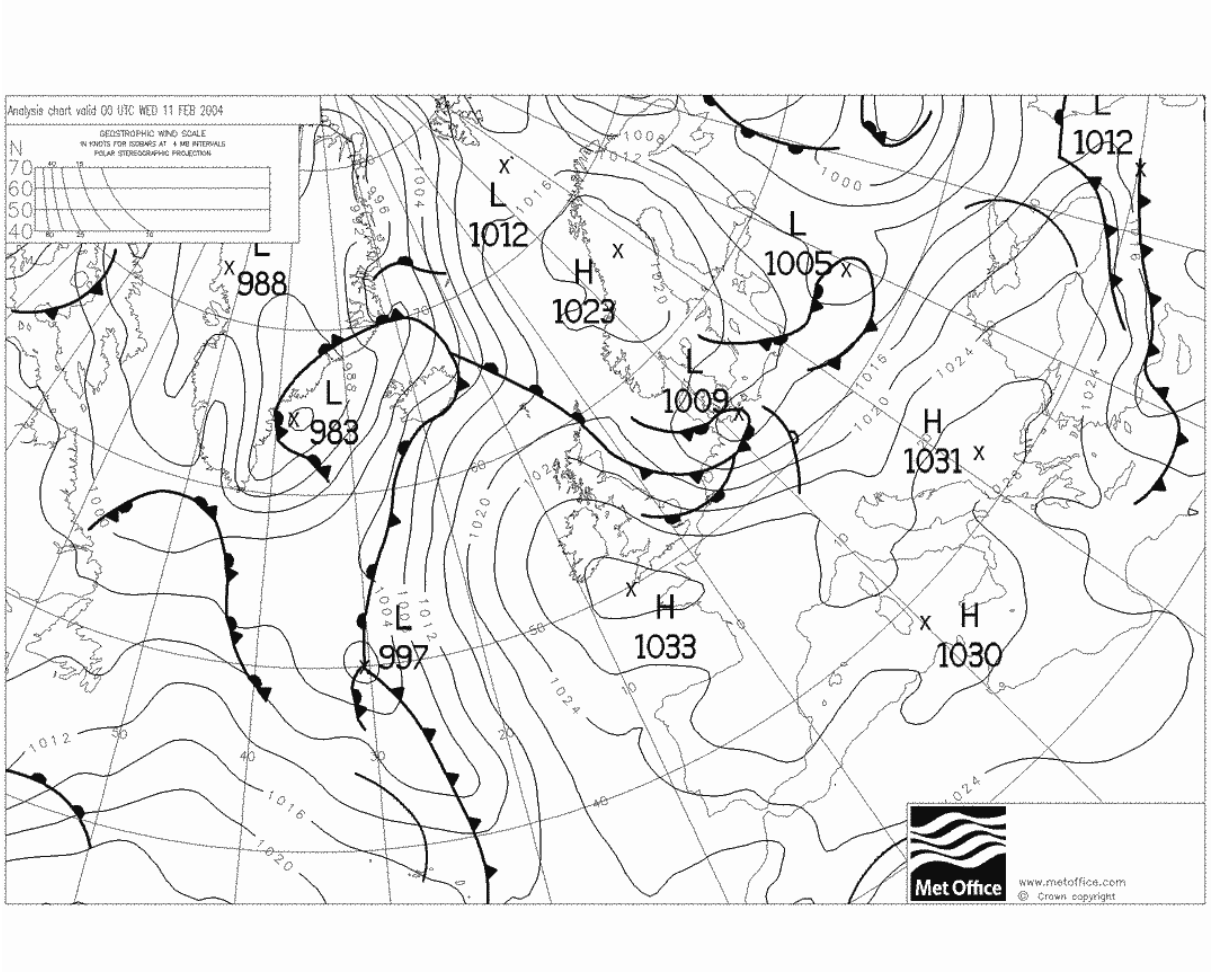

Figure 51: Meteorological Analysis: February 11, 2004

February 26, 2004: Meteorological Analysis

A series of closely bunched low pressure systems located over the North Sea, the Baltic and central Sweden combined to bring very strong northerly winds and precipitation to Britain and Scandinavia. Also with these systems was a weak cold front extending over central Europe through central France which brought only light precipitation to these regions. A low pressure system over the Black Sea had with it a warm front which connected it to two other low pressure system centred over southern France and southern Spain bringing rain to the western Mediterranean and Adriatic. A weak low brought light precipitation to Libya.

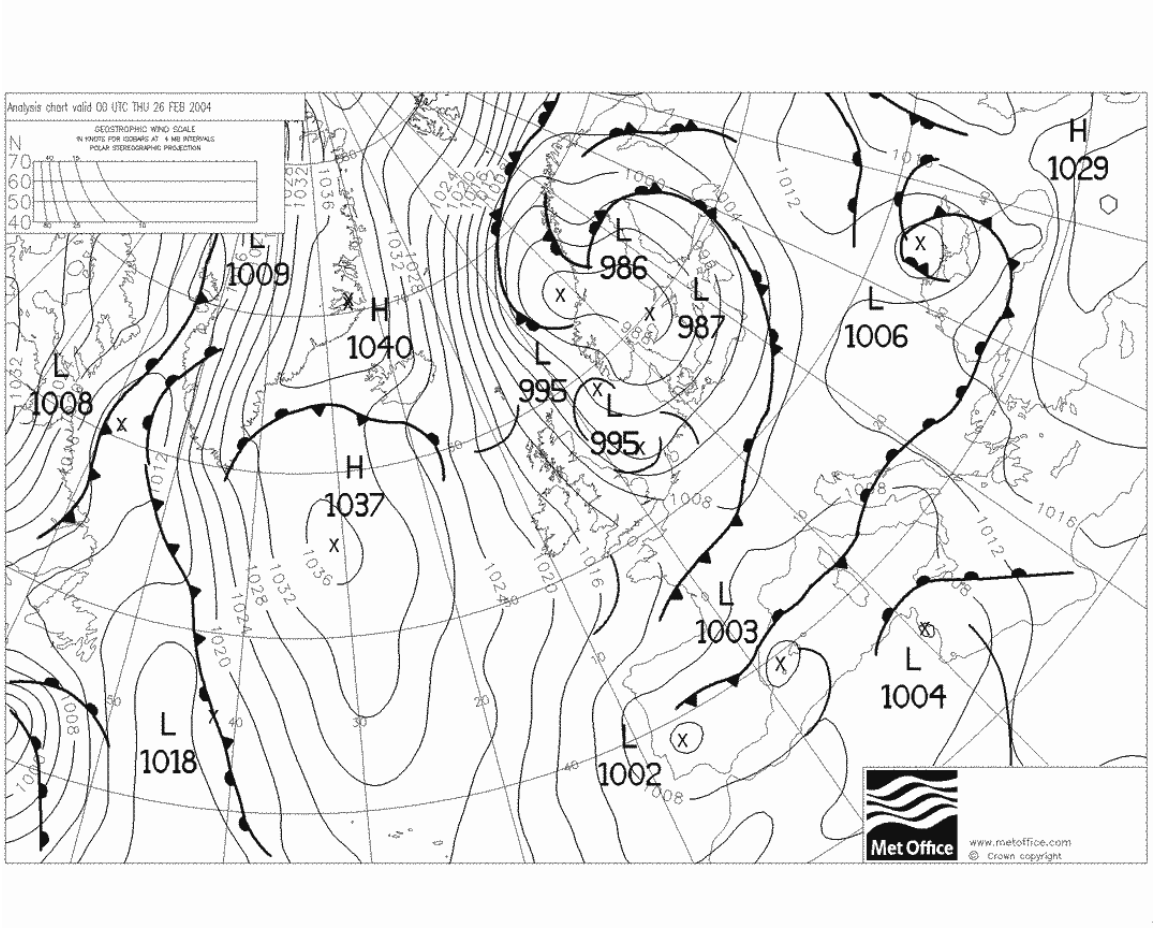

Figure 52: Meteorological Analysis: February 26, 2004

March 08, 2004: Meteorological Analysis

Although a series of deep low pressure systems over Iceland and the north Atlantic brought heavy winds and precipitation to these regions, an intense high pressure system located over northern Britain brought clear skies and light winds throughout western Europe. Low pressure systems over northern Italy and Corsica with associated warm and cold fronts over the central regions of the Mediterranean brought rain to Italy, Greece and the Balkans. A high pressure system over the western Mediterranean brought clear skies and calm conditions to north-western Africa. Another high located over the Black Sea brought clear skies and light winds throughout southern Russia.

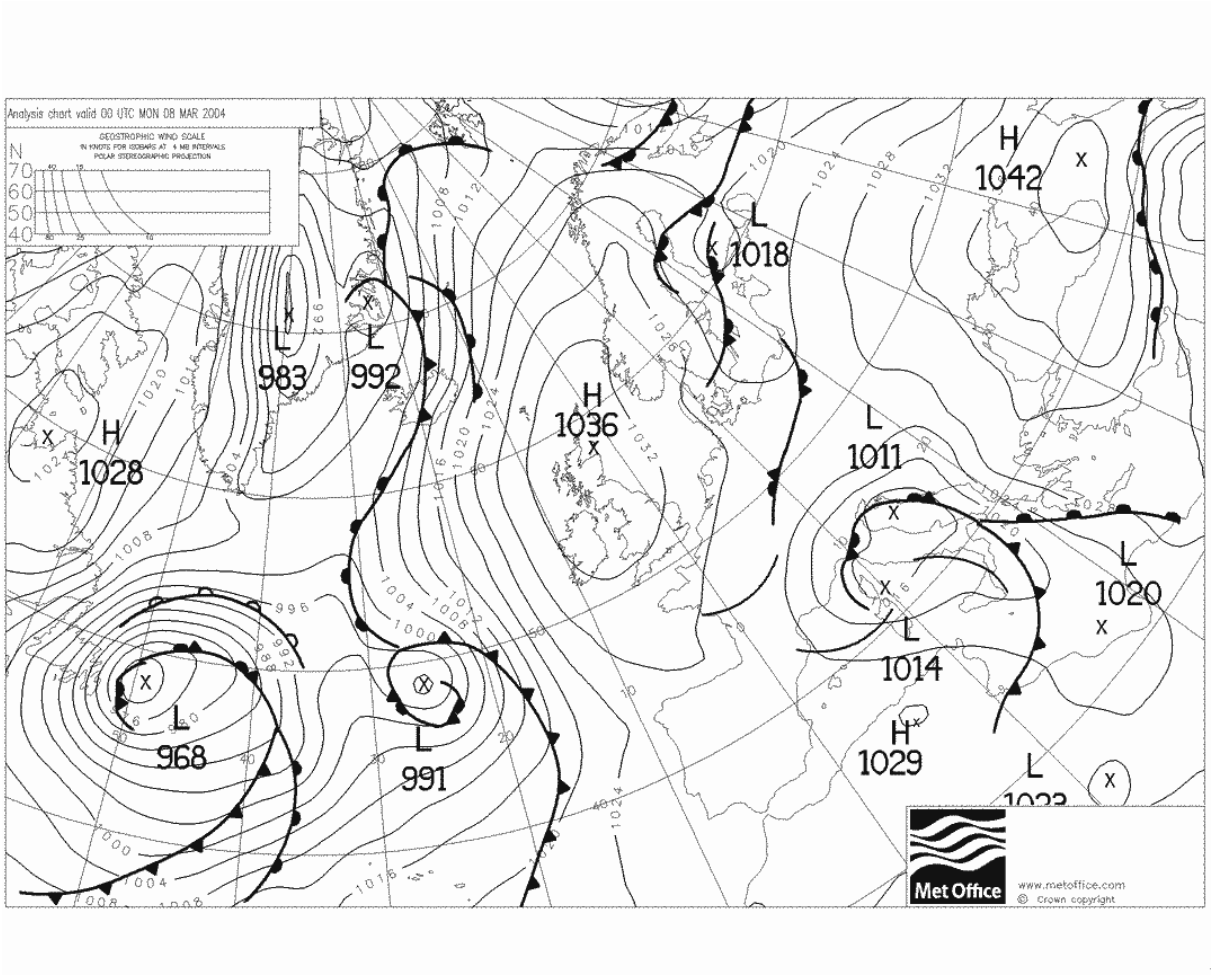

Figure 53: Meteorological Analysis: March 08, 2004

March 18, 2004: Meteorological Analysis

A low pressure system located over the Atlantic west of Iceland with an associated cold front extending southward over the Atlantic brought westerly winds and light precipitation to Britain. Another series of low pressure systems located off the coast of central Norway brought similar conditions to southern Norway. A strong high pressure system located over Austria brought clear skies and calm conditions throughout Europe except north of a line along the French coast of the English channel and the German coast of the North Sea where a cold front marked the dividing line. A weak low over the Black Sea brought light precipitation and westerly winds to the central and western parts of Russia.

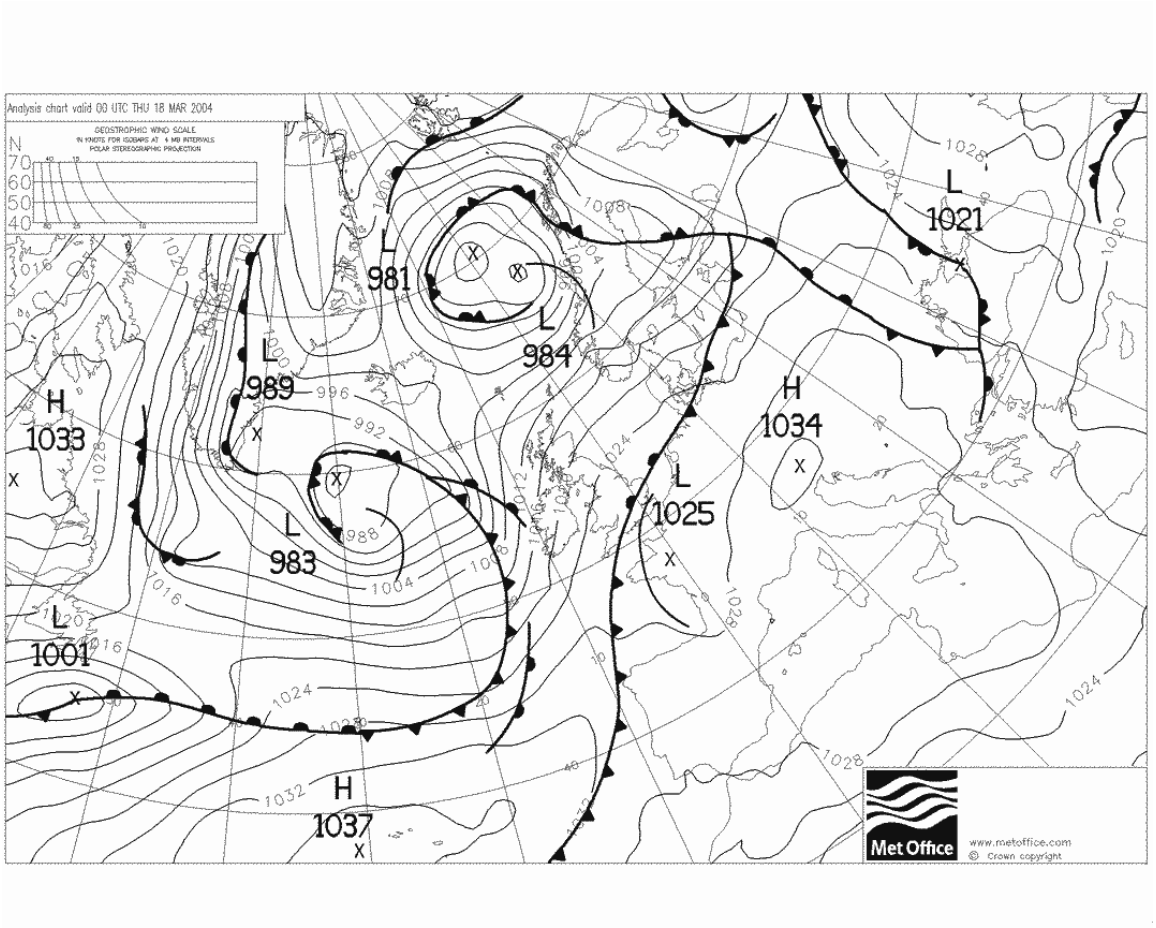

Figure 54: Meteorological Analysis: March 18, 2004

April 22, 2004: Meteorological Analysis

A low pressure system over northern Scotland brought light precipitation and westerly winds to Britain. A cold front from this system extended down through France and Spain and this, combined with low pressure systems located over the western Mediterranean, brought heavy rain to southern France and northern Spain. A low pressure system located over central-western Russia brought heavy precipitation but light winds to western Russia and eastern Poland. A low pressure system with its associated cold front over the Black Sea and central Turkey also brought heavy precipitation and light winds to Turkey and southern Russia.

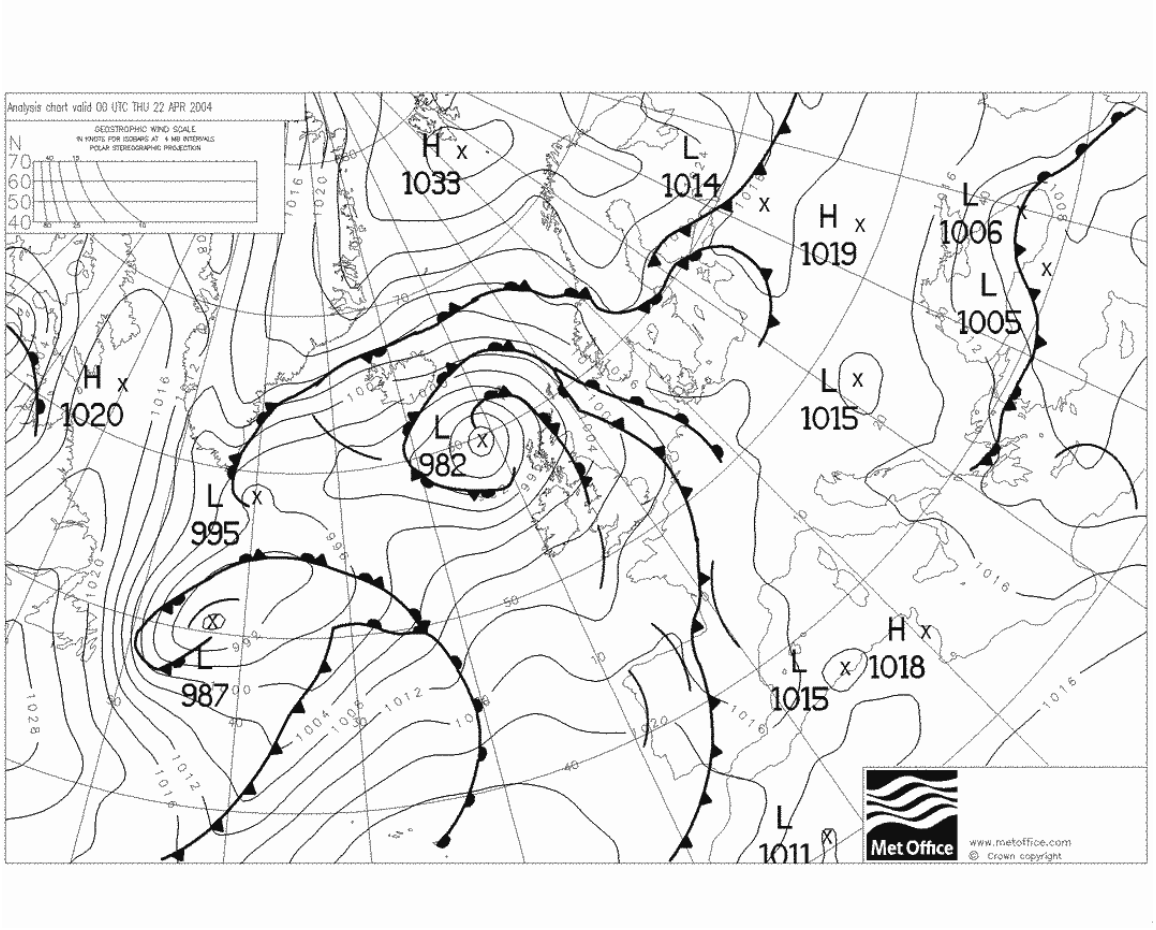

Figure 55: Meteorological Analysis: April 22, 2004

April 29, 2004: Meteorological Analysis

A low located over the Belgian coast brought precipitation and north-easterly winds to northern Germany. Along with this a low located off the north-western coast of France which was connected by a warm front to a low located north of Norway brought precipitation and north-westerly winds to Britain and northern France. Also associated with the French low was a cold front extending south to a low in southern Spain bringing precipitation all along this front. A low located over the western Mediterranean brought rain to southern France and Italy. Lows located over Romania, south-eastern Finland and the Black Sea brought rain and light winds to these regions. High pressure systems over central Greece and northern Libya brought clear skies and calm conditions to the eastern Mediterranean.

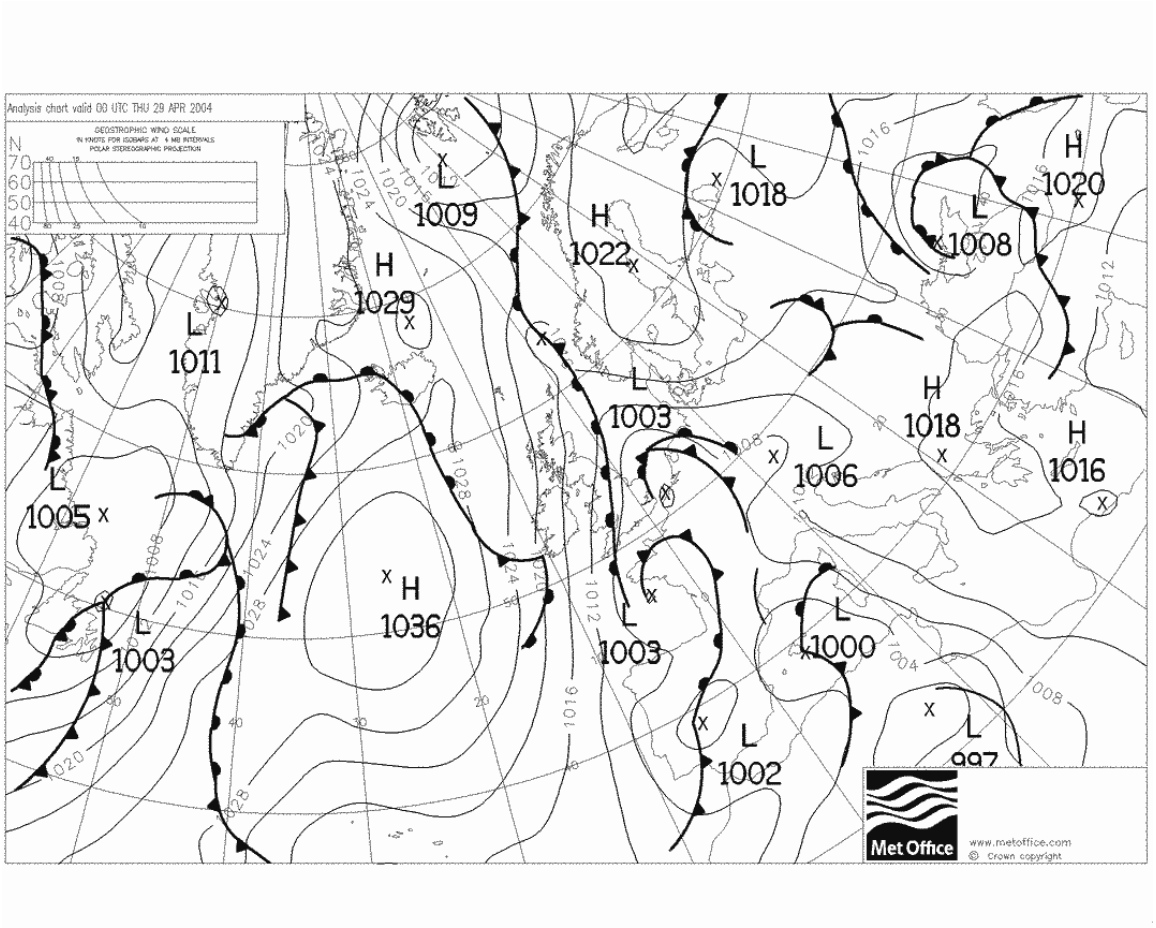

Figure 56: Meteorological Analysis: April 29, 2004

May 17, 2004: Meteorological Analysis

An intense low pressure system was located east of Iceland. With this low was a warm front extending through southern Norway and a cold front extending southward over the Atlantic. This brought strong westerly winds with a little precipitation to northern areas of Scotland and Scandinavia. A fast-moving but weak low located over the Balkans traveled to the Black Sea, bringing light rain and cloudy skies to the Balkans, Greece and Turkey. High pressure systems located off the western coast of France and southern England brought generally clear skies and light winds throughout Europe as far east as the Russian border.

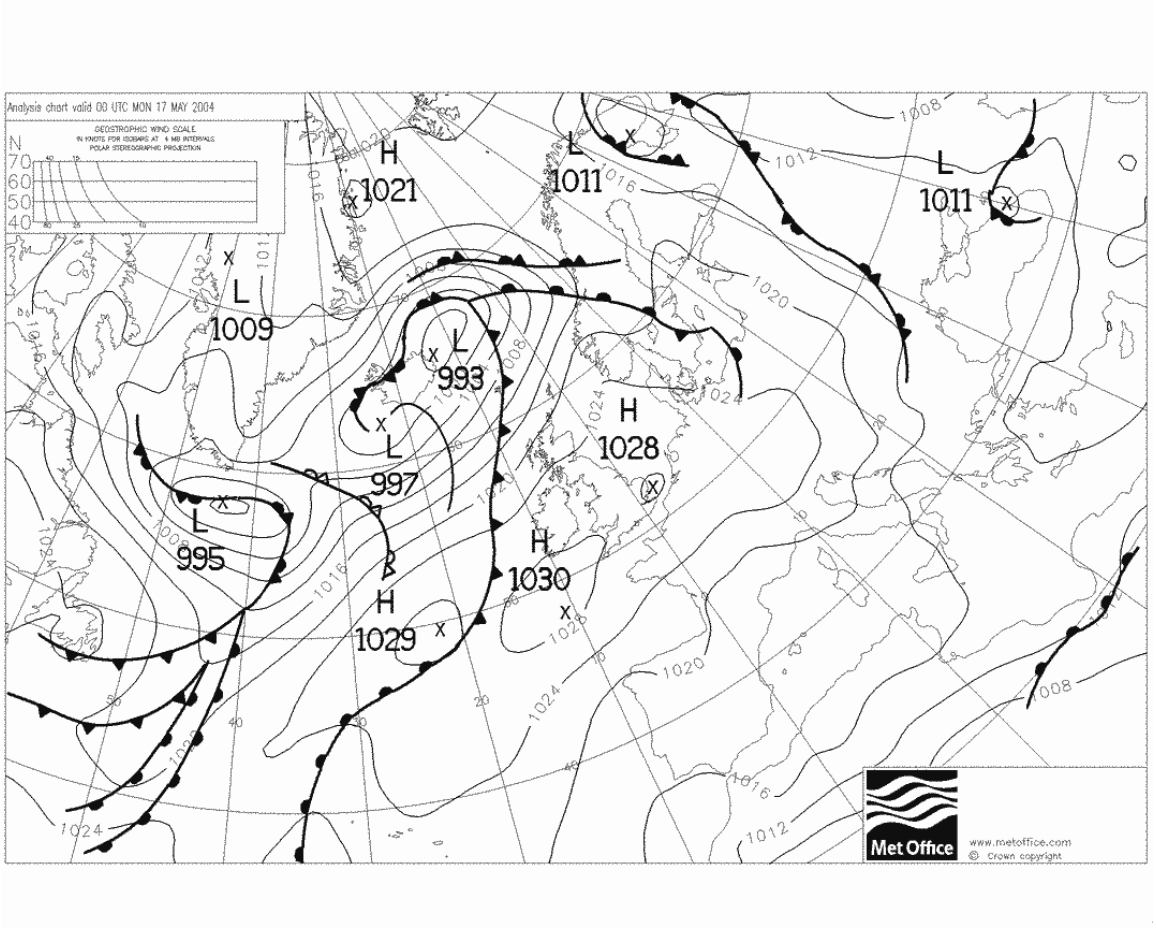

Figure 57: Meteorological Analysis: May 17, 2004

May 28, 2004: Meteorological Analysis

Low pressure systems located over the north Atlantic brought strong winds and precipitation to an area west of Ireland and south of Iceland. A low located over northern Italy with an extended cold front through central Russia and north to northern Finland brought moderate rain to central Italy and the area around southern Hungary. A warm front extending through eastern Turkey brought heavy rain to this region. A high pressure system centred over eastern England and one off the south coast of Spain brought clear skies and calm conditions to western Europe.

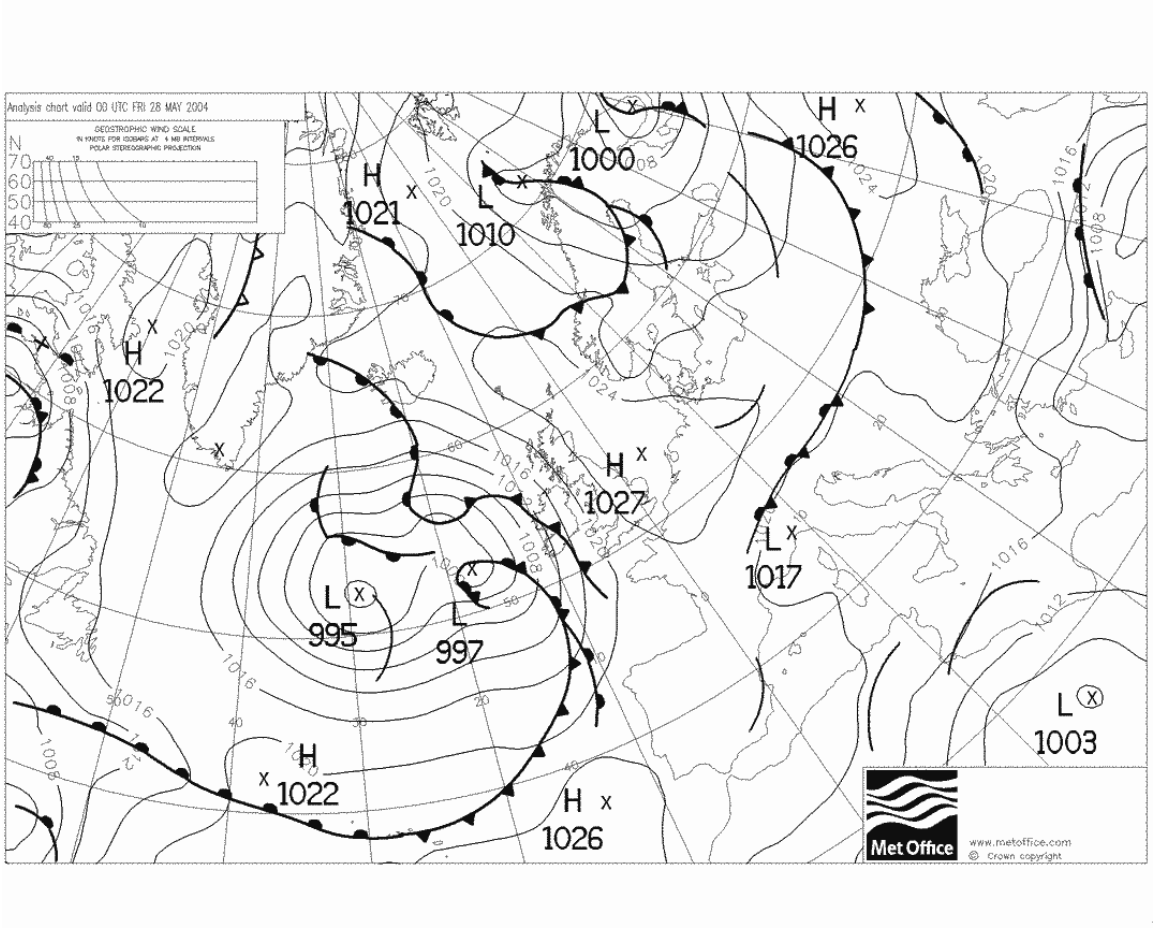

Figure 58: Meteorological Analysis: May 28, 2004

June 01, 2004: Meteorological Analysis

A warm front associated with a low centred over the Irish Sea moved through France bringing moderate to heavy rain and light winds to central France. A low centred over Hungary brought moderate to heavy rain from southern Germany south through to Bulgaria. The winds were low to calm throughout this region. Another low centred east of the Black Sea brought similar conditions to the areas around southern Russia, Georgia, Armenia and eastern Turkey. Weak lows over central Spain, southern France and Greece brought light rain and light winds to the northern shore of the Mediterranean. A high pressure system located over the central Mediterranean brought clear skies and calm conditions to the rest of the Mediterranean. A high located over the Baltic brought clear skies and calm winds to Scandinavia.

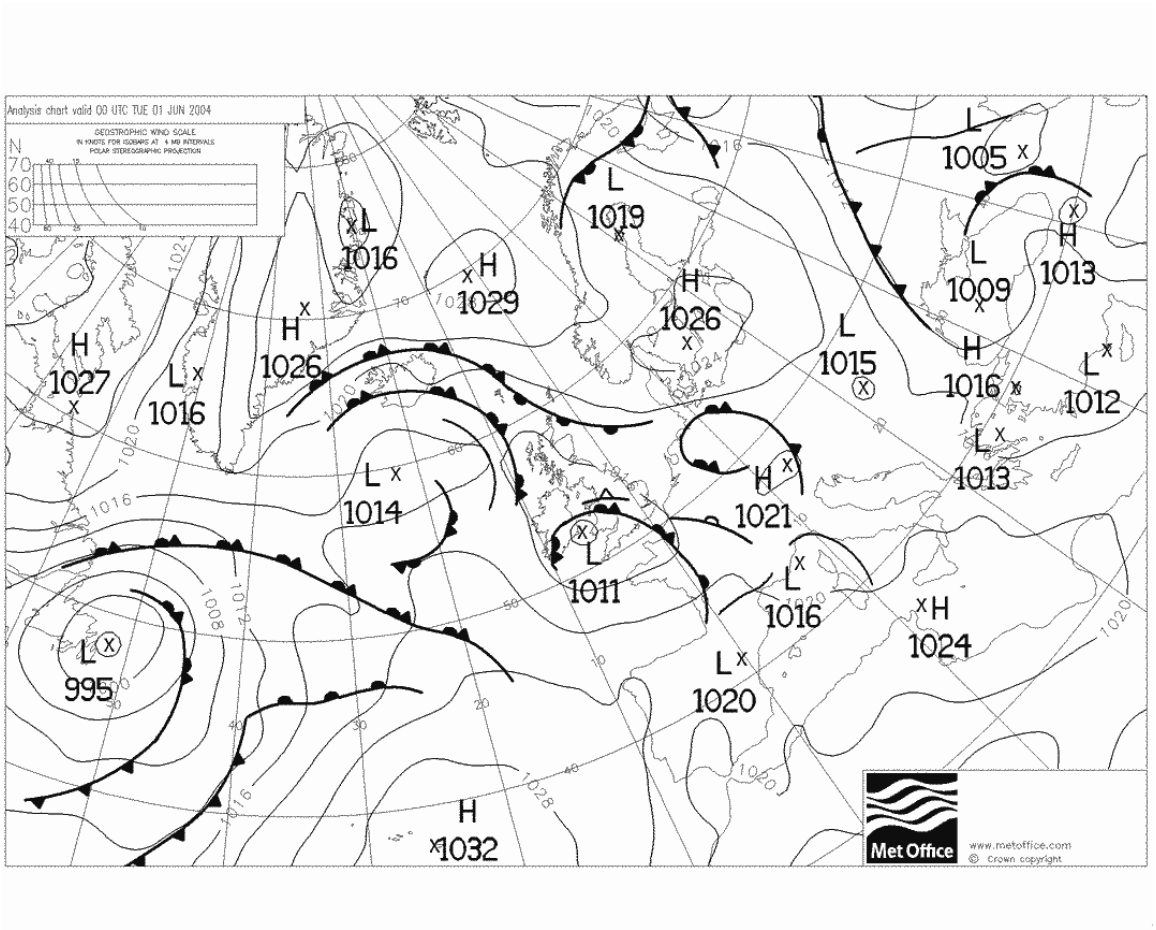

Figure 59: Meteorological Analysis: June 01, 2004

June 22, 2004: Meteorological Analysis

A deep low pressure system with an associated occluded front off the southeast coast of Britain brought heavy rain and strong south-easterly winds to Britain and the northern French coast. Another low located off the coast of central Norway brought moderate to heavy rain to southern Norway and central Sweden. A low off southern Finland had with it a cold front and extended southward through west-central Russia bringing moderate to heavy rain to the entire region. A low located east of the Black Sea brought heavy rain to southern Russia and eastern Turkey. Also a low centred over western Turkey brought moderate to heavy rain to northern Greece and south-eastern Balkans. High pressure systems located over the Atlantic off the south-western coast of Spain, over Sardinia and over the Adriatic brought clear skies and calm conditions to the Mediterranean areas.

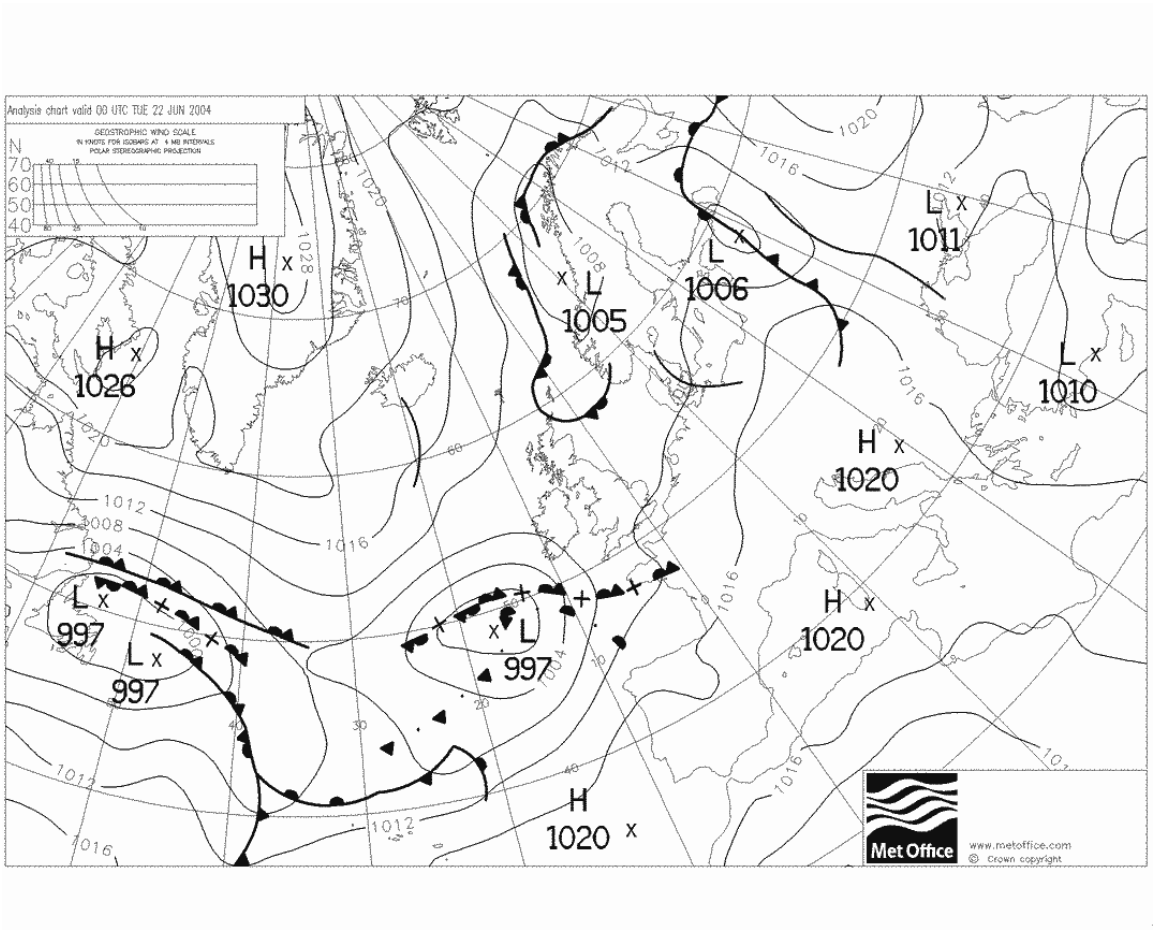

Figure 60: Meteorological Analysis: June 22, 2004

July 01, 2004: Meteorological Analysis

A warm front associated with a deep low pressure system located south of Iceland moved through Britain and France and then central Germany bringing rain and westerly winds. Another deep low centred over southern Finland with an associated warm front extending through north-western Russia brought heavy rains and light southerly winds to this region. A low over central Russia had a cold front extending down through the length of Turkey bringing rain which was heavy at times. A weak low pressure system passed quickly from southern Spain to northern Italy throughout the day bringing heavy rain at it passed. A high located over the Balkans brought clear skies to central Europe from Poland down through Greece.

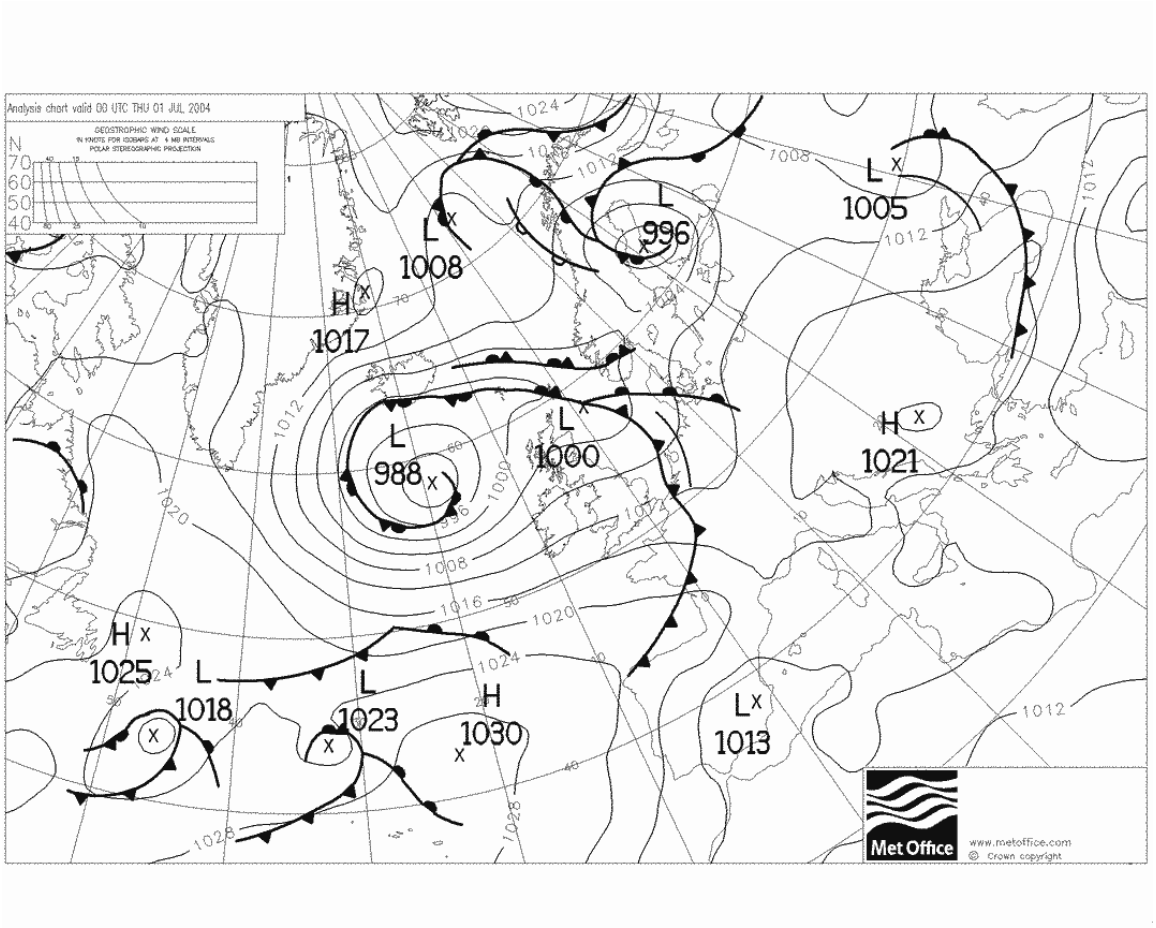

Figure 61: Meteorological Analysis: July 01, 2004

July 24, 2004: Meteorological Analysis

A cold front extending southward from a deep low pressure system located off the western coast of Denmark through Germany and into Italy brought strong westerly winds to most of western Europe and heavy precipitation to northern areas of Italy. A weak low over north-western Russia brought moderate rain to most areas of western Russia. A low near eastern Turkey brought rain to southern Russia and eastern Turkey.

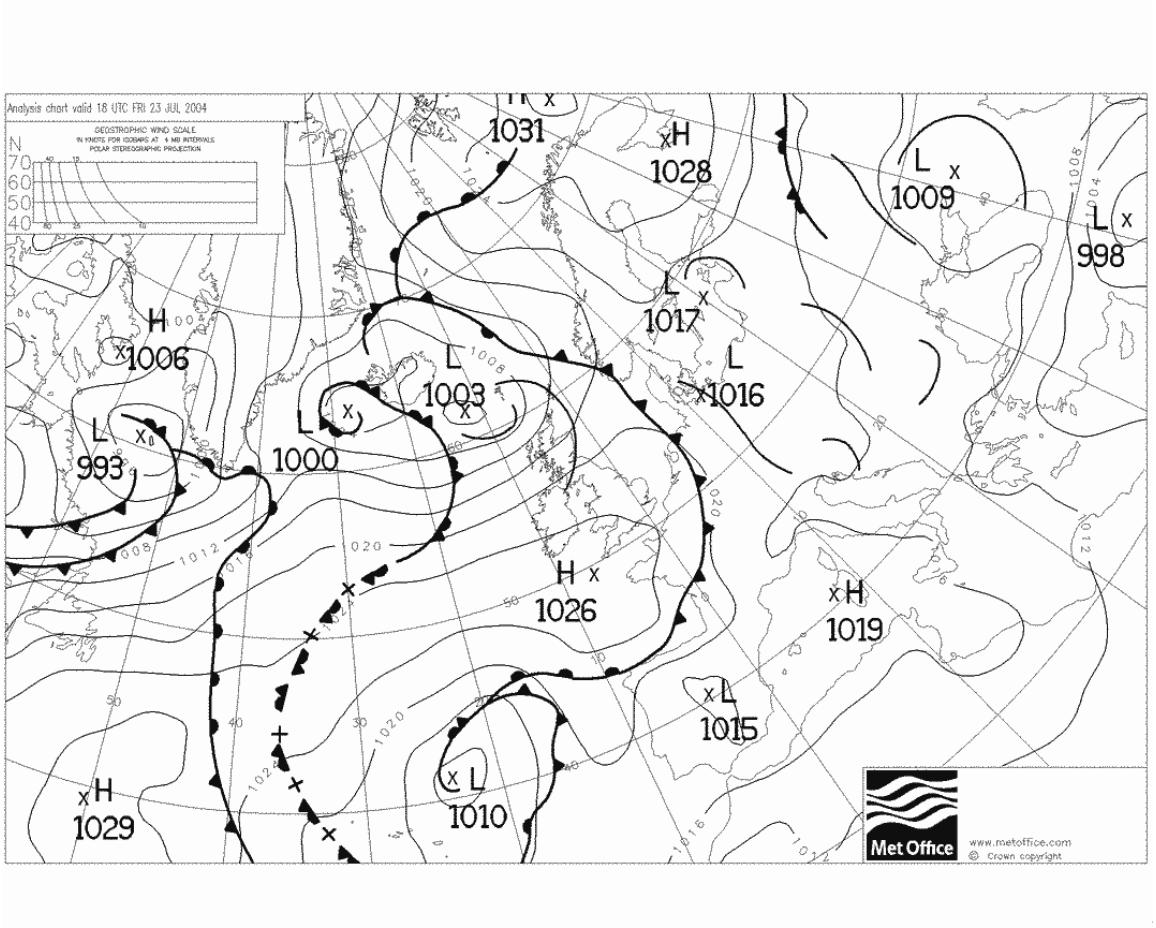

Figure 62: Meteorological Analysis: July 24, 2004

August 01, 2004: Meteorological Analysis

A warm front, associated with a low pressure system over southern Finland, extending from Finland through western Russia, brought very heavy rains and thunderstorms to this region. Weak troughs located over eastern and western Germany brought light rains to parts of Germany and northern Italy. The rest of Europe was clear and calm due to a high pressure system over the central Mediterranean.

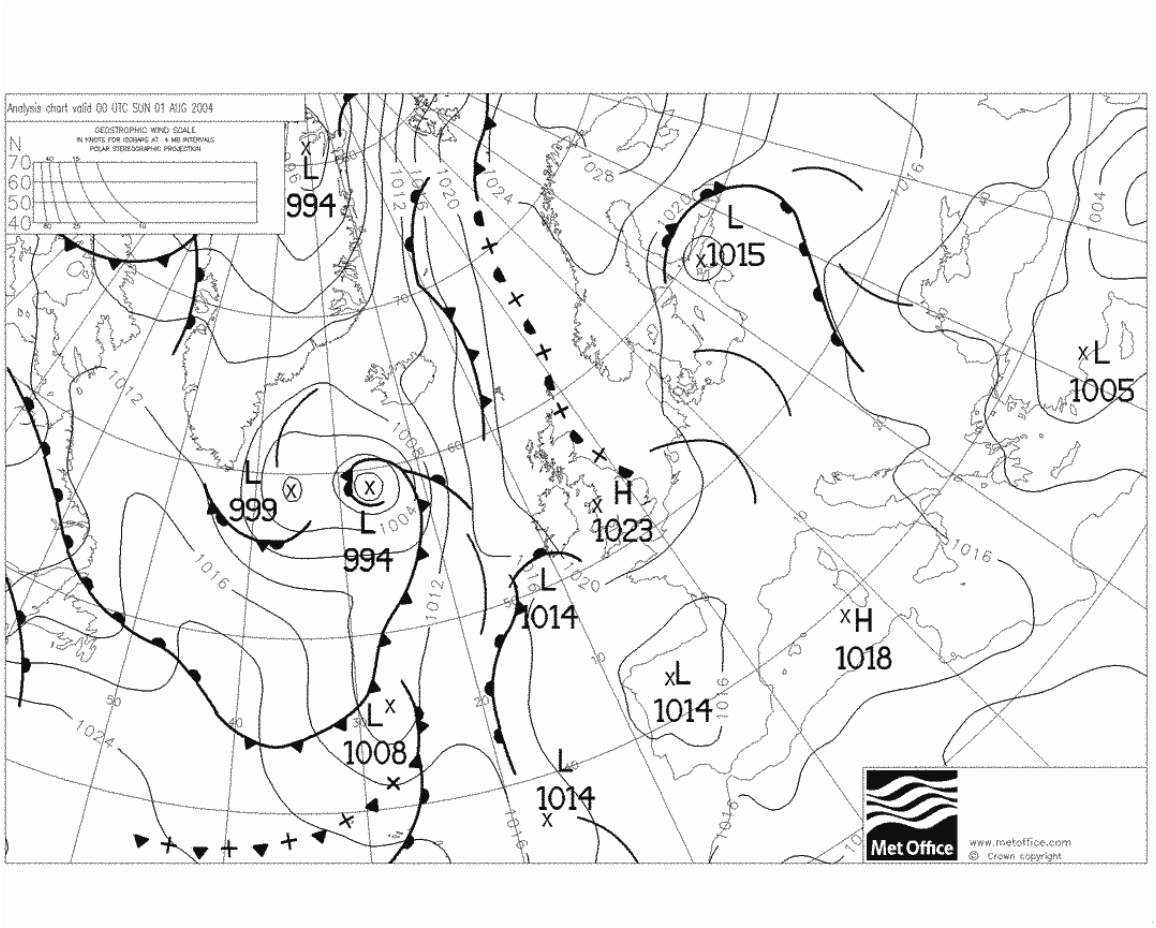

Figure 63: Meteorological Analysis: August 01, 2004

August 31, 2004: Meteorological Analysis

Low pressure systems located over Denmark and southern Sweden brought moderate rain and strong winds to most areas of Scandinavia and northern Europe. With these systems was an associated cold front which extended southward through Italy bringing heavy rain to areas of northern Italy. A low centred over central Spain brought heavy rain but light winds to this area. Another low and associated cold front brought rain to areas of north-western and western Russia. A low located over the Black Sea brought heavy rain to Ukraine and southern Russia. Highs located over the central and eastern Mediterranean brought clear skies and calm conditions to most of the Mediterranean.

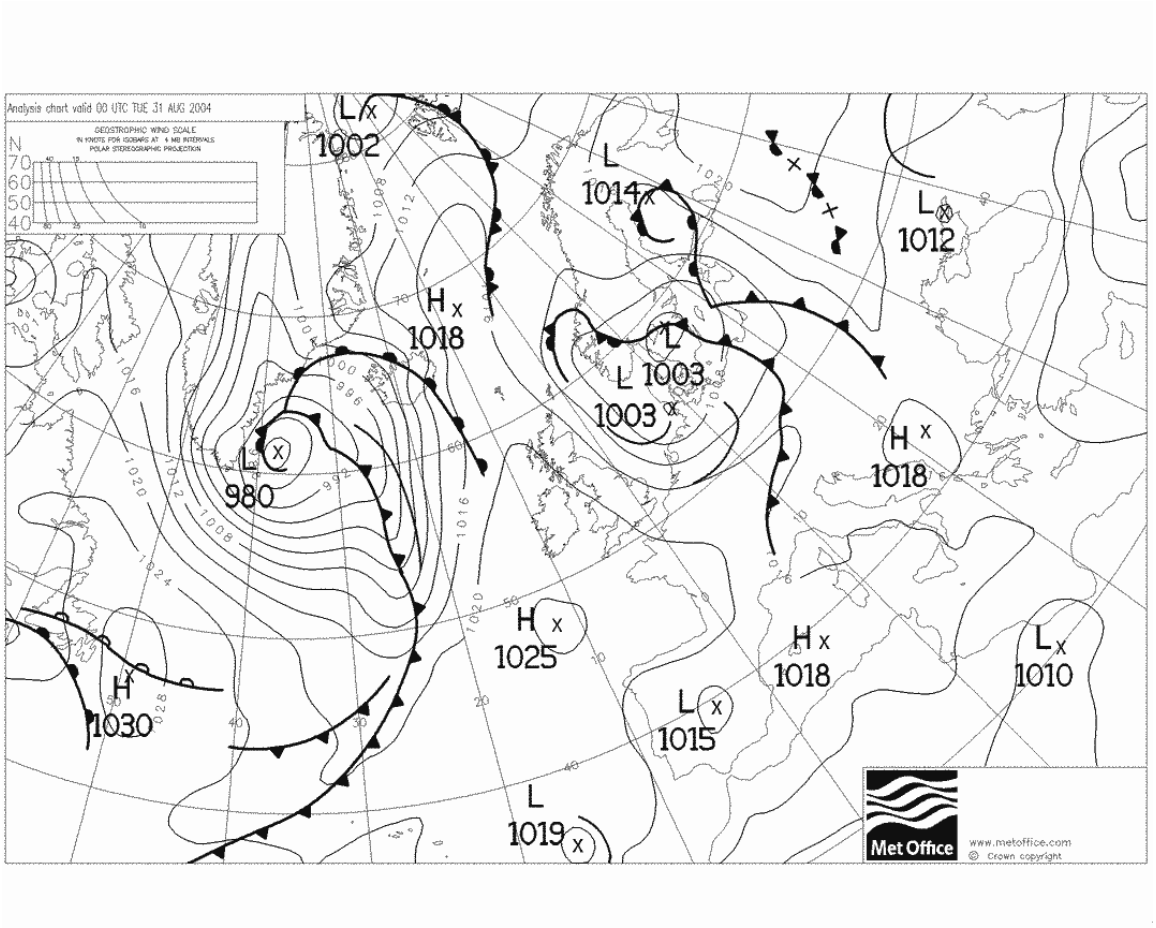

Figure 64: Meteorological Analysis: August 31, 2004

September 11, 2004: Meteorological Analysis

An intense low pressure system located off the western coast of Ireland brought strong westerly winds to western Europe. An associated cold front extended into France bringing moderate to heavy rain, and a warm front extending north-eastward to northern Scotland also brought rain. A low located north of Norway brought high winds and rain to the north shore of north-western Russia. More lows located in the north, central and southern areas of west-central Russia brought moderate-heavy rains and strong westerly winds. Dominating central and southern Europe was a large area of high pressure centred over Romania, which brought clear skies and calm to light wind conditions throughout most of Europe and the Mediterranean.

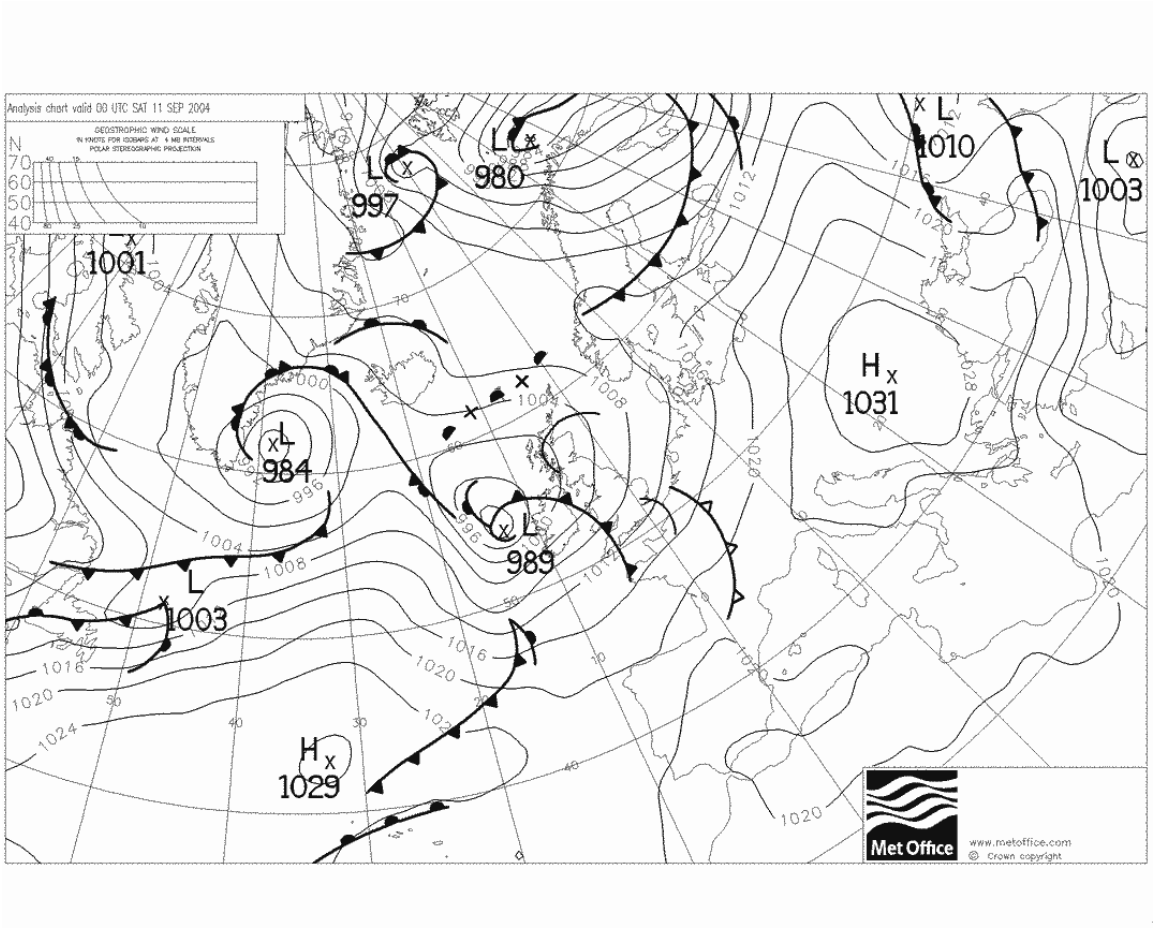

Figure 65: Meteorological Analysis: September 11, 2004

September 17, 2004: Meteorological Analysis

A very intense low pressure system south of Iceland brought very strong westerly winds to all of Britain. With this system two fronts passed in succession through Britain, first a warm front and then a cold front each bringing moderate to heavy rain. A low centred over Sardinia brought very heavy cold front-induced rains to central Italy. A low over northern Finland brought strong north-westerly winds and rain to north-western Russia. A low over eastern Turkey brought rain to this region. A large area of high pressure centred over central Germany brought clear skies and light winds to most areas of Europe.

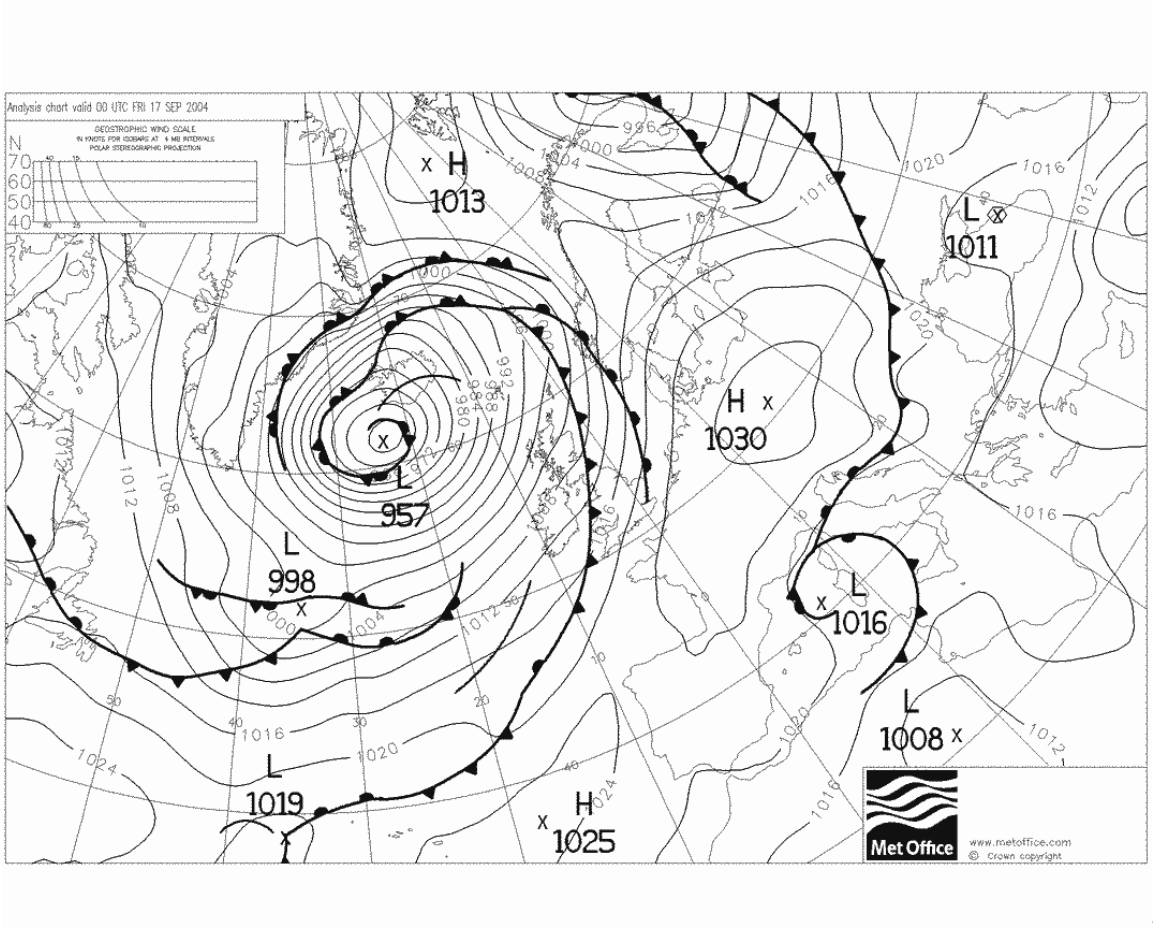

Figure 66: Meteorological Analysis: September 17, 2004

October 03, 2004: Meteorological Analysis

A deep low pressure system located north of Scotland brought strong westerly winds and moderate to heavy precipitation to the western parts of Britain. A series of cold fronts from this system passed through western Europe bringing short periods of heavy rain to all parts of Europe north of the Alps, including Scandinavia. A low centred over eastern Turkey brought rain, which was heavy at times, to southern Russia with its associated cold front. A series of high pressure systems located on both sides of Italy brought clear skies and calm conditions to the Mediterranean and North Africa.

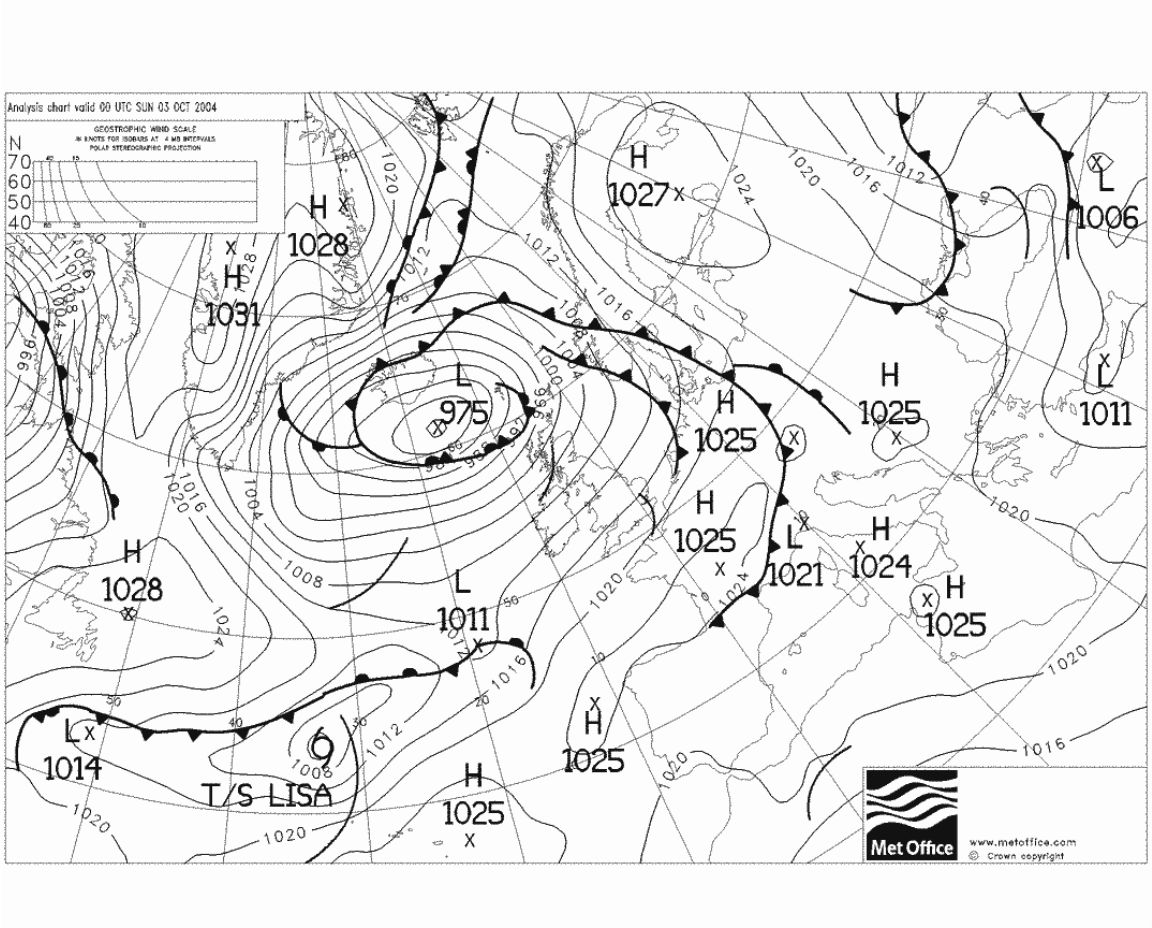

Figure 67: Meteorological Analysis: October 03, 2004

October 18, 2004: Meteorological Analysis

A deep low pressure system located over the Atlantic off the south-west portion of the Iberian Peninsula with an associated warm front, brought heavy rain and strong southerly winds to Portugal and southern Spain. A low located south of Iceland brought moderate to heavy rain and strong northerly winds to Iceland and moderate rain and less strong northerly winds to northern Scotland. A low pressure system located over southeast Sweden which brought strong westerly winds to northern Europe including Germany and Poland. With this system an associated cold front passed through bringing rain which was heavy at times. Another low pressure system located over the central portions of western Russia brought strong westerly and north-westerly winds and moderate to heavy rain to most of the northern sections of European Russia with an associated cold front. Highs located over the western and eastern areas of the Mediterranean and over the Adriatic brought clear skies and light winds to calm conditions to southern Europe.

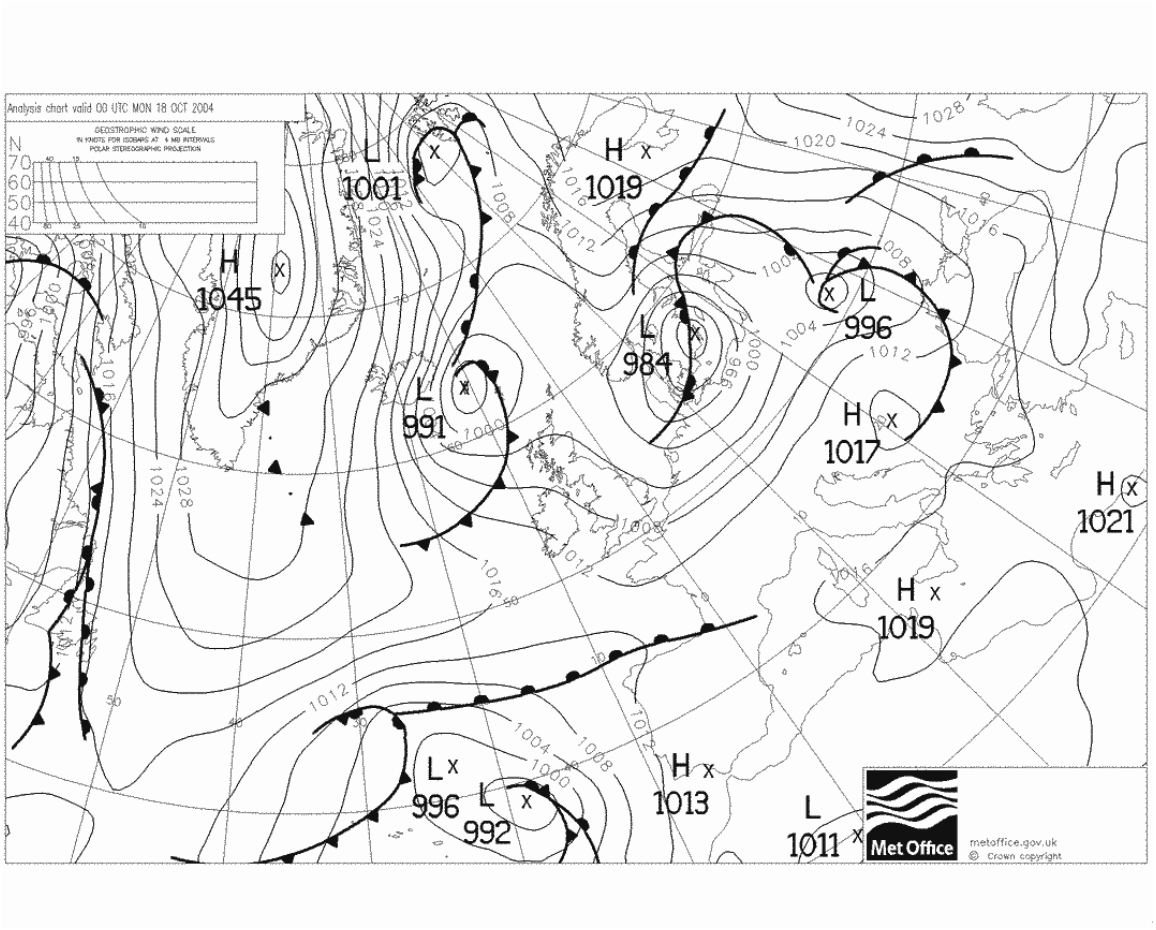

Figure 68: Meteorological Analysis: October 18, 2004

2. Additional Meteorological Files

a. Precipitation Rate (mm/hr)

PRATEsfc at 12Z Sat 10jan2004

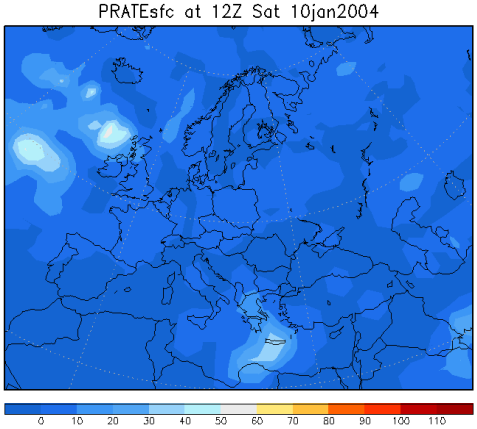

PRATEsfc at 12Z Tue 20jan2004

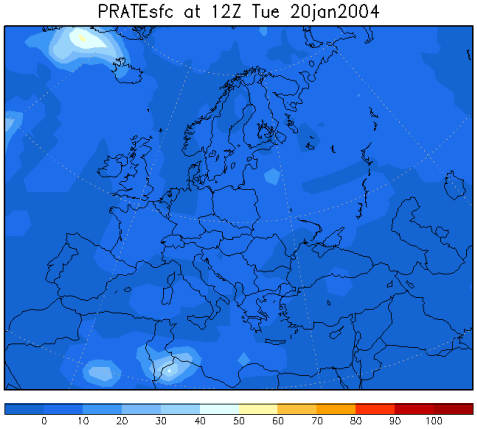

PRATEsfc at 12Z Wed 11feb2004

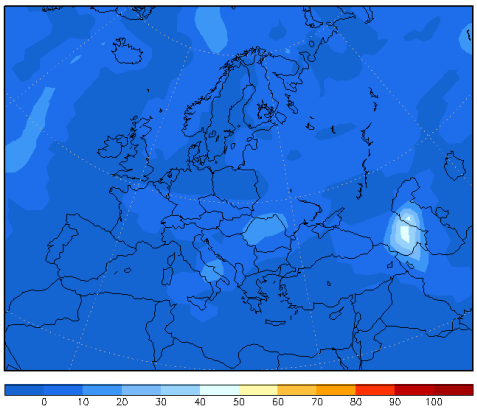

PRATEsfc at 12Z Thu 26feb2004

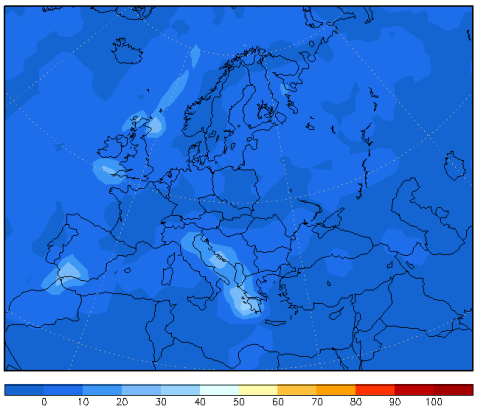

PRATEsfc at 12Z Mon 08mar2004

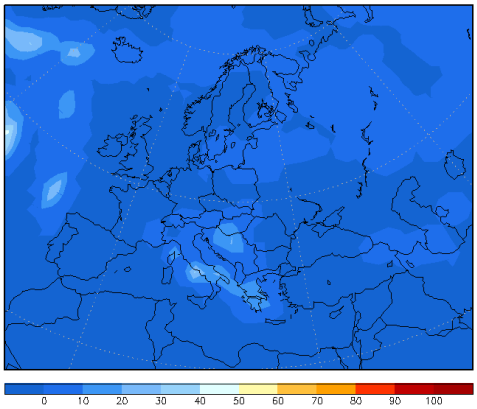

PRATEsfc at 12Z Thu 18mar2004

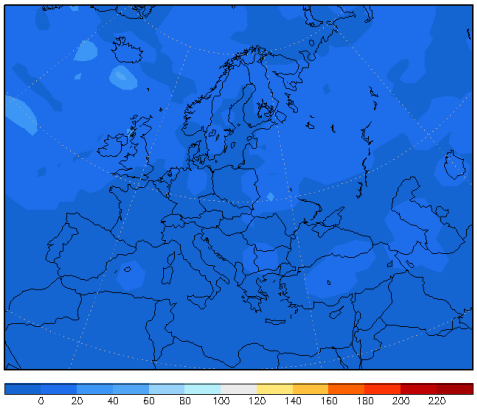

PRATEsfc at 12Z Thu 22apr2004

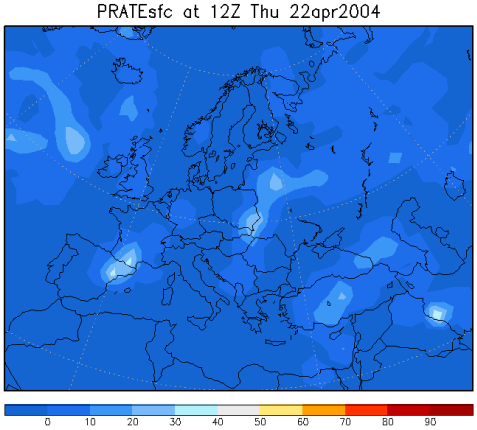

PRATEsfc at 12Z Thu 29apr2004

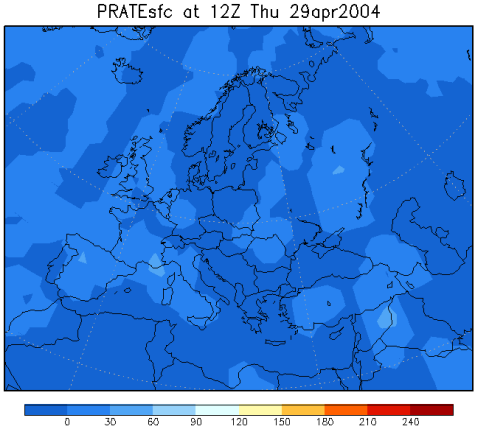

PRATEsfc at 12Z Mon 17may2004

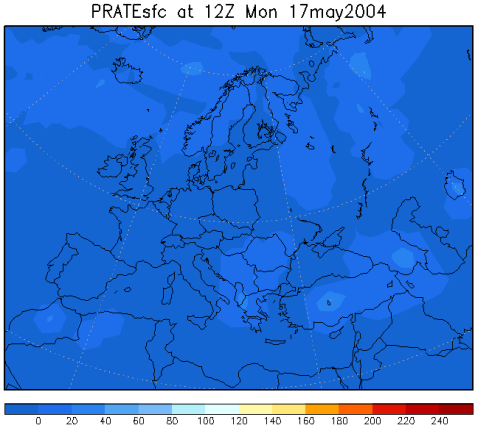

PRATEsfc at 12Z Fri 28may2004

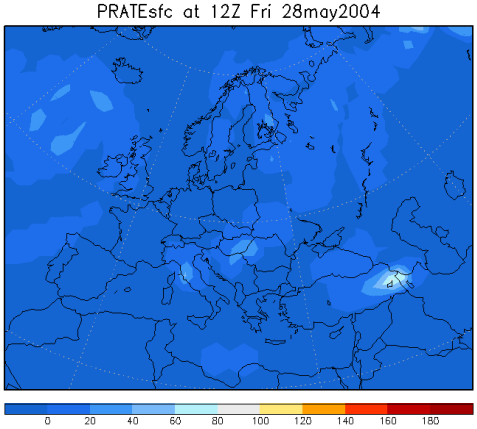

PRATEsfc at 12Z Tue 01jun2004

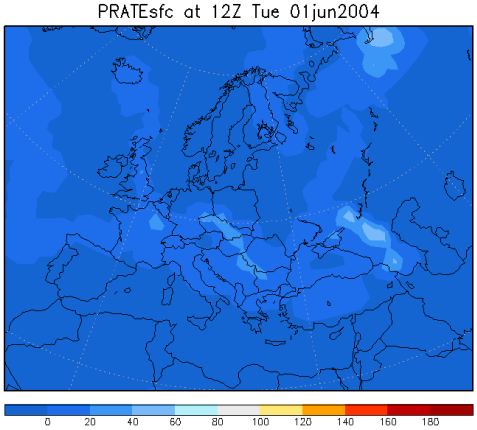

PRATEsfc at 12Z Tue 22jun2004

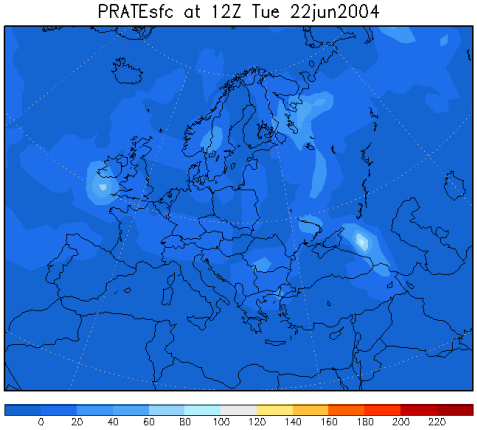

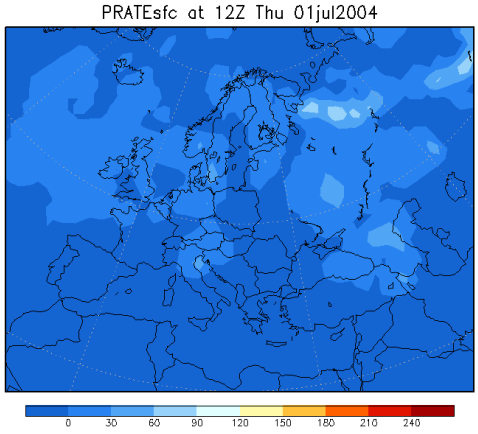
PRATEsfc at 12Z Thu 01jul2004
0 30 60 90 120 150 180 210 240

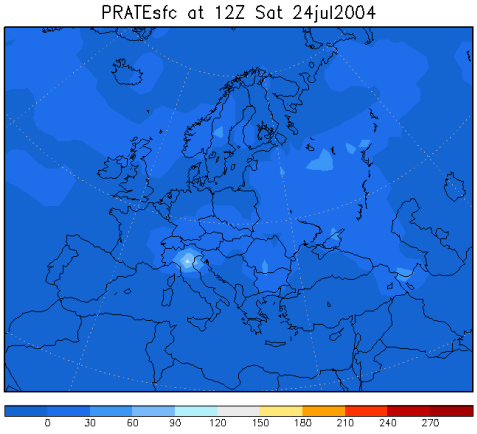
PRATEsfc at 12Z Sat 24jul2004
0 30 60 90 120 150 180 210 240 270

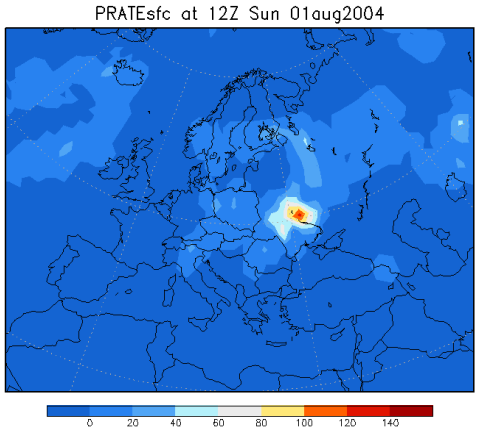
PRATEsfc at 12Z Sun 01aug2004
0 20 40 60 80 100 120 140

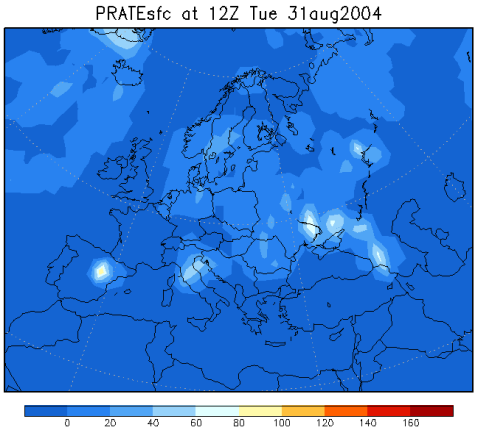
PRATEsfc at 12Z Tue 31aug2004
0 20 40 60 80 100 120 140 160

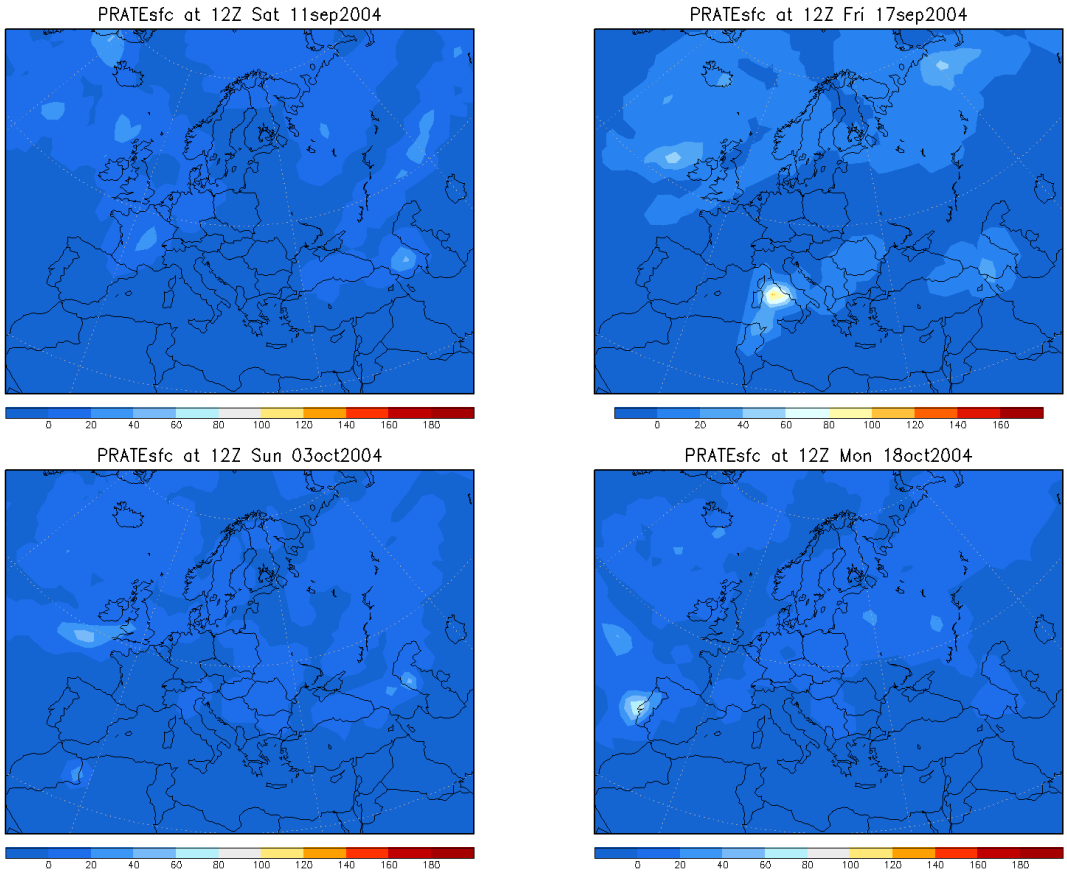

Figure 69: Precipitation Rate (mm/hr)

b. Temperature at FL 300 (C)

TMPprs at 12Z Sat 10jan2004

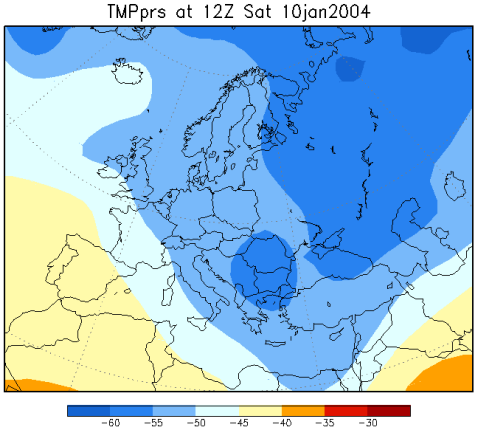

TMPprs at 12Z Tue 20jan2004

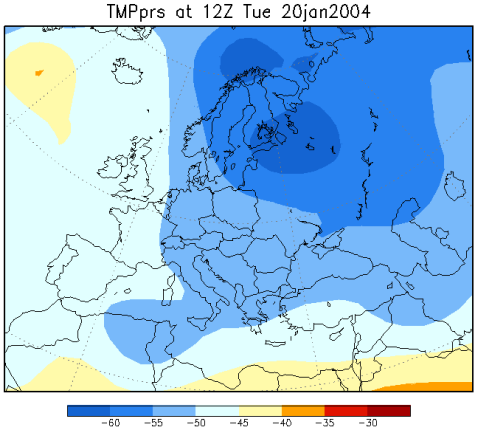

TMPprs at 12Z Wed 11feb2004

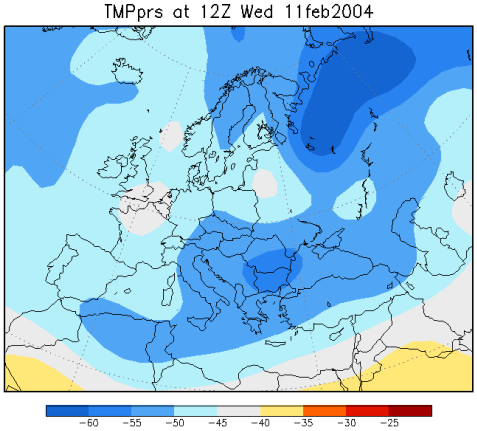

TMPprs at 12Z Thu 26feb2004

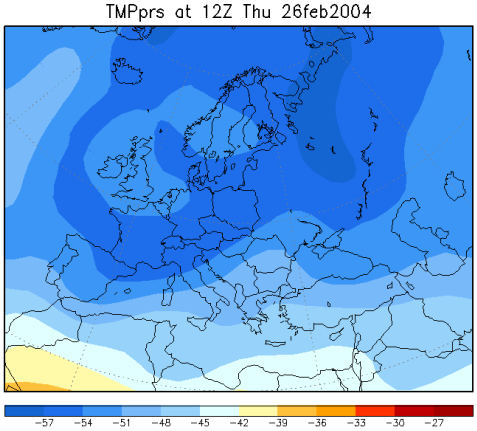

TMPprs at 12Z Mon 08mar2004

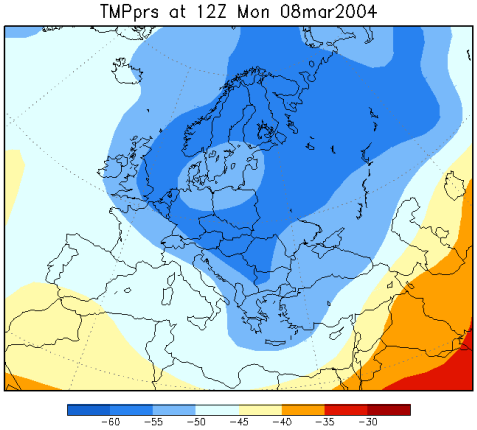

TMPprs at 12Z Thu 18mar2004

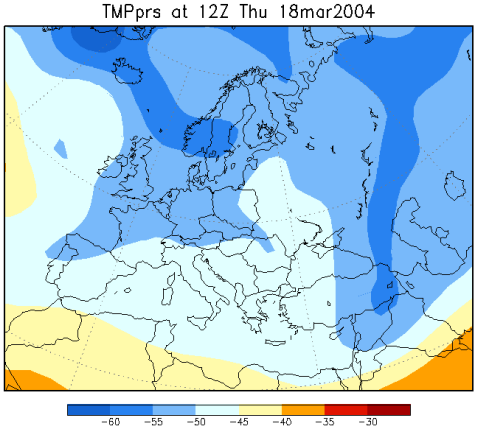

TMPprs at 12Z Thu 22apr2004

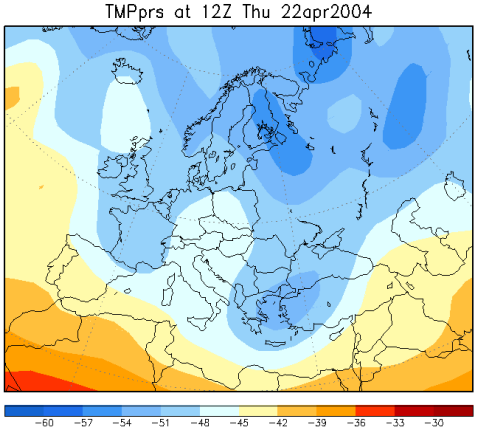

TMPprs at 12Z Thu 29apr2004

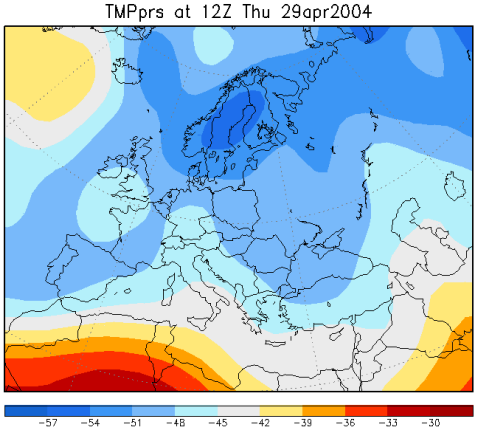

TMPprs at 12Z Mon 17may2004

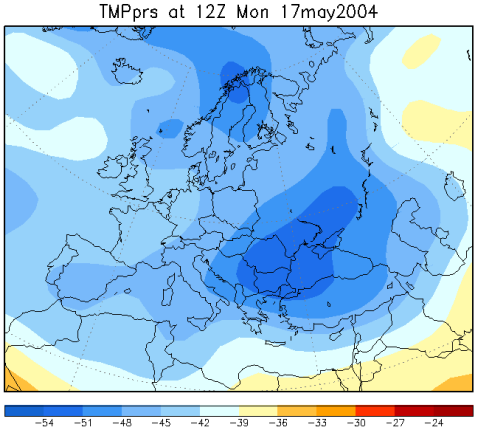

TMPprs at 12Z Fri 28may2004

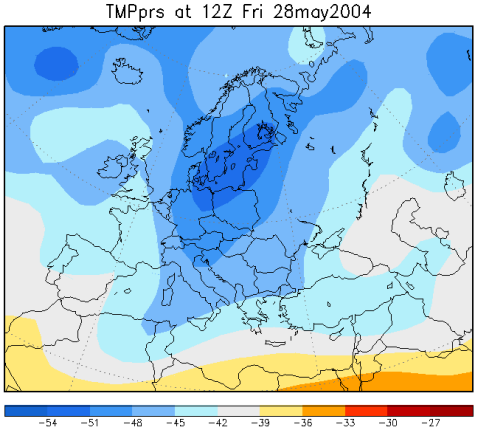

TMPprs at 12Z Tue 01jun2004

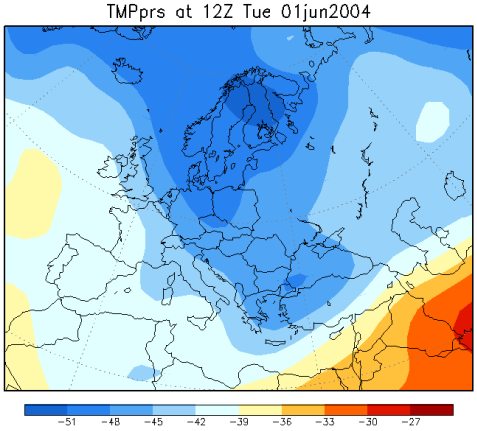

TMPprs at 12Z Tue 22jun2004

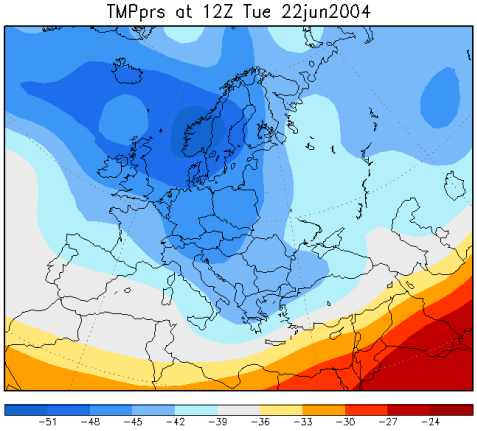

TMPprs at 12Z Thu 01jul2004

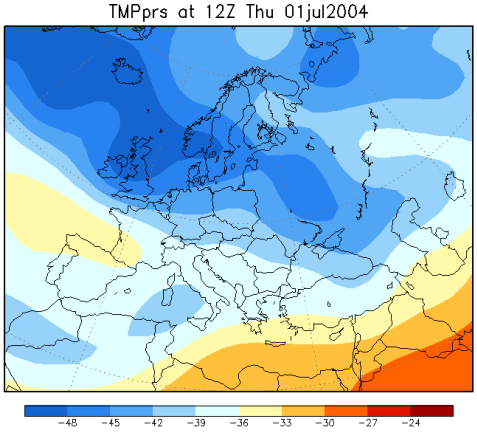

TMPprs at 12Z Sat 24jul2004

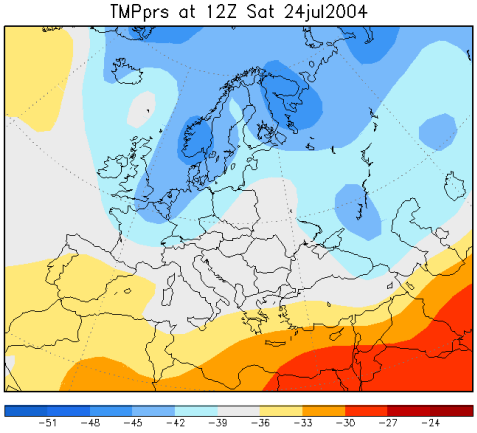

TMPprs at 12Z Sun 01aug2004

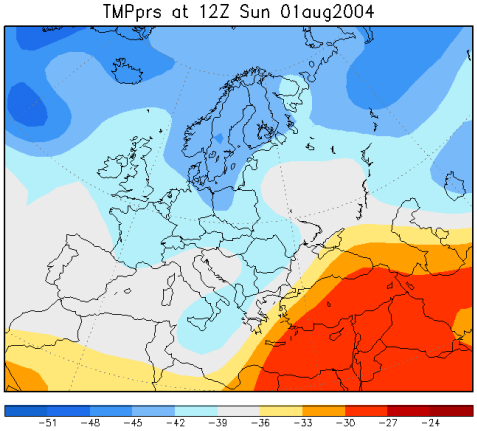

TMPprs at 12Z Tue 31aug2004

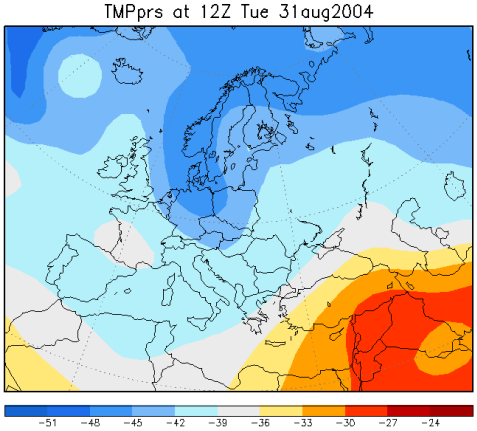

TMPprs at 12Z Sat 11sep2004

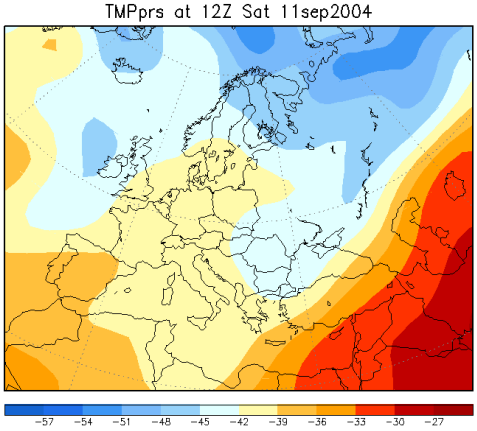

TMPprs at 12Z Fri 17sep2004

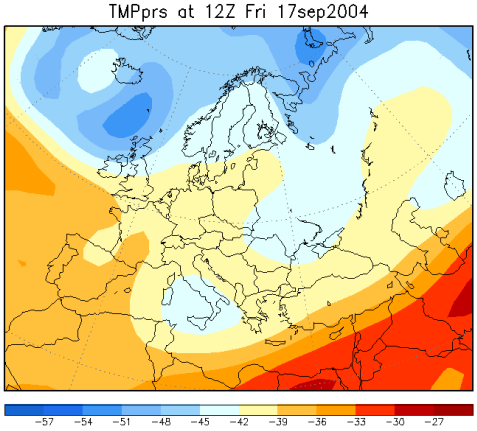

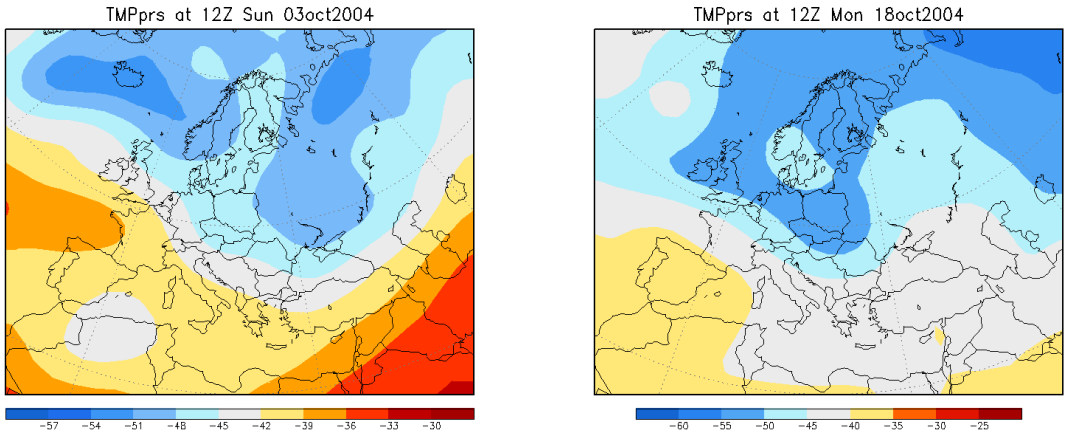

Figure 70: Temperature at FL 300 (C)

c. Relative Humidity at FL 300 (%)

RHprs at 12Z Sat 10jan2004

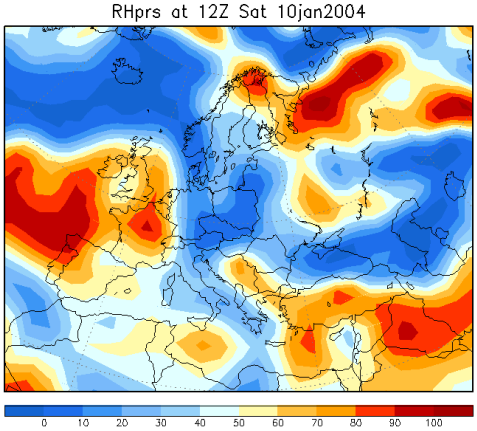

RHprs at 12Z Tue 20jan2004

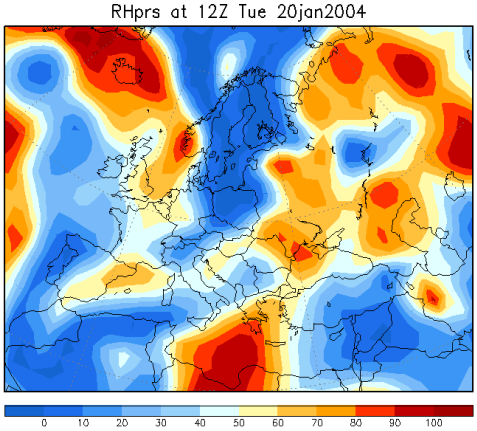

RHprs at 12Z Wed 11feb2004

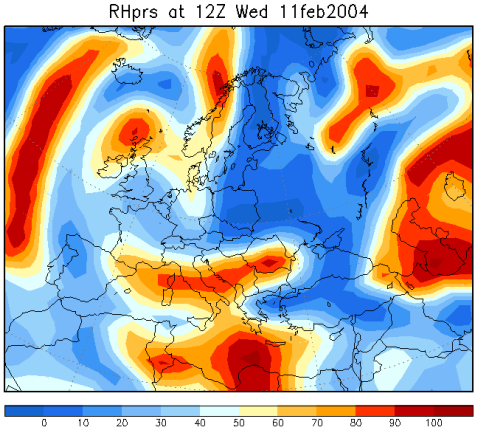

RHprs at 12Z Thu 26feb2004

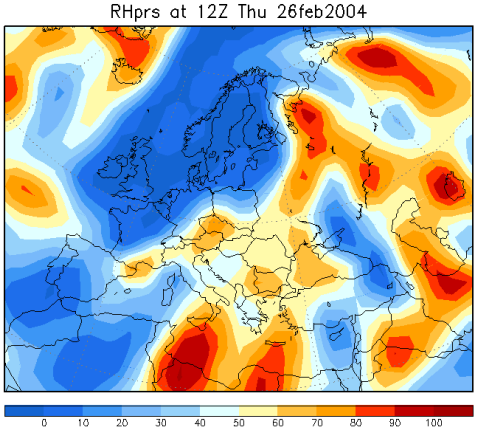

RHprs at 12Z Mon 08mar2004

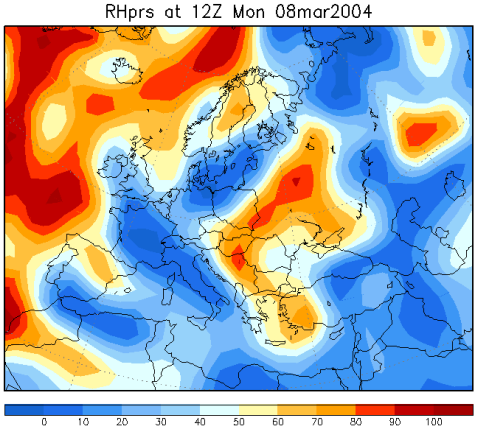

RHprs at 12Z Thu 18mar2004

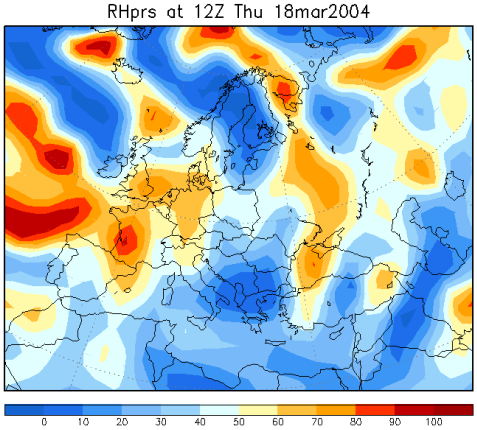

RHprs at 12Z Thu 22apr2004

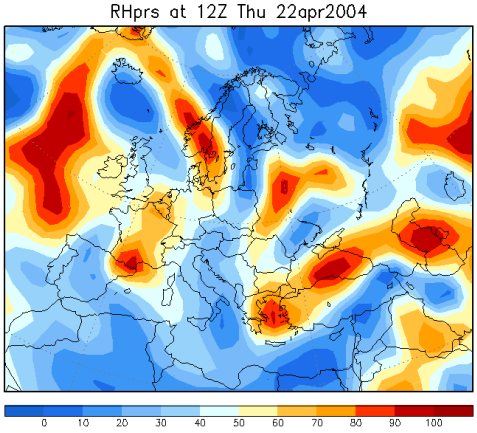

RHprs at 12Z Thu 29apr2004

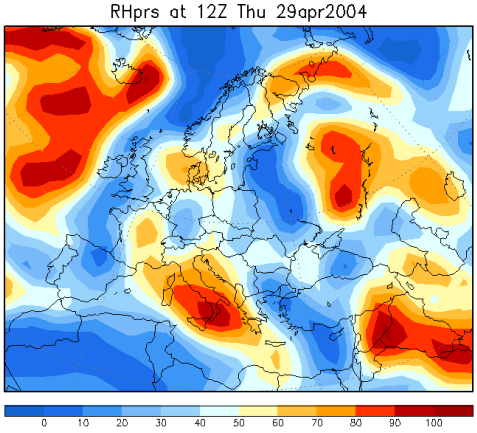

RHprs at 12Z Mon 17may2004

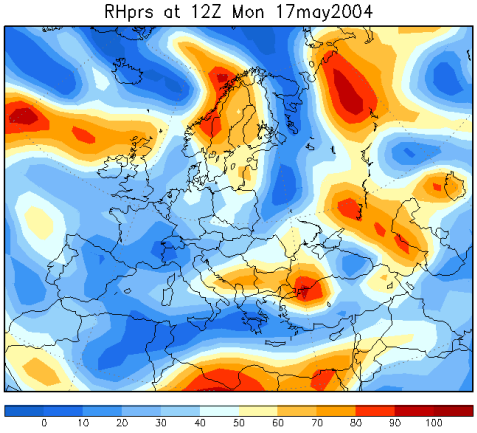

RHprs at 12Z Fri 28may2004

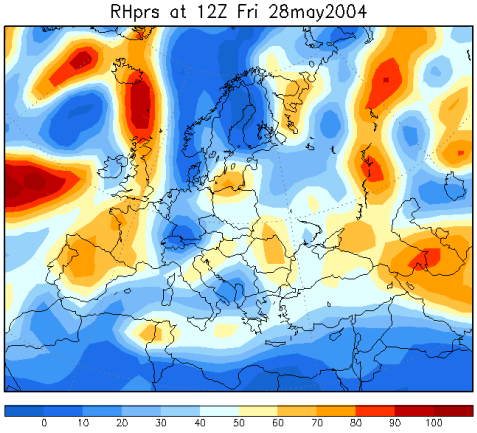

RHprs at 12Z Tue 01jun2004

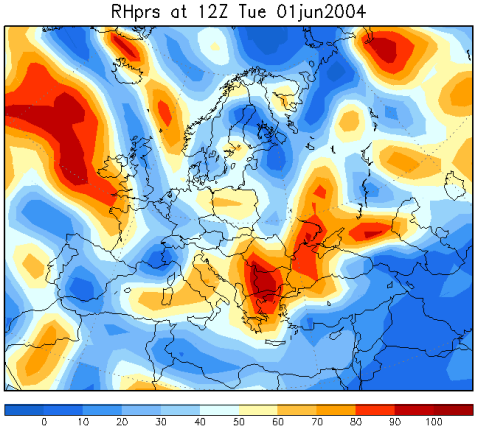

RHprs at 12Z Tue 22jun2004

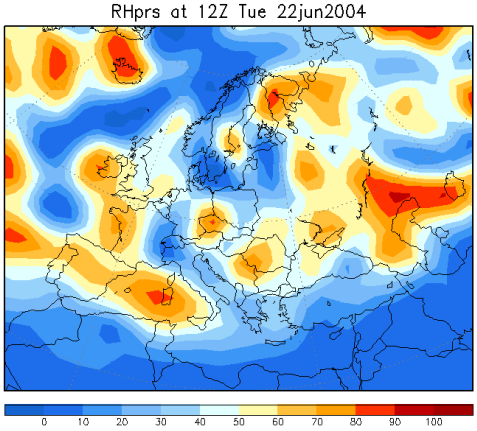

RHprs at 12Z Thu 01jul2004

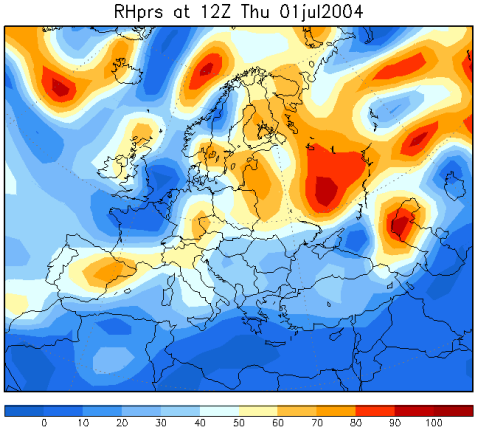

RHprs at 12Z Sat 24jul2004

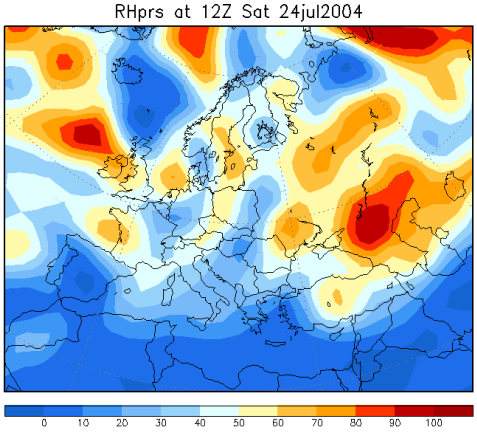

RHprs at 12Z Sun 01aug2004

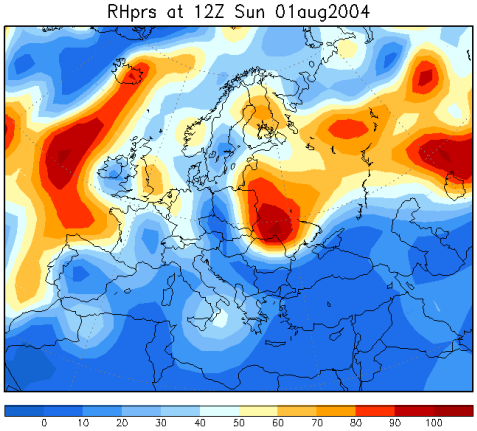

RHprs at 12Z Tue 31aug2004

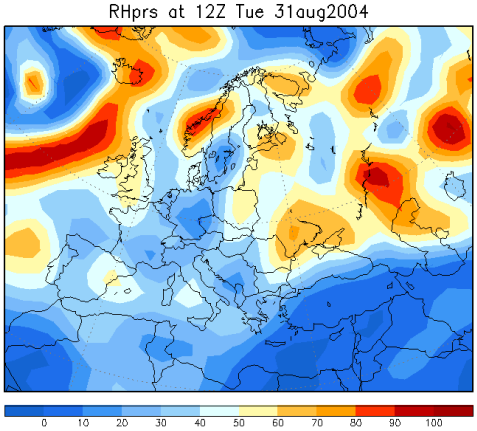

RHprs at 12Z Sat 11sep2004

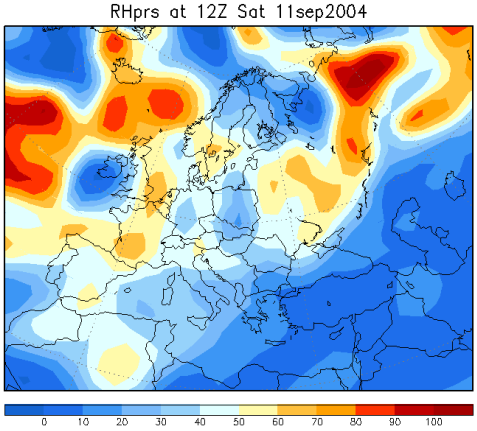

RHprs at 12Z Fri 17sep2004

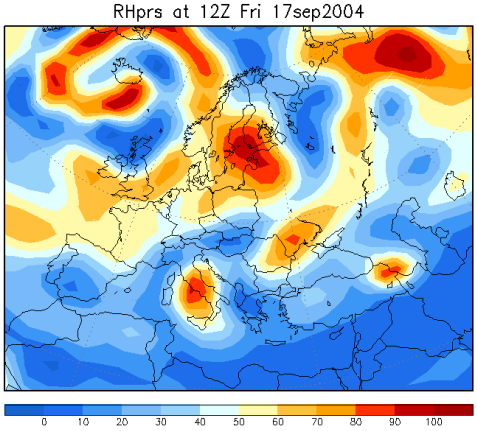

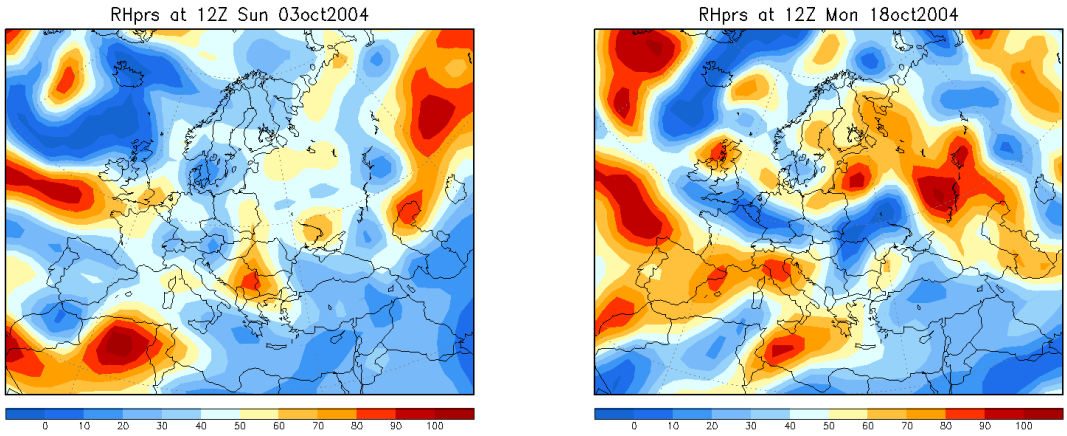

Figure 71: Relative Humidity at FL 300 (%)

ANNEX 6. DESCRIPTION OF CONTRAIL MODEL OUTPUT

For each day, the Contrail Model produces three kinds of output; a text file which contains all contrails produced for the day, a NetCDF file containing the gridded contrail coverage at the time of each satellite overpass, and a number of plots of the gridded contrail coverage for each satellite overpass. The contrail model text output is used to create gridded contrail maps. Since the contrail model does not include diffusion or transportation by winds of the contrails, the contrails used for the gridded output were those produced within 5 minutes of the satellite overpass time.

Contrail Model text file output format:

A text file containing all the contrails, as flight legs, produced for each day with the following format:

Start time of contrail, start latitude, start longitude, start flight level, end time of contrail, end latitude, end longitude, end flight level

An example of the text format is:

```
00:22:11,50.93,6.70,305.00,00:23:12,50.95,6.51,321.00
00:23:12,50.95,6.51,321.00,00:23:46,50.96,6.41,328.00
00:23:46,50.96,6.41,328.00,00:24:15,50.97,6.33,333.00
00:24:15,50.97,6.33,333.00,00:25:18,51.00,6.14,348.00
00:25:18,51.00,6.14,348.00,00:26:20,51.02,5.95,360.00
00:26:20,51.02,5.95,360.00,00:26:29,51.03,5.92,360.00
00:26:29,51.03,5.92,360.00,00:27:22,51.07,5.77,360.00
00:27:22,51.07,5.77,360.00,00:28:24,51.12,5.60,360.00
00:28:24,51.12,5.60,360.00,00:28:43,51.14,5.54,360.00
00:28:43,51.14,5.54,360.00,00:29:27,51.17,5.42,360.00
00:29:27,51.17,5.42,360.00,00:30:30,51.22,5.25,360.00
00:30:30,51.22,5.25,360.00,00:31:33,51.27,5.07,360.00
00:31:33,51.27,5.07,360.00,00:32:34,51.32,4.90,360.00
00:32:34,51.32,4.90,360.00,00:33:37,51.37,4.72,360.00
00:33:37,51.37,4.72,360.00,00:34:39,51.42,4.55,360.00
00:34:39,51.42,4.55,360.00,00:35:43,51.47,4.38,360.00
00:35:43,51.47,4.38,360.00,00:36:45,51.52,4.21,360.00
00:36:45,51.52,4.21,360.00,00:37:47,51.57,4.03,360.00
00:37:47,51.57,4.03,360.00,00:38:50,51.61,3.86,360.00
00:38:50,51.61,3.86,360.00,00:39:52,51.66,3.69,360.00
00:39:52,51.66,3.69,360.00,00:40:55,51.71,3.52,360.00
00:40:55,51.71,3.52,360.00,00:41:57,51.75,3.34,360.00
00:41:57,51.75,3.34,360.00,00:43:00,51.80,3.17,360.00
00:43:00,51.80,3.17,360.00,00:44:02,51.84,3.00,360.00
00:44:02,51.84,3.00,360.00,00:45:05,51.89,2.82,360.00
00:45:05,51.89,2.82,360.00,00:46:07,51.94,2.64,360.00
… etc.
```

Table 26: Example Text Output

NetCDF Format

NetCDF (Network Common Data Format) is an interface for array-oriented data access and a library that provides an implementation of the interface. The netCDF library also defines a machine-independent format for representing scientific data. Together, the interface, library, and format support the creation, access, and sharing of scientific data. The netCDF software was developed at the Unidata Program Center in Boulder, Colorado.

The NetCDF format is a self-describing binary grid format. Header information containing information about the dimensions and variables is followed by the latitude and longitude of the grid points and finally with the gridded data itself. When the format is converted to text (to view the data directly using a text dump utility) the output looks similar to the following:

```
netcdf contrails_2004-04-05 {
dimensions:
      lon = 120 ;
      lat = 80 ;
      time = 4 ;
variables:
      double lon(lon) ;
        lon:units = "degrees_east" ;
        lon:long_name = "longitude of lower left corner of grid cell" ;
      double lat(lat) ;
        lat:units = "degrees_north" ;
        lat:long_name = "latitude of lower left corner of grid cell" ;
      double time(time) ;
        time:units = "hours since 2004-04-05 00:00:00" ;
        time:long_name = "satellite overpass time" ;
      double contrails(time, lat, lon) ;
        contrails:units = "number of persistant contrails per grid cell" ;
        contrails:long_name = "contrail density at satellite overpass time" ;

// global attributes:
       :source = "Eurocontrol contrail model output" ;
data:

 lon = -10, -9.75, -9.5, -9.25, -9, -8.75, -8.5, -8.25, -8, -7.75, -7.5,
    -7.25, -7, -6.75, -6.5, -6.25, -6, -5.75, -5.5, -5.25, -5, -4.75, -4.5,
    -4.25, -4, -3.75, -3.5, -3.25, -3, -2.75, -2.5, -2.25, -2, -1.75, -1.5,
    -1.25, -1, -0.75, -0.5, -0.25, 0, 0.25, 0.5, 0.75, 1, 1.25, 1.5, 1.75, 2,
    2.25, 2.5, 2.75, 3, 3.25, 3.5, 3.75, 4, 4.25, 4.5, 4.75, 5, 5.25, 5.5,
    5.75, 6, 6.25, 6.5, 6.75, 7, 7.25, 7.5, 7.75, 8, 8.25, 8.5, 8.75, 9,
    9.25, 9.5, 9.75, 10, 10.25, 10.5, 10.75, 11, 11.25, 11.5, 11.75, 12,
    12.25, 12.5, 12.75, 13, 13.25, 13.5, 13.75, 14, 14.25, 14.5, 14.75, 15,
    15.25, 15.5, 15.75, 16, 16.25, 16.5, 16.75, 17, 17.25, 17.5, 17.75, 18,
    18.25, 18.5, 18.75, 19, 19.25, 19.5, 19.75 ;

 lat = 40, 40.25, 40.5, 40.75, 41, 41.25, 41.5, 41.75, 42, 42.25, 42.5,
    42.75, 43, 43.25, 43.5, 43.75, 44, 44.25, 44.5, 44.75, 45, 45.25, 45.5,
    45.75, 46, 46.25, 46.5, 46.75, 47, 47.25, 47.5, 47.75, 48, 48.25, 48.5,
    48.75, 49, 49.25, 49.5, 49.75, 50, 50.25, 50.5, 50.75, 51, 51.25, 51.5,
    51.75, 52, 52.25, 52.5, 52.75, 53, 53.25, 53.5, 53.75, 54, 54.25, 54.5,
    54.75, 55, 55.25, 55.5, 55.75, 56, 56.25, 56.5, 56.75, 57, 57.25, 57.5,
    57.75, 58, 58.25, 58.5, 58.75, 59, 59.25, 59.5, 59.75 ;

 time = 4.6, 10.6333333333333, 14.3333333333333, 20.3833333333333 ;

 contrails =
```

```
  0, 0, 0, 0, 0, 0, 0, 0, 0, 0, 0, 0, 0, 0, 0, 0, 0, 0, 0, 0, 0, 0, 0, 0,
    0, 0, 0, 0, 0, 0, 0, 0, 0, 0, 0, 0, 0, 0, 0, 0, 0, 0, 0, 0, 0, 0, 0, 0,
    0, 0, 0, 0, 0, 0, 0, 0, 0, 0, 0, 0, 0, 0, 0, 0, 0, 0, 0, 0, 0, 0, 0, 0,
    0, 0, 0, 0, 0, 0, 0, 1, 0, 0, 0, 0, 0, 0, 0, 0, 0, 0, 0, 0, 0, 0, 0, 0,
    0, 0, 1, 0, 0, 0, 0, 0, 0, 0, 0, 0, 0, 0, 0, 0, 0, 0, 2, 1, 0, 0, 0,
  0, 0, 0, 0, 0, 0, 0, 0, 0, 0, 0, 0, 0, 0, 0, 0, 0, 0, 0, 0, 0, 0, 0, 0, 0,
    0, 0, 0, 0, 0, 0, 0, 0, 0, 0, 0, 0, 0, 0, 0, 0, 0, 0, 0, 0, 0, 0, 0, 0,
    0, 0, 0, 0, 0, 0, 0, 0, 0, 0, 0, 0, 0, 0, 0, 0, 0, 0, 0, 0, 0, 0, 0, 0,
    0, 0, 0, 0, 0, 0, 0, 1, 0, 0, 0, 0, 0, 0, 0, 0, 0, 0, 0, 0, 0, 0, 0, 0,
    0, 0, 0, 0, 0, 0, 0, 0, 0, 0, 0, 0, 0, 0, 0, 0, 2, 2, 1, 0, 0, 0, 0,
  0, 0, 0, 0, 0, 0, 0, 0, 0, 0, 0, 0, 0, 0, 0, 0, 0, 0, 0, 0, 0, 0, 0, 0, 0,
    0, 0, 0, 0, 0, 0, 0, 0, 0, 0, 0, 0, 0, 0, 0, 0, 0, 0, 0, 0, 0, 0, 0, 0,
    0, 0, 0, 0, 0, 0, 0, 0, 0, 0, 0, 0, 0, 0, 0, 0, 0, 0, 0, 0, 0, 0, 0, 0,
    0, 0, 0, 0, 0, 0, 0, 1, 0, 0, 0, 0, 0, 0, 0, 0, 0, 0, 0, 0, 0, 0, 0, 0,
    0, 0, 0, 0, 0, 0, 0, 0, 0, 0, 0, 0, 0, 0, 0, 0, 1, 1, 0, 0, 0, 0, 0, 0,
  0, 0, 0, 0, 0, 0, 0, 0, 0, 0, 0, 0, 0, 0, 0, 0, 0, 0, 0, 0, 0, 0, 0, 0, 0,
    0, 0, 0, 0, 0, 0, 0, 0, 0, 0, 0, 0, 0, 0, 0, 0, 0, 0, 0, 0, 0, 0, 0, 0,
    0, 0, 0, 0, 0, 0, 0, 0, 0, 0, 0, 0, 0, 0, 0, 1, 1, 1, 1, 1, 1, 0, 0, 0, 0,
    0, 0, 0, 0, 0, 0, 0, 1, 0, 0, 0, 0, 0, 0, 0, 0, 0, 0, 0, 0, 0, 0, 0, 0, 0,
.. etc.
```

Table 27: Example NetCDF Output

Contrail Model Plots

Plots are produced for each satellite overpass in two formats; JPEG and WMF. An example plot is as follows:

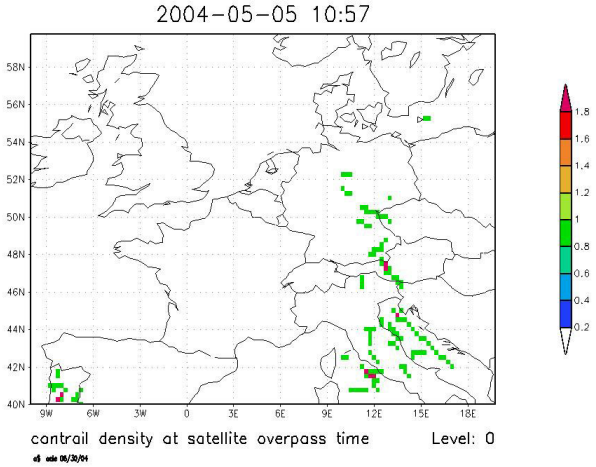

Figure 72: Example Contrail Map

ANNEX 7. CONTRAIL MAP FILE NAMES AND SATELLITE TIMES

The NetCDF files for Scenario 'Kerosene' are called **future_contrails_yyyy_mm_dd.nc**, and for Scenario 'Hydrogen' **H2_contrails_yyyy_mm_dd.nc.** The text files for Scenario 'kerosene' are called **future_contrails_yyyy_mm_dd.txt** and for Scenario 'Hydrogen' **H2_contrails_yyyy_mm_dd.txt** Two formats are available for each satellite overpass; a .JPEG format and a .WMF format. The files names are **yyyymmdd_#$.jpg** and **yyyymmdd_#$.wmf**, where # is the satellite overpass number that day and **$** = **A** for Scenario 2028K, **B** for Scenario 2050H and **C** for Scenario 2050K.

The Contrail Model time is taken as 2/3 of the time between the start and the end of the satellite overpass. This is used because the area of interest (central and Western Europe) is only a subset of the total satellite view. The following table shows the satellites overpass times for the project dates:

Date	Satellite Number	Satellite Start Time	Satellite End Time	Satellite Duration	CONTRAIL Model Time
10/01/2004	1	01:40:15	01:55:49	00:15:34	01:50:37
	2	09:38:46	09:53:30	00:14:44	09:48:35
	3	13:11:06	13:26:15	00:15:09	13:21:12
	4	15:58:40	16:13:06	00:14:26	16:08:17
20/01/2004	1	01:27:19	01:42:44	00:15:25	01:37:35
	2	09:12:30	09:26:11	00:13:41	09:21:37
	3	15:13:45	15:28:24	00:14:39	15:23:30
	4	20:39:07	20:54:09	00:15:02	29:49:08
11/02/2004	1	02:20:22	02:32:34	00:12:12	02:29:48
	2	09:16:54	09:26:37	00:09:43	09:23:22
	3	12:09:40	12:24:34	00:14:54	12:19:35
	4	16:16:11	16:28:55	00:12:44	16:24:40
26/02/2004	1	01:10:44	01:24:32	00:13:48	01:19:55
	2	10:12:37	10:27:38	00:15:01	10:22:37
	3	12:40:20	12:55:22	00:15:02	12:50:21
	4	20:00:02	20:14:38	00:14:36	20:09:45
08/03/2004	1	00:46:30	00:59:32	00:13:02	00:55:11
	2	05:53:20	06:06:30	00:13:10	06:02:06
	3	12:15:45	12:30:54	00:15:09	12:25:51
	4	15:37:18	15:52:08	00:14:50	15:47:11
18/03/2004	1	02:13:14	02:27:32	00:14:18	02:22:46
	2	10:36:07	10:50:33	00:14:26	10:45:44
	3	13:44:39	13:58:14	00:13:35	13:53:42
	4	20:23:14	20:38:05	00:14:51	20:33:08
22/04/2004	1	04:11:09	04:24:18	00:13:09	04:19:55
	2	10:42:55	10:56:48	00:13:53	10:52:10
	3	15:33:32	15:48:27	00:14:55	15:43:20
	4	22:08:51	22:21:03	00:12:12	22:16:59
29/04/2004	1	02:38:21	02:52:51	00:14:30	02:48:00
	2	11:22:39	11:35:55	00:13:16	11:31:36
	3	16:02:06	16:16:35	00:14:29	16:11:45
	4	21:08:12	21:23:04	00:14:52	21:18:06

17/05/2004	1	00:54:03	01:06:57	00:12:54	01:02:39
	2	02:34:24	02:48:58	00:14:34	02:44:06
	3	03:55:42	04:10:27	00:14:45	04:05:32
	4	04:15:17	04:26:23	00:11:06	04:22:41
	5	10:45:17	10:57:26	00:12:09	10:53:28
	6	11:14:34	11:27:41	00:13:07	11:23:18
	7	12:23:40	12:38:40	00:15:00	12:33:39
	8	13:41:38	13:54:40	00:13:02	13:50:19
	9	14:05:36	14:18:38	00:13:02	14:14:17
	10	15:19:51	15:34:51	00:15:00	15:29:50
	11	19:20:48	19:33:55	00:13:07	19:29:32
	12	20:59:17	21:14:06	00:14:49	20:29:09
28/05/2004	1	02:08:53	02:23:28	00:14:35	02:18:36
	2	03:49:56	04:02:44	00:12:48	03:58:28
	3	04:26:26	04:40:29	00:14:03	04:35:48
	4	06:05:42	06:18:24	00:12:42	06:14:09
	5	10:25:05	10:38:31	00:13:26	10:34:02
	6	12:00:09	12:13:05	00:12:56	12:08:46
	7	13:39:46	13:54:24	00:14:38	13:49:31
	8	14:10:36	14:24:44	00:14:08	14:20:01
	9	15:50:00	16:04:31	00:14:31	15:59:40
	10	20:09:57	20:24:12	00:14:15	20:14:27
	11	21:50:47	22:03:53	00:13:06	21:59:31
01/06/2004	1	12:14:17	12:25:01	00:10:44	12:21:26
	2	18:42:17	18:51:56	00:09:39	18:48:39
22/06/2004	1	00:45:52	00:59:03	00:13:11	00:54:39
	2	02:26:01	02:40:32	00:14:31	02:35:41
	3	04:06:37	04:18:42	00:12:05	04:14:40
	4	05:51:43	06:05:02	00:13:19	06:00:35
	5	09:16:18	09:30:29	00:14:11	09:25:45
	6	10:56:26	11:10:36	00:14:10	11:05:52
	7	12:15:16	12:30:32	00:15:16	12:25:26
	8	13:57:34	14:09:48	00:12:14	14:05:43
	9	15:35:43	15:50:32	00:14:49	15:45:35
	10	19:03:14	19:15:18	00:12:04	19:11:16
	11	20:41:41	20:55:47	00:14:06	20:51:05
01/07/2004	1	02:23:52	02:38:27	00:14:35	02:33:35
	2	03:50:21	04:04:38	00:14:17	03:59:52
	3	04:06:06	04:16:42	00:10:36	04:13:09
	4	05:30:31	05:44:24	00:13:53	05:39:46
	5	09:11:41	09:24:58	00:13:17	09:20:32
	6	10:51:54	11:05:55	00:14:01	11:01:14
	7	12:13:26	12:28:14	00:14:48	12:23:18
	8	13:37:16	13:49:10	00:11:54	13:45:12
	9	13:55:32	14:08:09	00:12:37	14:04:21
	10	13:56:47	14:08:08	00:11:21	14:04:21
	11	15:15:00	15:29:21	00:14:21	15:24:34
	12	20:36:16	20:51:05	00:14:49	20:46:08
24/07/2004	1	01:22:10	01:36:57	00:14:47	01:32:01
	2	03:02:54	03:17:31	00:14:37	03:12:38

	3	04:25:10	04:39:59	00:14:49	04:35:02
	4	06:05:22	06:17:58	00:12:36	06:13:45
	5	11:13:11	11:26:48	00:13:37	11:22:15
	6	12:52:38	13:07:47	00:15:09	13:02:44
	7	14:09:57	14:23:52	00:13:55	14:19:13
	8	15:49:20	16:03:55	00:14:35	15:59:03
	9	21:54:35	22:07:56	00:13:21	22:03:28
01/08/2004	1	04:28:32	04:43:17	00:14:45	04:38:18
	2	06:08:42	06:20:58	00:12:16	06:16:52
	3	09:06:52	09:19:42	00:12:50	09:15:25
	4	10:46:56	11:00:52	00:13:56	10:56:13
	5	12:27:26	12:37:23	00:09:57	12:34:03
	6	13:01:39	13:16:58	00:15:19	13:11:50
	7	14:13:10	14:27:29	00:14:19	14:22:42
	8	15:52:39	16:07:18	00:14:39	16:02:25
	9	20:31:37	20:45:59	00:14:22	20:41:11
	10	22:12:46	22:25:06	00:12:20	22:20:59
31/08/2004	1	00:50:19	01:04:26	00:14:07	00:59:43
	2	02:31:23	02:46:22	00:14:59	02:41:22
	3	03:50:32	04:05:06	00:14:34	04:00:14
	4	04:12:23	04:24:04	00:11:41	04:20:10
	5	09:23:54	09:38:19	00:14:25	09:33:30
	6	10:42:57	10:54:37	00:11:40	10:50:43
	7	11:03:47	11:17:59	00:14:12	11:13:14
	8	12:20:40	12:35:59	00:15:19	12:33:34
	9	13:36:41	13:49:11	00:12:30	13:41:53
	10	14:02:28	14:16:22	00:13:54	14:11:44
11/09/2004	1	02:05:48	02:21:00	00:15:12	02:15:56
	2	03:46:50	04:00:06	00:13:16	03:55:40
	3	04:19:54	04:34:48	00:14:54	04:29:49
	4	06:00:16	06:13:08	00:12:52	06:08:50
	5	10:13:46	10:27:41	00:13:55	10:23:02
	6	11:54:09	12:05:51	00:11:42	12:01:57
	7	13:36:27	13:51:24	00:14:57	13:46:24
	8	14:05:19	14:18:58	00:13:39	14:14:25
	9	15:44:10	15:58:52	00:14:42	15:53:58
	10	19:59:09	20:13:04	00:13:55	20:08:25
	11	21:39:07	21:53:07	00:14:00	21:48:26
17/09/2004	1	00:57:00	01:11:26	00:14:26	01:06:37
	2	02:38:09	02:53:05	00:14:56	02:48:06
	3	03:32:29	03:46:36	00:14:07	03:41:53
	4	04:19:04	04:30:39	00:11:35	04:26:47
	5	05:12:25	05:26:50	00:14:25	05:21:48
	6	06:52:57	07:03:04	00:10:07	06:59:41
	7	09:36:53	09:51:28	00:14:35	09:46:36
	8	10:49:36	11:01:29	00:11:53	10:57:31
	9	11:17:08	11:30:44	00:13:36	11:26:12
	10	12:27:43	12:42:47	00:15:04	12:37:45
	11	14:09:23	14:22:37	00:13:14	14:18:15
	12	14:56:23	15:11:24	00:15:01	15:06:23

	13	16:37:40	16:50:30	00:12:50	16:46:13
	14	19:23:27	19:36:27	00:13:00	19:32:07
	15	21:01:57	21:16:39	00:14:42	21:11:44
03/10/2004	1	01:14:19	01:29:00	00:14:41	01:24:06
	2	01:15:25	01:30:00	00:14:35	01:25:08
	3	02:55:07	03:09:59	00:14:52	03:05:01
	4	02:56:29	03:11:03	00:14:34	03:06:11
	5	03:38:40	03:53:03	00:14:23	03:48:15
	6	04:36:22	04:47:42	00:11:20	04:43:55
	7	04:37:41	04:47:59	00:10:18	04:44:32
	8	05:18:44	05:33:01	00:14:17	05:28:15
	9	10:12:09	10:26:14	00:14:05	10:21:32
	10	10:12:58	10:26:57	00:13:59	10:22:17
	11	11:07:20	11:19:33	00:12:13	11:15:28
	12	11:08:19	11:21:11	00:12:52	11:16:53
	13	11:52:00	12:04:26	00:12:26	12:00:17
	14	11:53:20	12:05:04	00:11:44	12:01:09
	15	12:45:56	13:00:46	00:14:50	12:55:49
	16	12:47:01	13:02:06	00:15:05	12:57:04
	17	13:25:38	13:36:44	00:11:06	13:33:01
	18	14:29:56	14:42:13	00:12:17	14:38:07
	19	15:02:44	15:17:37	00:14:53	15:12:39
	20	16:44:11	16:56:48	00:12:37	16:52:35
	21	19:58:19	20:12:20	00:14:01	20:07:39
	22	19:58:19	20:13:31	00:15:12	20:08:42
	23	21:37:50	21:52:12	00:14:22	21:47:24
	24	21:39:27	21:53:31	00:14:04	21:48:49
18/10/2004	1	01:43:54	01:59:03	00:15:09	01:34:00
	2	01:44:30	02:00:03	00:15:33	01:54:52
	3	03:24:50	03:39:04	00:14:14	03:34:19
	4	03:25:31	03:40:00	00:14:29	03:35:10
	5	04:09:15	04:24:20	00:15:05	04:19:18
	6	05:49:31	06:03:10	00:13:39	05:58:36
	7	09:30:04	09:44:28	00:14:24	09:39:39
	8	09:30:44	09:45:34	00:14:50	09:40:37
	9	11:10:13	11:24:04	00:13:51	11:19:27
	10	11:11:13	11:25:01	00:13:48	11:20:24
	11	11:35:52	11:49:45	00:13:53	11:45:07
	12	11:36:30	11:50:51	00:14:21	11:46:03
	13	13:15:17	13:30:30	00:15:13	13:25:25
	14	13:16:52	13:31:47	00:14:55	13:26:48
	15	13:54:54	14:08:26	00:13:32	14:03:55
	16	15:33:41	15:48:29	00:14:48	15:43:33
	17	19:17:36	19:30:28	00:12:52	19:27:15
	18	19:18:22	19:31:42	00:13:20	19:27:15
	19	20:56:25	21:10:43	00:14:18	21:05:57
	20	20:57:17	21:11:59	00:14:42	21:07:05

Table 28: Satellite Overpass Times

REFERENCES

[Ref 1] FAA, 2004, Aviation and Emissions – A Primer, Federal Aviation Administration, http://www.aee.faa.gov/emissions/

[Ref 2] "Airbus Global Market Forecast (Airbus GMF)", Airbus Industrie, 1999

[Ref 3] "Aviation and the Global Atmosphere", Intergovernmental Panel on Climate Change (IPCC), Cambridge University Press, 1999

[Ref 4] "Aero2K Global Aviation Emissions Inventories for 2002 and 2025" – CJ Eyers, P Norman, J Middel, M Plohr, S Michot, K Atkinson, RA Christou – QINETIQ/04/01113 – December 2004

[Ref 5] "Document de synthèse GIFAS GROUPE ENVIRONNEMENT" – J.M. JACQUET – Snecma Moteur – YY N° 358-01 /JMJ – April 2000

[Ref 6] "Airbus Global Market Forecast (Airbus GMF)", Airbus Industrie, 2004

[Ref 7] "Boeing Current Market Outlook 2004"

[Ref 8] ANCAT/EC2: Global Aircraft Emissions Inventories for 1991/92 and 2015 – Report by the ECAC/ANCAT and EC working group – Editor R.M. Gardner – 1998

[Ref 9] "Liquid Hydrogen Fuelled Aircraft – System Analysis", CRYOPLANE, Contract n° G4RD-CT-2000-00192, Project n° GRD1-1999-10014, September 2003

[Ref 10] "ESA-EEC/SEE Contrail Maps – Description of Product" – EUROCONTROL Experimental Centre / Isa Software – Smith, Jelinek, 2004

[Ref 11] Klaus Gierens and Susanne Marquat, Regions that are conditioned for Contrail Formation, DLR, 2001.

[Ref 12] Lee, D.S., I. Koehler, E.Grobler, F.Rohrer, R. Sausen, L.Gallardo-Klenner, J.g.J. Olivier, F.J. Dentener, A.F. Bouwam: Estimations of global NOx emissions and their uncertainties" Atmos.Env.,31, 1735-1749, 1997.

[Ref 13] WMO, 1995 WMO (World Meteorological Organisation): "Scientific assessment of ozone depletion: 1994", global ozone research and monitoring project, Report No.34, WMO, Geneva, 1995.

[Ref 14] Koehler and. al, 1997: Koehler, I., R.Sausen, R.Reinberger: "Contributions of aircraft emissions to the atmospheric NOx content" Atmos. Env., 31, 1801-1818, 1997

[Ref 15] Brasseur and. al., 1998: Brasseur, G.P., R.A. Cox, D. Hauglustaine, I.Isaksen, J. Lelieveld, D.H. Lister, R.Sausen, U. Schumann, A. Wahner, P. Wiesen: "European scientific assessment of the atmospheric effects of aircraft emissions", Atmos. Env., 32, 1998

[Ref 16] Travis, DJ, Carleton, AM and RG Lauritsen (2002) Contrails reduce daily temperature range. Nature 418:601.

[Ref 17] Evaluation of Air Pollutant Emissions from Subsonic Commercial Jet Aircraft; United States Environmental Protection Agency; EPA420-R-99-013; April 1999

[Ref 18] NASA Langley Cloud and Radiation Research - Minnis Group; http://www-pm.larc.nasa.gov/

[Ref 19] Environmental issues in flight – Global scale environmental impact of aviation; Sausen, R. AERONET II / X-NOISE II Joint Workshop on ENVIRONMENTAL INTERDEPENDENCIES IN AIR TRANSPORT; IATA, Geneva, 10-11 Feb 2003

[Ref 20] http://www.pa.op.dlr.de/contrails/

[Ref 21] ICAO Engine Exhaust Emissions Data Bank; ICAO; Doc 9646-AN/943 ; First Edition – 1995 ; Internet Issue 1(3/10/1998) ; Internet Issue2(8/2/99).

[Ref 22] Emission Indices – State of the Art; Literature Review; EUROCONTROL Experimental Centre; BU Environmental Studies; A.Celikel ; 1999 ; unpublished internal paper.

[Ref 23] Scheduled Civil Aircraft Emission Inventories for 1992: Database Development and Analysis; April 1996; NASA LRC; Contractor Report 4700; Steven L. Baughcum, Terrance G. Tritz, Stephen C. Henderson, David C. Picket

[Ref 24] "The Advanced Emission Model (AEM3) Version 1.5 – Validation Report", EUROCONTROL Experimental Centre; Society, Environment and Economics Business Area; Jelinek; Carlier; Smith; EEC/SEE/005/2003

[Ref 25] "Impact de la flotte aérienne sur l'environnement atmosphérique et le climat", Rapport no.40, Décembre 1997, Institut de France, Académie des sciences – Académie Nationale de l'air et de l'espace

[Ref 26] "Wasser als Treibstoff – Alternatives Antriebskonzept für die Luftfahrt" – FLUGREVUE – Ausgabe September 1998 Seite 66

[Ref 27] http://wave.prohosting.com/sunwater/aircraft.html

[Ref 28] "Methodologies for estimating emissions from air traffic future emissions" – MEET Project – Doc. N°97.177-006-Version1.1 – Sept. 1998 – Kalivoda, Kudrna, Fitzgerald

[Ref 29] "Cryogenic aircraft – Development of cryogenic fuel aircraft" – http://www.tupolev.ru

[Ref 30] "Hydrogen aviation" – Alexander Filatov – http://filas.narod.ru/docs/hydrogen_aviation_eng.htm

[Ref 31] "Les trois dimensions du défi énergétique pour l'avionneur" – Journée d'étude FEDESPACE – Feb. 2005 – Sébastien Remy – Airbus S.A.S.

[Ref 32] "Mit Wasser in die Luft gehen" – Wolfgang Birkenstock

[Ref 33] IPCC, 2001: *Climate Change 2001: The Scientific Basis. Contribution of Working Group I to the Third Assessment Report of the Intergovernmental Panel on Climate Change*, [Houghton, J.T.,Y. Ding, D.J. Griggs, M. Noguer, P.J. van der Linden, X. Dai, K. Maskell, and C.A. Johnson (eds.)]. Cambridge University Press, Cambridge, United Kingdom and New York, NY, USA, 881pp.

[Ref 34] CE Delft (2002) *External Cost of Aviation*.

Intentionally left blank

For more information about the EEC Society, Environment and Economy Research Area please contact:

Ted Elliff
SEE Research Area Manager,
EUROCONTROL Experimental Centre
BP15, Centre de Bois des Bordes
91222 BRETIGNY SUR ORGE CEDEX
France

Tel: +33 1 69 88 73 36
Fax: +33 1 69 88 72 11
E-Mail: ted.elliff@eurocontrol.int

or visit

http://www.eurocontrol.int/